PNL-4767
UC-66d

DO NOT MICROFILM
COVER

Geothermal Injection Treatment: Process Chemistry, Field Experiences, And Design Options

C. H. Kindle
B. W. Mercer
R. P. Elmore
S. C. Blair
D. A. Myers

September 1984

Prepared for the U.S. Department of Energy
under Contract DE-AC06-76RLO 1830

Pacific Northwest Laboratory
Operated for the U.S. Department of Energy
by Battelle Memorial Institute

Battelle

PNL-4767

DISCLAIMER

DISCLAIMER

PACIFIC NORTHWEST LABORATORY
operated by
BATTELLE
for the
UNITED STATES DEPARTMENT OF ENERGY
under Contract DE-AC06-76RLO 1830

Printed in the United States of America
Available from
National Technical Information Service
United States Department of Commerce
5285 Port Royal Road
Springfield, Virginia 22161

NTIS Price Codes
Microfiche A01

Printed Copy

Pages	Price Codes
001-025	A02
026-050	A03
051-075	A04
076-100	A05
101-125	A06
126-150	A07
151-175	A08
176-200	A09
201-225	A010
226-250	A011
251-275	A012
276-300	A013

PNL-4767
UC-66d

PNL--4767

DE85 002873

GEOTHERMAL INJECTION TREATMENT:

PROCESS CHEMISTRY, FIELD EXPERIENCES, AND DESIGN OPTIONS

Cecil H. Kindle
Basil W. Mercer
Rebecca P. Elmore
Steven C. Blair
David A. Myers

September 1984

Prepared for
the U.S. Department of Energy
under Contract DE-AC06-76RLO 1830

Pacific Northwest Laboratory
Richland, Washington 99352

ACKNOWLEDGMENTS

Several Pacific Northwest Laboratory staff members are acknowledged for their contributions to this report: D. W. Shannon for technical review and discussions; G. E. Zima for compilation of the case studies; P. L. Koehmstedt for assistance on the inhibitor section; O. H. Koski for the centrifuge separation analysis; O. J. Wick for gas flotation data; and L. L. Fassbender for the economic analysis, and S. K. Edler for editorial assistance and printing/graphics coordination. The support and encouragement of L. Lehr and A. D. Allen of the Division of Geothermal Energy, U.S. Department of Energy are also acknowledged.

ABSTRACT

The successful development of geothermal reservoirs to generate electric power will require the injection disposal of approximately 700,000 gal/h (2.6 x 10^6 l/h) of heat-depleted brine for every 50,000 kW of generating capacity. To maintain injectability, the spent brine must be compatible with the receiving formation. The factors that influence this brine/formation compatibility and tests to quantify them are discussed in this report. Some form of treatment will be necessary prior to injection for most situations; the process chemistry involved to avoid and/or accelerate the formation of precipitate particles is also discussed. The treatment processes, either avoidance or controlled precipitation approaches, are described in terms of their principles and demonstrated applications in the geothermal field and, when such experience is limited, in other industrial use. Monitoring techniques for tracking particulate growth, the effect of process parameters on corrosion and well injectability are presented. Examples of brine injection, preinjection treatment, and recovering from injectivity loss are examined and related to the aspects listed above.

CONTENTS

FIGURES

TABLES

1.0 SUMMARY

Fluid injection is not a new technology; oil companies have been injecting into oil fields to increase production for many years. However, oil field technology does not involve the high temperatures that are characteristic of a geothermal field and many aspects of the technology are not directly transferable. Oil field technology is more applicable to sedimentary rock formations than to the fractured systems often found at geothermal sites.

In the last two decades, geothermal development has been shifting from steam fields to the more common liquid-dominated reservoirs. To prolong the resource and to avoid degrading surface waters, the underground injection of the heat-depleted brine is increasingly becoming an accepted practice. Many brines, particularly those from the higher temperature reservoirs, undergo severe chemical disequilibrium during the energy extraction process because of temperature and/or pressure changes. As the brine regains equilibrium, precipitates form that can plug the injection process. Several approaches to treating the brine prior to injection have been used, tested, proposed, or are possible. This report describes these treatment options, the experience to date, how they relate to fluid and reservoir characteristics, and how these processes should be monitored. Documentation and references are provided.

The treatment of spent brine prior to disposal is not currently a standard practice. Plants in Mexico, Kenya, Hawaii, New Zealand, and El Salvador do not inject spent brine; the brine at these plants either percolates into the ground or is disposed of in surface waters. It is noteworthy that most plants anticipate initiating or expanding injection efforts to improve reservoir longevity and to minimize environmental damage. Experience has shown that treatment prior to injection will become standard practice because of the precipitates that form during the heat extraction process and block the injection well. Treatment possibilities include:

- immediate injection with no treatment; 1 h of aging prior to injection (Japan); 20% annual loss of injectivity
- maintaining temperature above silica precipitation levels (EL Salvador)
- maintaining temperature (silica control) and pressure for calcite control (United States)
- inhibiting silica precipitation by acidifying (United States)

- flocculating the silica by raising the pH with lime addition (New Zealand and Mexico)
- using a calcite inhibitor and maintaining high temperatures for silica control (United States)
- using a recycled sludge to seed precipitation (United States).

Operating experience is limited, much of the data is proprietary, and the reservoirs are so varied that general conclusions based only on operating experience are hard to support. The reservoir site and chemistry conditions still determine the treatment process.

Injection horizon reservoir characteristics, both those relating to the formation porosity and its connate water, have an impact on the injection treatment process. To maximize the injection zone area and the tolerance to particulates, the preferred practice is to inject into a fracture, especially if it does not short-circuit back to the production well. As the Japanese and the Roosevelt Hot Springs experiences indicate, high injection conductivity from fractures can partially compensate for what would otherwise be an unacceptable treatment process. This injection conductivity can only be reliably determined on the site by drilling a well; however, literature references can permit the estimation of formation mean grain size. Assuming that injection will be controlled by the porosity surrounding the wellbore, this can be correlated with different types of formation damage as a function of injected particulate size (Table 1.1).

The chemistries of the brines that require injection range from salinities of 5% to 800% that of seawater. Within this range of salinities there are a handful of scale species that give problems in geothermal conditions, and these problems can be aggravated by certain process operations (Table 1.2).

TABLE 1.1. Estimated Impact of Injected Particles on Formation

Reservoir and Well	Calculated Formation Grain Size, μm	Size of Injected Particles Estimated to Affect Well Performance, μm		
		No Effect	Deep Bed Invasion	Surface Impairment
Westmorland				
Dearborn 2	38	<0.5	0.5 to 3	>3
Landers 3	36	<0.5	0.5 to 3	>3
East Mesa				
Mesa 5-1	13	<0.5	0.5 to 1.2	>1.2
Magma 46-7	137	<0.5	>0.5	

TABLE 1.2. Effect of Process Parameters on Potential Scale Formation

Process Parameter	Equilibrium Effect on Potential Scale Species(a) SiO_2	$CaCO_3$	Sulfide	Sulfate
Temperature decrease (as in plant cycle)	●	o	●	o Ca ● Ba
Temperature increase (reheat during injection)	o	●	o	● Ca o Ba
Increased pH (as CO_2 is flashed)	● o pH >9	●	●	●
Decreased pH (acid addition)	o	o	o	o
Increased salinity (flashing; mixing)	●	o	o	o

(a) ● aggravates problem
o alleviates problem.

Among these species the most universal problem is caused by silica polymerization as the brine is concentrated and/or cooled by flashing or heat extraction. Silica precipitation kinetics is slow to moderate; deposition in the receiving formation can cause loss of injectivity that is expensive to rectify. Factors that depress the speed of silica precipitation include: decreased temperature, decreased supersaturation ratio, the absence of fluoride ion catalyst, and lowering the pH. Maintaining silica supersaturation ratios below 2 gives some opportunity for controlling precipitation at the pH ranges normally encountered in U.S. fields. Lowering the pH by one unit slows the kinetics by a factor of 10. As the pH becomes very acid (pH ~3) and the kinetics slows, the presence of fluoride catalyst can maintain the precipitation rate even in the face of further pH drops. Since silica equilibrium solubility increases with temperature, which partially offsets the temperature-based kinetic factors, the net effect is that the maximum rate of silica precipitation should occur when the brine is 25 to 50°C below the temperature for saturation at a given amorphous silica concentration.

Calcite precipitation is typically a production problem, although it may result from the injection of surface or incompatible waters as they are reheated. Sulfate scales are a similar problem where incompatible waters are involved. Sulfide scales frequently occur in conjunction with other scales, although as techniques are used to control these other scales, sulfide precipitates become more noticeable as geothermal scales on their own basis. The

sulfide chemistry is more complicated and less understood than the silica and calcite chemistry, and it deserves more investigation.

The various processes for controlling the chemical disequilibrium inherent in the geothermal energy extraction process can be grouped as either precipitation avoidance or controlled precipitation; brine purification methods (ion exchange, reverse osmosis) are inappropriate. Some of these specific techniques are more suitable for one type of scale than another and, even in the conceptual stage, can be matched to a particular reservoir or type of power cycle (Table 1.3).

Until the hot hypersaline brines from the Imperial Valley of California were produced and injected, the experience and development focused on precipitation avoidance techniques such as temperature control, acidification, inhibitors, or pressure maintenance. All of these are currently in use for main flow treatment in the United States. Silica chemical inhibitors have shown some effectiveness at high concentrations (economically unattractive); a sulfate inhibitor has demonstrated poor effectiveness in laboratory tests; $CaCO_3$ inhibition has been effective at low concentrations (ppm range) depending on the chemical used and the brine scaling tendency.

TABLE 1.3. Potentially Usable Treatment Techniques

Scaling Species	Precipitation Avoidance	Controlled Precipitation	Not Appropriate
Silica	Temperature maintenance Acid treatment Dilution Inhibitor	Crystallizer-clarifier Base treatment Aging/sedimentation	CO_2 injection[a] Pressure maintenance
$CaCO_3$	Pressure maintenance Inhibitor Acid treatment	CO_2 injection[b]	Temperature maintenance Crystallizer-clarifier[b]
Sulfides	Acid treatment Temperature maintenance	Crystallizer-clarifier Base treatment	Pressure maintenance CO_2 injection[a,c]
Sulfates	Compatible mixing Inhibitor		

(a) To the extent that the resulting brine pH is lowered, it may be beneficial.
(b) The speed of calcite deposition makes it unlikely that controlled precipitation techniques will be successful unless pressure is maintained.
(c) In the case of noncondensible gas (NCG) injection into some brines the presence of H_2S could aggravate the problem by causing metal sulfides to precipitate from the cooled brine.

In the late 1970s, the U.S. Department of Energy and San Diego Gas and Electric operated the Geothermal Loop Experimental Facility (GLEF) using hypersaline brine. Silica and sulfide scaling problems resulted in the successful testing of the first of the controlled precipitation techniques--recycling precipitate particles as seeds and completing the particulate growth in a reactor clarifier. This crystallizer-clarifier technology has been adapted by a privately owned 10-MWe Salton Sea plant, and other derivative plants are planned. Various methods of separating the produced solids from the brine are described and the geothermal experience and potential are discussed in this report.

Table 1.4 summarizes some treatment practices and their status. These treatment processes protect the injection system, which in turn is usually a factor in determining whether the plant itself can operate. Monitoring these treatment and injection systems can be a cost-effective way to maintain a high capacity factor and minimize expensive well recovery operations. The use and interpretation of injectivity data, filter tests, particulate analysis, and other techniques are described including a detailed example. Treatment process monitoring by brine composition changes and particulate content have detected unanticipated scaling and suspended solids transients that could impact injection well performance. Table 1.5 illustrates a composite view from two reservoirs of particulate concentrations observed at different geothermal process locations. These limited data indicate that the controlled precipitation treatment processes, despite clarification and filters, will inject an order of magnitude more suspended particles than the precipitation avoidance treatments. From this, it can be inferred that the location of a fractured or highly permeable injection zone will be more critical to the success of a controlled precipitation process than it is to a precipitation avoidance process. It is conceivable that in the future the identification of favorable injection horizons will become nearly as important as the location of favorable production zones.

Monitoring the process for corrosion is a straightforward way to assure that process conditions are consistent with the full operational lifetimes of the components. An economic analysis is presented, indicating that the life cycle cost of repeated well cleaning is greater than the cost of a properly operating injection treatment process.

TABLE 1.4. Brine Treatment Problems and Selected Technical Options

Problem	Occurrence	Possible Solution or Component	Geothermal Experience
Silica (Section 4.1)	Japan, El Salvador, Mexico, New Zealand, Hawaii, and Imperial Valley; most common problem for injection disposal.	Crystallizer-reactor clarifier technology (Section 5.2)	GLFE, Salton Sea 10-MWe.
		Acidification (Section 5.1.3)	Tested in New Zealand, Salton Sea; now used at Brawley 10-MWe.
		Add base/lime (Section 5.1.3)	Tested in New Zealand, Cerro Prieto, Los Azufres.
		Chemical inhibitors (Section 5.1.4)	Tested at Salton Sea and Cerro Prieto.
		Air flotation separation (Section 5.3.4)	Tested at Wairakei.
		Ponding/aging-sedimentation (Section 5.3.2)	Japan (Hatchobaru), Hawaii, and Cerro Prieto (no injection); unsuccessfully tested in New Zealand and at Brawley 10-MWe plant.
		Maintain temperature (Section 5.1.2)	El Salvador, East Mesa, Heber (under construction).
		High-rate settler (Section 5.3.2)	Tested at Los Azufres.
		Dilution (Section 5.1.5)	Tested in Iceland.
Calcite (Section 4.2)	Turkey, Azores, East Mesa, Desert Peak, and Brady Hot Springs. Mainly a production problem, although calcite crystals may nucleate silica particles.	Maintain pressure (Section 5.1.1)	East Mesa, Brady Hot Springs, Heber (under construction).
		Inject CO_2 (Section 5.2.1)	Desert Peak test.
		Acidification (Section 5.1.3)	East Mesa tests.
		Inhibitors (Section 5.1.4)	Roosevelt Hot Springs.
Sulfides (Section 4.3)	Salton Sea, Brawley, East Mesa, Desert Peak, and New Zealand; frequently in conjunction with other precipitates.	Acidification (Section 5.1.3)	Brawley 10-MWe plant.
		Crystallizer-clarifier (Section 5.2)	Salton Sea 10-MWe plant and GLEF.
Sulfates (Section 4.4)	Salton Sea	Avoid incompatible waters	

TABLE 1.5. Particle Loadings in Treatment Processes

Process	Location	Particle Concentration, mg/l
Precipitation avoidance: maintain temperature and pressure (binary plant)	Plant inlet	0.7
	Injection	1.1
Controlled precipitation: crystallizer, reactor clarifier, media filter (flash plant)	Reactor clarifier inflow	10 to 20,000
	Reactor clarifier outflow	50 to 200
	Media filter outflow to injection	10 to 20

2.0 INTRODUCTION

The use of geothermal energy to produce electric power has demonstrated a long-term annual growth rate of 8.3% (Figure 2.1) throughout the world, depending on the combination of resources, capital, and technical knowledge. As of 1983, 90% of the 137 operational plants were distributed about evenly among four locations: Europe, the Pacific Island countries, North America, and Central America. The remaining plants were located in mainland Asia and Africa. North and Central American plants (almost 30% of the total) tend to be larger than the average and represent half of the worldwide installed capacity.

Two types of geothermal reservoirs are represented: steam and superheated water (usually referred to as a liquid-dominated or brine reservoir even though the salinity may range from 1/20 to 8 times that of seawater). The steam fields are more desirable because they can produce power more economically and efficiently than the more common liquid-dominated reservoirs.

Several liquid-dominated reservoirs, using flash-to-steam or binary (organic Rankine cycle) plant technology, are being developed as energy resources. About 55% of the operating geothermal units currently work from liquid-dominated reservoirs. A by-product from this energy utilization is the production of large volumes of spent (heat-depleted) geothermal brines; a 50,000-kWe plant produces about 700,000 gal/h (2.6 million l/h).

The composition of geothermal waters can vary widely depending on the source of the water and the process used to extract energy. A geothermal power plant that operates on a steam source will produce and discharge water that is very low in dissolved salts (i.e., condensate). A geothermal power plant that operates on a hot brine source will produce and discharge water that is high in dissolved salts and may contain precipitated particulate matter.

The variability of the composition of geothermal waters from different reservoirs in the western United States is illustrated in Figure 2.2. The dominant elements are sodium, potassium, calcium, and chlorine. Of these, only calcium plays a direct role in the formation of scale and precipitated solids. The major sources of scale and precipitated solids that form during energy extraction from geothermal waters are 1) silica, 2) calcium carbonate and sulfate, and 3) heavy metal sulfides, sulfates, oxides, and carbonates. Other minerals such as strontium carbonate or barium sulfate may occur infrequently. The composition of geothermal waters in a reservoir is related to:

- the composition of the water entering the reservoir (for example, brackish or fresh water)

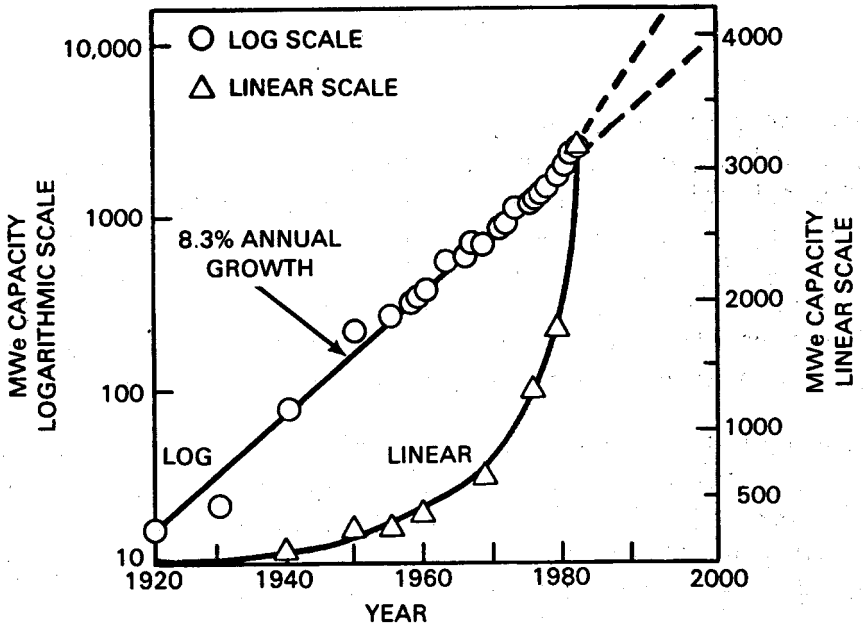

FIGURE 2.1. Geothermal Electric Plant Installed Capacity (DiPippo 1984)

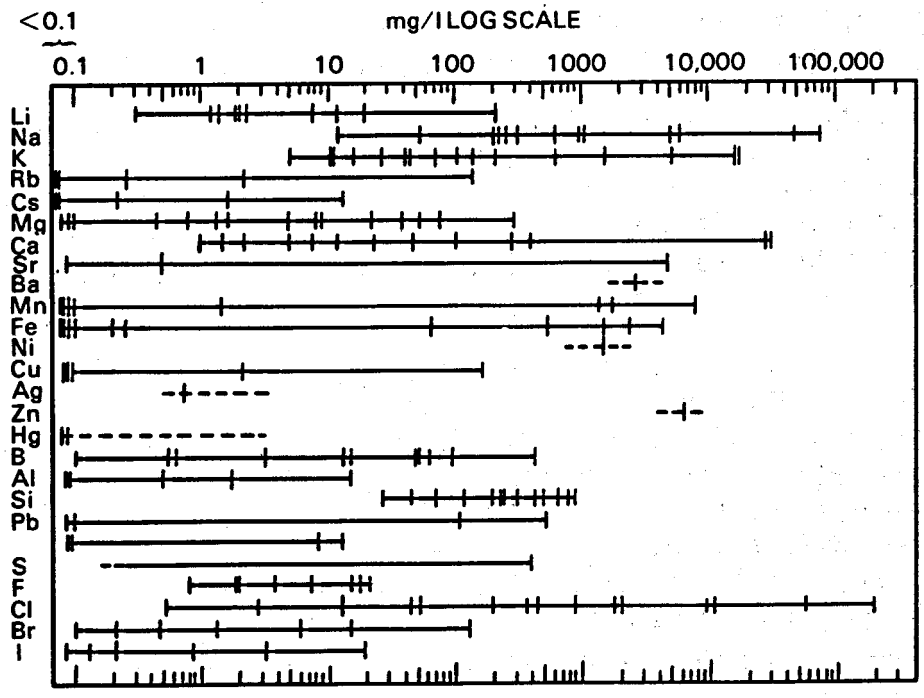

FIGURE 2.2. Concentration Ranges for Elements in Geothermal Waters (Douglas et al. 1972)

- temperatures within the reservoir
- geologic materials; water/rock reactions.

The solutes present in water entering a geothermal reservoir can also influence the final makeup of the water withdrawn for energy production. A high concentration of NaCl, for example, will increase the solubility of $BaSO_4$ (barite) but decrease the solubility of SiO_2. The types and quantities of minerals present in geologic strata containing the geothermal water in a reservoir affect the composition of the water. The scale- or precipitate-forming characteristics of geothermal waters are largely the result of mineral dissolution in the reservoir. Silica, frequently in the form of quartz, is a common constituent in the earth's crust and is frequently found in geothermal waters at concentrations sufficient to form scale or precipitates upon cooling. It is one of the more troublesome solutes because it is often slow to respond to physical/chemical alteration of the geothermal water; it fails to reach equilibrium quickly during precipitation or crystallization.

In general, the solvent capability of water for minerals in a geothermal reservoir is enhanced as the temperature increases. Notable exceptions are calcium carbonate and calcium sulfate over certain temperature ranges where the solubility decreases as the temperature increases. The causes of scale and precipitate formation are discussed in Section 4.

Elemental compositions of geothermal waters taken from various reservoirs in North America are presented in Table 2.1. These reservoirs either have existing power production units at the sites or have a potential for large-scale power production. All are hydrothermal, liquid-dominated reservoirs.

Because of construction scale-up risks, the high cost of capital, large brine disposal volumes, and the exploratory nature of building the first plant on any given reservoir, geothermal plants tend to be smaller than other base-load generating plants. The current median size is in the 10- to 20-MWe range. The larger geothermal plants are located on steam reservoirs, while smaller plants are on liquid-dominated fields. This arrangement works to the advantage of operators and engineers working in at least a partially unfamiliar field in that risks are smaller and more readily compensated for in a small process.

Several innovations are being explored and tested for specific geothermal applications, including: gravity head binary plants using downhole heat exchangers, binary plants utilizing direct contact (brine: organic working fluid) heat exchangers, a total flow rotary separator expander, CO_2 injection, and others. All of these options (except for the initial one) produce comparable volumes of waste fluids. The handling of these fluids is an area of intense current interest because development of new brine treatment processes

TABLE 2.1. Chemical Constituents in Unflashed Waters from Selected Geothermal Reservoirs[a]

Constituent	Reservoir, Location, and Well: Salton Sea USA/California Magnamax 1[b]	Cerro Prieto Mexico/Baja M-30b[c,d]	East Mesa USA/California Mesa 31-A[d]	Heber USA/California C. B. Jackson 1[d]	Ahuachapan El Salvador Ah 1 and 6[e]	Roosevelt Hot Springs, USA/Utah Phillips 54-3[d,f]	Beowawe USA/Nevada Vulcan 2A[d,g]
TDS[h]	183,000[i]	17,000	2900	15,300	15,000[i]	6440	855
Li	156	15	0.6	2.8	15	18	trace
Na	41,700	5,190	730	4690	4550	2400	214
K	7,350	1,220	85	181	792	565	9
Mg	97	0.55	<0.05	4.7	0.07	19	-
Ca	19,400	396	9	891	326	9	-
Sr	393	13	1.4	32	2.2	-	-
Ba	130	5.3	0.15	3	-	-	-
Fe	126	0.3	0.1	20	0.08	-	-
Mn	520	1.8	ND	1.3	0.19	0.15	<0.1
As	(12)[j]	0.31	0.025	-	7.8	3.5	-
Pb	21	-	0.6	0.6	≤0.0008	0.1	-
Cu	-	0.7	<0.1	0.4	≤0.0008	0.03	<0.1
Zn	203	0.007	0.1	0.4	0.005	0.04	-
F	(15)[j]	0.88	1.4	0.9	1.3	(5)	6
Cl	112,800	10,100	510	8,320	8,250	4,800	50
SiO_2	456	720	270	267	483	775	329
SO_4	(5.4)[j]	8.6	183	152	18	200	89
HCO_3	(>150)[j]	21	84.5	-	27	(200)	$_3$[k]
pH	(5.2 at 20°C)[j]	(8.10 at 25°C)	6.3	5.8	-	(6.5)	9.3
Temperature, °C	(340)[j]	(273)	174	-	240	(>260)	132

(a) Concentrations in ppm except where indicated otherwise; (-) signifies not available; and ND signifies not detectable.
(b) See San Diego Gas and Electric 1980.
(c) Data in μm; corrected for steam loss based on a factor of 0.665.
(d) See Cosner and Apps 1978.
(e) See Einarsson, Vides, and Cuellar 1975; Cuellar 1975.
(f) Data from Record 227 except that in parentheses is from Record 226.
(g) Uncorrected for steam loss (~7%).
(h) TDS - total dissolved solids.
(i) Sum of average major element concentrations.
(j) Well IID No. 1; see White 1968.
(k) CO^{-2} = 168 ppm.

will permit the tapping of selected geothermal reservoirs. In the recent past, some technologies addressing the handling of brine prior to injection have been tested; for example, crystallizer/clarifier technology adapted from municipal waste water treatment use. Investigators are looking at combining separate functions of this technology into a single component. Flotation technology from the minerals industry has seen limited testing to remove precipitates from spent brine as have filter presses, centrifuges, and settlers.

In all of these approaches to treatment before injection disposal, the brine chemistry, temperature, and pressure must be matched to the treatment process. The chemical engineering that exists is one of most challenging in the field because of the large flows involved and the rapid changes in temperature, pressure, and mineral solubilities.

This report was prepared by Pacific Northwest Laboratory (PNL)[(a)] to provide a technical understanding and description of the rapidly developing injection treatment field. Although many references are provided, it is the authors' intent to provide a stand-alone text to the extent practical, especially for the chemistry and treatment options areas. Discussions and evaluations of several techniques that have been proposed or could be tested for geothermal use are included. The underlying process chemistry principles are discussed in moderate detail because of the unusual chemistries involved and their large impact on process design and operation. Treatment options involving specific components are discussed with consideration to the nongeothermal background from which they are adapted. In many cases, these are not new and untried techniques; it is only their adaptation to the geothermal chemistry that is new.

The remainder of the report consists of:

- a description of design requirements for injection
- a discussion of the process chemistry involved
- a discussion of the treatment options
- a description of operational monitoring steps
- a discussion of the comparative economics
- a summary of injection experience throughout the world.

(a) Operated for the U.S. Department of Energy (DOE) by Battelle Memorial Institute.

3.0 DESIGN REQUIREMENTS FOR AN INJECTION TREATMENT PROCESS

To design a water treatment process, the effluent characteristics must be established so that the process is compatible with the injection formation. Two interrelated subjects are involved: the formation/fluid compatibility aspect and the geochemical problem to prevent scale from forming at an unanticipated location or rate. The latter is introduced in this section only, and calculational models are described. The changes that occur during a power cycle or treatment process and the effect on scaling are discussed in Section 4.

Injection experience and treatment processes vary from reservoir to reservoir, from brine to brine, and with temperature and pressure. These variables make it difficult, if not impossible, to determine design requirements for a successful treatment process; however, the tests used to arrive at such a determination for a particular site are discussed in this section. In general, this section assumes that injection permeability will be controlled by the matrix around the wellbore and not by fractures. Fracture-dominated permeability indicates that the formation will tolerate many more solids and that injection treatment may be minimal.

3.1 FORMATION/FLUID COMPATIBILITY

The main questions to be considered in treatment of fluids to be injected are: What are the major formation/fluid incompatibilities in a particular injection well and what are the potential well impairment mechanisms that may occur during injection? From design and operational standpoints, it is desirable to establish these impairment processes before trying to inject spent fluid because well plugging is often expensive or difficult to correct. In general terms, formation/fluid incompatibility can arise from either or both of two phenomena: 1) particulate plugging and 2) geochemical incompatibility. To diagnose injection problems in both of these areas, information on the geologic and hydrologic characteristics of the receiving formation and data on the injection composition, temperatures, and suspended solids content of the fluid are required. Formation/fluid compatibility is determined by each of these factors, and requirements and procedures for their characterization are discussed in this section.

3.1.1 Particulate Plugging

Particulate plugging is the most common type of impairment experienced in geothermal injection wells. It can arise from four processes that have been

described by Barkman and Davidson (1972) and Jorda (1980) among others.[a] These mechanisms are stated below and shown schematically in Figure 3.1:

- formation of a filter cake on the wellbore face
- particle invasion into the rock formation, which reduces available pore space or forms an internal filter cake

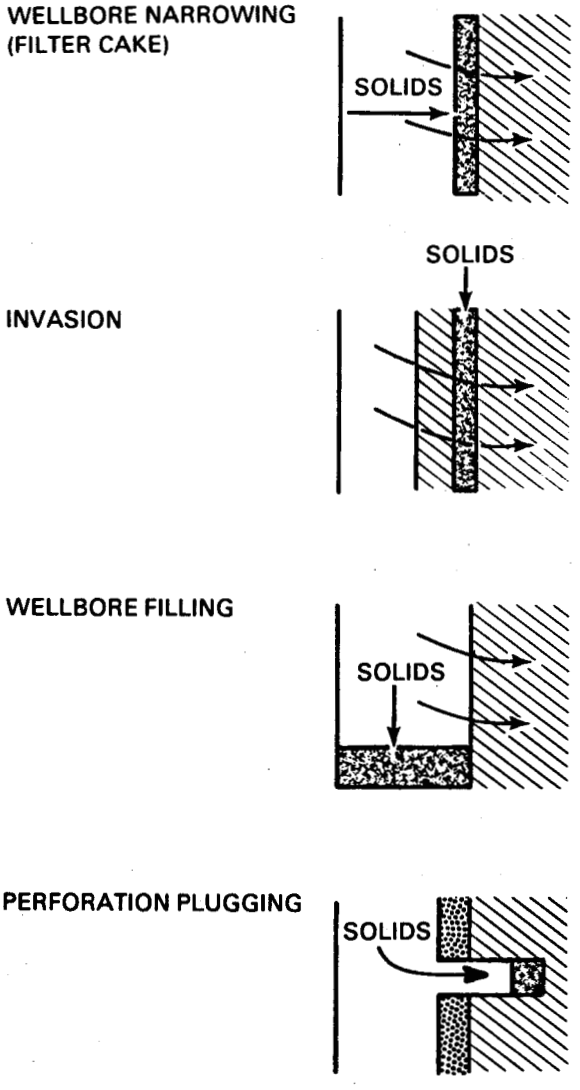

FIGURE 3.1. Types of Wellbore Impairment Caused by Suspended Solids (Barkman and Davidson 1972)

(a) Chasteen 1975; Davidson 1979; Earlougher 1977.

- wellbore filling
- well casing perforation plugging.

Particulate plugging in geothermal systems is often a combination of these mechanisms. Filter cake usually forms when the injected brine is high in suspended solids and the injection horizon has a mean pore size too small to accept all of the solid particles. Particle invasion occurs when the ratio of fluid particle size to porosity size is such that invasion of the formation occurs and an internal filter cake is formed. Injection impairment caused by wellbore narrowing, wellbore filling, or perforation plugging can sometimes be reversed by backflushing the well; however, impairment due to formation of an internal filter cake is much more difficult to remedy. Owen et al. (1979) investigated injectability testing of clarified hypersaline geothermal brine and concluded that wellbore narrowing and invasion were the most likely impairment modes.

Several authors have presented results that can be used to anticipate, diagnose, and prevent injection impairment by suspended solids. These methods are based on a thorough characterization of both the suspended solids in the injected fluid (including quantity and size distribution) and the receiving formation (permeability distribution of pore and grain sizes). These methods are discussed in more detail in Section 6 of this report; however, a basic rule has been derived to relate the diameter of the suspended solids to potential impairment: particles less than 0.45 μm in diameter generally pass through the formation without causing impairment and particles greater than 10 μm in diameter generally accumulate in the wellbore or are retained on the surface and form a filter cake. Particles with diameters between 0.45 μm and 10 μm can invade the formation and cause impairment, depending on the formation and the fluid properties. Thus, particles with diameters from 0.45 μm to 10 μm are potentially the most critical and represent a major candidate for injection treatment. Particles with diameters larger than 10 μm should also be considered for injection treatment even though the impairment that they cause is more easily recoverable. Because particles with diameters of 0.45 μm or less generally do not cause impairment, most membrane plugging and monitoring tests use a 0.45-μm filter. This simplified analysis may have to be shifted relative to the particle size, depending on the porosity and the degree of fracture of the receiving formation.

Suspended solids in a spent geothermal fluid can arise from a variety of sources. Major sources include fines from the production formation, fragments from pipe walls resulting from corrosion or precipitation, and freely suspended precipitates. Other sources may include chemical additives (kill fluids, grease for seals, drilling mud, makeup water, and scale and corrosion inhibitors), microorganisms, and mobilized fines in the receiving formation.

Permeability can also be impaired when gas bubbles enter and are entrained in the fluid stream. These bubbles can lodge in pore spaces and plug the formation, but this type of plugging can frequently be remedied by backflushing.

Spent fluid output from a plant can vary considerably in composition and suspended solids content with time. Operational considerations such as startup and shutdown of various sections of the system (wells, heat exchangers, etc.) will produce pulses of water with higher suspended solids and differing compositions. Care should be taken to assure that these changes in water conditions do not saturate treatment mechanisms and find their way into the wellbore.

Chemical Precipitation

Injection formation temperatures are generally higher than the temperature of the spent geothermal brine, and the injected fluids may be reheated upon entering the formation. This increase in fluid temperature can cause scaling of minerals with retrograde solubilities (solubilities that decrease as the temperature increases). The prime candidates are sulfate and carbonate scales that could form under one of two situations. The first situation is when CO_2 is lost in a flash cycle plant and shifts the pH toward a more basic, scale-forming condition. If a carbonate ($CaCO_3$) is close to its solubility limit in the cooled and altered brine on the surface, it may exceed its solubility limit as it is reheated during injection. The second situation is possible if makeup water is added to the brine prior to injection to add volume or dilute silica supersaturation. If this added water is not chemically compatible, precipitates may form during mixing or during the reheating process. Sulfates of barium, calcium, or strontium are of major concern; Kandarpa and Vetter (1981) describe an investigation relevant to the Salton Sea field. The correct approach is to establish the water chemistries and to use the geochemical models to verify compatibility for the range of operating temperatures.

Permeability Reduction with Clay Minerals

Clays are hydrous aluminosilicates that occur worldwide in sedimentary rocks. The most common clays are illite, kaolinite, montmorillonite and chlorite; and these minerals often occur together (Neasham 1977). Clay minerals are formed due to the interaction of formation water with rock, and clay mineralogy is very sensitive to water chemistry and can change very quickly in response to a change in water chemistry. Introducing foreign water can reduce permeability in two ways: 1) the clays may swell, reducing pore volume and blocking pore throats or 2) the clays may disperse, causing particulate plugging (Eickmeier and Ramey 1970). These phenomena can occur separately or together in all parts of the formation swept by the injection fluid.

Montmorillonite (smectite) is the only clay mineral known to swell substantially when contacted by foreign waters. It generally swells when connate water with a strong brine composition is replaced with a weaker brine (lower ionic strength) (Howak and Krueger 1951). Swelling is generally reversible; and formation permeability can be regained if the injected water is treated to have salinity, pH, and ionic strength equivalent to connate water and if the swelling permits the new fluid to reach the clay.

Clay minerals disperse (deflocculate) to some extent whenever fluids of different chemistries displace connate waters. The dispersion of clays and the introduction of clay particles into the fluid can cause particulate plugging. However, in an injection well, the dispersed particles are carried away from the wellbore; and, as the available pore space increases with the square of the distance from the well, plugging due to dispersion often does not occur.

Permeability impairment caused by swelling and dispersion of clays must be analyzed on a case-by-case basis. The response of clay minerals to injected water depends on the types and amounts of clay present and on the chemistry of the injected water. If the injected fluids are higher in salinity than the connate waters, clay swelling may not occur. At many locations (for example, the Salton Sea reservoir), the clay content of the receiving formations is low. Geopressure sites, where the clay content is often high, are exceptions. If changes in clay mineralogy are suspected to cause impairment, a series of tests should be performed to determine if clay swelling or dispersion is causing the problem. Laboratory analyses such as x-ray diffraction (XRD) and optical petrography should be used to determine the types, concentration, and location of the clay minerals. Neasham (1977) presents a detailed discussion of the effects of clays on fluid flow properties.

3.1.2 Geochemical Modeling

Geochemical modeling may be used to identify or understand chemical problems arising from injecting altered or foreign water into a geothermal reservoir. The chemical incompatibility that results from differences in composition and temperature may cause the precipitation of solid phases such as amorphous silica (SiO_2), $CaCO_3$, $CaSO_4$, $BaSO_4$, or $SrSO_4$. In some cases, knowledge of the nature and amount of potential precipitation as influenced by temperature and pressure could be critical in managing injection. The tendency of the brine to scale can be calculated by geochemical models. However, the kinetics of scale deposition is difficult to incorporate and is usually not addressed. For the two most common types of scale ($CaCO_3$ and SiO_2), the kinetics can be summarized as being very rapid in $CaCO_3$ precipitation and being slow to moderate in SiO_2 precipitation.

The objectives of this section are to:

- describe the modeling approach and the codes that are available and applicable
- review the necessary analytical data used as input for the geochemical models
- discuss advantages and shortcomings of using geochemical models as tools to manage the injection of waters into geothermal reservoirs.

Geochemical models use the principles of thermodynamics to calculate the tendency of reactions to occur as a system proceeds toward equilibrium. Computer codes that incorporate these models are used to calculate the nature of chemical reactions that will occur, given sufficient time; but it is again important to note that most current codes cannot predict how fast the reactions will occur.

These geochemical mass transfer codes can predict: 1) the final solution composition resulting from the dissolution or precipitation of a set of minerals and 2) the total mass of solid precipitated (or dissolved). More sophisticated mass transfer codes can predict the incremental changes in aqueous solution as the reactions proceed, but these codes have generally been written for metered dissolution of solids. These thermal "reaction path" models are based partly on chemical equilibrium and partly on the rate the solid is metered into the system.

Geochemical models can also predict the effects of temperature and pressure on precipitation reactions. Obviously, the ability to calculate temperature dependence is very important for injection schemes in which temperatures may cover a very wide range.

Some of the more recent versions of codes representing geochemical models are listed in Table 3.1. The minimum requirement for predicting precipitation during injection is a mass transfer model with temperature capability. The codes EQUILIB,[a] REDEQL-UMD, and MINTEQ satisfy this requirement. However, the PHREEQE and EQ3/EQ6 codes are required if the detailed sequence of precipitation or dissolution of solids needs to be known. The EQ3/EQ6 code has the advantage of being a reaction path model with high-temperature and high-pressure capabilities.

(a) EQUILIB is a copyrighted code of the Electric Power Research Institute, Palo Alto, California.

TABLE 3.1. Summary of Published Geochemical Models and Capabilities

Model	Type	Temperature Range, °C	Pressure Range, bar	Reference
SOLMNEQ	Aqueous speciation	0 to 300	1 to 1000	Kharaka and Barnes (1973)
WATEQ2	Aqueous speciation	0 to 100	1	Ball, Jenne, and Nordstrom (1979)
GEOCHEM	Mass transfer	25	1	Sposito and Mattigod (1980)
MINEQL/REDEQL2	Mass transfer	25	1	McDuff and Morel (1973); Westall, Zachary, and Morel (1976)
EQ3/EQ6	Reaction path	0 to 300	500	Wolery (1979)
MINTEQ	Mass transfer	0 to 100	1	Felmy, Girvin, and Jenne (1983)
PHREEQE	Reaction path	0 to 100	1	Parkhurst, Thorstenson, and Plummer (1980)

All geochemical codes are constrained by the accuracy of available thermodynamic data and the equilibrium assumption. In addition, without accurate and complete input data, the modeling effort can be restricted or misleading. The user of the code must provide the solution temperature, pH, and composition of the initial solution. Although it is not necessary to analyze for every element suspected to be present in the injection and aquifer waters, Ca, pH, CO_2, HCO_3, CO_3, Sr, Ba, SO_4, SiO_2, F, and sulfides should be determined as a minimum along with total dissolved solids (TDS).

Geochemical codes can identify reactions that will take place whenever an injection fluid is mixed with the solution in the reservoir. A code with mass transfer or reaction path capabilities could calculate the mass dissolved or precipitated as various mixtures of injected and native water react with the aquifer material and proceed toward equilibrium. This information could then be used to indirectly assess the potential damage to the aquifer. At the same time, the composition of the separate solution at equilibrium or combined solutions can be used to evaluate any potential precipitation (scaling) in the surface plant. Thus, the code could be used to identify potential problems.

Geochemical models cannot describe physical changes in the system. Although models can predict the mass of solids that might precipitate, they

cannot predict plugging of the reservoir. Dispersion of clays resulting from sudden changes in temperature or ionic strength can plug the pore throats of an aquifer, but a geochemical model cannot predict these reactions. None of the geochemical codes have been firmly based at high salt concentrations, which is a major constraint for some geothermal applications. Including Pitzer's formulation (1980, 1981) in future codes will improve the accuracy in very concentrated brines.

3.2 FLUID CHARACTERIZATION

Detailed knowledge of the suspended solids content and the fluid chemistry of injection fluids at a geothermal power plant is important. Fluid composition varies during initial plant startup and during startup and/or shutdown of various system components (production wells, heat exchangers, etc.).

3.2.1 Sampling and Analyzing Geothermal Fluids

In sampling and analyzing geothermal fluids, flow uncertainties, sampling biases, preservation difficulties, and analytical interferences may lead to unreliable results. As part of a DOE project, PNL developed a procedure for sampling and analysis that is particularly suited to liquid-dominated resources and adaptable to a variety of situations (Kindle and Woodruff 1981). The analytical methods were refined from the results of a 20-laboratory round robin on several geothermal samples.

The approach consists of recording flow conditions at the time of sampling, a specific insertable probe sampling system, a sample stabilization procedure, commercially available laboratory instruments, and data quality check procedures. Readily available equipment is utilized whenever possible.

The sampling system consists of a sampling probe (Figure 3.2) that is inserted into the flowing stream to avoid the possibility of contamination (corrosion products, dirt, scale) that is present in a normal service valve. The probe also permits easier identification of two-phase flows that bias sampling by allowing selection of a sampling position within the flow path to avoid trapped gas or stratified flow.

The sample flow must be cooled under pressure to eliminate flashing within the sample collection system and to facilitate handling. The geothermal sampling assembly designed by PNL is shown in Figure 3.3. Cooling coils followed by a flow-regulating valve permit pressure reduction without flashing or biasing the sample because of scale deposits and with a minimum of gas breakout. The entire sampling and analysis procedure is summarized in Figure 3.4. The required sampling apparatus, which containers and stabilizers to use, and the most appropriate analytical technical for each chemical component are shown. Suggested sample designations, sample volumes, and data quality checks are also included.

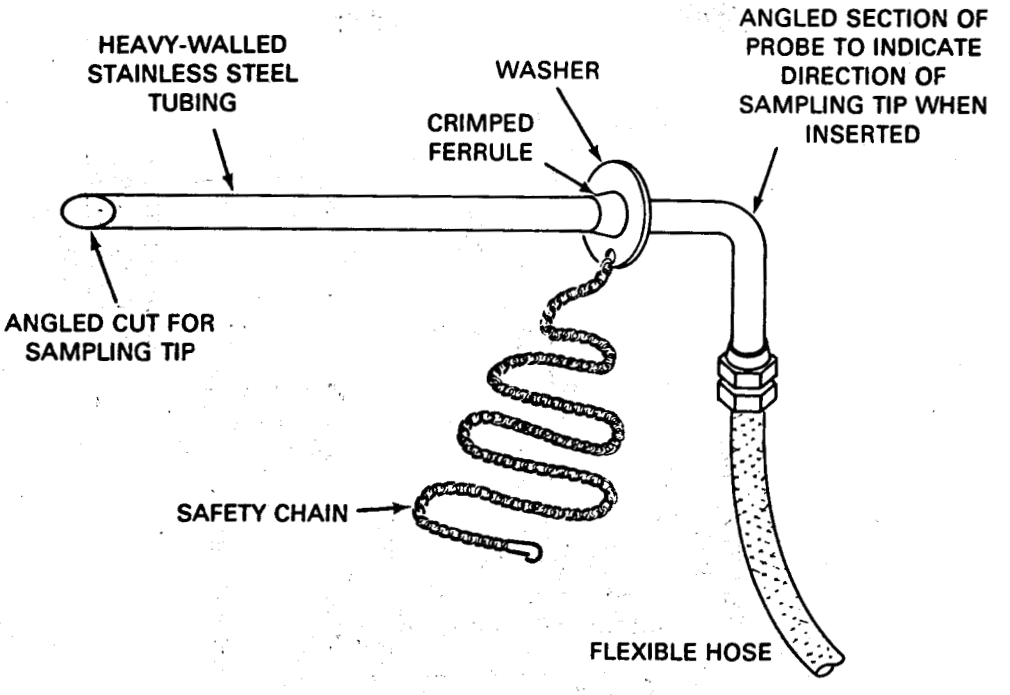

FIGURE 3.2. Probe for PNL Sampling Procedure (Kindle and Woodruff 1981)

Most sample components can be stabilized in the field for analysis in the laboratory:

- CO_2 is determined from a sample stabilized with NaOH.(a)
- H_2S is determined from a sample containing zinc acetate.
- Cations and NH_3 are stabilized by acidification.
- SiO_2 is diluted ten-fold to preserve it in solution.
- Hg samples are collected in glass bottles containing an acid-oxidizer mixture.
- The pH is measured in the field.

For laboratory analyses, a combination of standard techniques and commercially available instruments (as shown in Figure 3.4) produces satisfactory results. Specifically, these methods are:

(a) To estimate calcite scale problems, some prefer to determine CO_2 using a separator to unambigiously differentiate CO_2 from HCO_3^-.

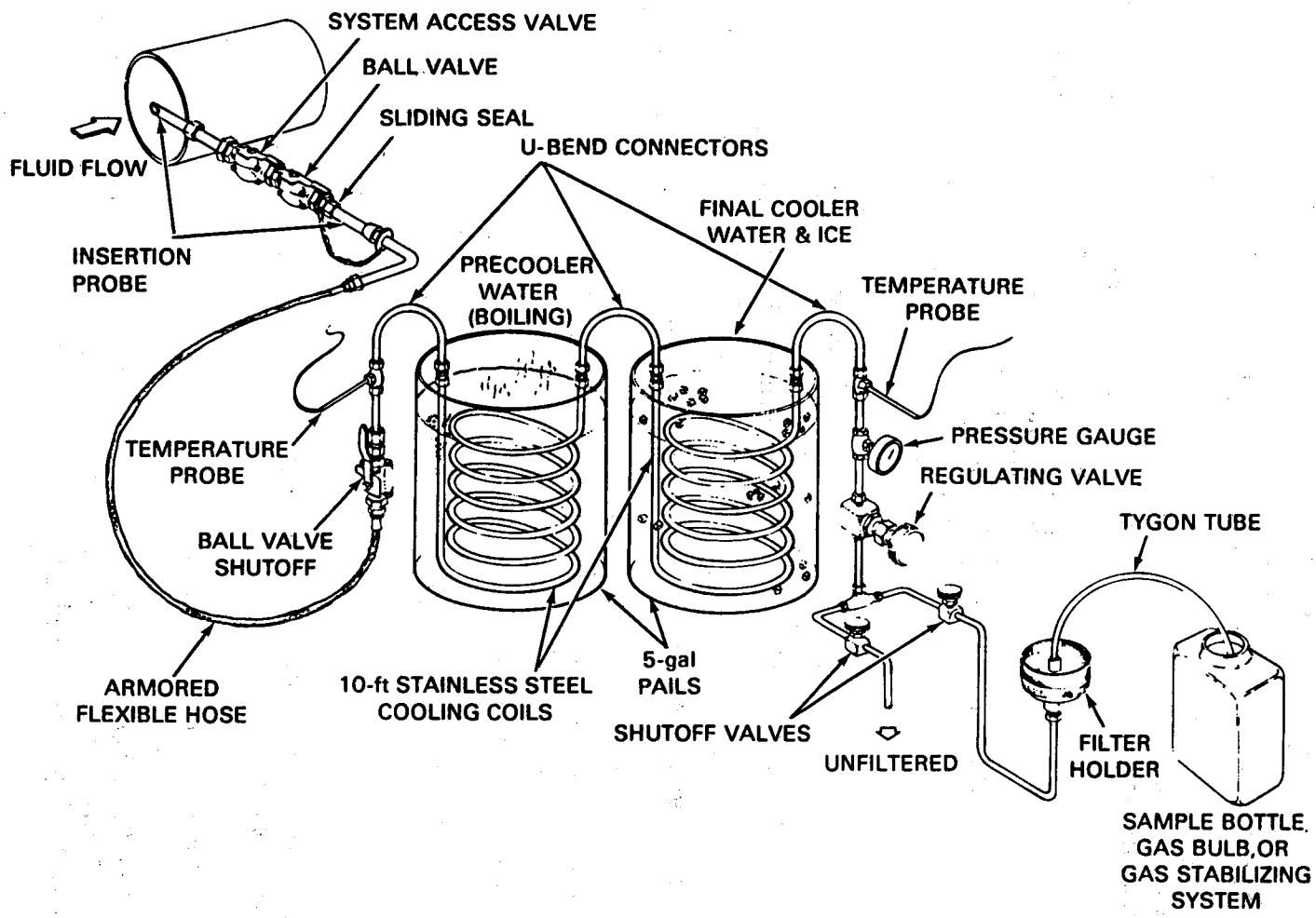

FIGURE 3.3. Geothermal Liquid Sampling Double Coil Assembly (Kindle and Woodruff 1981)

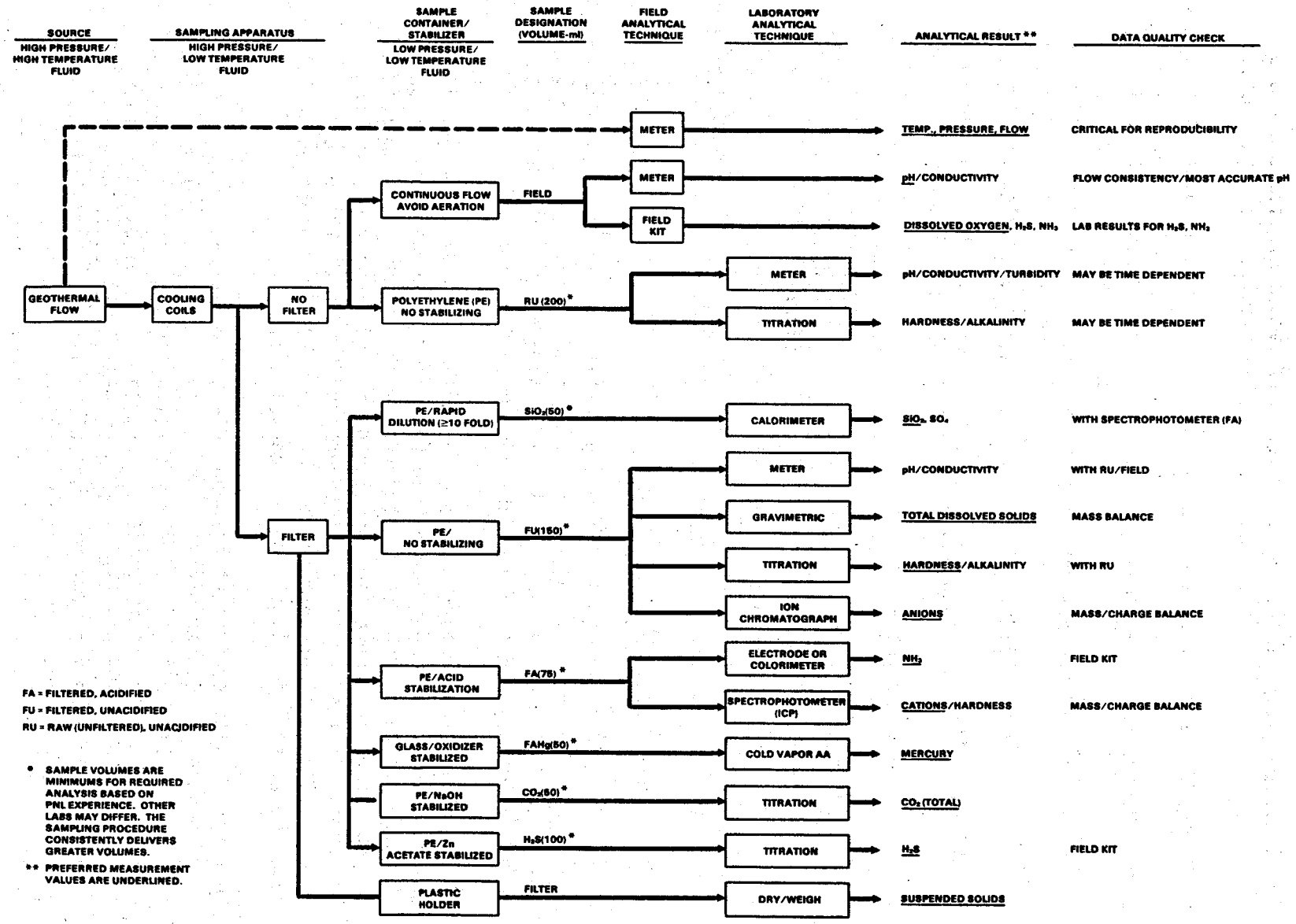

FIGURE 3.4. Flow Chart for Comprehensive Sampling and Analysis of Geothermal Source (Kindle and Woodruff 1981)

- spectroscopy--inductively coupled plasma (ICP) and atomic absorption (AA) - for cations
- colorimetry - for silica and ammonia
- ion chromatography - for anions
- selective ion electrode - for ammonia and pH
- titrations - for sulfide, alkalinity, hardness, CO_2, chloride
- gravimetry - for suspended and dissolved solids
- turbidimetry - for sulfate.

A data quality check is used to insure that the analytical results are consistent: a charge balance (anion-to-cation ratio) is calculated.

A collection of geothermal characterization techniques is available from the Environmental Protection Agency (Kindle et al. 1984). Liquid, gaseous, and environmental sampling techniques are included.

3.2.2 Inexpensive Site-Specific Testing

Brine treatment prior to injection may require a large capital investment and/or a significant risk of injection malfunction and plant shutdown. However, there are a few simple and inexpensive tests that can be run on the brine to give a preliminary indication of suitability. For example:

- test for direct injection - Sample the brine for silica content as described. Be sure to field dilute the sample. Compare the reconstructed silica content (corrected for flash, if any) with amorphous silica saturation curve (see Section 4) and the lowest process temperature. If the sample is not supersaturated under these conditions, silica will neither precipitate nor plug the injection well. Note the effect of salinity on silica solubility.
- test for gravity sedimentation/ponding - Collect a series of brine samples under simulated process conditions (flashing, cooling, etc.). Visually note and time any settling or gel formation; a portable turbidity meter provides quantitative results. At various times (0 to 8 h?) stop silica polymerization by dilution or acid addition. Analyze for remaining soluble silica, particle sizes, and numbers. From this, a curve can be generated showing time to relieve silica supersaturation (relates to holding time) and time to

generate a certain number and size of particulates (relates to evaluating best solids/liquid separation method).

- test for acid treatment - Collect a few samples under simulated process conditions (flashing, cooling, etc.). Using a pH meter calibrated at those conditions and HCl titrate the samples to a pH of 3, recording intermediate pH/acid levels every 0.25 pH unit. This procedure will generate a curve showing how much acid is needed to reach a particular pH. Collect a new series of samples as before and immediately stir in acid additions to reach selected pH levels (pH 4 to 5.5?). Follow the silica polymerization closely for several hours using the soluble silica concentration as an indication of how much acid is needed to arrest silica growth at a particular site. Analytical field kits are available for determining silica. Spectrophotometric methods (AA and ICP) can also analyze microparticulates in addition to dissolved silica unless the sample is filtered first through 0.22- or 0.45-μm filters. Try to perform this test with the last samples maintained at a temperature that is characteristic of a plant disposal system.

3.2.3 Sampling and Analyzing Suspended Solids

Suspended solids data are important because a high particle load in the fluid stream can quickly cause irreversible plugging of the injection well. The minimum suspended solids data that are required are the total suspended solids, which are defined as weight per volume of fluid.(a) It is also useful to know the particle size distribution, quantity of particles in each size range, and composition of the particles. By monitoring these suspended solids data, information can be obtained on what facility operations produce or increase their production and the effectiveness of removal methods. Determining the chemistry of the suspended solids can also provide insight into possible mechanisms of pipe corrosion, scaling phenomena, and production well performance. For these reasons, both the quantity of suspended solids and their chemical nature should be obtained. An example of the difficulty that affects the suspended solids determination in flashing geothermal brines is presented in the appendix.

Sampling for particulates in geothermal systems has unique problems that are partially due to the hostile environment. The high temperatures (~250°C) and pressures (~700 psig) that may be encountered require specialized sampling equipment that can contain these fluids safely. Another major concern in sampling geothermal systems is obtaining a representative sample. A number of factors should be considered in locating the sampling port; for example, the

(a) Usually milligrams per liter (mg/l) or parts per million (ppm).

geometry of the system and whether there is sufficient turbulent flow to carry all particles. A practical technique for withdrawing a sample through an upstream-facing probe inserted into the main flow is described by Shannon et al. (1980) and Kindle and Woodruff (1981).

The chemistry of the geothermal fluids also presents unique problems in sampling. For example, geothermal systems often contain NCG bubbles. These bubbles can cause erroneously high values when using light-scattering or sonic-counting on-line methods. For most sampling methods, the geothermal fluid needs to be cooled and depressurized, which can produce supersaturation in some minerals. These minerals may then precipitate and produce suspended solids values that are too high. It is important to note that the preservability of suspended solids in geothermal brine samples has not been established.

Samples can be obtained in several ways. The total stream can be sampled, or a representative part can be sampled. A sample can be taken at in-line conditions or after it is depressurized and cooled. The smallest sampling error is introduced by sampling the stream at in-line conditions. Unfortunately, the temperatures and pressures encountered reduce the number of total stream sampling techniques to on-line particle size analyzers. Several particulate-counting techniques have been tested: ultrasonic echo measurements, laser beam attenuation, optical-electronic method, mass flow, and x-ray attenuation. However, none of these instruments is currently configured for field use. The laser and optical-electronic techniques require a clean in-line optical window. Overall, in-line counting should lend itself to long-duration hands-off field monitoring when reliable instrumentation is developed. Turbidity measurements are also useful guides to water quality. These measurements are easier and do have an in-line capability but provide only qualitative data on suspended solids. Maintaining optical window clarity is difficult.

The hardware for obtaining a representative sample of brine from a large flowing volume has been successfully tested (Figure 3.5). The sampling system consists of an insertion probe, cooling coils, filter housing, and necessary valves and gauges. A more detailed description of the sampling hardware can be found in Shannon et al. (1980).

The suspended solids sampler or multiple-filter housing (Figure 3.6) sizes particles during sampling and collects sized particles for later chemical analysis. Cellulose filters can be used for cooled and depressurized sampling, and Teflon® filters can be used for sampling at temperatures and pressures of the geothermal system. However, some of the higher temperature geothermal resources may exceed the temperature stability limit for Teflon. For a fluid

® Registered trademark of E. I. du Pont de Nemours and Company, Inc., Wilmington, Delaware.

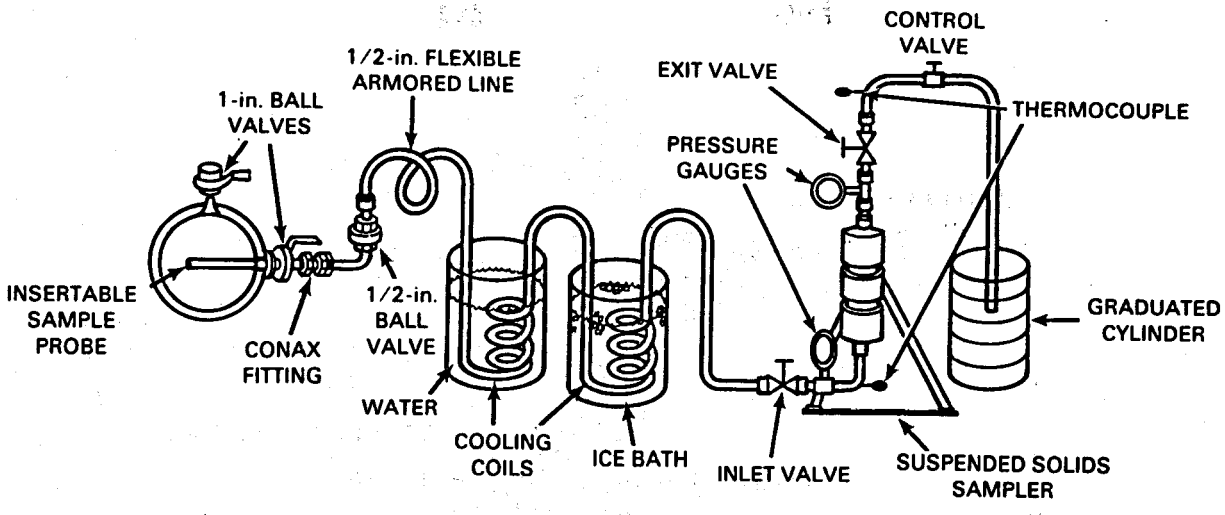

a) Cold Sampling System

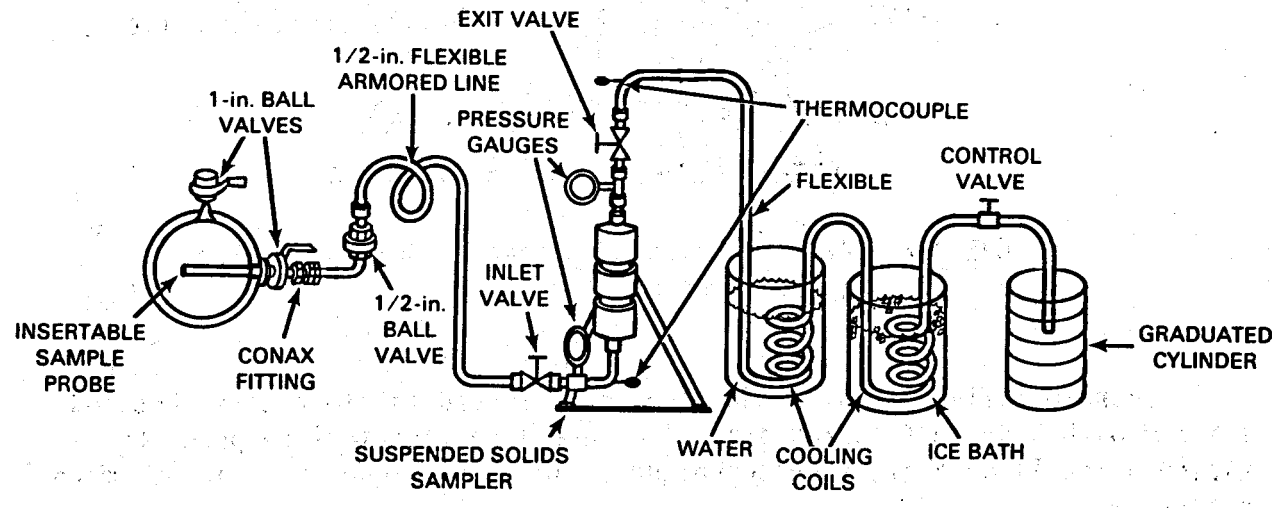

b) Hot Sampling System

FIGURE 3.5. Sampling System for Collecting and Measuring Suspended Solids (Shannon et al. 1980)

containing 2-mg/l particulates, filtering 5 l of brine was sufficient to obtain measurable weight gain on the filter even after correcting for residual salt. For multiple filters, more fluid is generally needed; but care must be taken not to develop filter caking to the extent that the effective filter pore size is reduced. The filter weight gain technique is a quick, inexpensive, and easily performed measurement of suspended solids.

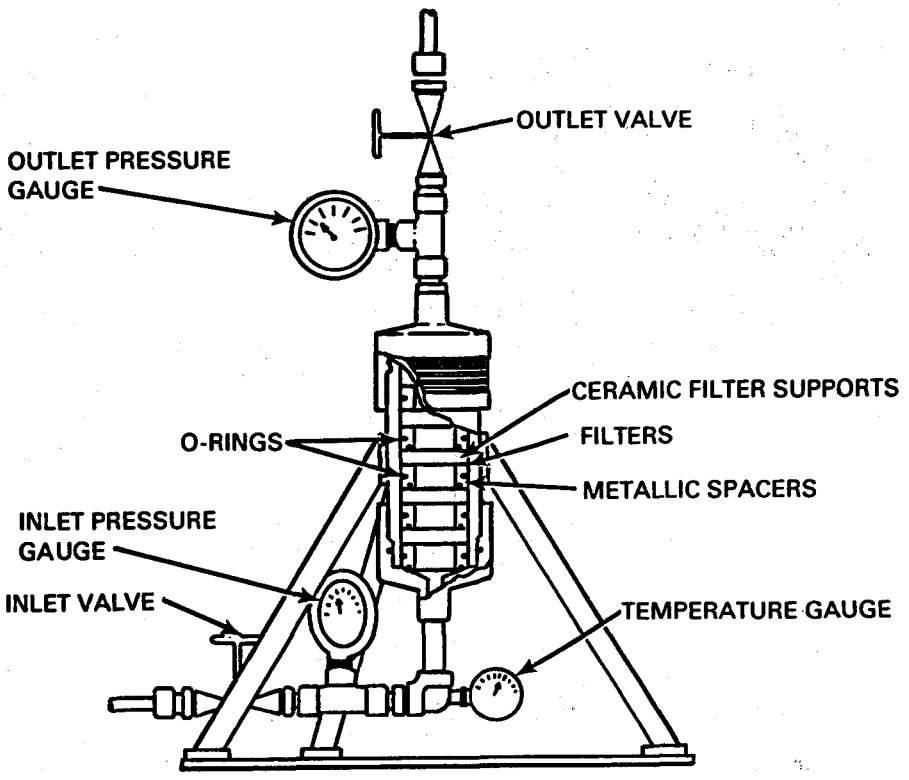

FIGURE 3.6. Cross Section of Suspended Solids Sampler (Shannon et al. 1980)

Geothermal fluid samples can also be collected in clear glass bottles (rinsed with 0.45-μm filtered distilled water) for particulate population sizing using light-scattering techniques. This technique is rapid but more expensive.

Numerous other particle-sizing methods exist: sedimentation, x-ray centrifuge sedimentation, electrical sensing zone methods, and wet sieving. Considering the particulate size range of interest, wet sieving is not appropriate. The other techniques all have the disadvantage that they do not work well for the concentrated fluids expected in geothermal systems. Microscopic sizing of particles collected on a filter is sometimes difficult due to high packing density that makes particle size definition impossible.

Fluid chemistry is important because fluid/fluid or fluid/rock incompatibility can cause serious impairment of an injection well. Injection fluids should be analyzed for TDS content and amount and type of anions and cations. Special attention should be given to characterization of SiO_2, Ba, Ca, Sr, CO_3, SO_4, pH, fluoride, and sulfide content.

Fluid characteristics are very sensitive to pressure, temperature, and flow conditions; and fluids should be sampled and analyzed in such a manner that results are representative of the actual operating conditions in the plant. For example, the compositions measured within wells flowing in artesian flow, pumped flow, or two-phase flow can be different. A detailed fluid sampling plan should be formulated to gather data for the design of an injection treatment facility. Complete fluid characterization should be conducted on:

- geothermal production fluid for each well and their mixtures
- fluid existing at the production plant, if available
- any foreign waters that are to be mixed with spent fluid
- the mixture of spent and foreign fluids; it is especially important that these measurements be made at pressure, temperature, and concentrations appropriate to the plant if the water treatment system is to be added to an existing plant.

For more details on a field study in suspended solids sampling, their chemical interpretation, and the effects on injection well productivity, see the appendix and Shannon, Elmore, and Pierce (1981).

3.3 FORMATION CHARACTERIZATION

The disposal of large quantities of spent geothermal fluids by injection into the hot reservoir requires consideration of numerous construction, geological, and hydrological factors. Improper planning or incomplete knowledge of these aspects may result in insufficient injection capacity or even detrimental changes in reservoir thermal characteristics.

3.3.1 Field Measurements

Important data for the design and operation of a injection field can be collected from the exploratory and production holes drilled for field delineation and resource evaluation. The yield capacity of a supply well is related to the capacity of the same well or an equivalent structure to accept fluids in an injection mode. Experience has shown that in single-phase fluid systems, injection capacity is commonly about 80% of production capacity. In geothermal

installations, the differences in fluid characteristics between production and injection are significant both physically (temperature, viscosity, etc.) and chemically (TDS, particulates, etc.) and may be less amenable to this rule-of-thumb approach.

Well testing is discussed in detail by a number of authors; the most comprehensive texts are by Earlougher (1977) and Matthews and Russell (1967). Although these texts are directed at oil field engineering, the principles and techniques are very similar or identical to those applicable to geothermal reservoir analysis. Determining initial well conditions using flow and pressure testing is highly recommended.

The tests that are listed in Table 3.2 generally require little specialized equipment; their cost is low compared with geophysical logging. Because the cost is moderate and several of the tests can be done while the plant is operating, they are ideal for injection well monitoring. The tests should be performed shortly after construction to establish preoperational conditions of the injection wells.

Geophysical logging of the proposed injection well prior to on-line operation is essential. The background data provided by preoperational tests are the basis for ascertaining what damage has occurred during operation and the effect of rehabilitation procedures. The following logs should be run:

- caliper - to record borehole diameter over the entire well profile
- gamma density - to record the porosity of the injection interval
- temperature - to provide a record of ambient thermal distribution
- flowmeter - to delineate zones where water enters or leaves
- natural gamma - to indicate the clay mineral fraction and location of clay-rich zones.

Spontaneous potential and resistivity (SP&R) logs can be used to delineate zones of higher permeability or potential zones for injection. A full set of logs is advisable so that no factor is overlooked.

Predictions of injection performance can be estimated quickly and inexpensively using the method developed by Barkman and Davidson (1972). Briefly, this method entails flowing the disposal fluid through a membrane filter (usually 0.45 μm) under constant driving pressure (between 80 and 100 psig recommended) while recording the cumulative volume of the filtrate at set times. The result is a K_c value, which is then compared with the known formation permeability (K_f) (Figure 3.7) to estimate the potential type of well

TABLE 3.2. Well Monitoring Tests

Test	Equipment	Data	Done Under Normal Plant Operations
Downhole pressure profile	Downhole pressure gauges with a surface recorder.	Changes in pressure at different horizons related to changes in the aquifer.	Yes
Transient pressure test	High-precision pressure gauge at wellhead.	Pressure variations with time after flow rate of well is changed reflect permeability of reservoir rock around well and the number of aquifers.	Yes
Interference test	Pressure changes recorded in observation well (the closed well) with time; downhole quartz crystal pressure gauges capable of resolving pressures to within 0.01 psi.	Directional reservoir flow patterns, porosity, anisotropic directional reservoir permeability obtained from data. An alternate test is "pulse testing" where rapid pressure changes occur at one well and are recorded at another.	No
Drill stem test (DST)	Most DST tools include several pressure gauges, packets, and flow valves. Tool is attached to drill stem and lowered to the test depth. A surface recorder is also needed.	A DST yields a sample of the type of reservoir fluid present at each test depth, an indication of flow rates, a measure of static and flowing bottomhole pressures, and a short-term pressure transient test.	No
Falloff test	Surface pressure gauges and recording instruments.	Injection or flow is constant until the well is shut. Pressure data are taken immediately before and during the shut-in period. The pressure falloff behavior can be analyzed to determine reservoir permeability and skin factor.	No

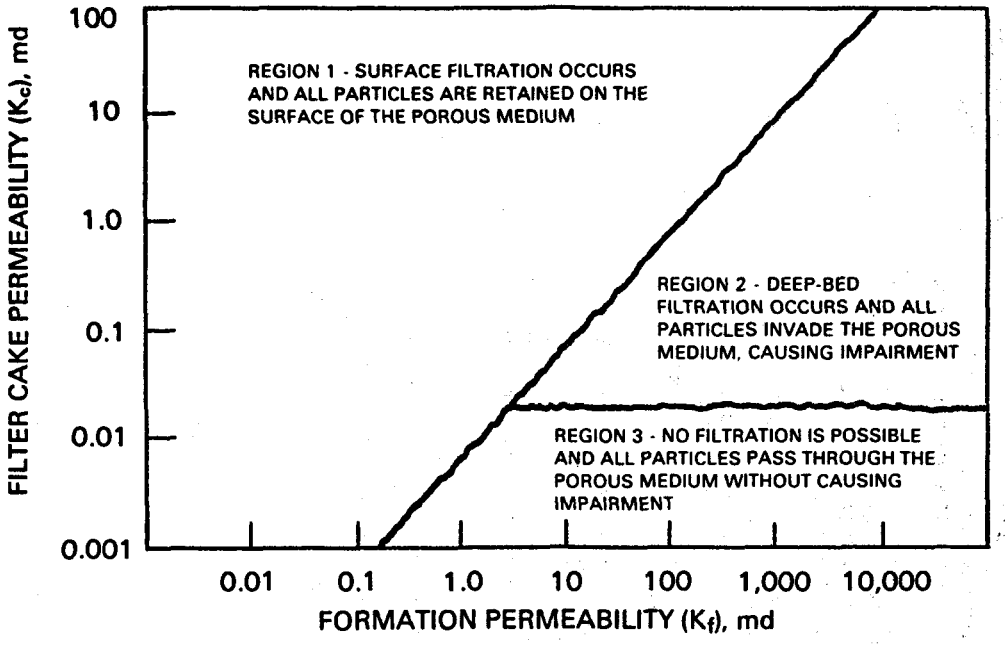

FIGURE 3.7. Relationship Between Filter Cake and Formation Permeabilities in Flow or Particle-Laden Fluid Through Porous Media (Jorda 1978)

impairment. The K_c value obtained from the membrane test can also be used to estimate the half-life of the injection well, assuming that wellbore narrowing occurs. An example is presented in Figure 3.8 (from Jorda 1978) for the case where K_c/K_f is greater than 0.05 and wellbore narrowing is the means of well impairment. The hatched rectangle shows the corridor for well operation where the suspended solids are rigid particles larger than 10 μm and range from 0.0 to 1.0 ppm and K_c is larger than 7.5 md.

It is also important to design the well to assure that it will withstand the stresses that will be applied to it. Thermal interference between injection and production wells should also be avoided. One method of accomplishing this is to assure adequate well separation. Determining what distance is adequate will depend on hydrologic characterization of the reservoir. Numerical modeling of the reservoir using computer codes may provide insight into the spatial problems of well placement. Typically, however, reservoir models do not easily accommodate fractures and may be of only modest value in a poorly understood geothermal reservoir.

Operational procedures that can theoretically minimize the effects of well interference involve multiple injection wells used alternately. The wells are used alternately so that the cool water plume will be reheated by the reservoir

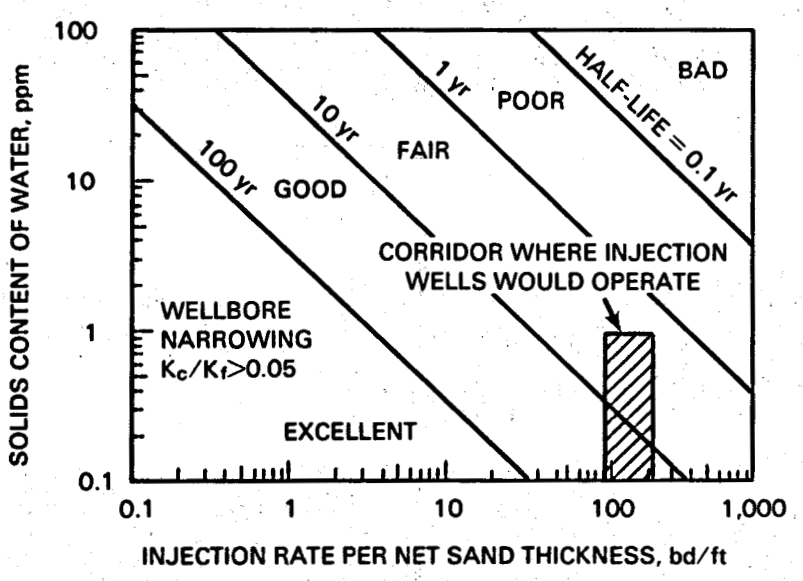

FIGURE 3.8. Calculated Half-Life for the Case of Wellbore Narrowing with High-Permeability Filter Cake (Jorda 1978)

rocks during the unused period. The length of time a well is unused is determined by the reservoir temperature, the amount of water injected, and the proximity of the injection and production wells. Numerical simulation of reservoir response is again recommended. Injection wells lose capacity more rapidly if they are used intermittently; therefore, a balance must be made between minimizing thermal interference and maximizing capacity.

3.3.2 Downhole Sampling (coring)

Two types of sampling methods are commonly used in the drilling industry: conventional coring and sidewall sampling. In conventional coring, an open-centered bit bores through formations. Core samples up to a few inches in diameter and up to 10 to 30 ft long can be collected in competent rock, and continuous coring can produce a sample of the entire thickness of a formation. However, core recovery is usually less successful in friable or unconsolidated zones.

Sidewall sampling is an alternate method of obtaining subsurface samples. A percussion device drives a series of small coring tools into the formation face. These sampling tools are attached to the main tool body via cables and can be retrieved. This method yields smaller samples (1.125 in. diameter by 2.125 in. long) than conventional coring, requires skilled operators, and is limited to a maximum temperature of 300°F. However, it can be very useful, especially for providing samples to ascertain impairment mechanisms and to evaluate the effectiveness of well stimulation techniques.

Conventional core handling and preserving techniques should be used, and core samples should be logged and properly archived by a geologist. Carefully prepared descriptive core logs can be used to estimate the maximum theoretical permeabilities of layers in the injection zone based on the following equation:

$$d = \sqrt{\frac{K}{14.44}} \qquad (3.1)$$

where d = grain diameter in microns; estimated from the core description (i.e., very fine grained sand implies grain sizes from 0.0625 to 0.125 mm)
K = permeability in millidarcys (md).

These permeability estimates can then be used with well and pump design data to estimate maximum well injectivity (see example from Jorda 1980). Theoretical permeability can be compared with laboratory permeability measurements, and corresponding corrections can be applied to injection system design.

3.3.3 Laboratory Measurements

While geophysical logging and surface geophysical measurements have the obvious advantage of providing data on in situ parameters, they often do not provide adequate spatial resolution or the appropriate technique to sufficiently characterize an injection zone for geothermal use. A drill stem test may provide these data, but injection zone data may also be obtained from core samples taken while drilling. The properties of these samples are then studied in laboratory tests. While coring has not been a frequent practice in geothermal injection wells, there is evidence in the literature[a] that core tests can help identify and avoid injection problems. Jorda (1980) presents a detailed discussion of the use of laboratory core tests to characterize injection formations and much of the following discussion is based on his report. In this discussion, only the types of measurements and their primary utility are presented.

Porosity

Porosity is formally defined as the ratio of the pore space volume in a rock to the total volume of the rock; it is usually stated as a percent. However, this definition includes all isolated voids in the rock and does not indicate the transmissive properties of the rock. A more useful concept is that of effective porosity or the porosity of the interconnected pore network

(a) See Gray and Rex (1966); Gruesbeck et al. (1979); Jorda 1978; McCune (1977).

in a rock. Effective porosity can be used to calculate fluid storage capacity of a formation if the thickness and areal extent are known. Effective porosity can be measured by the following techniques:

- comparing saturated sample weight versus dry sample weight; this method requires that the bulk volume of the sample and the density of the fluid be known

- using a Boyle's Law porosimeter to measure gas displacement in a dried sample.

Jorda (1980) presents a detailed discussion on the concept and measurement of porosity for geothermal application.

Permeability

Permeability is defined as the ability of rock to conduct fluid through an interconnected pore network. Permeability in flow regimes encountered in injection in sedimentary formations is thought to follow Darcy's Law, which describes laminar, viscous, and linear flow of fluids through porous media. Darcy's Law for flow through a cylindrical sample is given by:

$$K = \frac{q l \mu}{A P} \qquad (3.2)$$

where K = permeability, darcys
q = flow rate, ml/s
l = sample length, cm
μ = fluid viscosity, centipoise
A = sample cross-sectional area, cm^2
P = pressure drop across sample, atm.

Laboratory permeability measurements predict well performance, simulate well stimulation techniques, and investigate physicochemical processes active in the injection zone (migration of fines, clay swelling, dissolution/precipitation, and other phenomena). While permeability measurements can provide more information on subsurface phenomena than other laboratory measurements, they are more difficult to obtain and the results must be carefully interpreted. For example, laboratory permeability measurements yield data on the matrix permeability of a formation; however, this value should be considered as an order of magnitude number only because permeability variations can be as high as 10:1 in poorly sorted or otherwise heterogeneous formations. Moreover, it is important to have a measure of the permeability of the matrix, especially in sandstone formations.

Since permeability may change with temperature, measurements should be made at temperatures equal to those of the injected fluid. Flow rate is also important for determining impairment mechanisms, and laboratory tests should simulate flow rates at the wellbore rock face. Permeability may also vary with confining pressure; therefore, laboratory tests should simulate the downhole pressure.

Pore Size Distribution

The pore size distribution of a rock defines the percentage of porosity as a function of pore size. Pore size distribution is generally presented as a semilog plot of cumulative size percent versus pore size (μm). Pore size distribution can be used in conjunction with particle size distribution in the injected fluid to predict if 1) all particles will bridge on the well face, 2) invasion of all particles will take place, or 3) both types of particle distribution will take place (Brownell et al. 1947).

It is generally acknowledged that the ratio of pore size to particle size necessary to cause surface filtration lies between 10:1 to 3:1 (often called the bridging ratio). This bridging ratio is based on the guidelines presented by Thormeer et al. (1977), who conducted laboratory studies using well-sorted and rounded-to-subrounded sand grains and particles:

- If the pore throat diameter is less than three times the particle diameter, the solids bridge on the rock face.
- If the pore throat diameter is more than three times but less than 10 times the particle diameter, shallow invasion of solids will take place and a damaging internal filter cake will form.
- If the pore throat diameter is more than 10 times the particle diameter, deep invasion of solids will take place and a nondamaging condition will exist.

Unfortunately, this range of bridging ratios is not sufficiently narrow to totally optimize injection well design. Few injection systems have the precisely defined sand grains and water-borne particles used in these experiments; and, frequently, the formation characteristics are not accurately known.

Purcell (1949) developed a technique for determining pore size distribution using data derived from a high-pressure mercury porosimeter. Pore size distribution measurements are described by several authors; Jorda (1978) presents a thorough discussion of their use and interpretation.

Grain Size Distribution

Grain size distribution analysis is important for sand control in injection zones in unconsolidated sands or in consolidated sands that have been disturbed. The grain size distribution is used with the particle size distribution in the treated injection fluid to design the gravel pack for completion of the injection well. Median gravel size must be about 4 to 6 times as large as the median grain size of the formation to achieve effective sand control (Jorda 1980).

Grain size distribution can be used to estimate potential injection well impairment. By comparing the diameter range of the particles in the fluid with the diameter range of the formation particles, the potential for and the causes of well impairment can be estimated by comparing the diameter ranges shown in Figure 3.9. Grain size can be determined using conventional sieving apparatus and analysis techniques. Detailed discussions of analysis and application of grain size data from core, sidewall, and bailer samples are presented by Jorda (1978).

The median grain size of a formation can also be estimated directly from formation permeability measurements using Equation (3.1) or from a combination of permeability and porosity data using the expression:

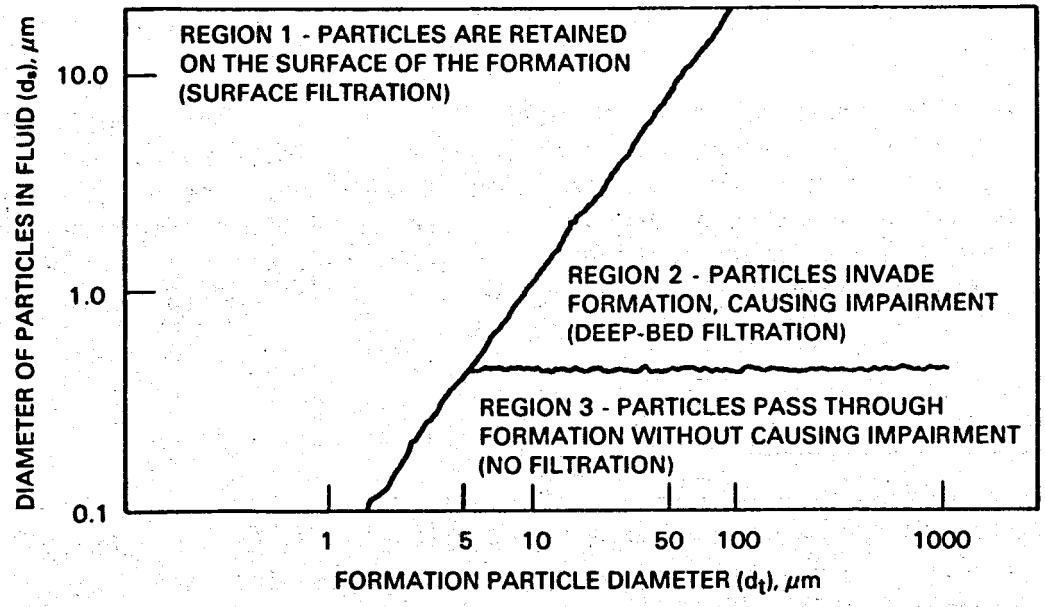

FIGURE 3.9. Particle Distribution in Systems Where Particles in Fluid and Reservoir Particles Are Spheroids (Jorda 1978)

$$d_\mu = \sqrt{\frac{K_f\ (1 - \phi)^2}{\phi^3}} \qquad (3.3)$$

where d = mean grain size, μm
K_f = formation permeability, md
ϕ = formation porosity, %.

Equation (3.1) is actually derived from Equation (3.3) by assuming that the formation is composed of closely packed spheres. An example of estimating suspended solids impairment using both laboratory and field data is provided in Table 3.3. In this example, formation permeability and porosity are input into Equations (3.1) and (3.3) to predict mean grain size, which is then used with Figure 3.9 to predict the type of injection impairment expected from particles of different sizes.

Examples of porosity and permeability ranges encountered in geothermal injection systems are listed in Table 3.3. For each well, the mean grain diameters of the formations were calculated from the porosity/permeability data using both Equation (3.1), which relates the square of the grain diameter to the formation permeability over a constant, and Equation (3.3), which describes grain diameter in terms of the permeability and porosity of the formation. The two mean grain diameters calculated by the equations for a given formation differ by more than an order of magnitude, which results in quite a significant difference in estimating the mechanism of well impairment for various diameters of injected particles. The predictions obtained from Equation (3.3) appear to be more reasonable.

This exercise demonstrates how to use the information contained in this section to estimate the diameter range of injected particles that could cause trouble. The need for careful interpretation is apparent. The differences highlight the advantage of using actual data as a guide in arriving at the design parameters for a water treatment process prior to injection. These data could be obtained from prior injection experience at the same formation or by running the tests described earlier on core samples.

3.4 INJECTION WELLS AND PIPELINES

If the brine treatment relies on maintaining the temperature to avoid solids/scale formation until the spent brine is injected into the reservoir, it will be necessary to allow for cooling in the injection pipelines. Based on New Zealand experience (Henley 1983), the cooling in injection pipelines follows the relationship:

TABLE 3.3. Comparison of Calculated Formation Mean Grain Sizes

Geothermal Reservoir	Field Data: Typical Porosity, %	Field Data: Permeability (K_ϕ), md	Laboratory Data: Porosity, %	Laboratory Data: Permeability (k_c), md	Laboratory Data: Type of Rock	Equation (3.1): Mean Grain Size, μm $d = \sqrt{K/14.44}$	Equation (3.1): Estimated Impairment Particle Size/Location[b]	Equation (3.3): Mean Grain Size, μm $d_\mu = \sqrt{K_\phi(md)\,(1-\phi)^2/\phi^3}$	Equation (3.3): Estimated Impairment Particle Size/Location[b]
Westmorland, California									
Dearborn 2[c]	0.25	40.16	--	--	Unconsolidated sand, silt, and clay.	1.7	>0.1 μm/surface	38.0	>3 μm/surface 3 to 0.45 μm/deep bed <0.45 μm/none
Landers 3[c]	0.2657	45.57	31.34	201.85 (air)	Unconsolidated sand, silt, and clay.	1.8	>0.1 μm/surface	36.2	
Raft River, Idaho[d]									
RRGI-7[c]	0.17 to 0.30	25 to 165	--	--	Fractured metamorphic above quartzite.	1.3 to 3.4	>0.23 μm/surface <0.23 μm/deep bed	59.2; 54.7	>8.0 μm/surface 8 to 0.45 μm/surface <0.45 μm/none
East Mesa, California									
Magma 46-7[e]	0.28	800	--	--	Sands, shales, silts, and clays.	7.4	>0.85 μm/surface 0.85 to 0.45 μm/deep bed <0.45 μm/none	137.4	>0.45 μm deep bed <0.45 μm/none
Mesa 5-1[c]	0.27	6	--	--	Sand and silt stone.	0.64	>0.1 μm/surface	12.7	>1.2 μm/surface 1.2 to 0.45 μm/deep bed <0.45 μm/none

(a) Conclusions vary depending on which equation is used; Equation (3.3) results in more reasonable calculations.
(b) Type of particulate plugging determined by Figure 3.9.
(c) See Republic Geothermal 1979.
(d) See Kunze 1978.
(e) See Jorda 1980.

$$\Delta T\left(\frac{^{0}C}{1000\ ft}\right) = \frac{15.24}{D} \qquad (3.4)$$

where D is the pipeline diameter, in. This is equivalent to a 1.3°C (2.3°F) drop per 1000 ft for a 12-in. diameter pipe. Precise estimates would include site-specific temperatures, insulation thicknesses, and flow velocities.

Optimum construction requirements for injection wells may differ significantly from requirements for production wells, although common practice is to turn an unsuccessful production well into an injection well. Wells that allow for continuous injection simplify construction requirements, which must account for cyclical thermal stressing and the accompanying mechanical stressing of casing strings due to expansion and contraction. A gravel pack surrounding the slotted injection casing reduces flow velocities at the well formation interface to levels where laminar flow is assured. Gravel pack components should be carefully sized in conjunction with particle size analysis of both the formation and the suspended solids retained in the injection fluid (Jorda 1980). Well impairment caused by drilling mud is well known in the oil industry and has been investigated by several authors.(a) These researchers generally agree that invasion of the formation by mud particles can cause permeability impairment. Abrams (1977) summarized the results of several studies on this subject:

- Invasion and formation damage can occur with all drilling muds.
- Impairment usually occurs in the first 1 to 2 in.; however, invasion and damage could exist as deep as 1 ft.
- Damage is most likely to occur in higher permeability formations.
- Where invasion occurs, backflushing does not remove the impairment.

Experimental results indicate that it is possible to minimize this impairment by designing the mud to include properly sized bridging material (Abrams 1977). The bridging material must be selected so that the median particle size is equal to or slightly greater than one-third the size of the median pore size of the formation and the mud mix must contain 5 vol% bridging size solids. A detergent solution or plain water is being used in place of mud in some geothermal drilling to avoid the possibility of formation permeability damage.

Numerous chemical solutions are often added to the geothermal fluid: kill fluids, grease for seals, scale and corrosion inhibitors, and other treatment fluids such as coagulants. Each of these additives could potentially reduce

(a) See Barna and Patton (1972); Glenn and Slusser (1957); Kennedy (1971); Krueger and Vogel (1954).

well injectability by introducing suspended solids or by adverse chemical alteration of the injecting fluid. The addition of these solutions should be monitored along with well injectability. An example of a scale inhibitor that reduced injectability at high concentrations is presented by Harrar (1981).

Injection well construction/operation is a separate subject from injection treatment and is only mentioned to identify its relationship to the parameters discussed here. A discussion of geothermal well completion is available (Nicholson 1984).

3.5 SUMMARY OF DESIGN REQUIREMENTS

Injection wells generally become impaired because available flow channels are reduced, which results in decreased injection flow or increased injection pressure or both. The impairment can occur in the wellbore or in the receiving formations. Flow channel reduction is usually caused by particulates. Their source can be suspended solids in the injected fluid, particles formed by fluid or fluid/fluid insolubilities, or mobilized fines in the receiving formation. Clay swelling can potentially reduce flow channels at some sites. All of these are caused by injecting incompatible fluid.

Table 3.4 summarizes the tests mentioned in this section to determine if well impairment is likely to occur. Other tests that delineate the character of the injection system are also presented. It would require a substantial budget to perform each of the listed tests; but appropriate tests can be selected by interpreting site data. The amount of geophysical logging, flow testing, and chemical analysis is subjective. For example, if the clay content of the receiving formation is low, tests on clay swelling would be omitted.

Besides the total quantity of suspended solids and their size range, the nature of the suspended solids needs to be considered. Gelatinous, soft suspended solids (such as amorphous silica) typically cause a quicker decline in well injectivity than rigid particles. Removing these soft particles will maximize injection well performance.

A few generalizations can be made for establishing the design requirements for an injection treatment system at a geothermal facility. An injection fluid with a suspended solid content below 5 ppm is generally considered to be suitable, but the particle size distribution is as important as the total concentration of suspended solids. Particles with diameters less than 0.45 μm generally pass through the formation without causing impairment; particles with diameters between 0.45 μm and 10 μm can invade the formation and cause the least recoverable form of impairment; and particles with diameters greater than 10 μm cause impairment, generally by remaining in the wellbore or by being retained at the surface of the formations. These ranges are simplified, and the relationship

TABLE 3.4. Tests to Characterize the Injection System and Estimate Impairment

A. Establish chemistry and gas content of injected fluid

B. Suspended solids analysis, quantity, size range, and chemistry
   1. Membrane filter tests
   2. Light-scattering techniques

C. General area geology including faults and fracture systems, hydrology, geophysical data, and history of earthquake activity

D. Core analysis for injection horizon
   1. Petrology (clay content)
   2. Connate water chemistry (from each main aquifer)
   3. Directional permeabilities
   4. Porosity and nature of pore spaces

E. Geophysical logs
   1. Caliper
   2. Gamma density
   3. Temperature
   4. Natural gamma
   5. Spontaneous potential
   6. Resistivity

F. Pressure/flow tests
   1. Downhole pressure profile of well
   2. Transient pressure testing
   3. Interference tests
   4. Drill stem tests
   5. Falloff tests
   6. Production or injection tests

G. Predicting injection system performance
   1. Core flooding
   2. Membrane plugging
   3. Filter cake permeability versus formation permeability (Figure 3.7)
   4. Calculated half-life (Figure 3.8)
   5. Pore-to-particle size ratios
   6. Suspended particulates (Figure 3.8)

between impairment and particle size distribution should be established individually for each injection system and receiving formation. Some of the alternate treatment methods for allowing precipitation to occur in a controlled manner (see Section 4) can result in the formation of particulates with diameters $\leq$10 μm. Obviously the process needs to be designed and operated to remove these particulates.

4.0 PROCESS CHEMISTRY

Successful underground injection of geothermal waters generally requires a stable solution that is essentially free of suspended matter to avoid plugging the geological strata. Two approaches can achieve these conditions: 1) precipitate or crystallize supersaturated constituents and remove them from the brine or 2) prevent precipitation/deposition of solids by avoiding supersaturation or by adding chemicals that prevent scale formation. The process designs using the precipitation approach must include methods for accumulation and disposal of sludges produced by treatment processes.

Electric power production from geothermal brines typically involves large temperature reductions and, in the case of flash processes, the loss of steam and NCG such as CO_2 and H_2S from the brines. As a result of these physical and chemical changes, the brine may become unstable and one or more of its dissolved constituents may precipitate or build up scale on surfaces inside pipes, tanks, and other equipment. Precipitates or solid deposits may also form in the injection well and geological strata receiving the brine, rendering the system inoperable or substantially reducing the flow. This section includes a description of the chemical processes involved in spent brine treatment. The process equipment that may be used and field applications of the equipment are discussed in Section 5.

To understand the rationale for designing a treatment system prior to injection, it is necessary to understand the involved chemistry of the brine and the changes that it undergoes during the plant cycle. The chemistries involved with the following major scaling species in a geothermal environment are discussed in this section:

- silica - precipitation can occur when the fluid is cooled below the amorphous silica saturation level, which is a function of temperature and salinity
- calcite (carbonate) - precipitation can occur at high temperatures when CO_2 flashing/breakout occurs and at low temperatures when the temperature increases (due to the retrograde solubility of $CaCO_3$)
- sulfide - metal sulfide scales form in geothermal flows through poorly understood mechanisms that may be a combination of incompatible water mixing, temperature decreases, or pH changes due to CO_2 breakout

- other (sulfate) - calcium, barium, and strontium sulfates can precipitate due to temperature changes or the mixing of incompatible waters.

The effect of some process parameters on the potential scale species is summarized in Table 4.1.

4.1 SILICA PRECIPITATION

The current experience with geothermal injection indicates that silica fouling is the most widespread concern. To avoid this fouling by polymerized/precipitated silica, a process must be designed to: 1) eliminate the thermodynamic driving force toward precipitation or 2) affect the kinetics to have precipitation occur where it can be handled readily or delayed until the brine has been injected into the reservoir (and possibly reheated). Because of the dominant importance of silica control and the high cost of achieving this control, the two subjects of thermodynamics and kinetics are described in some detail.

TABLE 4.1. Effect of Process Parameters on Potential Scale Formation

Process Parameter	Equilbrium Effect on Potential Scale Species(a)			
	SiO_2	$CaCO_3$	Sulfides	Sulfates
Temperature decrease (as in plant cycle)	●	o	●	o Ca ● Ba
Temperature increase (injection into warm formation)	o	●	o	● Ca o Ba
Increased pH (as CO_2 is flashed)	o pH >9	●	●	●
Decreased pH (acid addition)	o	o	o	o
Increased salt concentration (flashing; mixing)	●	o	o	o

(a) ● aggravates problem
o alleviates problem.

4.1.1 Silica Precipitation Thermodynamics

The concentration of silica (SiO_2) in geothermal waters in reservoirs is usually controlled by the dissolution of quartz from the geological strata of the reservoirs. The deposition of silica as a scale, however, is controlled by its polymerization and precipitation as amorphous silica, which is more soluble than quartz. The solubilities of quartz and amorphous silica as a function of temperature are illustrated in Figure 4.1. If the geothermal water in the reservoir is in equilibrium with quartz at 300°C, for example, the water will become supersaturated with amorphous silica when brought to the surface and cooled to 100°C by an energy recovery process. Precipitation of silica may occur immediately or some time after cooling depending on the pH and supersaturation ratio, but the precipitate that forms will be amorphous silica rather than quartz.

Although quartz is thermodynamically more stable than amorphous silica, extreme conditions of temperature, pressure, and/or alkalinity are required for the growth of quartz at measurable rates in aqueous solutions (Weres, Yee, and Tsao 1980). In the example given above, 630 mg of SiO_2 will be dissolved at equilibrium for quartz at 300°C in pure water (see Figure 4.1). When this

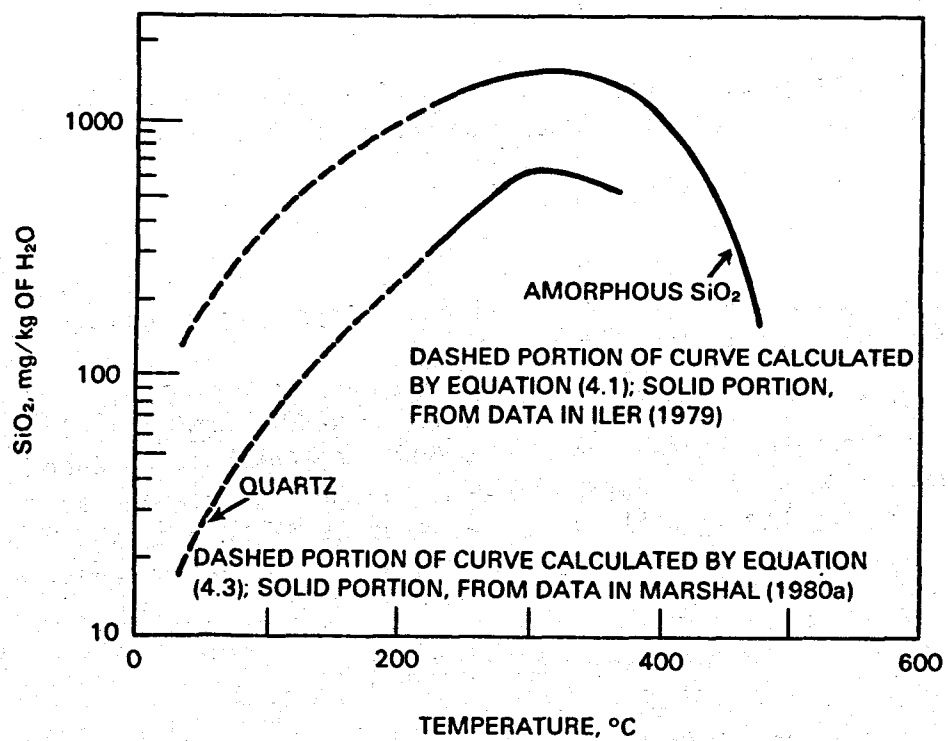

FIGURE 4.1. Solubility of Quartz and Amorphous Silica in Pure Water as a Function of Temperature

water is cooled to 100°C, it will be supersaturated at a ratio of 630 to 400 mg/l (1.58) with respect to amorphous silica. The greater solubility of amorphous silica relative to quartz is a distinct advantage for geothermal power plants because it limits the precipitation of silica from spent brines. The solubility curves of amorphous silica and quartz both increase with temperature to ~300°C and then decrease due to the decreasing density and solvent power of water. The decrease becomes rapid as the critical point of water (374°C) is exceeded.

Dissolved salts and pH also affect the solubility of silica in aqueous solutions.[a] The effect of NaCl molality and temperature on amorphous silica and quartz solubility is shown in Figure 4.2.

(a) The solubility of amorphous silica in pure water previously shown in Figure 4.1 (dashed portion of curve) and Figure 4.2 (0 molality of NaCl) was calculated by the empirical equation of Marshal (1980a):

$$\text{Log } s^o = -0.1185 - \left(1.1260 \times \frac{10^3}{T}\right) + \left(2.33 \times \frac{10^5}{T^2}\right) - \left(3.6784 \times \frac{10^7}{T^3}\right) \quad (4.1)$$

where s^o = molal solubility of amorphous silica in pure water
T = temperature in Kelvin.

The solubility of amorphous silica in NaCl solutions was calculated for Figure 4.2 from the classic Setchenow equation (Setchenow 1892):

$$\text{Log } (s^o/s) = Dm \quad (4.2)$$

where s = molal solubility of amorphous silica in the salt solution
D = a parameter that varies with salt type and temperature
m = molality of the added salt.

Values for D have been determined for NaCl, $NaNO_3$, $NaSO_4$, $MgCl_2$, and $MgSO_4$ solutions for temperatures from 25 to 300°C by Marshal and Chen (1982) using experimental data (Marshal 1980a; Marshal 1980b; Chen and Marshal 1982). The solubility of quartz up to 220°C was calculated for Figure 4.1 (dashed portion of curve) using the following equation (Weres, Yee, and Tsao 1980):

$$\text{Log } c_o = -\frac{1160}{T} + 1.93 \quad (4.3)$$

where c_o is the equilibrium solubility of quartz in g/kg of water. Data for the solubility of quartz in NaCl solutions shown in Figure 4.2 were taken from data reported by Weres, Yee, and Tsao (1980).

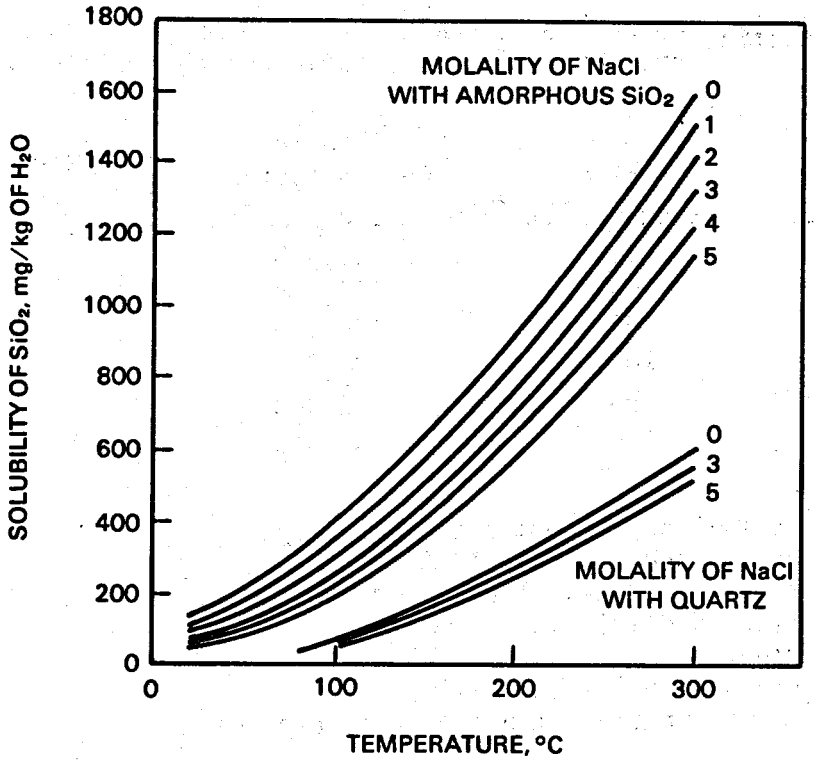

FIGURE 4.2. Effect of NaCl Molality on Solubility of Amorphous Silica and Quartz as a Function of Temperature (1 m NaCl = 58,400 ppm)

The curves in Figure 4.2 show decreasing solubility for both amorphous silica and quartz with increasing NaCl molality, but the effect is more pronounced with amorphous silica. The saturation ratios for amorphous silica resulting from cooling brines in equilibrium with quartz at 300°C down to 100°C increase with increasing NaCl molality. The value of 1.58 previously given for pure water solutions increases to 2.66 for 5 m NaCl. The higher supersaturation ratios for amorphous silica in cooled brines increase the kinetic driving force for precipitation of amorphous silica.

Estimates for saturation values of amorphous silica were computed for several cooled geothermal brines using Equation (4.2) and D values for NaCl reported by Marshal and Chen (1982) using the assumption that all of the chloride in the geothermal brine was NaCl. Comparing these calculated values to actual geothermal field data (Table 4.2) shows good agreement, especially when the kinetic factors that influence field solubilities are considered. These factors confirm the validity of calculating the amorphous silica solubility in this manner.

The temperatures at which amorphous silica saturation is reached upon cooling without water loss by flashing (for example, binary power plant) are

TABLE 4.2. Comparison of Calculated and Analyzed Values for Amorphous Silica in Cooled Geothermal Brines

Brine Source	Brine Temperature, °C	Chloride Concentration, ppm	Analyzed SiO_2, ppm	Calculated Solubility of SiO_2, ppm
GLEF No. 1[a]	90	112,000	183	166
GLEF No. 2[a]	90	145,400	144	124
GLEF No. 3[b]	100	134,500	192	156
GLEF No. 4[c]	105	125,000	185	181
Cerro Prieto[d,e]	95	12,940	370	369
Ahuachapan[f]	150	9,340	570[g]	632

(a) GLEF - Geothermal Loop Experimental Facility.
(b) See San Diego Gas and Electric 1980.
(c) See Featherstone and Powell 1981.
(d) See Weres, Tsao, and Iglesias 1980.
(e) Simulated brine.
(f) Einarsson, Vides, and Cuellar 1975.
(g) Assumes 18% concentration of brine from reservoir.

given in Table 4.3 for the geothermal waters listed in Table 2.1. Silica concentrations are low enough at East Mesa that saturation would not be reached by cooling this brine to below 100°C. Maintaining process temperatures above the saturation limit is the principle of the silica-free operation of the East Mesa Binary Plant (Magma Power Co.). Figure 4.3 illustrates how process conditions in a flash plant can change the saturation temperature for dissolved amorphous silica.

Attempts to use Equation (4.2) adapted for mixed electrolytes (Marshal and Chen 1982) and substituting D values for $MgCl_2$ in place of $CaCl_2$, which is high in Salton Sea geothermal brines, gave even lower amorphous silica estimates for GLEF brines. The D values for $MgCl_2$ and $CaCl_2$ did, however, compare favorably at 25°C (Marshal and Warakomski 1980); but additional work is needed to develop $CaCl_2$ (and KCl) data at higher temperatures to verify the usefulness of the mixed electrolyte equation. Values for D with NaCl at temperatures from of 25 to 300°C are given in Figure 4.4.

The solubility of silica is substantially independent of pH until the pH increases into the alkaline range. An expression for the relationship between pH and the solubility of monomeric silica is given by the following equation (Wahl 1977):

TABLE 4.3. Temperatures for Amorphous Silica Saturation for Geothermal Waters

Reservoir[a]	Molality	Silica Concentration[b]	Temperature, °C
Salton Sea	3.6	560	183
Cerro Prieto	0.30	733	167
East Mesa	0.01	270	63
Heber	0.23	270	70
Ahuachapan	0.23	500	123
Roosevelt Hot Springs	0.14	782	174
Beowawe	0.001	329	83

(a) From Table 2.1.
(b) Calculated from ppm of SiO_2 by correcting for TDS.

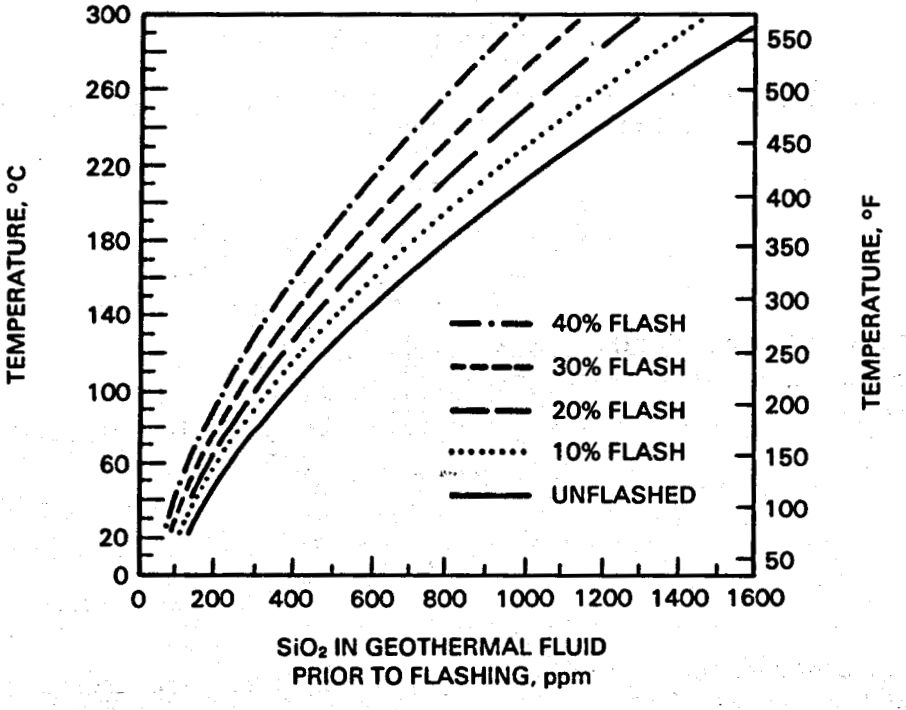

FIGURE 4.3. Process Flash Effect on Saturation Temperature for Amorphous Silica (Barnes and Rimstidt 1976). Conditions: pH < 8; precise work would include site-specific total salt concentrations.

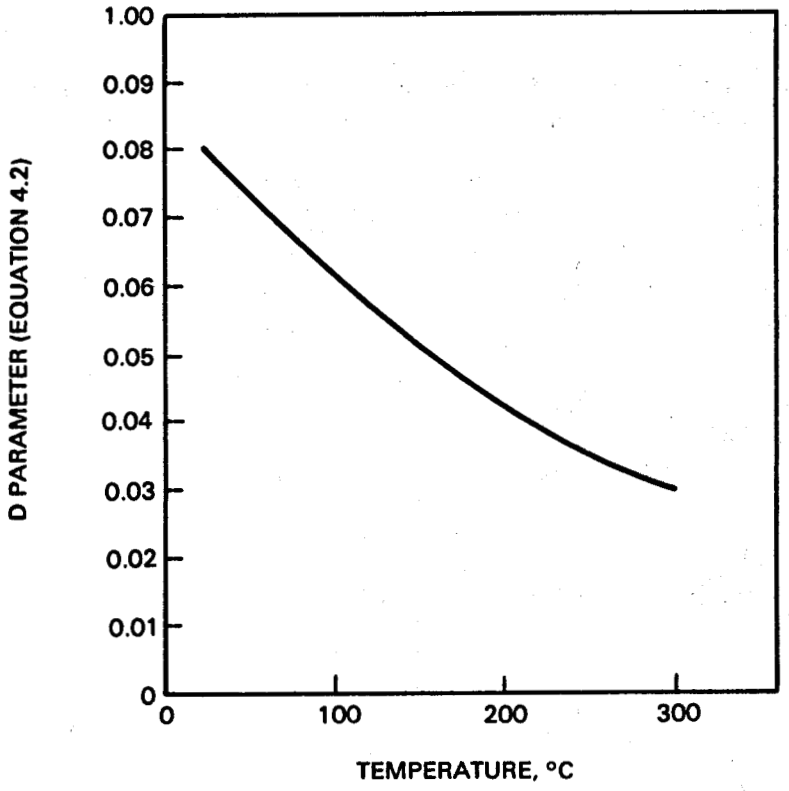

FIGURE 4.4. D Parameter (NaCl) as a Function of Temperature (Marshal and Chen 1982)

$$\log \frac{w_s - w_m}{w_m} = pH + \log K_1 \qquad (4.4)$$

where w_s = total solubility of monomeric silica
w_m = weight percent of molecular silicic acid
K_1 = first ionization constant for molecular silicic acid or

$$H_4SiO_4 = H_3SiO_4^- + H^+ \qquad (4.5)$$

$$K_1 = 10^{-9.7} \text{ at } 25^0C$$

The ionization constant can be calculated at higher temperatures using the following equation (Wahl 1977):

$$\ln K_1 = -16.76 - \frac{1661}{T} \qquad (4.6)$$

where T = temperature, K
ln = 2.303 log.

Solubility curves for amorphous monomeric silica (Figure 4.5) at 25°C and 100°C were calculated from Equation (4.4) using w_m values of 0.012 and 0.0402 wt% (120 and 402 ppm) and log K_1 values of -9.70 and -9.21 at 25°C and 100°C, respectively. The solubility curve at 25°C agrees reasonably well with experimental data except that the latter increases somewhat below pH 5.

The effect of pH on the equilibrium solubility of monomeric silica is of little practical significance under typical brine conditions when the pH is below 8. However, as discussed below, the kinetics of silica deposition slows dramatically as the pH is lowered into the acid range.

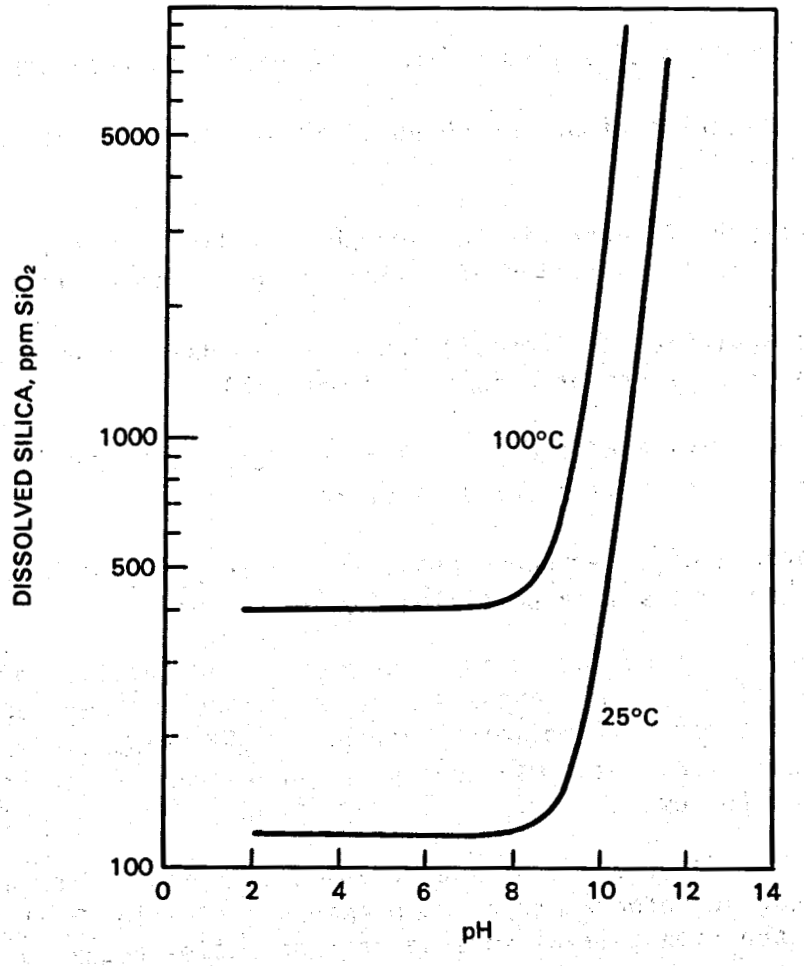

FIGURE 4.5. Silica Solubility as a Function of pH. Calculated from Equation (4.4); experimental data at 25°C show a slight increase in acid waters with a solubility minimum near pH 7.

4.1.2 Silica Precipitation Kinetics

In addition to the various factors affecting silica equilibrium solubility, other factors affect the rate at which silica comes out of solution. These kinetics are influenced by the degree of supersaturation, temperature, catalysts (fluoride), and nucleation site availability. Looking at just the temperature factors, the maximum rate of silica precipitation will occur at a temperature 25 to 50°C below the saturation temperature as the brine cools. Another rule of thumb is that once the supersaturation ratio nears 2 silica precipitation commences without delay.

The silica precipitation process consists of the following steps (Weres, Yee, and Tsao 1980):

- Step 1 - formation of silica polymers of less than nucleus size
- Step 2 - nucleation of an amorphous silica phase in the form of colloidal particles
- Step 3 - growth of supercritical amorphous silica particles by further chemical deposition of silicic acid on their surfaces
- Step 4 - coagulation or flocculation of colloidal particles to give either a precipitate or a semisolid material
- Step 5 - cementation of the particles in the deposit by chemical bonding and further deposition of silica
- Step 6 - growth of a secondary phase in the interstices between the amorphous silica particles (occurs rarely).

A solid surface in contact with a supersaturated solution of amorphous silica may have a layer of amorphous silica on it and further deposition may proceed by Step 3 alone. If colloidal amorphous silica particles form in the supersaturated solution, these may adhere to the surface in analogy to Steps 4 and 5; Step 6 may follow.

The formation of amorphous silica colloidal particles from a supersaturated solution can be referred to as homogeneous nucleation. It is the dominant process at the high initial supersaturation ratios required for rapid polymerization of amorphous silica. Heterogeneous nucleation applies to the deposition of amorphous silica on pre-existing colloidal amorphous silica particles, but it is not actually a nucleation process. Nucleation by other scale particles can also occur to provide surfaces for amorphous silica deposition. The formation of the amorphous silica on Fe(II) is most likely, followed by silicates of aluminum, magnesium, and calcium.

The nucleation process frequently involves an induction or lag time during which the concentration of molecular silicic acid remains constant. After some period of time, the concentration of molecular silicic acid begins t decrease, which indicates that nucleation is occurring. This induction time phenomena has been interpreted in two ways. First the approximate time required for sub-critical clusters of amorphous silica to grow to critical nucleus size and slightly beyond it is considered to be the induction time. The induction time is longer at lower saturation ratios because the critical nucleus size is larger at these ratios. For a batch process, the nucleation rate builds, peaks, and falls again as the saturation ratio decreases as a consequence of nucleation and particle growth.

In the second interpretation, induction time is viewed as simply the length of time required for enough particles to nucleate and grow to a point where the concentration of molecular silicic acid decreases. Rapid attainment of steady-state nucleation is implicit in this interpretation; therefore, an initially slower nucleation rate may be ignored for practical purposes. This interpretation applies to induction times observed for both homogeneous and heterogeneous nucleation.

A threshold value for amorphous silica supersaturation is apparent in some of the reported literature on amorphous silica nucleation. Iler (1973) reported a certain maximum deposition rate for molecular silicic acid on colloidal amorphous silica. Attempts to increase this rate by increasing the concentration of molecular silicic acid led to the homogeneous nucleation of new particles of amorphous silica as well as sustained growth of pre-existing particles. Weres, Yee, and Tsao (1980) reported that other researchers conducted their amorphous silica nucleation studies above a saturation ratio of 2.0, apparently to avoid inconveniently slow reaction rates.

Experimental studies have been conducted at Lawrence Berkeley Laboratories (LBL) to determine heterogeneous and homogeneous amorphous silica nucleation rates under specific conditions. Using both batch and continuous flow experimental results (Figure 4.6), Weres, Yee, and Tsao (1980) developed an empirical equation to calculate the rate of molecular deposition of amorphous silica over a broad range of temperature and molybdate active silica concentrations. Colloidal silica was added to solutions of molybdate active silica to determine heterogeneous nucleation (deposition on colloidal amorphous silica surfaces). Concentrations were ~0.6, 0.8, and 0.85 g/l at 50, 75, and 100°C, respectively. The colloidal silicas used in these experiments were Ludox® TM, HS, and SM, which had specific surface areas of 157, 242, and 359 m^2/g of SiO_2, respectively. The total surface area of the colloidal silicas varied between 143 and

® Product of E. I. du Pont de Nemours and Company, Inc., Wilmington, Delaware.

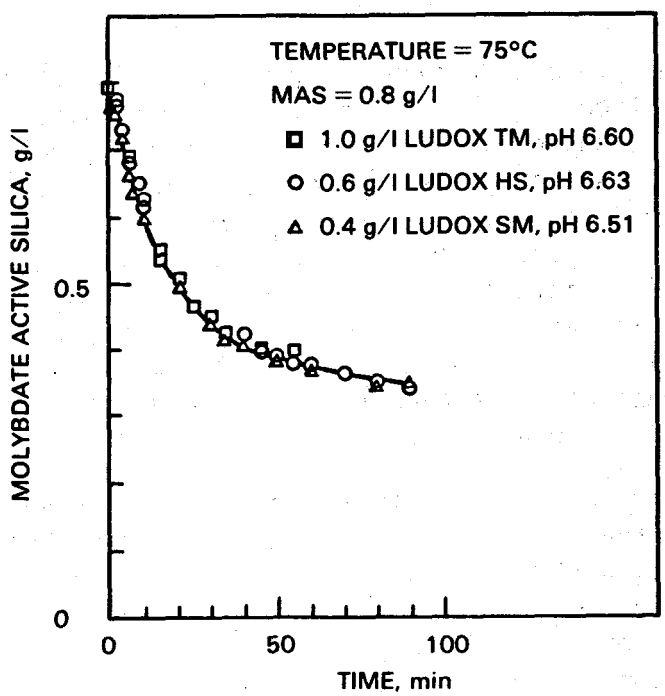

FIGURE 4.6. Reduction in Molybdate Active Silica (MAS) as a Function of Time Following Addition of Colloidal Silica (Weres, Yee, and Tsao 1980)

157 m^2/l for 1 g/l Ludox TM, 0.6 g/l Ludox HS, and 0.4 g/l Ludox SM. The reduction in molybdate active silica concentration with time following addition of colloidal silica is illustrated in Figure 4.6. Sodium molality in these experiments was ~0.07 due to buffering agents and the use of sodium silicate solutions to prepare the molybdate active silica. According to Figure 4.2, saturation of amorphous silica would be 290 ppm at 75°C; therefore, ~90% of the supersaturation was relieved in 90 min and about half of the supersaturation was relieved in 15 min.

Molybdate active silica is experimentally the same as unpolymerized silica. The amorphous silica molecular deposition rate (R_{md}) (grams of $SiO_2/cm^2/min$) is calculated from the following equation:

$$R_{md} = F(pH, pH_{nom})k_{OH}(T)f_f(S_a)(1 - S^{-1}) \qquad (4.7)$$

where $F(pH, pH_{nom})$ = factor expressing pH and salt effect on deposition rate (see Figure 4.7)

$K_{OH}(T)$ = rate constant at temperature T = $antilog_{10}$ (3.1171 - 4296.6/T)

S = saturation ratio (SiO_2 concentration/amorphous silica saturation concentration)

$$f_f(S_a) = S_a^5 \text{ if } S_a < S_t \text{ where } S_t = \text{antilog}_{10}\ (0.0977 + 75.84/T) \text{ or}$$

$$= S_t^5 + 5S_t^4\ (S_a - S_t) \text{ if } S_a > S_t$$

$$S_a = (1 - \alpha)S \text{ where } \alpha = \text{fraction of } SiO_2 \text{ in ionic form.}$$

The rate of molecular deposition at various molybdate active silica concentrations in low salinity solutions at 100°C is illustrated in Figure 4.8. The rate values were calculated with $S = S_a$, which is approximately true in low salinity solutions. Values from the curves in Figure 4.8 may be corrected by multiplying by $(1 - 1/S)/(1 - 1/S_a)$. Although this correction factor may be neglected in most cases because it is usually very close to 1, it can be important if S is close to 1. Only the area outlined by a solid line is approximately covered by experimental data; the other curves are extrapolations based

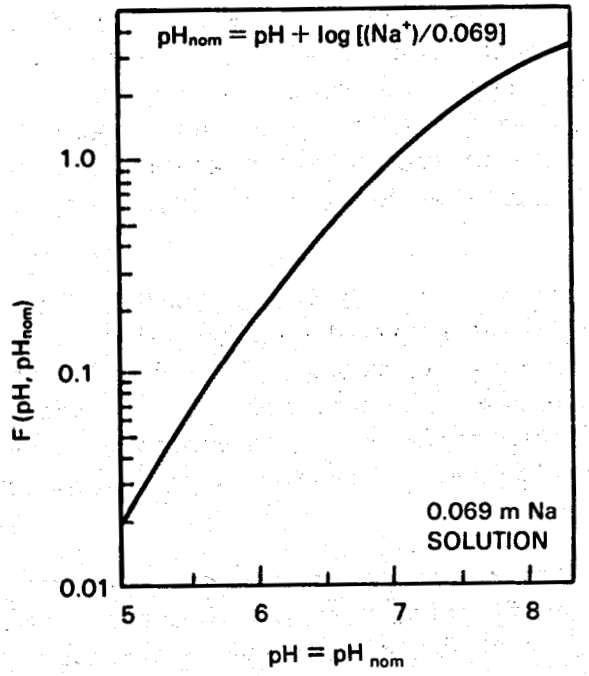

FIGURE 4.7. Variation of Silica Deposition Rate Factor with pH (Weres, Yee, and Tsao 1980)

on Equation (4.7). The dotted line represents the boundary between first-order kinetics (on the left of the dotted line) and fifth-order kinetics (on the right of the dotted line).

The effect of silica concentration on the rate of deposition is clearly evident in Figure 4.8. The deposition rate increases by almost three orders of magnitude by a three-fold increase in concentration (0.4 to 1.2 g/l) at 100°C. However, the indicated rate of molecular deposition of amorphous silica is still very slow and would cause a buildup of only 3 mm of scale over a period of a year.

This rate is considerably less than the 38 mm/month observed downstream from the second-stage flash vessel at the GLEF (San Diego Gas and Electric 1980). The rapid buildup of silica scale on equipment surfaces in contact with silica-supersaturated geothermal waters is attributed to deposition of excess molecular silicic acid on colloidal particles, which in turn adheres to the equipment surfaces and accelerates scale formation (Weres, Tsao, and Iglesias 1980). It is also evident that silica deposits more rapidly on precipitated silica sludge particles than indicated in Figure 4.8. For example, mixing 1.8 wt% precipitated sludge with spent geothermal brine for 20 min in a reactor clarifier at the GLEF lowered the silica content from 390 to 200 mg/l SiO_2 (San Diego Gas and Electric 1980). If an average 10-μm sludge particle size is assumed (Awerbuck and Rogers 1981) and the density of the particle is 1.4, the calculated silica deposition rate is 2×10^{-5} g/cm^2/min. The equivalent molecular silicic acid deposition rate from Figure 4.8 would be $\sim 10^{-9}$ g/cm^2/min. As can be seen from Figure 4.8 and from various literature sources (for example, Owen 1975), silica precipitation kinetics increases with increasing temperature and then decreases for a given concentration as the supersaturation ratio drops toward 1.0.

The rate of homogeneous nucleation at 100°C and neutral pH is illustrated in Figure 4.9 for different molybdate active silica starting concentrations in experiments similar to those previously described but without colloidal silica addition. Figure 4.10 shows the same data reinterpreted to illustrate the effect of supersaturation ratio on the polymerization induction period. These curves were corrected for small differences in pH and are therefore to be considered approximate.

In addition to temperature and degree of supersaturation, pH, dissolved salt concentration, and fluoride ions can affect the rate of silica nucleation. Weres and others have related the increase in molecular deposition rates (i.e., heterogeneous nucleation) to pH and Na^+ as illustrated in Figure 4.7, which shows about an order of magnitude increase in deposition rate by increasing the pH from 5 to 6. An increase in Na^+ from 0.069 to 0.69 m would also increase the deposition rate by an order of magnitude at pH 5 (pH_{nom} = 6 with 0.69 m Na^+ at pH 5). The effects of varying pH and NaCl concentrations in homogeneous

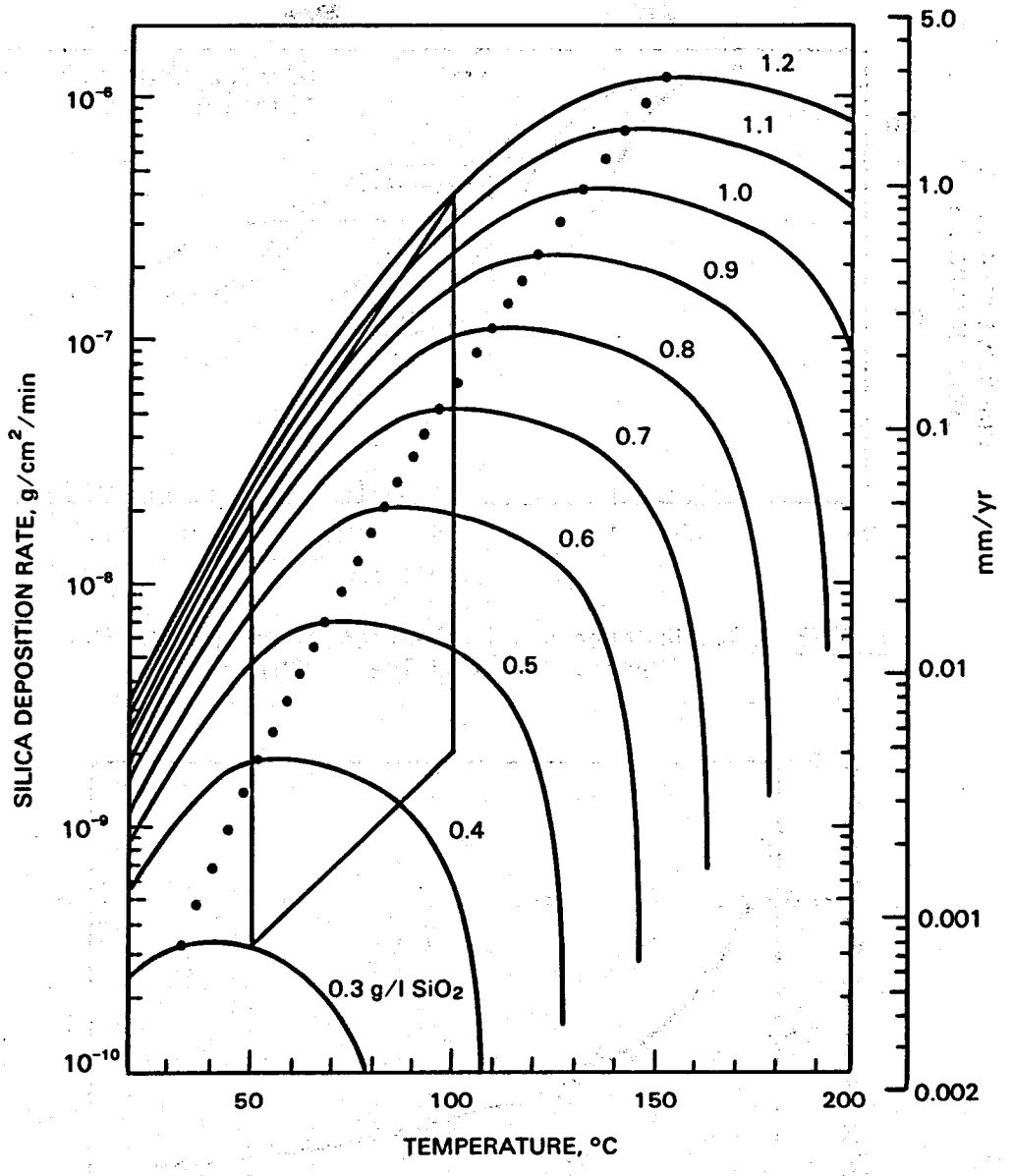

FIGURE 4.8. Rates of Molecular Deposition of Amorphous Silica at pH 7 (Weres, Yee, and Tsao 1980). Experimental data obtained within the four-sided figure; other curves are calculated. The maximum deposition rate for a specific concentration (dots) is the point where temperature-based increases in kinetics are counterbalanced by temperature-based increases in solubility. The vertical scales are considered by the authors to be quantitatively unreliable for predicting actual plant and well deposition rates.

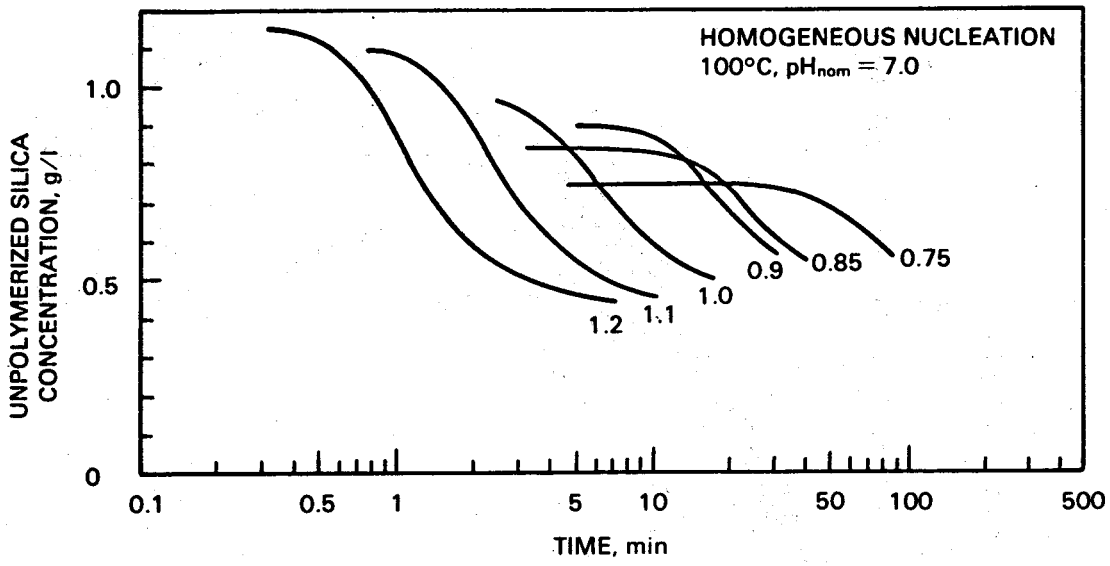

FIGURE 4.9. Homogeneous Nucleation of Silica at 100°C (Weres, Yee, and Tsao 1980)

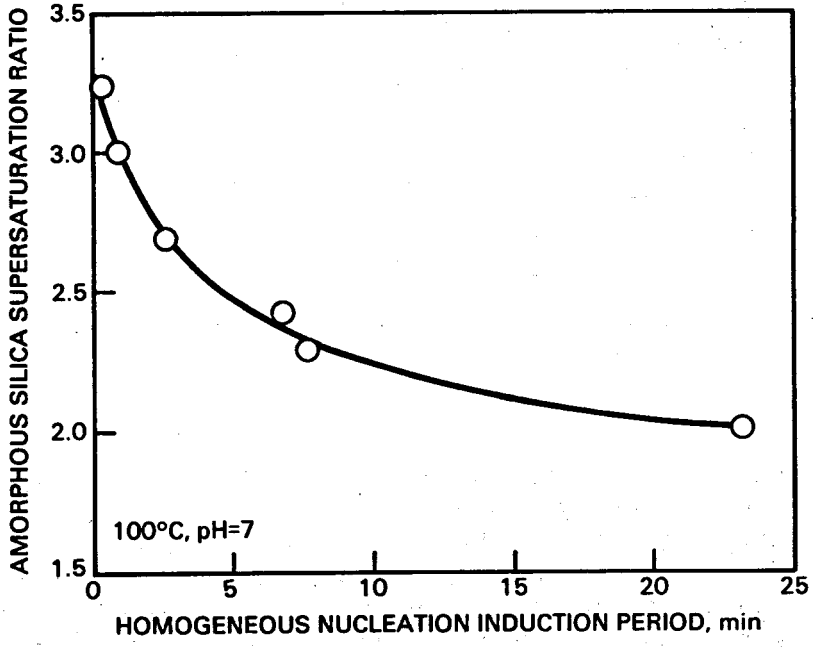

FIGURE 4.10. Effect of Silica Supersaturation on Induction Period (adapted from Figure 4.9)

nucleation experiments are illustrated in Figures 4.11, 4.12, and 4.13. The effects of fluoride catalysis and pH on homogeneous nucleation are shown in Figures 4.14. The "no F" curve in Figure 4.14 was estimated for pH 3.3 from an

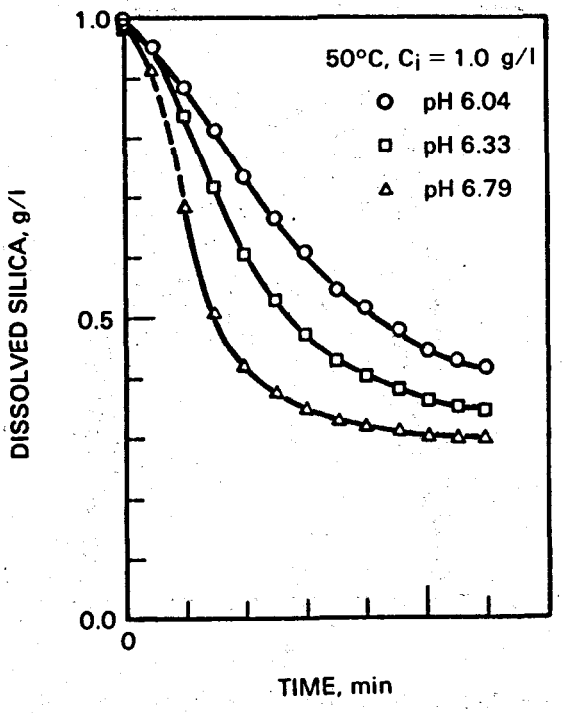

FIGURE 4.11. Effect of Varying pH on Homogeneous Nucleation of Silica (Weres, Yee, and Tsao 1980). Precipitation kinetics slows as solution becomes more acidic.

experiment conducted at a pH higher than 3.3 (Weres, Yee, and Tsao 1970). The specific fluoride levels described in this figure are high for geothermal fluids and would not normally be encountered; however, the figure does illustrate the dramatic catalytic effect of the fluoride ion at low pH.

A theoretical approach to the formation of colloidal silica particles by homogeneous nucleation was developed at LBL and was incorporated into the computer code SILNUC (Weres, Tsao, and Iglesias 1980). The availability of the SILNUC code should make this involved work on silica kinetics simpler for geothermal use. Awerbuck, Van der Mast, and Rogers (1982) used an exponential decay curve (such as is used to describe radioactive decay) to estimate the kinetics for the design parameters for a controlled precipitation process--a flash crystallizer-clarifier. However, the general relationships of Weres' work are confirmed by other investigators of silica chemistry:

- Weres reported that the rate of silica deposition is proportional to the sodium ion concentration; Iler (1979) reported that dissolved NaCl promoted faster solubility equilibrium.

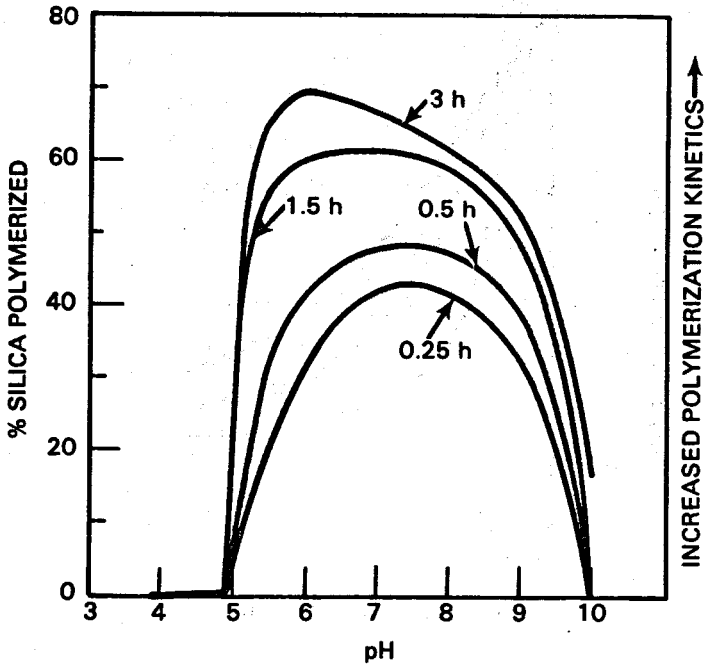

FIGURE 4.12. Silica Polymerization Kinetics Versus pH at Room Temperature. Amorphous silica supersaturation ratios of 3 to 4 (500 to 600 ppm). Original data from Kitahara (1960); reinterpreted and regraphed; not quantitative.

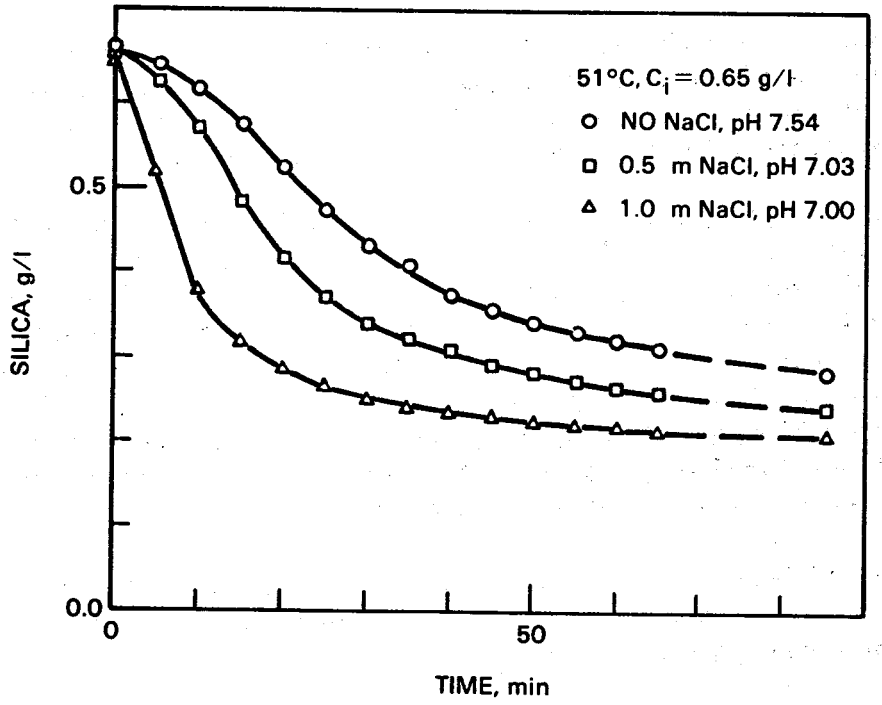

FIGURE 4.13. Effect of Varying NaCl Concentration on Homogeneous Nucleation of Silica (Weres, Yee, and Tsao 1980)

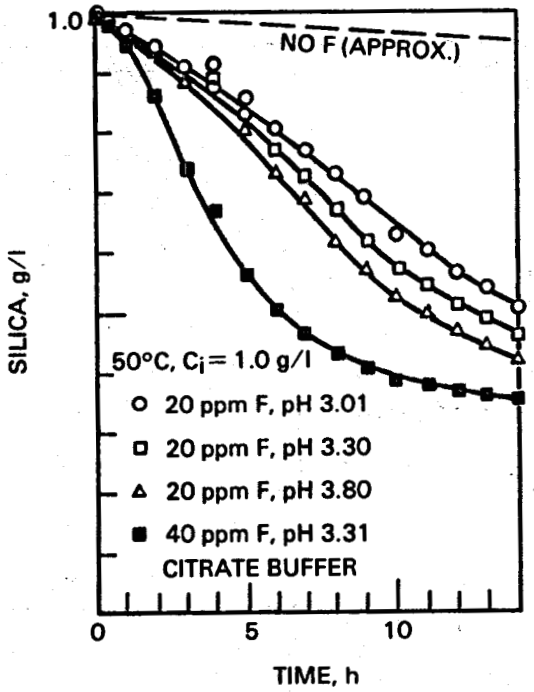

FIGURE 4.14. Effect of Fluoride Catalysis on Homogeneous Nucleation of Silica at Low pH (Weres, Yee, and Tsao 1980). Due to the impact of the kinetic impact of pH alone, fluoride catalysis becomes much less dramatic as pH rises.

- Weres reported a ten-fold increase in deposition rates with an increase from pH 5 to 6; Baumann (1955)--Figure 4.15--found that the rate of dissolution varied similarly within the approximate pH range of 3 to 6.

- Weres reported fluoride catalysis of silica polymerization; Iler (1979) discussed this effect and confirmed its significance in low pH waters.

The subject of silica precipitation kinetics is difficult to assess quantitatively without field tests. Among calculational options, the DOE/Berkeley code (SILNUC) and possibly the EPRI codes (EQUILIB, FLOWSCALE) are the most usable methods. For an initial design parameter, the kinetics can be estimated from the relationships discussed in this section and summarized in Table 4.4.

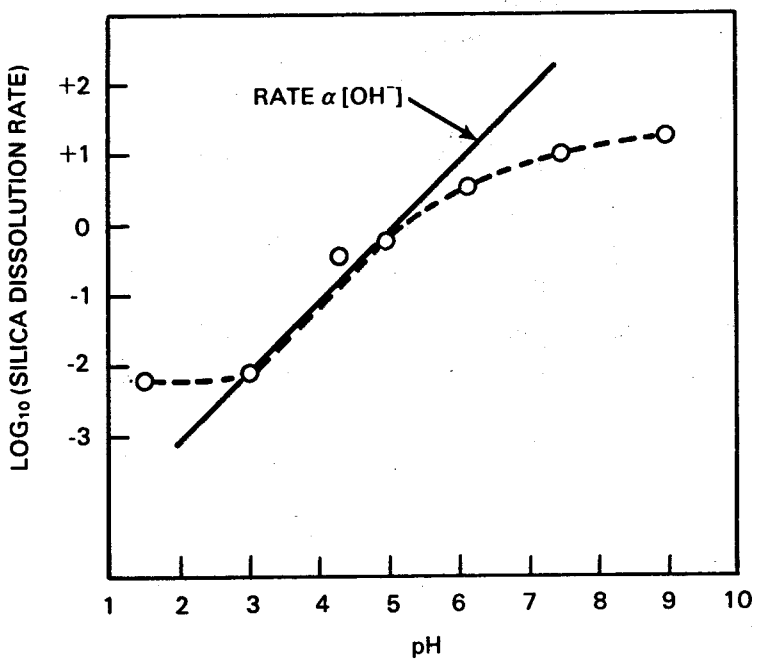

FIGURE 4.15. pH Dependence of Silica Kinetics for Dissolution Equilibrium, Indicating that Dissolution and Precipitation Have Similar pH Dependencies (Baumann 1955)

4.2 CARBONATE PRECIPITATES

Carbonate precipitates or scales can form in geothermal waters by the combination of carbonate ion with certain metal ions, the most prominent of which is Ca(II). Calcium ion can unite with carbonate ion in geothermal waters to form calcite, one of the crystalline forms of calcium carbonate. Aragonite, a different crystalline form, can also form but it is less common. Calcium carbonate deposits form very rapidly once the thermodynamic conditions are correct. For practical purposes, the calcite kinetics can be assumed to be instantaneous. Other alkaline earth metals, such as Sr(II) and Ba(II), and certain heavy metal ions, such as Fe(II) and Pb(II), can also contribute to carbonate precipitates or scales under appropriate conditions. Many of the heavy metal ions, excluding the alkaline earth metals, may be preferentially precipitated as sulfides instead of carbonates if sufficient $S^{=}$ is present because of the lower solubility of the sulfide compounds of these heavy metals. Alkaline earth sulfides are relatively soluble.

If the geothermal resource is a bicarbonate-dominated water (i.e., the pH is controlled by the CO_2/HCO_3^- equilbrium), alkaline earth carbonate precipitates and scale can be formed when flashing for steam production occurs.

TABLE 4.4. Factors Affecting Silica Deposition Kinetics

Factor	Impact	Comments
pH	Lowering pH slows kinetics by a factor of ~10 for every pH unit.	
Supersaturation ratio	Precipitation becomes rapid as the ratio exceeds 2.	Reduce pH and temperature
Temperature	Kinetics slows dramatically as temperature drops, which counteracts the increase in supersaturation ratio as a saturated solution cools.	The maximum silica deposition rate may occur 25 to 50°C below the temperature at which the cooled solution reaches amorphous silica solubility limits.
Salinity	Increased salinity increases kinetics of deposition	
F catalyst	This equilibrium (precipitation) accelerator may become the dominant controller of deposition in lower pH brines (pH 3?) where the normal precipitation mechanism is pH inhibited.	
Chemical inhibitors	Retards growth of silica particulates	Limited testing described in the Inhibitor Treatment section.

The loss of carbon dioxide and the associated pH increase are the principal causes for alkaline earth carbonate precipitation. The solubility products (K_{sp}) of calcium, strontium, and barium carbonate minerals at 25°C and 100°C are presented in Table 4.5. All the carbonate minerals listed exhibit decreasing solubility as the temperature increases from 25 to 100°C. The K_{sp} of calcite continues to decrease from 100 to 250°C, which limits its solubility (see Figure 4.16). However, the presence of CO_2 under moderate to high pressure in a geothermal reservoir enhances its solubility. This dissolution reaction may be expressed as:

$$CaCO_3(s) + H_2O(\ell) + CO_2(g) \rightleftharpoons Ca^{+2} + 2\ HCO_3^- \qquad (4.8)$$

As the bicarbonate ion dissociates to form carbonate ion, the pH rises:

$$HCO_3^- \rightleftharpoons OH^- + CO_2 \qquad (4.9)$$

TABLE 4.5. Solubility Products of Alkaline Earth Carbonate Minerals

Mineral	Chemical Formula	K_{sp} at 25°C[a]	K_{sp} at 100°C[b]
Calcite	$CaCO_3$	2.4 to 4.8 x 10^{-9}	3.2 x 10^{-10}
Strontianite	$SrCO_3$	1.6 x 10^{-9}	1.4 x 10^{-12}
Witherite	$BaCO_3$	8.1 x 10^{-9}	1.4 x 10^{-13}

(a) See Wahl 1977; Chemical Rubber 1962.
(b) See Ellis 1963.

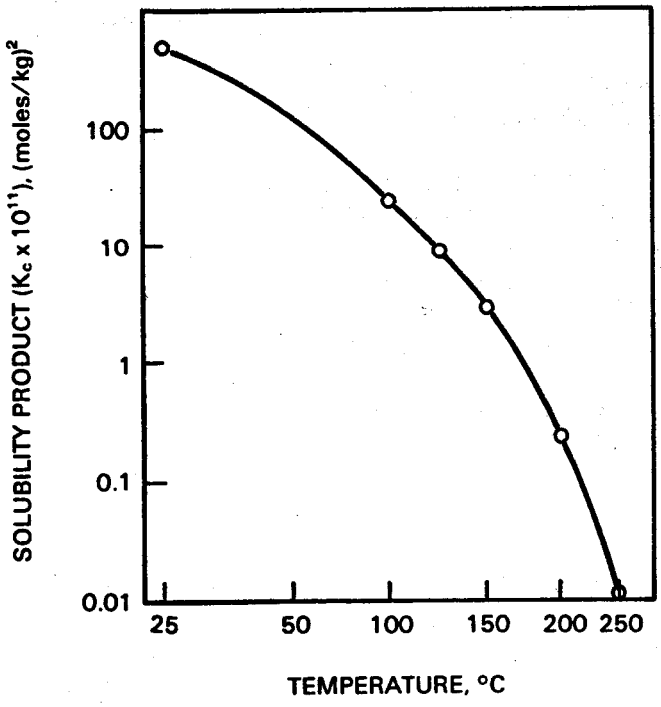

FIGURE 4.16. Solubility Product of Calcite as a Function of Temperature in Water (Wahl 1977; Ellis 1963)

But the equilibrium of Equation (4.9) is shifted to the left under the influence of increasing CO_2 pressure, which decreases the pH:

$$H_2CO_3 \rightleftharpoons H^+ + HCO_3^- \qquad (4.10)$$

The $CO_3^=$ concentration, which controls the solubility of calcite and the other minerals listed in Table 4.5, is given as a function of temperature and CO_2 pressure in Figure 4.17 for geothermal water from the East Mesa reservoir. Flashing of this water, which contains 400 ppm of HCO_3^-, increases the pH from 6

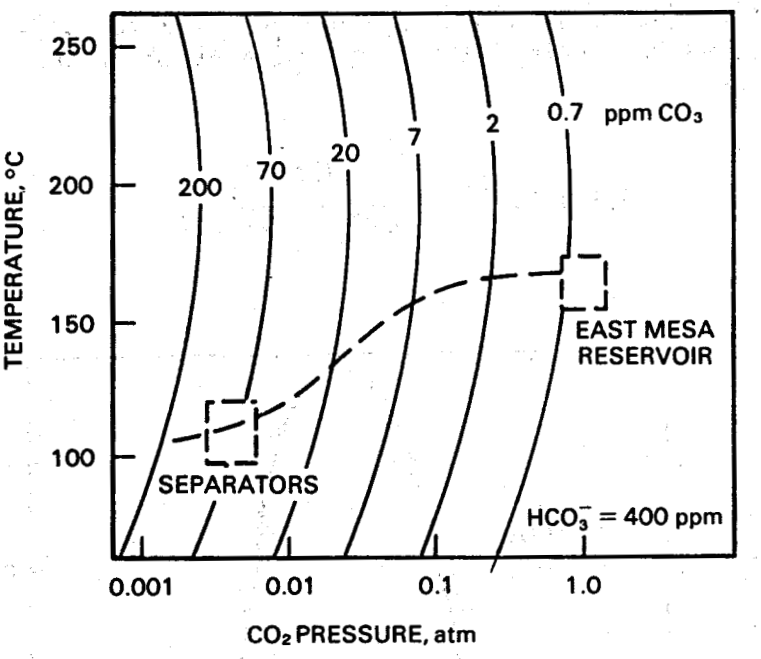

FIGURE 4.17. Isopleths Showing $CO_3^=$ Concentrations Versus Temperature and CO_2 Pressure (Michels 1979)

or 7 to 9 or 10 and increases the $CO_3^=$ concentration from <0.7 to ~70 ppm. This change causes the precipitation of ~7 ppm of Ca as $CaCO_3$ (Michels 1979). The soluble Ca in a pure water solution with 70 mg/l $CO_3^=$ would be ~0.01 mg/l Ca(II); however, the presence of complexing agents (for example, $SO_4^=$ and F^-) could increase this value in actual geothermal water. The fraction of $CO_3^=$, HCO_3^-, and H_2CO_3 (CO_2aq) present as a function of pH at 100°C is shown in Figure 4.18. In the case of the water containing 400-ppm HCO_3^- and CO_2(aq), if only the available CO_2 illustrated in Figure 4.18 were flashed with steam, the pH of the solution would appear to approach 9 rather than exceed it as discussed in the East Mesa example. Some of the HCO_3^- decomposes to yield water and CO_2 (volatilizes with the flashing steam) and $CO_3^=$ that hydrolyzes to increase the pH above 9 (Michels 1979):

$$2\ HCO_3^- \xrightarrow{\text{boiling}} H_2O + CO_2\uparrow + CO_3^= \qquad (4.11)$$

and

$$CO_3^= + H_2O \rightleftharpoons OH^- + HCO_3^- \qquad (4.12)$$

From Equation (4.10), there is always some CO_2 and H_2O available (as H_2CO_3) at equilibrium in a solution containing HCO_3^-. The equilibrium constant

(K_1) for Equation (4.10) at 100°C is 5.8×10^{-7} (Table 4.6). Although Figure 4.18 indicates zero mole fraction of H_2CO_3 at pH 9, the mole fraction calculated from:

$$K_1 = 5.8 \times 10^{-7} = \frac{(H^+)(HCO^-)_3}{(H_2CO_3 + CO_2\ aq)} \qquad (4.13)$$

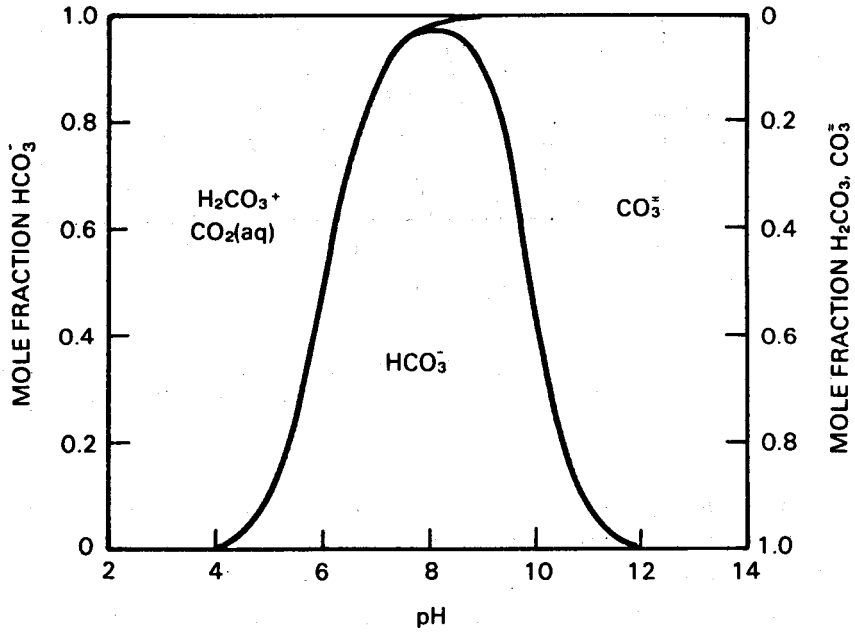

FIGURE 4.18. Fraction of H_2CO_3, HCO_3^-, and $CO_3^=$ as a Function of pH at 100°C

TABLE 4.6. Equilibrium Constants K_1 and K_2 for Equations (4.13) and (4.9), Respectively, at Temperatures from 25 to 200°C[a]

Temperature, °C	$K_1 \times 10^7$	$K_2 \times 10^{11}$
25	4.45	4.69
50	5.16	6.73
100	5.8	7.3
150	4.7	5.6
200	2.8	3.8

(a) See Ellis 1959b.

is actually a finite amount (H_2CO_3 = 0.0017 mole fraction). The amount of H_2CO_3 (or $CO_2 + H_2O$) may be very small; but due to the high volatility of CO_2 dissolved in water, the CO_2 is readily removed by boiling or steam stripping to pH levels above 9. Experiments with shale oil waste water containing $NaHCO_3$ have shown that pH levels increased from 8.6 to as high as 10 by steam stripping for ammonia,[a] which also removes CO_2 by decomposition of the HCO_3^- (Mercer et al. 1982). Steam stripping of the CO_2 available from Equation (4.13) becomes less efficient as the pH increases because the fraction of CO_2(aq) becomes smaller (for example, at pH 10 and 100°C, the mole fraction of H_2CO_3 is only 1.7×10^{-4}).

The $CO_3^=$ concentration can be computed from the following equation (Stumm and Morgan 1981):

$$CO_3^= = \frac{K_1 K_2}{(H^+)^2}(K_H)\left(P_{CO_2}\right) \qquad (4.14)$$

where K_1 and K_2 = the first and second ionization constants for carbonic acid; Equations (4.10) and (4.9), respectively, and Table 4.6

K_H = the inverse of Henry's law constant in moles/l/atm (see Figure 4.19)

P_{CO_2} = the partial pressure of CO_2 in atmospheres.

A value of 81 mg/l $CO_3^=$ was calculated from Equation (4.14) using constants from Table 4.6 and Figure 4.19 for 100°C, a pH of 9, and a pressure of 3×10^{-3} atm for $CO_3^=$. This $CO_3^=$ concentration falls within the zone for the steam separators shown in Figure 4.17.

4.3 SULFIDE PRECIPITATES

Precipitation of heavy metal sulfides is also influenced by temperature reduction and loss of CO_2. However, compared with the alkaline earth carbonates, the temperature reduction generally decreases the solubility of the heavy metal sulfides (see Figure 4.20). The loss of CO_2 increases the pH, which also enhances the precipitation of the heavy metal sulfides. At pH values normally seen in geothermal waters (pH 4 to 9), most sulfide is present as H_2S or HS^- ion; however, solubility products are expressed in terms of sulfide ($S^=$).

(a) Steam stripping NH_3 causes a reduction in pH in pure water.

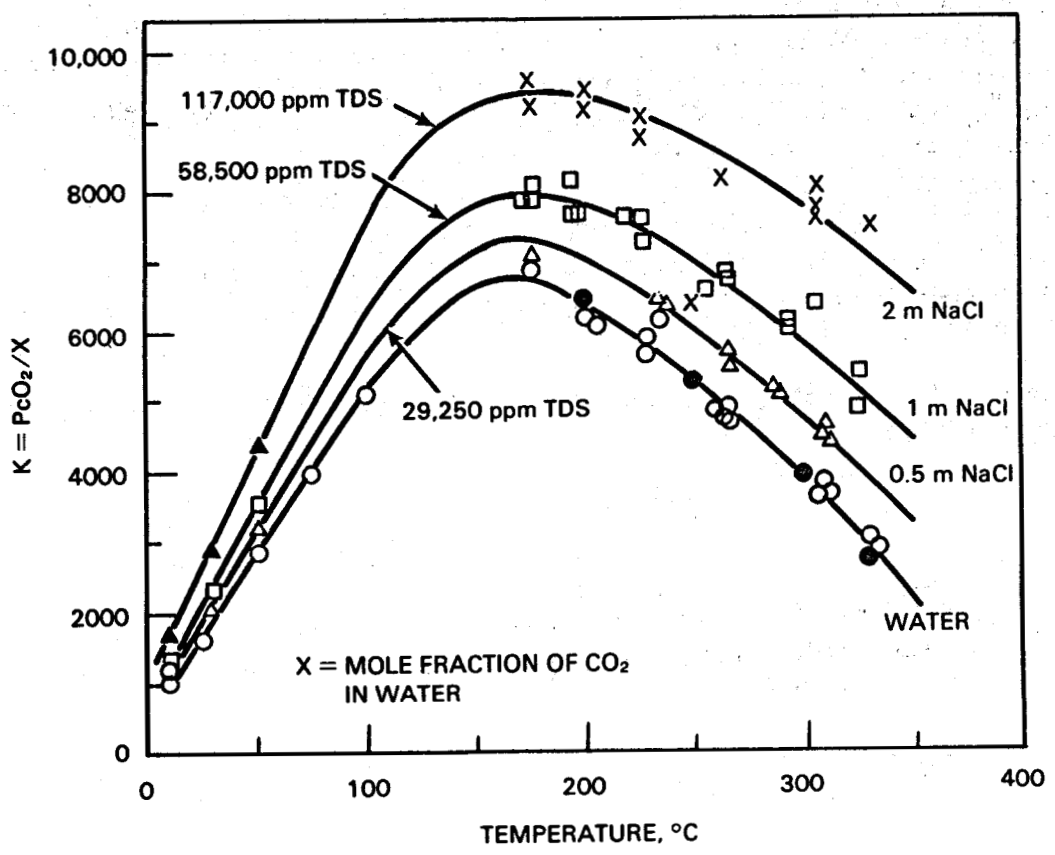

FIGURE 4.19. Henry's Law Constant (K) for CO_2 in Water and NaCl Solutions as a Function of Temperature for CO_2 Pressure Below 50 atm (Ellis and Golding 1963)

Sulfide ion is formed from H_2S, commonly found in geothermal waters by the following reactions:

$$H_2S \leftrightharpoons HS^- + H^+ \quad (4.15)$$

$$HS^- \leftrightharpoons S^= + H^+ \quad (4.16)$$

An increase in pH shifts Equation (4.16) to the right increasing the concentration of sulfide ion available for precipitating heavy metals. The effect of pH on the solubility of several heavy metal sulfides is illustrated in Figure 4.21. These solubilities decrease rapidly with increasing pH.

Comparing Ag_2S solubility in a neutral solution of water (Figure 4.21) with its solubility in 3 M NaCl (Figure 4.20) illustrates the effect of chloride complexing for increasing the solubility of the Ag_2S. The concentration of Ag_2S is 10^{-14} m in water compared with $\sim 10^{-9}$ m in 3 M NaCl. The

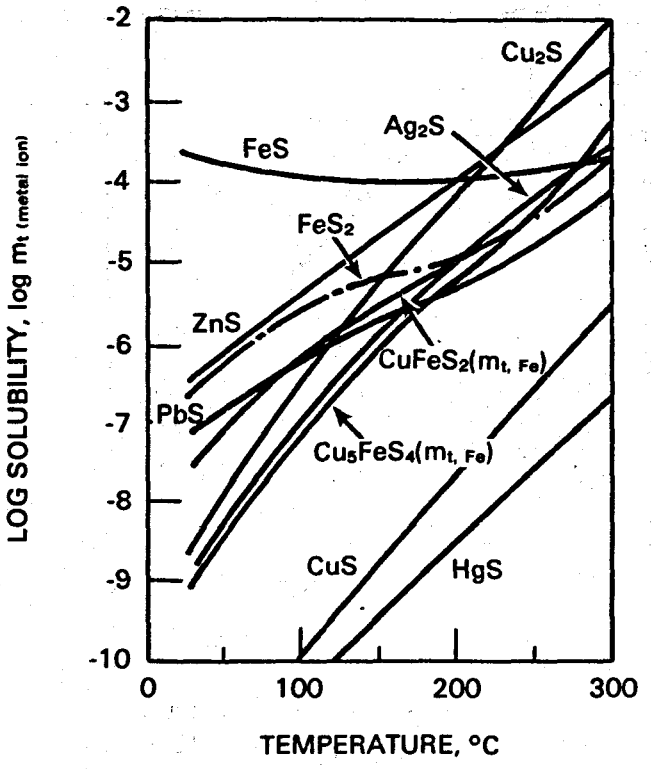

FIGURE 4.20. Solubilities of Sulfides in 3 M NaCl (Helgeson 1969)

complexing action of chlorides, HS^-, and other ligands makes it difficult to predict heavy metal sulfide solubilities in geothermal waters. Hopefully, the development of computer programs will greatly simplify the task of calculating solubilities of sulfides and other species in geothermal waters.

Heavy metal sulfides, especially galena or lead sulfide, formed a hard black scale in the piping and valves leading to the first-stage flashing vessel at the Salton Sea GLEF (Featherstone and Powell 1981). Beyond the first-stage flashing vessel, the precipitation of silica begins to dominate; however, the precipitate is dark colored due to the intermixing of metal sulfides with the silica. It is also known that cooled brines at this plant precipitated heavy metal sulfides if the NCG from the separator bubbled through the brine. The H_2S in the gas reacts with the cooled solution under the new solubility conditions and sulfide precipitates form. Although this results in less H_2S being released, the specific application to a brine treatment process has not been explored.

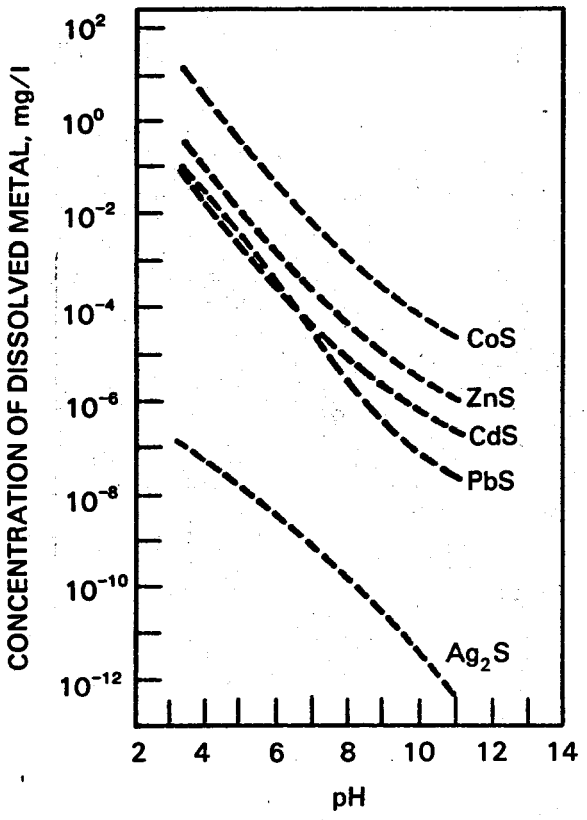

FIGURE 4.21. Metal Sulfide Solubility in Water as a Function of pH at 25°C (EPA 1980)

4.4 OTHER PRECIPITATES

A wide variety of precipitates other than the ones discussed above are possible when geothermal waters are processed for energy recovery. Alkaline earth metals, Ca, Sr, and Ba comprised 10% of the washed filter cake from injection water treatment at the Salton Sea plant (Featherstone and Powell 1981). A substantial portion of these metals, especially Ba (4.8%), probably precipitated as sulfate since there was 6.38% sulfate in the filter cake. Calcium and strontium sulfates have retrograde solubilities in water from 30 to about 300°C. Although NaCl increases the solubility of these two sulfates, the solubility remains retrograde in this temperature range for $SrSO_4$ up to 2 m NaCl and for $CaSO_4$ up to 5 m NaCl (Holland and Malinin 1979). The solubility of barium sulfate is prograde in water to ~100°C; however, the presence of NaCl concentrations above 1 m can raise this temperature to at least 300°C. Therefore, brine solutions (>1 m NaCl) saturated with $BaSO_4$ at 300°C can precipitate $BaSO_4$ as they are cooled. The addition of sulfuric acid as a pH control agent

can also cause the precipitation of Ca, Sr, and Ba sulfates by increasing the $SO_4^{=}$ concentration of the water. The mixing of incompatible waters may be a prime cause of sulfate scales.

Hydroxide, silicate, and fluoride precipitates are also possible in geothermal waters. These precipitates are of minor or theoretical interest except for iron hydroxide, which has been observed in some brines after exposure to air (oxygen). The most noteworthy cases of this iron (III) hydroxide to date have been in the hypersaline Imperial Valley brines.

5.0 TREATMENT OPTIONS

There are two approaches that can be used to extract the usable energy from the production flow without damaging the spent brine injection system: 1) choosing an energy cycle or process that avoids precipitation or 2) using one that controls precipitation so that it occurs in a location designed for that purpose. With the second approach, one of several subsystems can be chosen for separating the solids from the liquids on a continuous basis. Rather than concentrate on the four or five practiced injection treatment systems (GLEF, Salton Sea, Brawley, Magma's Binary Magmamax, and the Japanese aging technique) as detailed case studies, the options (including many subsystems not currently in use) are described as individual technologies and components. Where there is relevant geothermal experience, it is described and referenced. Those readers interested in how industry has integrated, or plans to integrate, these into whole processes may prefer reading the section on "Current Brine Processing Experience." The status of detailed operating information of the practiced treatment system is listed below:

- GLEF - dismantled; comprehensive information published
- Salton Sea - discussed in this report; additional details would require proprietary operational data
- Brawley - same comments as for Salton Sea only Brawley is not functioning as smoothly
- Magmamax - a proprietary approach to avoiding precipitation whose performance is well known in the field; specific examples are discussed
- aging - discussed in this report, but the experience indicates it is usable only with certain brines and with fracture-dominated injection capability.

Precipitation avoidance will require either limiting the temperature drop of the brine (limiting the energy input into the power plant) or adding pressure/chemicals to the brine to control or alter the chemistry (raises costs). Controlled precipitation requires additional facilities and energy for removing and pumping the solids (raises costs). The principles of the treatment options are described in reasonable detail just as the process chemistry principles were. Except possibly for the use of certain inhibitors as precipitation avoidance tools all of the treatment techniques are adaptations of existing water treatment processes in use in municipal water treatment plans or industrial applications.

It is exceedingly difficult to estimate a specific detailed system for a generic geothermal plant since the individual chemistries and reservoir characteristics influence the choice so much. As a hypothetical resource becomes hotter (that is, the energy is higher grade and overall power conversion efficiencies improve), more capital investment and expense can be tolerated in extracting this desirable energy compared to a lower grade, lower temperature resource. This implies that hotter fields will see the use and development of treatment processes, which has been observed in the United States.

5.1 PRECIPITATION AVOIDANCE

Process parameters (pressure and temperature) and additives (acid, inhibitors, and water) that can be used to control scaling before and during the injection process are discussed in this section. The use of CO_2 injection is described in Section 5.2 because its use can both avoid and control $CaCO_3$ scale, depending on the particular injection point. The use of lime (a base) to accelerate silica deposition is discussed in Section 5.1.3 because it is complementary to acidification (a precipitation avoidance technique).

5.1.1 Pressure

If sufficient pumped pressure is applied to the geothermal liquid to keep the CO_2 in solution, $CaCO_3$ scale is avoided, which allows the designer to concentrate on avoiding silica precipitation. In the case of pumped binary cycle plants, silica precipitation is avoided by maintaining a certain minimum temperature. Pressure is effective at preventing $CaCO_3$ scale that occurs in many wells as a result of chemical pH changes accompanying CO_2 exsolution, but it is ineffective at preventing other types of particulate scale formation.

It is necessary to predict accurately the minimum pressure necessary to prevent $CaCO_3$ scale formation in fluids that show a tendency to scale in this manner. This pressure will be a function of temperature, salinity, and individual flow chemistry. The usual and safest approach is to insure that neither flashing of the brine into steam nor dissolved gas breakout occurs and then boost the pressure to account for flow composition changes and hydraulic pumping factors.

If the calculations were sufficiently precise, some of the CO_2 could be lost (lower pressure means lower pumping costs) as long as enough remained to prevent $CaCO_3$ formation. This precision is exceedingly difficult because CO_2 is lost very rapidly during the initial flash stages (see Figure 5.1). To avoid this two-phase flow, the design must take into account CO_2 pressure, other NCG pressures, and brine flash pressures. Downhole pressures must also include hot static wellhead pressure and drawdown allowances.

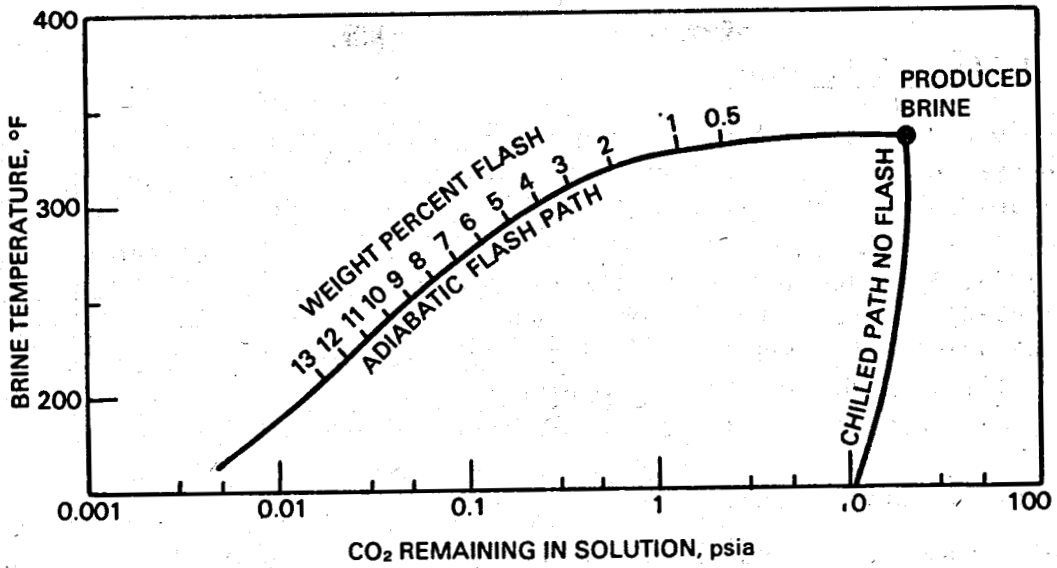

FIGURE 5.1. Loss of CO_2 as Flash Progresses (Michels 1981)

If two-phase flow is avoided throughout the process, no $CaCO_3$ will deposit. The only conceivable exception would be if the brine were mixed with another somewhat incompatible water. Because $CaCO_3$ solubility decreases with increasing temperature (retrograde solubility), $CaCO_3$ could also precipitate and plug the injection zone as it is reheated.

5.1.2 Temperature

In a geothermal cycle (where the fluid starts off as a superheated brine, heat is extracted from it, and the fluid is disposed of in a potentially warm aquifer), adverse injectability may be caused by particulate gel or crystal growth due to silica, metal sulfides, or barium sulfate. These growths can be avoided by controlling the lowest temperature prior to injection. Problems with silica are commonly encountered at geothermal sites, and it is the chemistry of this mineral that determines the minimum temperature and therefore the energy available and the economics. Barium sulfate and metal sulfide injectability problems are more site or well specific.

The simplest and most certain way to avoid silica problems is to keep the silica concentration below the amorphous silica saturation level. To avoid silica supersaturation, it is necessary to control the temperature for a binary plant (or injection process alone) or the degree of flashing for a flashed brine plant. Controlling the temperature is the normal brine treatment method for binary cycle power plants. Awerbuck, Van der Mast, and Rogers (1982) proposed a flow sheet in which a flash cycle effluent is diluted with reheated steam condensate to avoid the silica supersaturation problem.

5.1.3 Brine pH Adjustment

Scale and particulate formation are caused by chemicals re-equilibrating in a changed process environment. This environment can be changed by adding mineral acids/bases to effect a pH environment and prevent the formation of selected solids. CO_2 gas to lower the pH is discussed in another section. All of the major scaling elements in geothermal systems (silica, calcite, sulfides, and sulfates) are less troublesome as the pH is reduced. The solubility is higher as acidity increases and silica polymerization kinetics slows dramatically. Silica solubility is at a minimum at pH 7; it increases slightly in acid waters and dramatically as the pH rises above 8 and becomes more basic.

Acid Addition - Silica

The effect of reduced pH to retard silica polymerization is well known and has been tested at several sites. A good test is to titrate the brine to determine how much acid is needed to reach a specific pH. This information coupled with a test on the speed of polymerization at a specific pH will permit calculation of the amount of acid required, which will permit an economic analysis (should incorporate an allowance for increased corrosivity of the acidified solution). Instruments are available to permit on-line monitoring of corrosive attack and remaining wall thickness.

A conceptual flow process incorporating acid treatment is shown in Figure 5.2. Although it is a simple flow sheet, acid treatment had not been used

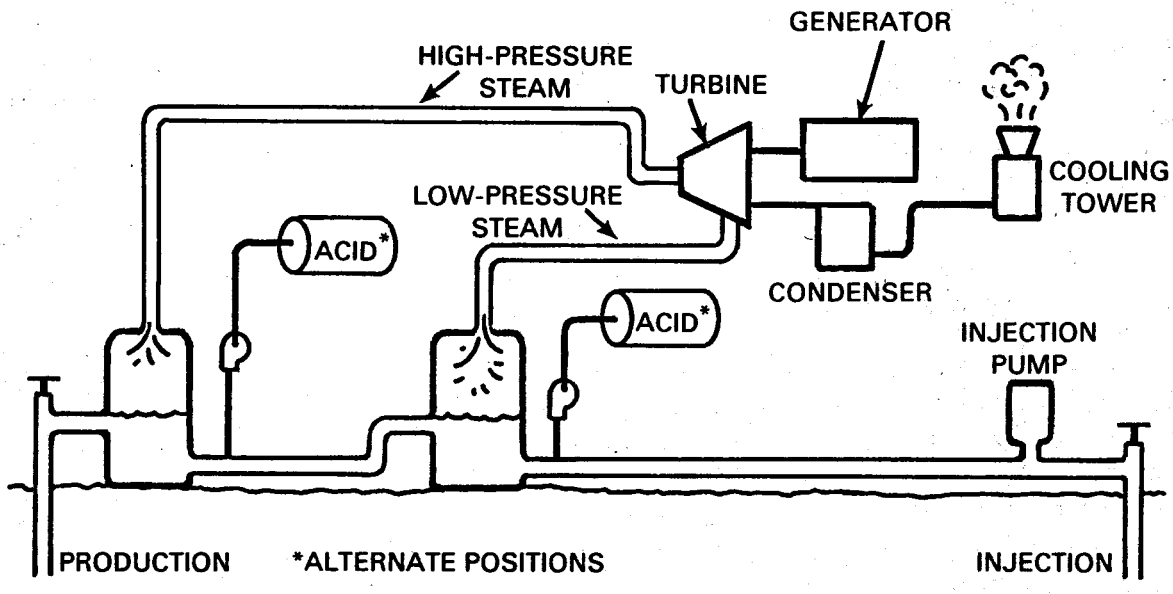

FIGURE 5.2. Process Flow Acidification Scale Prevention

on an operational basis until the Brawley plant instituted its use on hypersaline brine. It has advantages of flexibility because the dose can be readily altered to fit different flows and because acidification is effective against all the major scaling species. HCl would probably be the acid of choice because it is readily available and it does not introduce any new contaminants into the process chemistry. H_2SO_4 introduces sulfate ion, which could aggravate problems with sulfate precipitates (Ca, Sr, Ba), exactly opposite to what was intended. Repressurizing the brine with CO_2 (such as from NCG) can lower the pH; however, depending on the amount of CO_2 and the brine chemistry, it may or may not be sufficient to retard silica growth.

The acidification option has two technical disadvantages. The first, accelerated corrosion of steel piping, is discussed more in Section 6.2 (Corrosion). There are some data and experiences indicating that pH decreases into the pH 4 to 5 range may not raise corrosion rates to unacceptable levels. The second disadvantage is that increased evolution of NCG can result, particularly if the fluid is near neutral or basic in pH and has dissolved carbonate or sulfide species. These gases degrade turbine performance and may cause a disposal problem if they are mixed with steam, suggesting that acidification should occur after the separator in many resources; thus, additional corrosion protection of the separator is not needed. In the uncommon event that a particular well or combination of wells has a $BaSO_4$ precipitation tendency, there is some indication that acidification accelerates precipitation.

Salton Sea tests of acidification were carried out by several groups. Grens and Owen (1977) found acidification on postseparator brine (+200°C) to be effective in controlling silica, metal sulfide, and mixed scales in surface piping and equipment (Figure 5.3). By their estimate the cost of the acid would amount to 6% of the value of the produced electricity at the bus bar. It is important to note that their work involved scaling on surface equipment, and they did not consider suspended particles or downhole precipitation.

Harrar (1981) studied the effect of pH on suspended solids formation in a Salton Sea brine at 90°C. These results show the effectiveness of acidification in delaying precipitation under hypersaline conditions (Figure 5.4). This figure is a good example of some of the testing recommended in Section 3.2.2.

Tests on New Zealand spent brines (approximately 3000 ppm TDS and 75°C) showed that acidification to pH 4 reduced scaling rates on pipes by a factor of 18 at Broadlands (silica is 900 ppm) and 100 at Wairakei (silica is 560 ppm) (Rothbaum et al. 1979).

As of 1984, the steam supply system at the Brawley 10-MWe Demonstration Plant (Imperial Valley, California) is using acidification to help control the high scaling tendencies of the hypersaline brine. The particular acid and the injection point are currently proprietary.

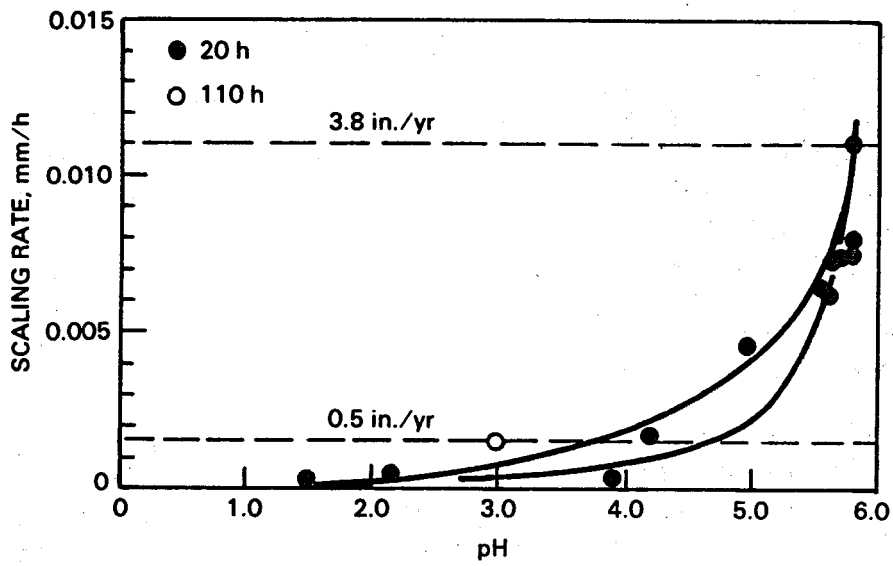

FIGURE 5.3. Effect of pH on Scale Deposition of Separated 200 to 230°C Brine from Salton Sea Geothermal Field (Grens and Owen 1977). Compare with Figure 4.12.

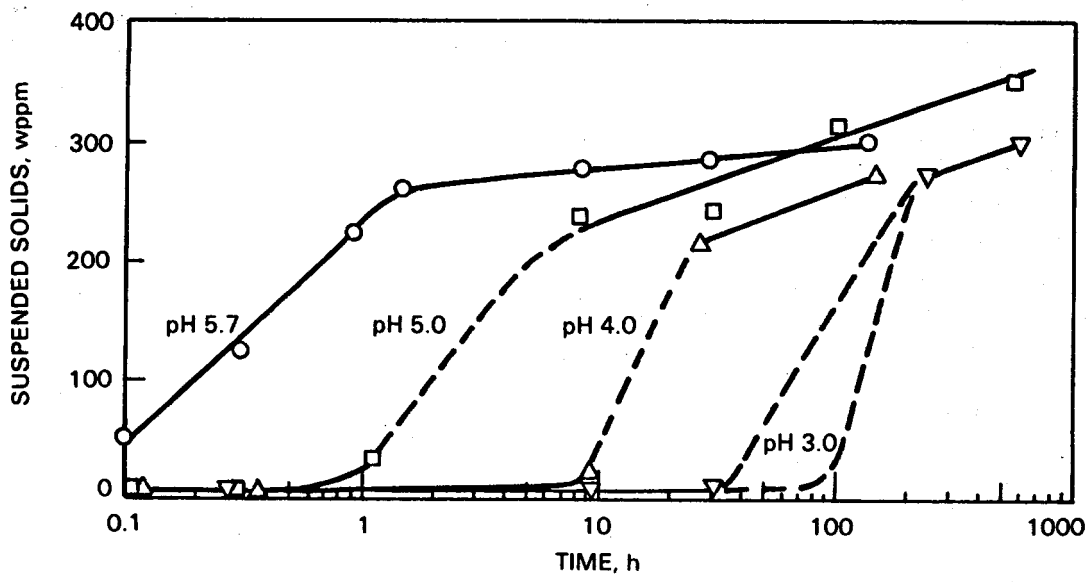

FIGURE 5.4. Effect of pH on Delaying Particulate Formation in Brine. 220,000 ppm TDS and 90°C from Salton Sea; starting dissolved silica concentration 450+ ppm (adapted from Harrar 1981). Broken lines are presumed curves where particulate growth is most rapid. Note good agreement with Figures 4.7.

Gudmundssen (1983) discusses a study on silica deposition at an Icelandic geothermal field and concludes that acidification, possibly including the use of naturally acidic condensate, would be effective at controlling silica scale.

Acid Addition - Calcite

Adding acid upstream from calcite deposition spots will eliminate scaling. However, it is not an attractive method in geothermal situations due to the following factors:

- the cost of the acid
- the thermodynamic penalty of adding cool acid degrades the resource before the energy is extracted from it
- the addition of acid at the head end of the production line means that acid-accelerated corrosion will be a concern for the entire brine system.
- the possibility of using noncorrosive scale inhibitors.

Acid Addition - Sulfides

Sulfide solubilities increase rapidly as the solution becomes more acidic. Little attention has been paid to sulfide scaling alone; it is usually found in conjunction with other scales.

Base Addition

The addition of lime (CaO) to waste geothermal brine has been tested at several locations and especially in New Zealand to remove silica and arsenic prior to surface disposal. Although this is not a precipitation avoidance method, it is discussed here because of the natural juxtaposition with the foregoing acid addition section. The increase in pH speeds up the polymerization kinetics, causing silica flocs to form and settle out on standing. Since silica solubility is at a minimum at pH 7, any increase above that will increase solubility equilibrium and further mitigate silica problems. The amount of lime required will be site dependent and will be affected by buffering capacity, specific flow chemistry, and process conditions. It would be best to experimentally test the effectiveness of raising the pH at a particular site rather than relying on a calculation model or experience.

Weres, Tsao, and Iglesias (1980) found that an increase of one-half pH unit to pH 7.8 in a synthetic Cerro Prieto brine caused a floc to form that settled at the rate of 60 cm/min. This work estimated that 37 ppm of lime--$Ca(OH)_2$ in this case--was needed to achieve this floc production. The high

concentration of divalent cations present (specifically Ca^{+2}) contributed to the effectiveness of low treatment levels.

Tests at the major Mexican field--Cerro Prieto--show good results from a combined process involving 10 to 15 min aging, 20 to 40 ppm lime addition, and sedimentation in a clarifier (Hurtado et al. 1981). Their analysis showed this approach cost 25% less than that of a reactor clarifier approach from which they were unable to get good results.

Lime addition has been tested in New Zealand as part of a larger process to remove arsenic from spent geothermal waters prior to surface disposal (Rothbaum and Anderton 1975). The trace arsenic was oxidized to a state that coprecipitated with silica as the pH was raised. The relatively low salinity and alkaline waters required a substantially higher lime addition rate (Figure 5.5) than the Cerro Prieto testing. The comparison is clouded, however, because of the different purposes of the tests: arsenic removal in New Zealand and suspended solids removal at Cerro Prieto.

Testing at the Mexican Los Azufres field demonstrated a similar experience to that of New Zealand. The field tests (Martinez et al. 1983) were to reduce arsenic, boron, and silica with the possible objectives of surface disposal, reverse osmosis cleanup, or injection. These tests indicated that the settling rate of the floc was related to the "aging" period of the brine (Figure 5.6).

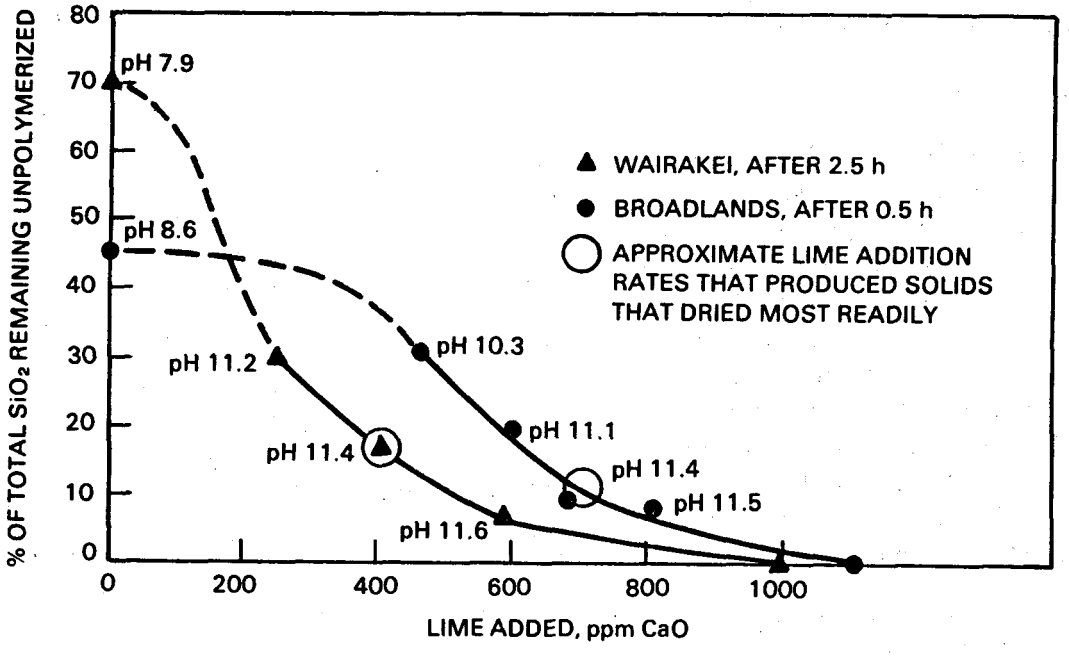

FIGURE 5.5. Effect of Lime Treatment on Silica in New Zealand Brines (data originating from Rothbaum and Anderton 1975)

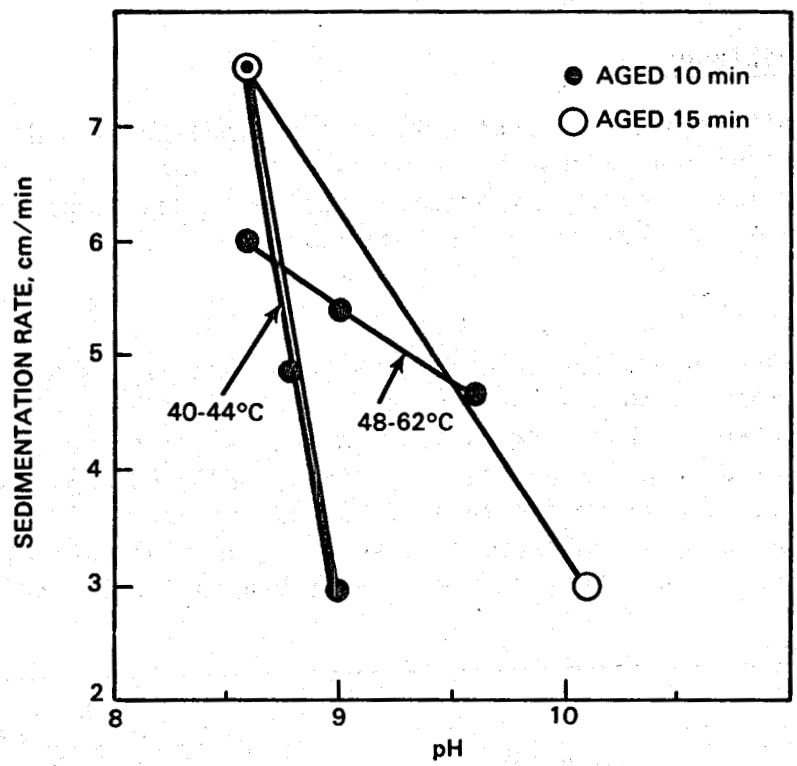

FIGURE 5.6. pH Versus Silica Sedimentation Rate for Los Azufres Brine (data originating from Martinez et al. 1983). Note possible complicating effect of temperature.

A high-rate lamella settler worked well with the lime addition and resulted in a 24-fold reduction in required settling time.

Field tests at the Salton Sea GLEF demonstrated similar behavior of base (NaOH) in reducing supersaturated silica (Quong et al. 1978). Adding 25 ppm NaOH increased the pH from 5.5 to 5.9 and decreased soluble silica by 16% after 30 min. These tests indicated that temperatures between 40°C and 85°C had no effect on base addition (or any other coagulants).

Process Equipment

The equipment used or recommended by these three tests is very similar. The brine passes through an aging tank into a mixing tank where lime is added. After this pH adjustment (an on-line pH monitor would be appropriate), the precipitating brine goes into a settler/clarifier where the sludge is separated and the brine clarified. A final sludge disposal/dewatering step is necessary. Because of the aging affect on the efficiency of the flocculation, the optimum aging period/flow rate should be determined for a specific site.

5.1.4 Scale Inhibitors

Scale inhibitors are used routinely in many industries and processes that deal with thermodynamically unstable processes or waters. The geothermal problem differs from most industry experience because of the temperatures, compositions, and large brine flow rates that are involved.

Silica Inhibition

The most thorough evaluation of silica scale inhibitors has been conducted by Harrar and coworkers in the late 1970s (see Harrar 1982 and listed publications). The purpose of this work was to find an inhibitor that would function in the hypersaline Salton Sea geothermal brines (>200,000 ppm TDS; >450 ppm SiO_2; >200°C). Tests were conducted at 90°C and some at 125°C and 220°C. A comparison of the results indicated that scale prevention data at 90°C did not correlate with results at higher temperatures; Figure 5.7 is an example. This

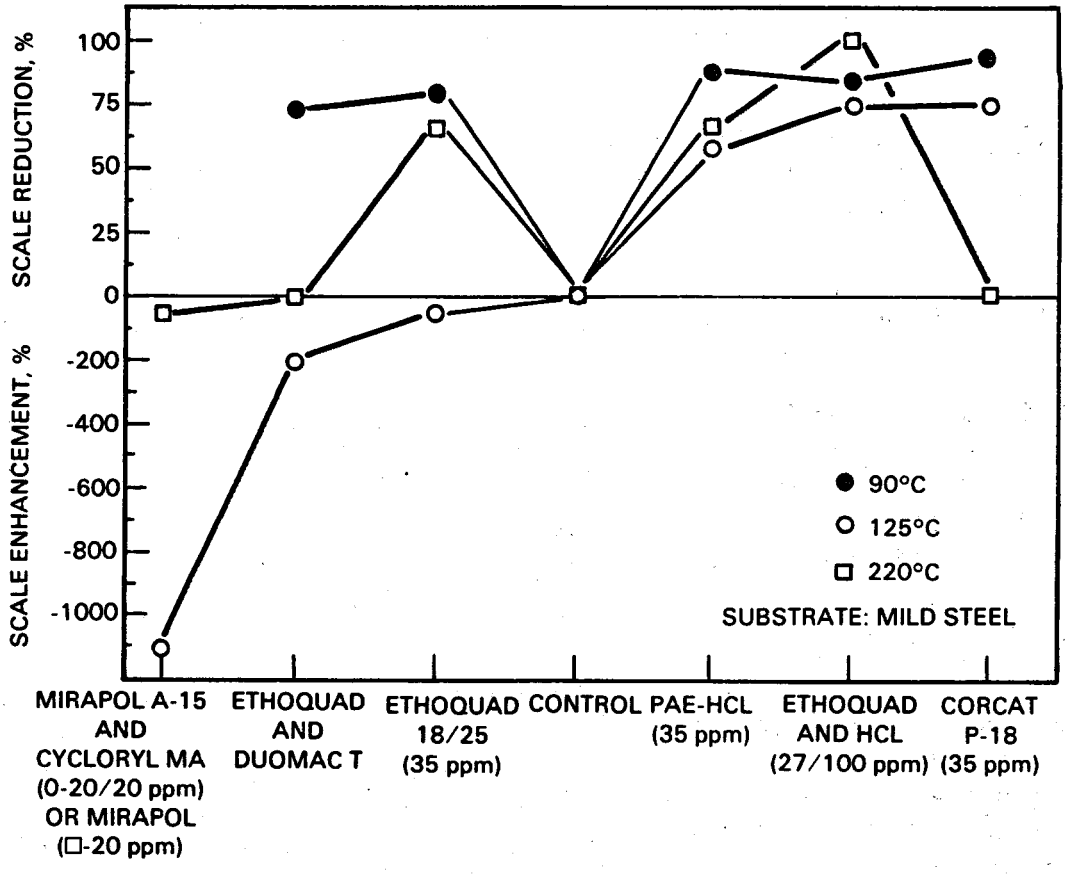

FIGURE 5.7. Relating Silica Inhibitor Performance to Different Temperatures. Poor extrapolation to different temperatures is evident. Data from Harrar, tested in Magmamax-1 brine.

lesson is important to every other investigator; inhibitor testing should (must) be done at process temperatures.

No pure organic inhibitor proved effective at 210°C; only a solution called PAE-HCl (Dynapol, Inc.) had any beneficial effect (probably due to the acid group). Figure 5.8 demonstrates the relative performance of pH control and organic inhibitors at the lowest temperature tested (90°C). Corcat P-18 (Cordova Chemical Co.) and PAE-HCl were effective at 125°C, and the Corcat P-18 also acted as a corrosion inhibitor for mild steel. An examination of Figures 5.7 and 5.8 demonstrates the relative performance advantage that acid has over organic silica inhibitors. Harrar's analysis concluded that chemicals containing ethylene oxide and/or polymeric nitrogen showed the most promise for further testing. He concluded that the most effective inhibitor could probably be a three-way mixture of an organic silica inhibitor (as above), acid (to slow silica precipitation kinetics), and a $CaCO_3$ scale inhibitor (crystals may serve as precipitation sites for SiO_2). Dequest 2060 was suggested as the $CaCO_3$ scale inhibitor.

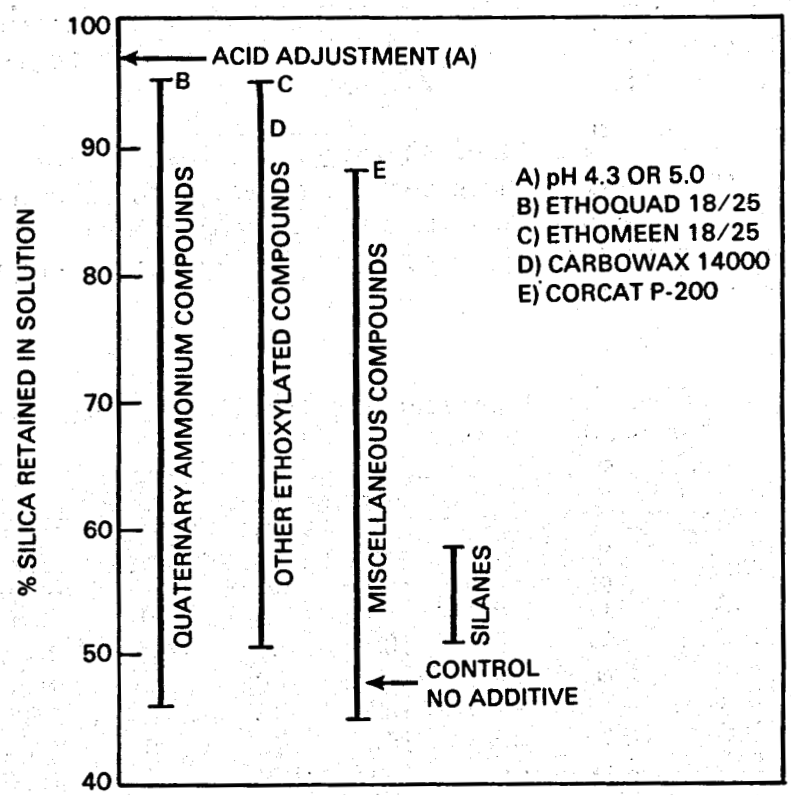

FIGURE 5.8. 90°C Silica Inhibitor Performance (20 ppm concentration in Magmamax No. 1 brine after 1 h). Data from Harrar. In a separate test PAE-HCl performed at point D under slightly different salinity conditions. Relative effectiveness of pH adjustment can be seen.

Chemical inhibitors that proved largely ineffective in Harrar's work at retarding silica growth included: polyacrylates, polymaleic acid, sulfonates, lignosulfonates, phosphate esters, phosphonates, nonethoxylated cellulose derivatives, technical proteins, and silanes. Some inhibitors--including oxysilanes, polyoxypropylane glycols, and a mixture of polyethylene imines--actually behaved as flocculants in mildly acidified brine (pH 4).

The effect of acid and scale inhibitors on the corrosion rate is discussed in Section 6.

Carbonate/Sulfate Inhibition

Oil field brine scale ($CaCO_3/CaSO_4/BaSO_4$) formation has been shown to be inhibited by adding small quantities of aminomethylene phosphonate (Ralston 1969). The effectiveness of this phosphonate is a function of the molecular weight of the compound along with the degree of supersaturation and the temperature. Other phosphonates are being investigated for geothermal use. To date, geothermal experience has witnessed calcite scaling in the production well. It is conceivable that calcite could form during injection, but a treatment process that would lead to this would probably involve foreign water addition, NCG injection, or lime (base) treatment.

Vetter (1972) tested a series of inhibitors at temperatures up to 350°F (177°C). His results comparing phosphonates, esters, and polyelectrolytes to inhibit $BaSO_4$, $CaSO_4$, and $CaCO_3$ as a function of temperature and inhibitor concentration are shown in Tables 5.1, 5.2, and 5.3. The conclusions from this oil-field oriented work are:

TABLE 5.1. Effect of Temperature on Inhibitor Effectiveness for $BaSO_4$ Precipitation[a,b]

Inhibitor Concentration, ppm	% of Precipitation Prevented								
	Polyelectrolyte			Ester			Phosphonate		
	73°F	210°F	350°F	73°F	210°F	350°F	73°F	210°F	350°F
0	0	0	0	0	0	0	0	0	0
2	100	80	0	100	100	0	100	100	0
4	100	90	20	100	100	0	100	100	5
8	100	100	40	100	100	0	100	100	9
12	100	100	60	100	100	0	100	100	30
20	100	100	100	100	100	0	100	100	55
50	100	100	100	100	100	0	100	100	100
250	100	100	100	100	100	0	100	100	100

(a) Vetter 1972.
(b) Initial concentration = 5×10^{-4} mol; NaCl = 0.5 mol = 2.92%.

TABLE 5.2. Effect of Temperature on Inhibitor Effectiveness for $CaSO_4$ Precipitation[a,b]

Inhibitor Concentration, ppm	% of Precipitation Prevented								
	Polyelectrolyte			Ester			Phosphonate		
	73°F	210°F	350°F	73°F	210°F	350°F	73°F	210°F	350°F
0	0	0	0	0	0	0	0	0	0
2	0	0	0	2	0	0	2	0	0
4	15	0	0	60	2	0	4	2	0
8	70	0	0	80	4	0	20	4	2
12	80	0	0	90	10	0	40	6	8
20	80	0	0	90	10	0	40	8	10
50	80	0	0	90	20	0	70	15	20
250	90	0	0	90	30	0	90	80	20

(a) Vetter 1972.
(b) Initial concentration = 0.08 mol; NaCl = 0.5 mol = 2.92%.

TABLE 5.3. Effect of Temperature on Inhibitor Effectiveness for $CaCO_3$ Precipitation[a,b]

Inhibitor Concentration, ppm	% of Precipitation Prevented								
	Polyelectrolyte			Ester			Phosphonate		
	73°F	210°F	350°F	73°F	210°F	350°F	73°F	210°F	350°F
0	0	0	0	0	0	0	0	0	0
2	47	0	0	40	7	0	100	10	7
4	100	0	0	100	10	0	100	20	10
8	100	20	0	100	15	0	100	50	35
12	100	32	10	100	25	0	100	100	38
20	100	35	20	100	55	0	100	100	42
50	100	40	40	100	65	0	100	100	42
250	100	100	50	100	65	0	100	100	45

(a) Vetter 1972.
(b) Initial concentration = 0.08 mol; NaCl = 0.5 mol = 2.92%.

- $BaSO_4$ inhibition - Polyelectrolytes showed the best performance at high temperatures, closely followed by phosphonates. All three types were equally effective at lower temperatures.

- $CaSO_4$ - Phosphonates showed good relative performance at 350°F, but esters were more effective at lower temperatures.

- $CaCO_3$ inhibition - Phosphonates showed fair to good performance up to 350°F, the highest temperature tested. Esters and polyelectrolytes were much less effective.

This work was extended to look at a particular phosphonate inhibitor. Dequest 2060 (Monsanto Chemical) was investigated at a calcite scaling geothermal production well in the East Mesa field and in the laboratory (Vetter and Campbell 1979). The field tests at temperatures of 320°F (160°C) indicated 1 vppm of the inhibitor prevented all scaling while 7.5 vppm precipitated a calcium phosphonate salt from the inhibitor itself. There was some indication that this "inhibitor scale" had retrograde solubility, which could represent a complication when injecting into a warm/hot reservoir.

One additional field study of scaling in East Mesa brines (Lindemuth et al. 1977) involved four inhibitors: Dearborn 8010, Calgon CL-77W, Drewplex 502 (all crystal growth inhibitors), and Calgon SL-500 (a chelating agent). The results are summarized in Table 5.4. Follow-up experiments found that 7 to 10 ppm was the optimum concentration for Dearborn 8010, the most effective of the four inhibitors (Crane and Kenkeremath 1981).

Later laboratory work by Vetter Research (1982) looking specifically at geothermal injection in the Imperial Valley conclued that "the phosphonate inhibitors performed better than inhibitors based on polymers, polymaleic acids, and phosphate esters." This conclusion was severely qualified by:

- inhibitor effectiveness was temperature and time dependent
- inhibitor effectiveness was diminished in the presence of dissolved iron
- when forced to mix incompatible waters, it might be better to remove the $SO_4^=$ ion first rather than rely on the inhibitor to prevent precipitation.

TABLE 5.4. Results of $CaCO_3$ and $BaSO_4$ Scale Inhibition Tests at East Mesa[a]

Additive	Concentration, ppm	Average Ca Recovery,[b] %	Average Ba Recovery,[b] %
Dearborn 8010	25 to 30	140	104
Calgon CL-77W	25 to 30	82	65
Drewplex 502	25 to 30	105	87
Calgon SL-500	70 to 80	128	65

(a) Lindemuth et al. (1977).
(b) Average percentage recovery is the percentage amount of cation in the brine that is removed by the additive; recovery in excess of 100% indicates that additional cation is taken out of the existing scale in the system.

It is significant to note that Vetter, working on calcite scale inhibition, experienced problems in reconciling laboratory and field results just as Harrar, who worked on silica scale inhibition. The lesson is worth highlighting: inhibitor testing should be done under actual process (field) conditions, and most laboratory studies have not reproduced these conditions.

Italian laboratory investigations (Corsi 1984) involving brines with $CaCO_3$ scaling tendencies arrived at the following conclusions:

- Chelating inhibitors are effective.
- These inhibitors (especially Monsanto Dequest 2066) remain effective for 3 h or more.
- Salinity and temperatures below 200°C do not alter the effectiveness of the inhibitors; above 200°C, additional inhibitor concentration is required.
- trace brine constituents (for example, As and Mn) do not influence the results.

Sulfide Inhibitions

Little attention has been paid to inhibiting sulfide precipitation despite the widespread occurrence of these usually dark-colored scales. Conventional wisdom indicates that sulfide scale forms after silica deposition has begun (Austin et al. 1977). Many of the scales found in the Salton Sea (hypersaline) brines are mixtures of silica/sulfide mixtures. Acid is, of course, effective at preventing sulfide precipitation (see Harrar et al. 1982 as an example); but the amount of acid needed to control sulfide has not been studied at various sites. Other sulfide-specific inhibitors have not been investigated.

Despite the common view of sulfide formation being related to silica, sulfide scale has been found in locations where silica scale has not been observed. Shannon, Elmore, and Pierce (1981) noted thin films of sulfide scale on top of carbonate scale during coupon tests in an East Mesa brine. The initial field demonstration of the CO_2 injection process to successfully control calcite scale in the well bore did encounter a thin coating of black sulfide scale (Kuwada 1982).

The lack of knowledge about sulfide precipitation chemistry in brines may present a modest long-term constraint on certain geothermal practices. If sulfide scaling tendencies are present and only waiting for a site to crystallize on, then the formation interface in the injection well might provide those sites and restrict injectivity. Sulfide scale chemistry is an aspect of geothermal power production that would benefit from further research.

5.1.5 Dilution

The dilution technique for water treatment has some potential applications to geothermal injection; however, the problems of implementing it at a particular site have prevented its use. The principle is that water will be added to the brine after it has been flashed, changing the brine chemistry into a nonscaling condition. Of the two major geothermal scales--$CaCO_3$ and SiO_2--this technique would be usable only for preventing the slower SiO_2 formation. The kinetic behavior of $CaCO_3$ deposition is too fast; $CaCO_3$ would deposit before any dilution could take place.

There is interest at some geothermal locations in adding water prior to injection simply to add to the volume, thus making up the water that is flashed to steam to minimize subsidence concerns. The potential problems with the dilution approach include:

- lack of water - Most U.S. hydrothermal resources are located in arid or semiarid regions where water is scarce.

- inappropriate water characteristics - The available water may be chemically incompatible with the brine, actually precipitating scale. Barium, calcium, and strontium sulfates and carbonates might be particularly troublesome. Diluting with steam condensate would solve this problem; however, the condensate would not be available for consumption by the heat rejection cycle (cooling towers).

- suspended solids - A chemically compatible water diluent could still cause problems if it carries suspended solids that plug injection wells.

- temperature - The effect of the reduced temperature on scale solubilities after dilution must be taken into account.

Techniques that might be considered in series with dilution for application at a particular site are: acidification (to prevent scale), inhibitor addition (to prevent scale), or a controlled precipitation technique such as a reactor clarifier. Because these techniques can serve as a water treatment approach without the addition of nongeothermal fluid, it is unlikely that surface water dilution will be considered as a brine treatment option unless: there is a good source of compatible water, silica scaling is the only injectivity problem, and there is a regulatory or reservoir management reason for injecting additional water volume.

The only actual data on the effect of dilution on geothermal brine precipitation is that of Harrar et al. (1977) on the hypersaline Magmamax 1 brine

at 90°C. They were primarily interested in studying the effect of acidification; the dilution tests were of secondary concern. The conclusion was that a 20% dilution was approximately as effective as acidifying to pH 4 or 5 (from the original pH 5.7) in controlling solids formation. Dilution and mild acidification were very effective at reducing solids formation; dilution was approximately as effective as lowering the pH another unit or more. These results are illustrated in Figure 5.9.

There is one conceptual geothermal situation where dilution with chemically compatible water would be a very desirable treatment. If the power extraction step (whether a flash or pumped binary cycle) leads to a brine supersaturated in silica (but only moderately so that the precipitate does not form immediately), then an immediate dilution could be very beneficial in slowing the formation of solids. Such a dilution would probably have to be pumped in against the brine pressure, and any oxygen content in the added water would be corrosive.

No relevant full-scale geothermal experience exists, although Bechtel has developed a conceptual flow sheet using a condensate dilution/reheat approach (Awerbuck, Van der Mast, and Rogers 1982). An Icelandic direct-use application did use 35% wellhead dilution to prevent silica scaling. The resulting large temperature drop is not desirable for power generation unless it is done after steam/brine separation, preferably with a low pH water such as some steam condensates.

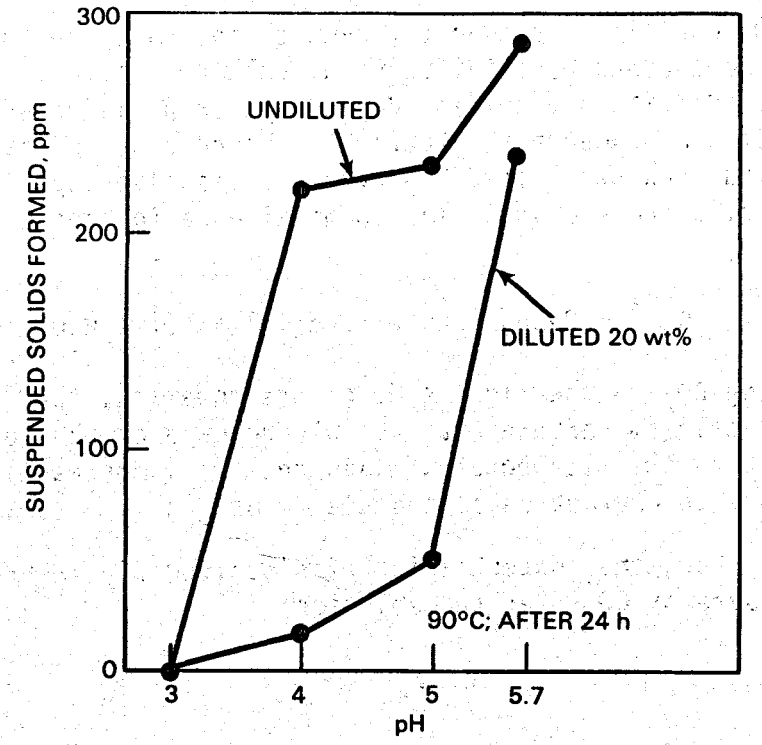

FIGURE 5.9. Effect of Dilution on Solids Formation in Brine as a Function of pH for Magmamax 1 Brine (Harrar et al. 1977)

5.2 CONTROLLED PRECIPITATION

When it is uneconomic to prevent precipitation, it may be possible to design the process so that scale formation occurs at a location and in a form that can be manipulated at minimal cost. Among these techniques is the use of crystallizers, crystallizer-separators, reactor clarifiers, and CO_2 injection. The first three control the location of geothermal scaling to surface vessels and keep the injection well usable. They will be most usable for silica/sulfide/silicate scales that have moderate to slow kinetics; $CaCO_3$ scale, with its rapid kinetics, will probably form in a pipe without waiting to reach the vessel. CO_2 injection is a mechanism to control $CaCO_3$ scaling by shifting the chemical equilibrium and will serve primarily as a production tool rather than as an injection treatment.

Two additional methods of controlled precipitation (aging and adding base) are described in other sections. Aging the brine in a tank or pond, is described in Section 5.3.2 (Sedimentation) because the facilities are of similar design and, perhaps, overlap in purpose. Base addition is described in Section 5.1.3 (Brine pH Adjustment) because of its natural relationship to acid addition.

5.2.1 CO_2 Injection

$CO_2/HCO_3^-/CO_3^=$ equilibria frequently control the pH of geothermal liquids. Many scales can be avoided by acidification; calcite, silica, and sulfides are sensitive to pH. Calcite and sulfide dependence on pH is based on equilibrium factors; the silica dependence is kinetically based. By injecting CO_2, the pH and the equilibrium can be shifted to favor the dissolved species at the expense of the solid scale phase. The chemical equation for calcite scaling can be simplified as:

$$Ca^{2+} + 2HCO_3^- \rightleftarrows CaCO_3\downarrow(\text{scale}) + CO_2 + H_2O \qquad (5.1)$$

Thus, by supplying CO_2 on the right side of the equation, the equilibrium is shifted from the calcium carbonate to the bicarbonate on the left. Calcium stays in solution as the bicarbonate. This chemistry process is the basis for using CO_2 pressure to prevent calcite scale formation.

From Henry's Law, the concentration of dissolved CO_2 is proportional to the applied pressure of CO_2 over the solution:

$$k(CO_2) = P_{CO_2} \qquad (5.2)$$

where k is a proportionality constant (Henry's Law constant). By applying CO_2 pressure to the solution, it can be made unsaturated with respect to $CaCO_3$ (a

nonscaling condition). Ascertaining the amount of CO_2 pressure necessary to prevent scale formation requires a site- and process-specific calculation. Figure 5.10 illustrates the effect of temperature and the concentration of dissolved calcite on the pressure of CO_2 necessary to avoid scale formation. Michels (1981) provides a good discussion of the subject of CO_2 and carbonate chemistry as applied to geothermal engineering. Figure 5.11 relates Henry's Law (expressed in engineering units) as a function of temperature and salinity (Michels 1981).

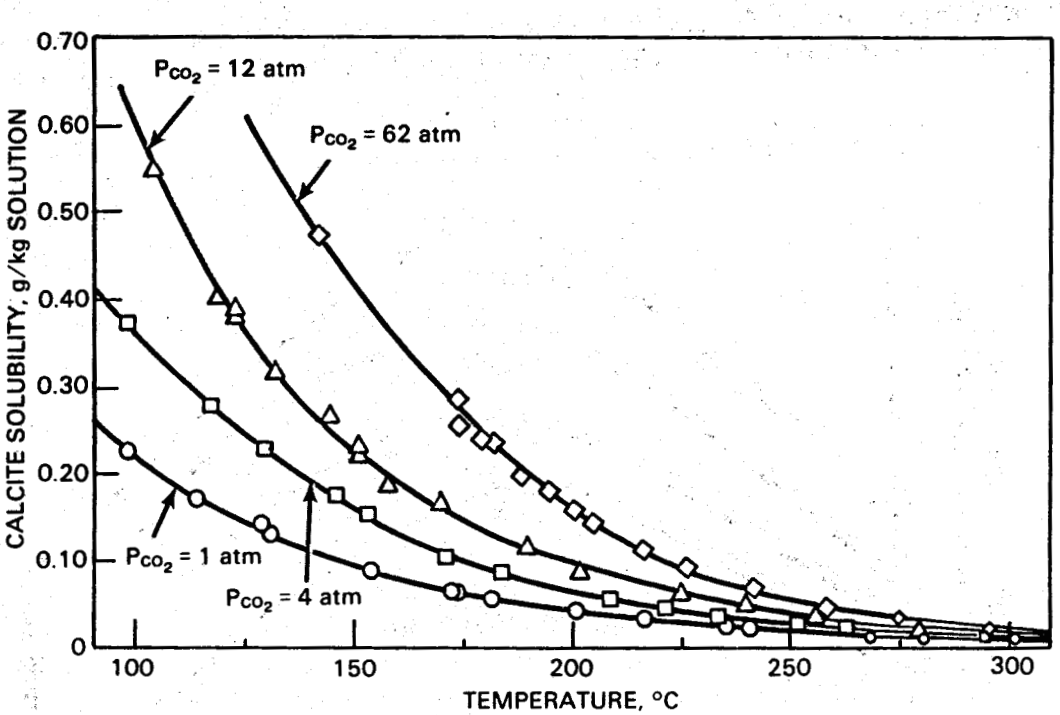

FIGURE 5.10. Solubility of Calcite in Water up to 300°C at Various Partial Pressures of Carbon Dioxide (Ellis 1959a). The solubility values have been revised downward slightly by Ellis (1963). As the temperature increases, the pressure of CO_2 needed to avoid scaling increases rapidly.

The most likely area to use CO_2 injection to control scale and brine flow properties is the production well because this is the area where calcite scale is most likely to form. Calcite scaling in the production well is a common problem in many geothermal fields worldwide.(a)

Scaling in the injection side is also possible if the brine equilibrates at reduced surface temperatures mixed with incompatible waters and is then reheated during injection into warm aquifers (calcite solubility is retrograde with respect to temperature). These conditions could occur during extended brine ponding/aging or if surface waters are mixed with the brine during injection. CO_2 injection has not been demonstrated to benefit silica scale control

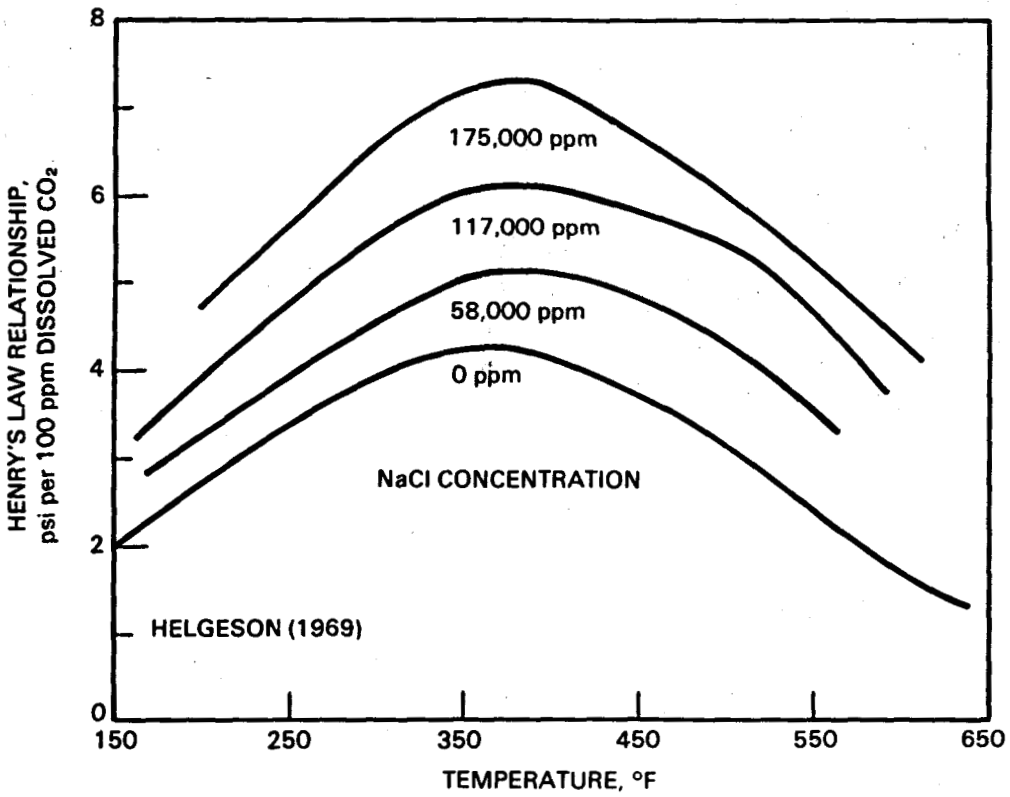

FIGURE 5.11. CO_2-Henry's Law Relationship in Engineering Units as a Function of Temperature and Salinity (Helgeson 1969). Note similarity and agreement with Figure 4.19.

(a) Kizildere (Turkey), Azores, Molagasy Republic, East Mesa, and many basin and range resources are known to have severe $CaCO_3$ scale potential. With this potential, there is an enormous range of CO_2 contents: East Mesa has a CO_2 pressure of 35 ±20 psi; the Niland field is generally above 300 psi (Michels 1981); and Kizildere has a CO_2 content of 15,000 ppm (Kuwada 1982).

efforts. The addition of CO_2 will not drive the pH down into the range that is needed to arrest silica precipitation (pH 4); however, the pH shift may affect marginal silica scaling in some cases and prove to be an effective site-specific treatment.

Production-Side CO_2 Injection

Although this is not primarily an injection treatment process, it is a brine treatment approach that has implications for injection treatment. CO_2 is injected into the producing well below the calcite-forming level by means of tubing. The additional CO_2 pressure in the gas phase keeps the carbonate equilibrium shifted to the nonscaling bicarbonate. The addition of gas also lowers the effective density of the producing fluid and the flow increases (Figure 5.12). All of the pumps and maintenance problems are on the surface rather than downhole, which is an operational advantage when compared with the use of downhole pumps for the same purposes. The conceptual application of CO_2 injection to a flash plant is shown in Figure 5.13. It is a technically interesting and potentially versatile process that warrants additional testing. However, at least partially offsetting the positive features are four items needing attention during detailed design:

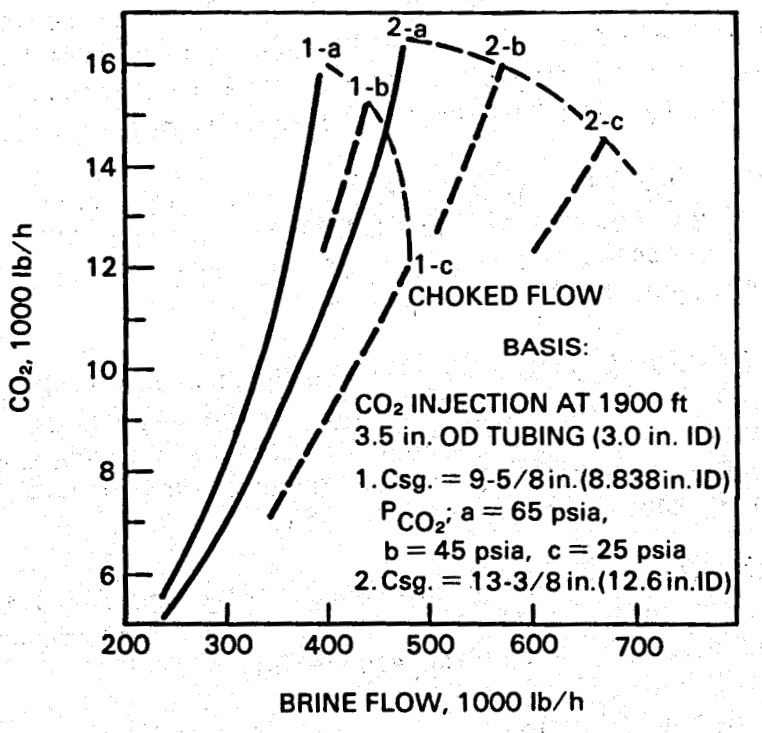

FIGURE 5.12. Effect of CO_2 Injection Rate on Brine Production (Kuwada 1982)

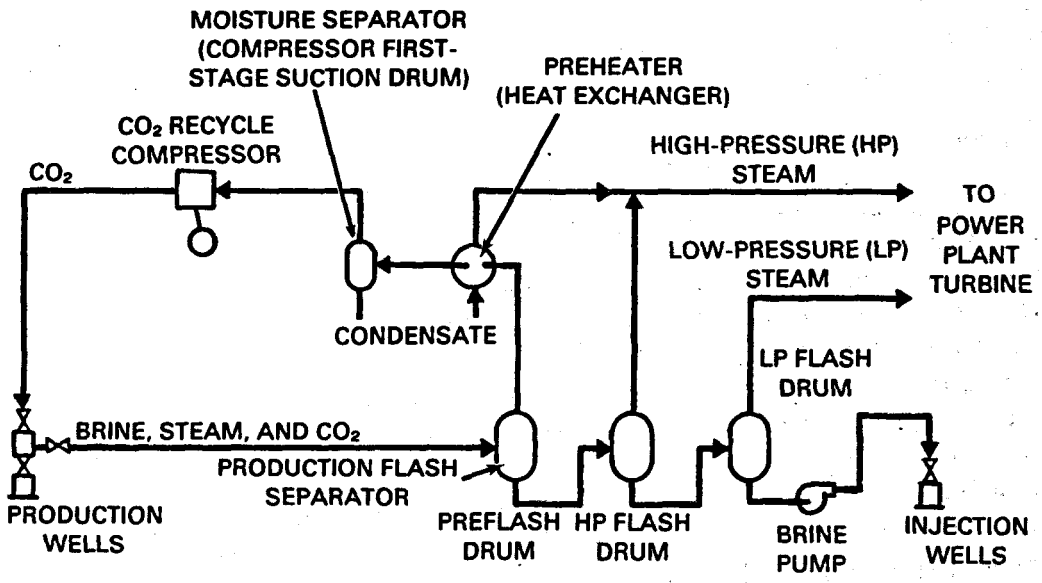

FIGURE 5.13. CO_2 Injection in Flash Cycle Concept (Kuwada 1982)

- $CaCO_3$ will form in the separator when the CO_2 pressure is released during steam flashing. At a test in 1982 at Desert Peak, Nevada, the deposit was easily removed and may have been aragonite rather than calcite. Cycling between two separators may be feasible.

- Non-CO_2 gases (N_2, CH_4) will tend to increase in concentration in the recycled gas because of the differences in solubility. During the Desert Peak test, the recycled gas was only 15% to 20% CO_2 (Rodgers Engineering 1982).

- Although injecting CO_2 does increase brine production in a given configuration, lowering a tube to deliver the CO_2 results in a lower cross-sectional area available and more friction for brine flow. A 3-1/2-in. outside diameter (OD) tube inserted down a 9-5/8-in. OD casing reduces the available area by 16%.

- The extra CO_2 will make the brines more acidic and corrosive. The degree to which this occurs will be site and process material specific and may be of minor consequence.

Injection-Side CO_2 Addition

This process has not been tested because the situation involving $CaCO_3$ plugging of the injection well has not been experienced to date in the United States. A conceptual flow sheet is shown in Figure 5.14.

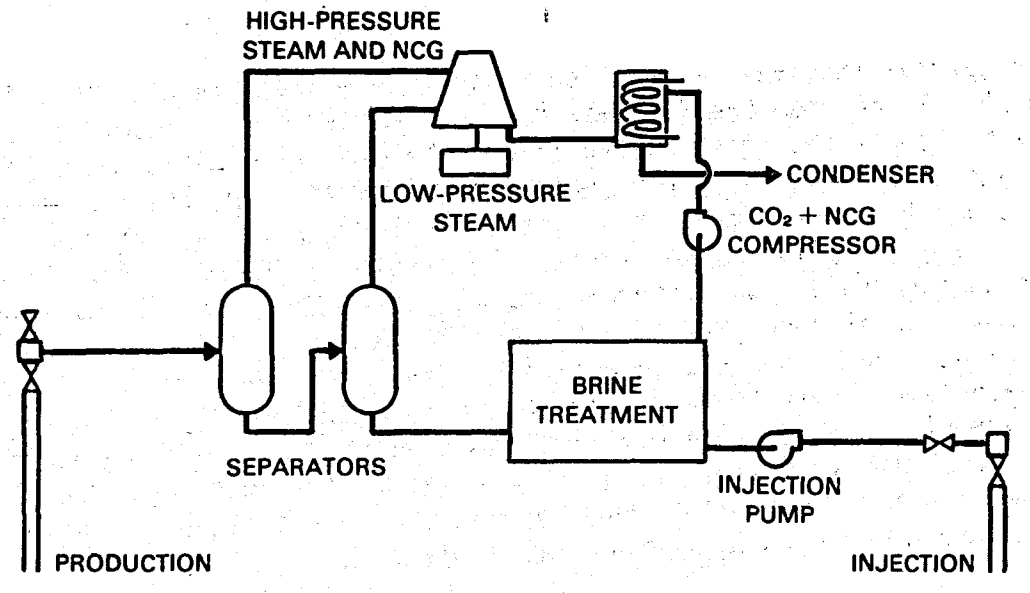

FIGURE 5.14. CO_2 Addition to Injection Flow--Conceptual Flow Sheet

If $CaCO_3$ precipitates during injection, it may be a result of adding slightly incompatible waters or chemicals during brine treatment or concentrating Ca by evaporation prior to injection. A side benefit of injecting the CO_2 and NCG (as shown Figure 5.14) is that nuisance gases such as H_2S are injected.

5.2.2 Flash Crystallizers

Flash crystallizers are a recent innovation developed to reduce or prevent scale formation in flash vessels used for low-pressure steam recovery. This development was an outgrowth of the successful application of a solids-contact clarifier used in a pilot-plant testing program at the GLEF near Niland, California, at the Salton Sea geothermal reservoir (Featherstone and Powell 1981). A solids-contact clarifier (described in more detail in a later section) promotes particle growth by coagulation/flocculation or crystallization, thereby facilitating the settling of the particles. Both particulate growth and sedimentation for clarification of the treated water are accomplished in one unit.

The autocrystallization or precipitation reactions are driven to equilibrium faster when the supersaturated solutions are allowed to contact a preformed sludge. The sludge contains seed particles to promote the crystallization/precipitation processes. Because of the severe scaling problems encountered at some fields in low-pressure flash vessels, pipes, and valves, it was felt that the solids-contact principle could be applied to these vessels to transfer the growth of insoluble matter from the surfaces of the equipment to the sludge particle surfaces.

A natural internal circulation flash crystallizer is illustrated in Figure 5.15. Brine from the first-stage flash vessel is introduced through a pipe in the bottom of the flash crystallizer; the pipe terminates inside a draft tube that is elevated from the bottom to permit fluid recirculation. Flashing takes place inside the draft tube above the influent pipe, and two-phase flow occurs above the point where flashing is initiated (Hedrick 1982). Fluid is driven up the draft tube by the low-density two-phase flow; it is then circulated down the high-density single-phase fluid outside the tube where a substantial portion is recirculated back up the draft tube. Sludge from the solids-contact clarifier is introduced near the bottom of the flash crystallizer vessel and mixes with the recirculating fluid. Effluent consisting of a slurry of sludge with spent brine is withdrawn from the side of the flash crystallizer for further flashing and treatment to reduce supersaturation to a level compatible with underground injection of the spent brine.

The primary purpose of the flash crystallizer is to reduce or prevent scaling in the brine feeding the low-pressure steam system; however, the operation of this equipment is discussed in this section because it initiates the precipitation/crystallization process needed to stabilize the brine for injection. This equipment has successfully controlled scaling problems at the

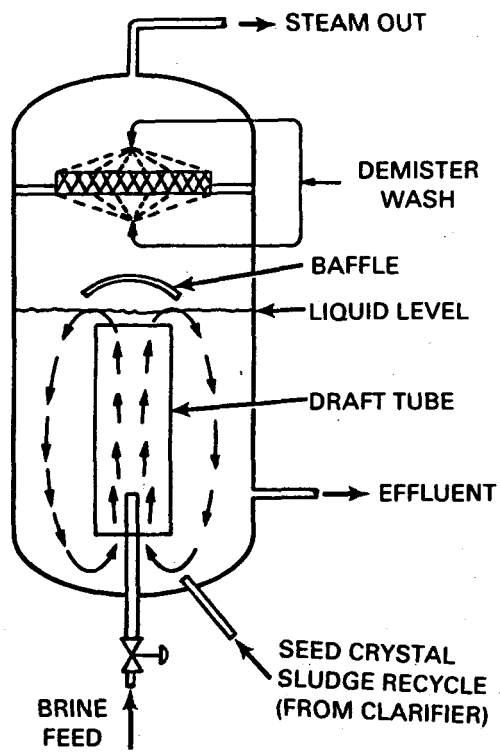

FIGURE 5.15. Natural Internal Circulation Flash Crystallizer

Salton Sea 10-MWe demonstration plant (Chemical Engineering 1983). Detailed proprietary design and operational data on the flash crystallizers used in this plant are not available at this time.

Operational data have been reported by Featherstone and Powell (1981) on the pilot-plant tests conducted with a forced external recirculation flash crystallizer (illustrated in Figure 5.16). This pilot-plant flash crystallizer was initially operated at 11-psig pressure for 760 h with a scale buildup of 0.016 in. on the wall of the crystallizer. Minor scale deposits formed on surfaces in the system where nonturbulent conditions existed (flow velocity = 2.5 ft/s). No deposits formed in later tests at higher flow velocities. Scale was prevented in the crystallizer at optimal operating conditions of 0.5% to 1.0% solids and a residence time of 8 min. Test runs at 1% solids level indicate that the pilot flash crystallizer was operating at near saturation levels of amorphous silica (Table 5.5).

Downhole Injection

The concept of a flash crystallizer with vigorous circulation as a mechanism to promote precipitate formation as particles points to an alternate

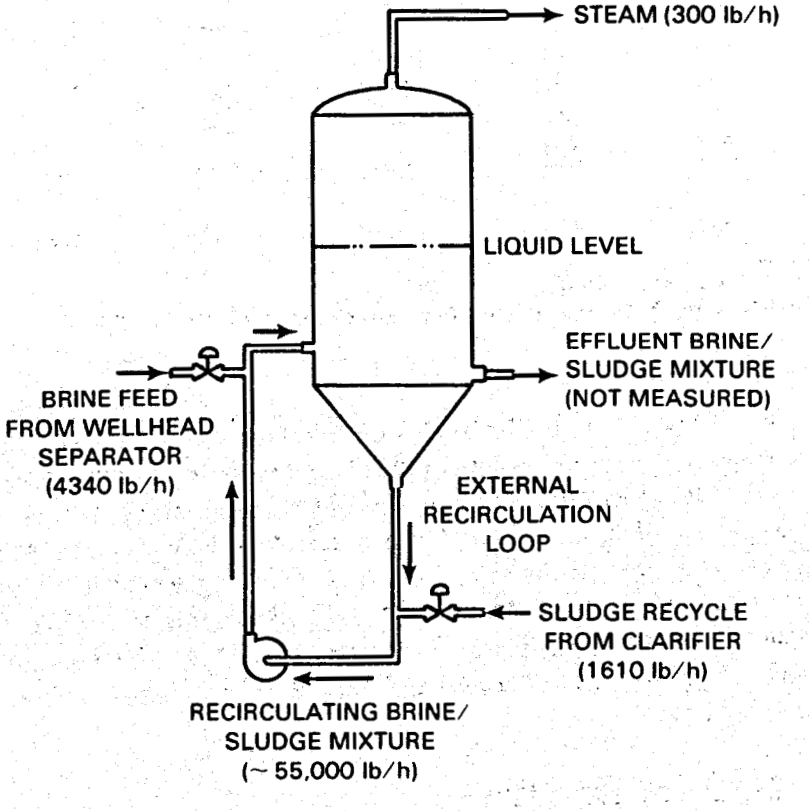

FIGURE 5.16. Pilot-Plant Second-Stage Flash Crystallizer

TABLE 5.5. Silica Solubility in Pilot Flash Crystallizer Tests with Salton Sea Geothermal Brine[a]

Conditions[b]	Sample 1	Sample 2	Sample 3
Crystallizer pressure, atm	1.23	2.59	3.74
Operating temperature, °C	131	146	157
Operating SiO_2 concentration, mg/l	364	388	412

Time After Shutdown, min	Sample 1		Sample 2		Sample 3	
	SiO_2 Concentration, mg/l	Temperature, °C	SiO_2 Concentration, mg/l	Temperature, °C	SiO_2 Concentration, mg/l	Temperature, °C
2	--	--	385	147	--	--
5	370	132	--	--	--	--
6	--	--	362	144	413	153
9	364	131	--	--	415	153
11	--	--	362	143	--	--
12	--	--	--	--	404	152
15	332	129	--	--	--	--
17	--	--	368	142	--	--
18	342	128	--	--	--	--
19	--	--	--	--	396	151
20	--	--	372	142	--	--
22	--	--	--	--	407	151
23	332	128	--	--	--	--
26	--	--	372	141	402	150
28	336	127	--	--	--	--
32	342	126	--	--	--	--
Average constant value	337	129	367	143	402	152

(a) See San Diego Gas and Electric 1980.
(b) Residence time = 8 min; solids concentration = 1% in all runs.

approach. The CO_2 injection technique controlled calcite precipitation by recycling CO_2 downhole; it may be possible to recycle sludge downhole to control silica/sulfide scaling. Since calcite frequently comes out in the wellbore, the presence of sludge seed particulates may reduce narrowing by calcite. Negative aspects might include a dampening effect on production through the injection of a cool dense liquid, although the effect might be modest with a small volume recycle. The use of the producing wellbore as a recycling natural flash crystallizer would appear to deserve testing and/or site-specific evaluation.

5.2.3 Flash Crystallizer Separators

A modification of the flash crystallizer is currently being researched by Bechtel Group Inc. under contract with the Electric Power Research

Institute.[a] The modification involves the addition of a solids-contact clarifier section to a flash crystallizer, which eliminates the need for a follow-up reactor clarifier to achieve a stabilized effluent. A conceptual diagram of the flash crystallizer separator (FCS) is illustrated in Figure 5.17. The FCS concept, which is scheduled for pilot testing in the near future, combines the functions of controlled precipitation and solids separation.

The FCS operates similarly to the flash crystallizer in the center of the unit. Geothermal brine is introduced into a venturi where it entrains a portion of the brine/slurry. Steam is released as the third phase, the solids/liquid vapor mass expands into the enlarged cone. The steam is largely released as it is discharged against the baffle plate and then exits through the top of the FCS. The brine/solids mixture cycles down beside the venturi where a portion again enters the venturi; the remainder flows through the sludge blanket. The particulate matter grows in size and eventually becomes large enough to descend through the sludge outlet at the bottom of the FCS. A

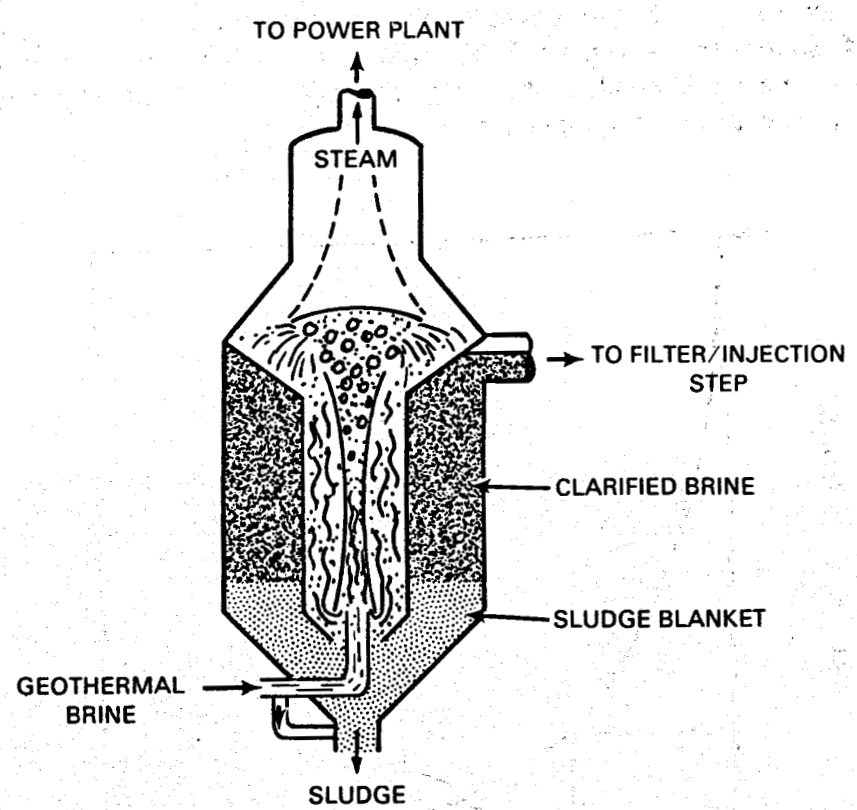

FIGURE 5.17. Flash Crystallizer Separator Concept

(a) Awerbuck and Rogers 1981; Awerbuck, Van der Mast, and Rogers 1982.

small brine flow is maintained upflow through the sludge outlet to return any small particles that escape into the sludge blanket for further growth. Elimination of small particles facilitates any subsequent sludge dewatering step.

The exponential decay equation used to predict the retention time in the Bechtel FCS pilot-plant design to achieve a desired supersaturation level is plotted in Figure 5.18. The value of B in the equation is a function of many factors, including temperature, degree of supersaturation, particle surface area, pH, ionic strength of the brine, and concentration of catalytic agents (for example, fluoride for silica precipitation). As discussed in the section on autoprecipitation, silica deposition becomes very slow as the supersaturation ratio approaches 1.0. The FCS is anticipated to relieve only 80% of the supersaturation. This approach substantially reduces the time requirement in the FCS and minimizes the size of the units. If 80% of the silica saturation is relieved, Bechtel believes that significant scaling in the FCS units and associated piping and equipment will be prevented. The entire system is closed and operates above atmospheric pressure. Long residence times in high-pressure vessels must be avoided or these vessels become very large and very expensive. The residual 20% supersaturation will be eliminated after the second-stage FCS by diluting the brine with condensate from the power plant and by increasing the temperature using a vapor compressor.

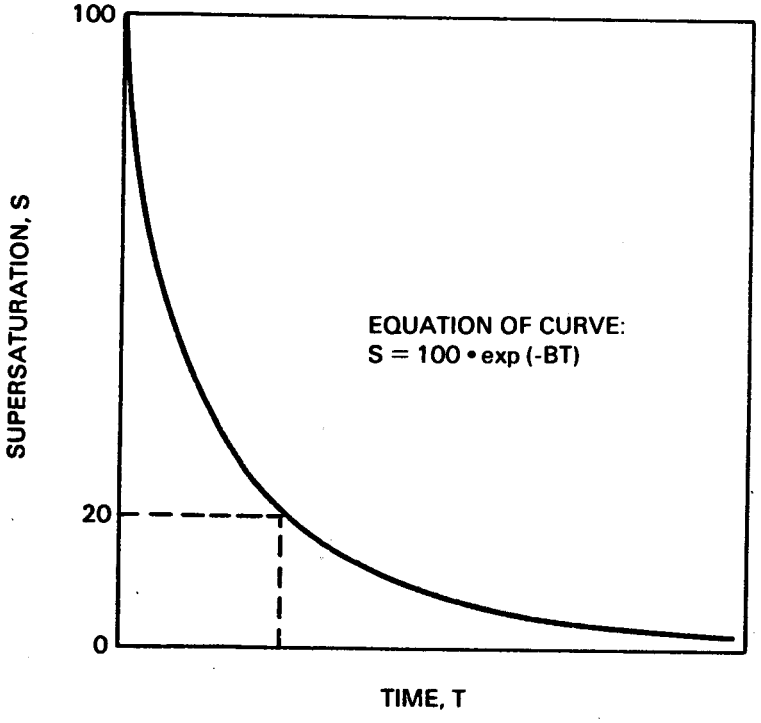

FIGURE 5.18. Predicted Reduction in SiO_2 Supersaturation with Time (curve used by Bechtel for FCS design)

5.2.4 Reactor Clarifier and Fluidized Bed

Process Description

A reactor clarifier controls precipitation and separates particulates and liquids. Reactor clarifiers were originally developed for use in water treatment, although the principles have been successfully used in waste water applications (Culp, Wesner, and Culp 1978). Reactor clarifiers have been particularly useful in settling flocculant and low-density sludges. Sedimentation units of this type have been variously termed solids-contact clarifiers, upflow clarifiers, sludge blanket clarifiers, and many trade names.

Several equipment configurations are offered by manufacturers; a major portion of the volume of the solids-contact clarifier may be taken up by mixing and reaction zones as shown in Figure 5.19. These mixing and reaction zones coupled with the sludge blanket or slurry pool can be very effective for solids removal. Flow enters the clarifier through a pipe to the mixing zone and proceeds to the reaction zone. Chemicals may be added to the incoming stream or directly to the mixing zone to enhance flocculation or sedimentation. The large circulation patterns in these zones provide an opportunity for thorough mixing and particle contact to enhance flocculation or particle growth. Treated waste water leaves the reaction zone and passes through the sludge

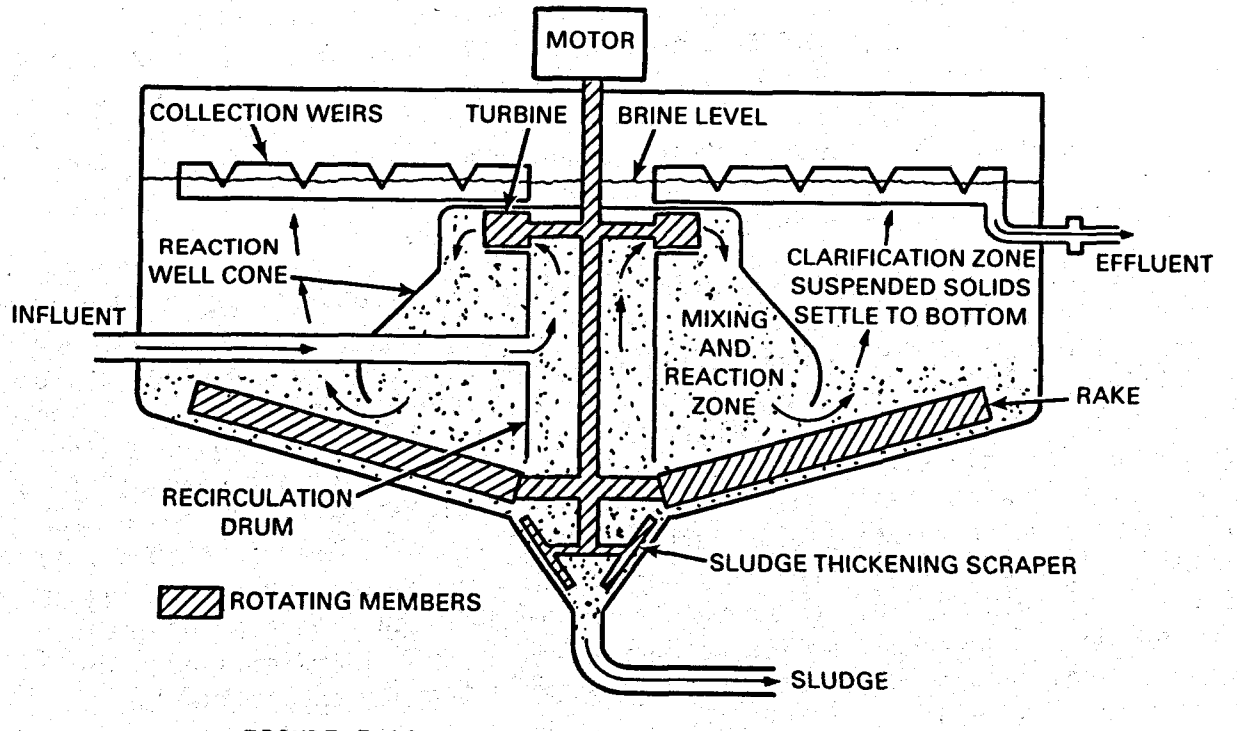

FIGURE 5.19. Solids-Contact Reactor Clarifier

blanket or slurry pool where essentially all of the particulate matter is retained. Clarified water flows up from the sludge blanket and overflows to the effluent line. Sludge is collected in the concentrator and discharged at a rate designed to maintain an optimum solids concentration in the sludge blanket.

Process Application

A full-scale reactor clarifier operated continuously for 10 weeks at the GLEF to evaluate its performance in precipitating and removing silica and other substances (San Diego Gas and Electric 1980). The objective of the operation was to render the spent brine suitable for underground injection, and the equipment was considered to be the fundamental component of the brine injection processing system. Due to the availability of only one production well, flow from the GLEF averaged only 525 gpm during the test period. Since the design flow of the reactor clarifier was 1600 gpm, 680 gpm of clarified brine was recycled from the injection pump to the clarifier. The total average influent flow was therefore 1205 gpm or only 75% of the design flow.

Data from a pilot test program indicated that the best results were obtained when the sludge blanket was carried considerably above the lower outside edge of the reaction zone. It was not possible to achieve this condition in the 55-ft diameter reactor clarifier due to several factors. First, the design flow rate was not attainable; and second, solids settled more rapidly in the large clarifier (2.1 gpm/ft^2) than in the pilot clarifier (1.5 gpm/ft^2), which indicated that the large clarifier could actually be sized for 2300 gpm. As a result, the sludge blanket could not be properly expanded to achieve good particle growth. The pilot clarifier produced an effluent containing 50 mg/l of suspended solids while the full-scale clarifier produced an effluent containing 100 mg/l of suspended solids (average values).

The sludge blanket of a reactor clarifier could contain enough suspended solids so that it would operate with hindered settling (for example, Type 3 settling, discussed in Section 5.3.2). The effective operation of a reactor clarifier depends on maintaining a sufficient solids concentration and sludge blanket depth to reduce silica supersaturation to acceptable levels while achieving particle sizes that settle well. In the case of hindered settling, the settling velocities are inversely proportional to the solids concentration in the zone where the particles settle. Settling rates as a function of suspended solids are illustrated in Figure 5.20. Upflow velocities as high as 2.4 gpm/ft^2 (0.5 ft/min) can be maintained in this reaction zone or sludge blanket when a suspended solids concentration of 0.5% is maintained. The upflow rates must be decreased accordingly when the percent solids is increased. Therefore, a compromise exists between continuous stable production of silica-saturated effluent and the maximum permissible upflow rate in the clarifier. A solids concentration of 1.35% will produce a silica-saturated

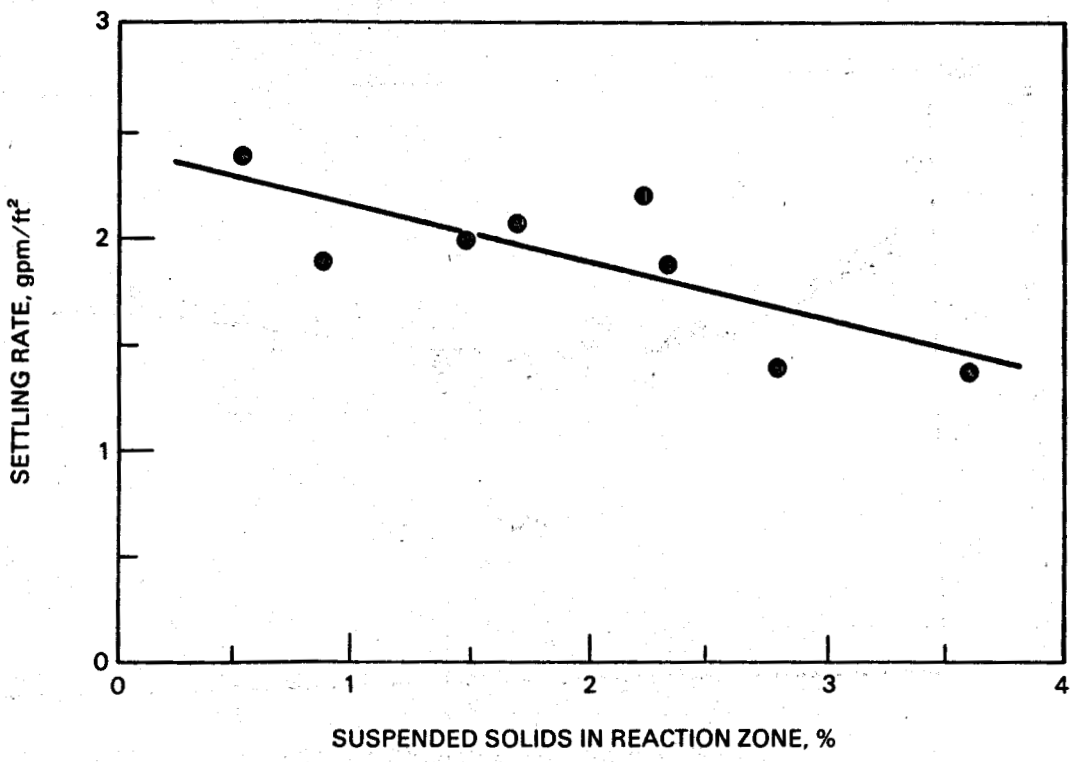

FIGURE 5.20. Settling Rate Versus Suspended Solids Concentration in the GLEF Reactor Clarifier (San Diego Gas and Electric 1980)

effluent (190-ppm SiO_2) (Figure 5.21). An upflow rate of 2.1 gpm/ft^2 is indicated in Figure 5.20 to achieve a solids concentrations of 1.35%. Clarifier manufacturers frequently design these units for about one-half the settling velocity at optimum solids loading. This conservative design gives an upflow velocity of 1.05 gpm/ft^2 at 1.35% suspended solids. A summary of the average measurements of operating parameters for the full-scale reactor clarifier at the GLEF are presented in Table 5.6. Dahlstrom, Moore, and Emmett (1982) report on the GLEF reactor clarifier from an equipment manufacturer's perspective.

Vetter, Kandarpa, and Jackson (1981) reported a 42-day test of reactor clarifier technology at the Mercer 2 well in the Imperial Valley. Increased residence time slightly increased the particle size and the number of particles $\geq$9 µm in size. The most common particle size was 5 to 10 µm in the reaction/growth areas of a reactor clarifier and 5 to 7 µm after the settling (clarifier) portion.

Reactor clarifiers have been used successfully at the Salton Sea demonstration plant since the July 1982 startup. Operational data are not available at this time; however, these units are reported to be operating successfully. No chemical coagulants are used. The output of these reactor clarifiers is

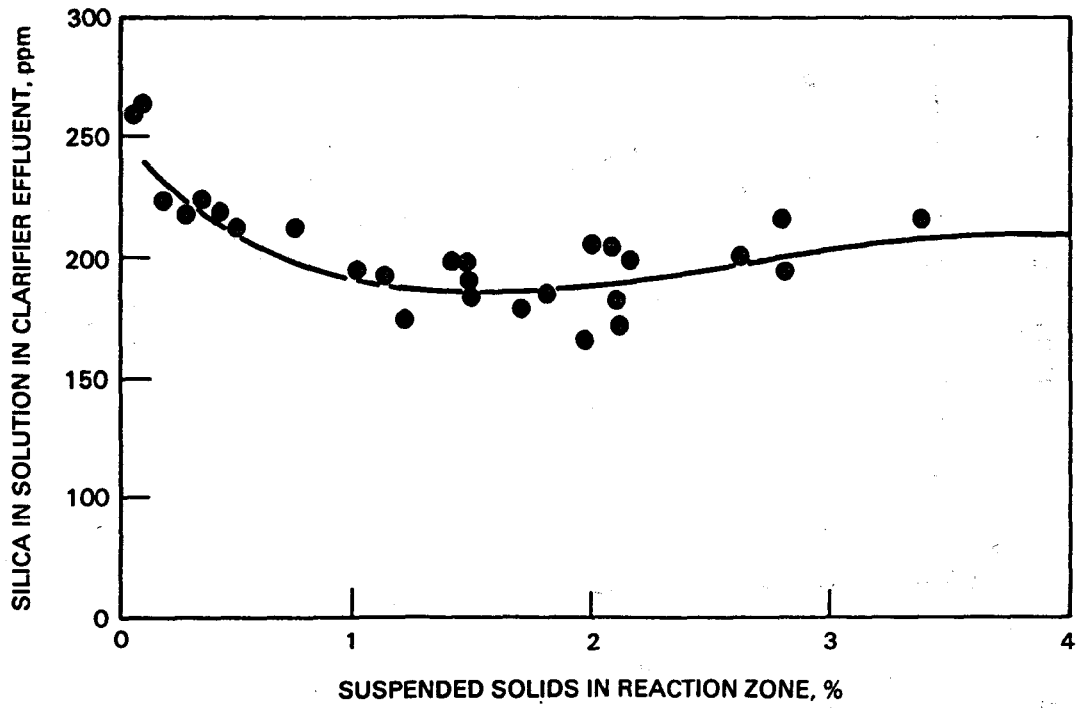

FIGURE 5.21. Silica in Solution in GLEF Clarifier Effluent Versus Suspended Solids in Reaction Zone (San Diego Gas and Electric 1980)

believed to be primarily ≤10-μm silica particulates that range from 50 to 200 mg/l in concentration, depending on the routine/transient nature of the process at that time.

Field experiments at Cerro Prieto in Mexico attempted to duplicate the successful use of the reactor clarifier at the GLEF. Although a pilot-scale commercial unit was used, it did not adequately prevent scale (Hurtado et al. 1981). Dissolved silica at the overflow was 3 to 400 ppm; suspended solids were 250 ppm; and solids in the reaction zone were 0.9%. Cerro Prieto brine has a salinity of 30,000 ppm TDS and silica concentration of 1000 ppm. Other tests indicated that aging, lime addition, and settling produced superior results at this site (Hurtado et al. 1981); this last step was performed in a clarifier, although the lime addition makes it a different process than the natural pH particulate growth of the reactor clarifier at GLEF or the Salton Sea plant.

Fluidized Beds

Fluidized beds, as the generic concept is applied to geothermal brine treatment, are a location where particles are fluidized in the brine flow. In

TABLE 5.6. Operating Parameters for the 55-ft Diameter GLEF Reactor Clarifier[a]

Parameter	Average Measurement
Clarifier influent (brine feed)	Temperature = 104°F Suspended solids = 180 ppm Silica in solution = 390 ppm pH = 5.4 Total flow = 1205 gpm GLEF flow = 252 gpm
Clarifier reaction zone	Suspended solids = 1.8 wt%
Clarifier draft tube	Suspended solids = 2.7 wt%
Clarification zone at a point 50 ft vertically from bottom of side	Suspended solids = 0.06 wt%
Upflow velocity	0.51 gpm/ft^2
Settling velocity	2.0 gpm/ft^2
Clarifier effluent	Temperature = 102°C Turbidity = 15 NTU Suspended solids = 100 ppm Silica in solution = 200 ppm pH = 5.1

(a) See San Diego Gas and Electric 1980.

this position they act as seed crystals to focus the precipitation of (silica) minerals on these crystals. As more precipitation occurs, the particles grow in size until they settle out and are ready for disposal.

If the particles are self-generating scale particles, it is a similar technology to that applied in the reaction sludge blanket zone of a clarifier process (for example, Vetter et al. 1981 and Kandarpa et al. 1981).

If the particles are not self-generating scale particles but are a foreign dense material (perhaps a mineral sand), then the technology is indeed different from that described earlier; it is closer to the usual concept of a fluidized bed. Because of the scale growth, a continuous supply of fresh foreign particulates must be introduced to the fluidized bed unless they are recycled. R. C. Axtmann (1980) patented a process for removing silica via a fluidized bed with particles being recycled after cleaning in a ball mill. This process was

field tested at the New Zealand Broadlands site using a continuous ball mill; the operation/technical details will be available in the fall of 1984.

Two DOE-funded projects[a] looked at the use of fluidized beds to prevent fouling of heat exchangers in binary cycle plants. Tests at East Mesa were effective at preventing calcite and iron sulfide scale on the metal vessel surfaces. To prevent injection plugging, such a heat exchanger would presumably have to be followed by a filter to remove the unadhered scale particles from the brine unless the particle sizes and further scaling tendencies of the brine were compatible with the formation, which is unlikely. Fluidized bed particles with adhered scale would have to be cleaned and the solids separated.

5.3 LIQUID/SOLIDS SEPARATION

The selection of the process to remove solids from geothermal brines requires addressing the following considerations:

- smallest particle size to be removed
- physical properties of the system, such as fluid density, solids density, and viscosity
- solids burden carried by the fluid
- processing rates.

Generally, as the solids burden and the particle size increase, artificial or natural gravity separation becomes the method of choice. Centrifugation is applicable from a submicon range; hydroclones, from ~5 μm up; and settling, from ~1 μm up. As the particle size and the solid burden decrease, filtration and enhanced settling (thickeners; flocculation) become more attractive with respect to power consumption and technical feasibility. Traditional operating ranges are shown in Figure 5.22. The available data indicate that geothermal injection treatments yield particles less than 20 to 30 μm; however, no geothermal data are available on many of the streams and subsystems, especially those that yield larger particles that end up as sludge.

(a) Addomms, Breindel, and Gracey (1978); Allen, Lawford, and Van Haaften (1978).

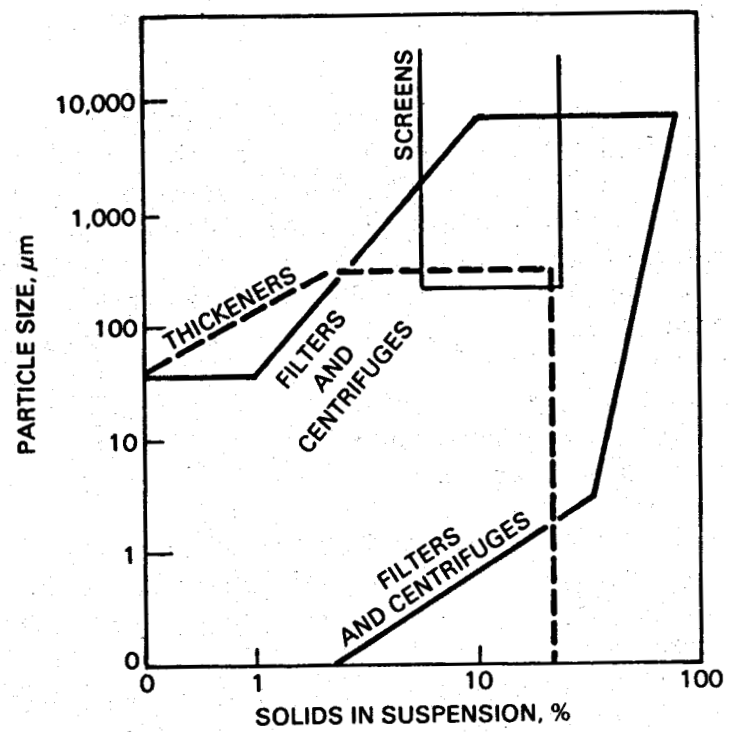

FIGURE 5.22. Operating Ranges for Traditional Liquid/Solids Separation Mechanisms

5.3.1 Chemical Coagulation/Flocculation

Inorganic Coagulants

Effective removal of suspended matter from waste water by sedimentation and/or filtration processes requires that the particles of suspended matter be large enough to either settle in a relatively short period of time or be removed by entrapment in the void spaces of a filter bed. Because a significant fraction of the suspended matter in waste water often consists of particles too small for effective settling or filtration, the aggregation of these particles by coagulation and flocculation into larger, more readily settleable or filterable aggregates is common practice.

Coagulation and flocculation are terms that are frequently used interchangeably; however, in this document, coagulation is defined as a process where chemicals are added to waste water to reduce the forces that keep the suspended particles apart. Coagulation occurs immediately after the chemicals are rapidly mixed into the waste water. Flocculation involves the bonding together of the coagulated particles to form settleable or filterable solids by agglomeration, which is hastened by gently stirring the water to increase the

collision of coagulated particles. Flocculation requires longer time intervals than coagulation. Culp, Wesner, and Culp (1978) discuss these principles in detail.

The detailed mechanisms of coagulation and flocculation are not well understood, and considerable research has been conducted to understand these phenomena. Mechanisms that occur during coagulation and flocculation include: 1) chemical and physical reactions with colloidal particles during coagulation, 2) physical enmeshment or entrapment of particles during flocculation and sedimentation, and 3) adsorption. The relative importance of each of these mechanisms has not been established, but it is believed that all three play a role. Although current theory helps to explain these processes, chemical clarification remains as much an art as a science. To determine the proper dosages of chemicals, laboratory and pilot-plant testing is usually required using the actual waste water to be processed.

Coagulation is generally carried out in a rapid mix or flash mix tank or basin; coagulation reactions are very rapid and occur within 1 s. The rapid mixing disperses the coagulating chemical into the waste water as quickly as possible. The rapid mix tanks or basins are usually equipped with high-speed mixing devices designed to create velocity gradients of 300 ft/s-ft or more with retention times in the tank ranging from 15 to 60 s.

Inorganic chemicals commonly used in waste water coagulation are aluminum sulfate (alum), lime, and iron salts such as ferric chloride. The chemical reactions involved with waste water containing bicarbonate ion or calcium bicarbonate are:

- $Al_2(SO_4)_3 \cdot 14\ H_2O + 6\ HCO_3^- \rightarrow 2\ Al(OH)_3 \downarrow + 3\ SO_4 + 6\ CO_2 + 14\ H_2O$
- $Ca(OH)_2 + Ca(HCO_3)_2 \rightarrow 2\ CaCO_3 \downarrow + 2\ H_2O$
- $FeCl_3 + 3\ Ca(HCO_3)_2 \rightarrow 2\ Fe(OH)_3 \downarrow + 3\ CaCl_2 + 6\ CO_2$.

The addition of sufficient lime to raise the pH to ~11 will also precipitate magnesium hydroxide, which is a gelatinous precipitate and a good coagulant.

Two principal theories have been proposed to explain coagulation and flocculation mechanisms: 1) a chemical theory that assumes that colloids are aggregates of definite chemical structural units and coagulation occurs because of a specific chemical reaction between these aggregates and the coagulating chemical and 2) a physical theory that proposes that colloidal suspension consists of very fine particles that carry an electric charge on their surface. The particles are repelled from one another by this charge, which causes them to remain in suspension. The stability of colloidal suspensions in water is based on the ability of the particles to retain the surface charge. This

charge must be overcome if the particles are to aggregate (coagulate) and form larger particles (flocculate) that settle easily (Metcalf and Eddy 1979). Coagulation is brought about by overcoming the effect of the electrical charge or by reducing the charge, which may be accomplished by adding electrolytes to the solution.

Organic Polymers

Organic polymers (often called polyelectrolytes) may be divided into two categories: natural and synthetic. Important natural polyelectrolytes include those of biological origin and products derived from starch, cellulose, and alginates. The synthetic polyelectrolytes that are currently being used in the water and waste water treatment field can be divided into three categories of long-chained organic polymers: 1) neutral (nonionic), 2) negatively charged (anionic), or 3) positively charged (cationic).

Polyelectrolytes can perform three functions in the coagulation/flocculation of suspended matter in waste water (Metcalf and Eddy 1979). First, the polyelectrolytes can act as coagulants by reducing the charge on colloidal particles. Since waste water colloidal particles are normally negatively charged, cationic polymers can serve as primary coagulants by neutralizing the charges on these particles. Second, bridging can take place whereby the polymers become attached to the colloidal particles at a number of adsorption sites on the polymer. Anionic and nonionic (usually anionic to a slight extent) polymers collect two or more particles along the chain of the organic molecule to form larger masses. These bridged particles become intertwined with other bridged particles to form still larger masses that settle readily. Third, extremely high molecular weight cationic polyelectrolytes not only reduce the charge of the colloidal particles but also form particle bridges.

Polyelectrolytes are often used with inorganic coagulants to improve flocculation. Treatment of certain types of waste waters with inorganic coagulants alone produces very fine flocs that settle slowly. The addition of a suitable polymer prior to the flocculation tank frequently increases the size of the floc and substantially improves the settling process (Culp, Wesner, and Culp 1978).

Acid/Base Treatment

The pH of a geothermal water may be adjusted with an acid or base addition to initiate or accelerate precipitation/coagulation reactions. Lime was used to increase the pH of the Cerro Prieto brine from 7.35 to ~7.8; the treatment was very effective for flocculating silica (Weres and Tsao 1981). These experimental results suggest a simple preinjection brine treatment process that

consists of aging the brine for 10 to 20 min in a closed holding tank, adding 30- to 40-ppm lime, mixing for 5 min, and separating the flocculated silica with a conventional clarifier.

Coagulant Tests on Geothermal Brine

Laboratory jar tests were conducted on GLEF Salton Sea spent brine to evaluate several inorganic coagulants for removing suspended solids (Quong et al. 1978; Quong, Schoepflin, and Stout 1978). The coagulants tested included $FeCl_3$, $Fe_2(SO_4)_3$, MgO, and $Al_2(SO_4)_3$.

The inorganic coagulants proved slightly beneficial; $Fe_2(SO_4)_3$ at 100 ppm was the most effective. The most notable feature of the jar test results was the amount and rapidity of floc formation in the control samples, which was apparently due to mixing of spent brine (see Table 5.7). Significant improvement in sedimentation rate of the coagulated particles and effluent clarity was achieved when coagulation was combined with sludge contact.

Inorganic coagulants were rejected in favor of organic polymers for coagulation and flocculation during the pilot solids-contact clarifier testing at the GLEF. Although inorganic coagulants are commonly used for waste water treatment prior to underground injection, there are no known geothermal water treatment examples prior to injection. Mexican and New Zealand experience has included adding CaO (lime) to remove silica and toxic metals prior to surface disposal.

Polymer Tests with Geothermal Brines

Kochelek and Zienty (1981) tested some of their company's organic flocculants on a heat-depleted Imperial Valley brine processed through a pilot-scale clarifier. These tests involved Tretolite chemical TFL-362 and TFL-4100 (Petrolite Corporation) with residence times of 45 to 90 min. The results showed a reduction in effluent suspended solids that ranged from 29% to 65% with added chemical concentrations in the 1- to 5-ppm range. Their analysis indicated that this could be an economical way to decrease the size of the clarifier and reduce up-front capital expenditures.

Anionic polymers in combination with sludge contact were highly effective for settling solids in jar tests conducted with GLEF spent brine; a 5-ppm polymer dosage was required (Quong et al. 1978). Cationic polymers were somewhat beneficial as coagulants (see Table 5.7), and their effectiveness was substantially improved by sludge contact. A range of 5- to 10-ppm cationic polymer was needed for good sedimentation.

An anionic polymer (hydrolyzed polyacrylamide) was used in pilot testing of a reactor clarifier at the GLEF. A 3-ppm concentration of this polymer was added to the rapid mix tank to precipitate supersaturated silica. The best

TABLE 5.7. Jar Test Results for Chemical Additives with Magmamax No. 1 Spent Brine from GLEF[a]

Test	Polyelectrolyte[b]	Type	Concentration, ppm	Inorganic	Concentration, ppm	Initial Temperature, °C	Final Temperature, °C	Final pH	Observations
1-1	Control	-		-		85	~55	5.5	Rapid floc formation in all tests with only slight improvement with polymer and $FeCl_3$ and alum addition.
2	B-1100	Anionic	1	-				5.5	
3	B-1130			-				5.5	
4	B-1100			$FeCl_3$	200			2.8	Supernatant liquid in Test 4-1 was clear.
5	B-1130			$FeCl_3$	20			5.5	
6	B-1100			Alum	20			5.5	
1-2	Control	-		-		85	~55	5.2	Rapid floc formation in all tests with only slight improvement with polymer addition.
2	B-1175	Cationic	2	-					
3	B-1180			-					
4	B-1185			-					
5	B-1190			-					
6	B-Poly Floc 3	Nonionic	20	-					
1-3	Control	-				82	~55	5.1	Rapid floc formation in all tests with only slight improvement with polymer and $FeCl_3$ addition. Tests 4-3 and 5-3 gave the best results.
2	B-1175	Cationic	2	$FeCl_3$	20				
3	B-1180								
4	B-1185								
5	B-1190								
6	B-poly Floc 3	Nonionic	20						
1-4	Control	-				80	~55	4.9	Rapid floc formation in all tests with only slight improvement with polymer addition.
2	B-1175	Cationic	10	-					
3	B-1180			-					
4	B-1185			-					
5	B-1190			-					
6	B-Poly Floc 3	Nonionic	20	-					
1-5	Control	-				81	~55	5.3	Same as above.
2	B-1175	Cationic	20	-					
3	B-1180			-					
4	B-1185			-					
5	B-1190			-					
6	B-Poly Floc 3	Nonionic		-					
1-6	Control	-				39	NA[c]	5.5	Samples cooled for 1.5 h before testing. Rapid floc formation in all tests with polymer and $FeCl_3$ addition. Test 3-6 gave the best results. Aging for 1.5 h did not appear to help floc formation.
2	B-1185	Cationic	2	-				5.5	
3	B-1185	Cationic		$FeCl_3$	20			5.3	
4	B-1130	Anionic		-				5.4	
5	B-1130	Anionic		$FeCl_3$	20			5.3	
6	-			$FeCl_3$	20			5.2	
1-7	Control					81	~55	5.3	Samples were held at 81°C for 1.5 h before testing. Rapid floc formation in all tests with only slight improvement with polymer and $FeCl_3$ addition. Test 3-7 gave the best results. Aging for 1.5 h did not appear to help floc formation.
2	B-1185	Cationic	2	-				5.3	
3	B-1185	Cationic		$FeCl_3$	2C			5.1	
4	B-1130	Anionic		-				5.3	
5	B-1130	Anionic		$FeCl_3$	20			5.1	
6	-			$FeCl_3$	20			5.1	

TABLE 5.7. (contd)

Test	Polyelectrolyte[b]	Type	Concentration, ppm	Inorganic	Concentration, ppm	Initial Temperature, °C	Final Temperature, °C	Final pH	Observations
1-8	Control					84	~55	5.5	Rapid floc formation in all tests with no improvement noted with polymer, $FeCl_3$, and alum addition in Tests 2-8, 3-8, and 6-8. Supernatant liquid in Test 4-8 was clear.
2	B-1185	Cationic	2	$FeCl_3$	20			6.1[d]	
3	-			$FeCl_3$				6.1[d]	
4	B-1185	Cationic	2	Alum				4.4[e]	
5	B-1185	↓	↓	Alum				5.4	
6	B-1185			Alum	↓	↓	↓	6.0[d]	
1-9	Control					84	~55	5.5	Rapid floc formation in all tests with only slight improvement with polymer and many air coagulant addition. Test 3-9 gave the best results of inorganic coagulants studied.
2	-			MgO	50			5.8	
3	-			$Fe_2(SO_4)_3$	100			5.4	
4	B-1130	Anionic	5	-				5.5	
5	DC Z-6070	Anionic	50	-					
6	UC A-1100	Anionic	50	-	↓	↓	↓	↓	
1-10	Control					86	~55	5.1	Good flocs produced, particularly with higher MgO additions.
2	ZT-646	Anionic	5	MgO	50			5.4	
3	↓	↓	↓	↓	100			5.6	
4					200			5.8	
5					300			6.0	
6					500	↓	↓	6.1	
1-11	Control					87	~55	5.2	Test 4-11 gave the results.
2	-			NaOH	150			5.8	
3	-			MgO	500			6.1	
4	ZT-646	Anionic	5	MgO	500			6.3	
5				-				5.3	
6				NaOH	150	↓	↓	5.9	

(a) See Quong et al. 1978.
(b) B = Betz
DC = Dow Corning
CU = Union Carbide
ZT = Zimmite; ZT 628, 636, 644, 651 also tested up to 20 ppm by company representative; ZT-646 produced best results.
(c) NA - not available.
(d) NaOH added.
(e) HCl added.

clarifier performance produced an effluent with 44-ppm suspended solids, which showed that clarification alone could remove at least 80% of the solids (Quong et al. 1978).

Synthetic organic flocculants (see Table 5.8) and caustic additions were evaluated in the laboratory for removal of silica in Cerro Prieto high and low Ca synthetic brines (Weres and Tsao 1981). These synthetic solutions were buffered with barbital (5,5'-diethylbarbituric acid) to facilitate pH control because carbonate buffering (in natural brines) would be difficult to control under the experimental conditions. In the tests, 300 ml of synthetic brine was rapidly mixed for a few seconds after chemical addition; and then the silica was allowed to settle. Samples were periodically withdrawn from the supernatant for suspended silica analysis (Tables 5.9 and 5.10). A cationic polymer--Magnifloc 573C--gave the most promising results with high Ca synthetic brines, but several others were also promising. None of the organic flocculants was effective with low Ca synthetic brines. Raising the pH to ~7.8 quickly reduced the suspended silica concentration and gave a final value below 5 mg/l in all

TABLE 5.8. Synthetic Flocculants Tested in Synthetic Cerro Prieto Brines[a]

Manufacturer	Name	Chemical
American Cyanamid	Magnifloc 572C	Probably a monomeric quaternary amine[a]
American Cyanamid	Magnifloc 573C	Probably a monomeric quaternary amine[a]
American Cyanamid	Magnifloc 577C	Probably a monomeric quaternary amine[a]
American Cyanamid	Magnifloc 585C	Probably a monomeric quaternary amine[a]
American Cyanamid	Magnifloc 587C	Probably a monomeric quaternary amine[a]
American Cyanamid	Magnifloc 591C	Probably a monomeric quaternary amine[a]
American Cyanamid	Magnifloc 1563C	Cationic polymer; otherwise unknown
American Cyanamid	Magnifloc 2535C	Cationic polymer; otherwise unknown
Calgon	M503	Cationic polymer; otherwise unknown
Calgon	M570	Cationic polymer; otherwise unknown
Calgon	M580	Cationic polymer; otherwise unknown
Calgon	M590	Cationic polymer; otherwise unknown
Dow	Separan CP7	Probably a cationic polyacrylamide
Dow	Purifloc C31	Probably a cationic polyacrylamide

(a) See Weres and Tsao 1981.
(b) American Cyanamid product literature did not identify the chemical nature of their products. However, the Magnifloc 500C series products are stated to be of low molecular weight, and a shipping label on a package of samples identified the contents as quaternary ammonium compounds. The Dow product literature states that most of the products in the Separan and Purifloc series belong to this chemical class.

TABLE 5.9. Flocculation Experiments with High Ca Synthetic Brine[a]

Date	Flocculant	Quantity Used	Initial SiO_2, ppm	Initial pH	Suspended SiO_2, ppm 30 min	Suspended SiO_2, ppm 40 min	Final Suspended SiO_2 ppm	Final Suspended SiO_2 at (min)
12/12/78	None	-	1000	7.40		151	5.6	>96
12/11/78	None	-	1000	7.17	321		3.9	>100
2/02/79	pH raised to 7.77	-	800	7.41	459[b]	20	3.9	>50
12/19/78	pH raised to 7.79	-	800	7.18	<10	<10	1.7	>70
1/05/79	pH raised to 7.74	-	900	7.29	44	15	3.3	>60
12/21/78	pH raised to 8.01	-	900	7.12	460[b]	27	3.5	>48
12/13/78	pH raised to 7.75	-	1000	7.24	15	<10	3.3	>60
6/11/79	MF 572C[c]	2 ppm	1100	7.23	69		>34	>33
5/30/79	MF 572C	2 ppm	1100	7.20	<10		5.0	>30
1/10/79	MF 573C	1 ppm	1000	7.25	449[b]	36	2.4	>50
1/09/79	MF 573C	2 ppm	1000	7.27	576[b]	<10	1.0	>60
4/27/79	MF 573C	5 ppm	900	7.27	<10		4.0	51
1/08/79	MF 585C	5 ppm	1000	7.17	34	13	1.8	>50
6/12/79	MF 591C	2 ppm	1100	7.33	60		>32	>32
12/20/78	MF 1563C	2 ppm	800	7.09	295[b]	26	5.3	>60
12/18/78	MF 2535C	2 ppm	1000	7.23	64	31	13	>67
2/07/79	MF 836A	2 ppm	1000	7.34	78	58	28	>60
2/06/79	MF 836A	20 ppm	1000	7.25	39	40	22	>50
4/30/79	Calgon M 503	5 ppm	1100	7.31	19		3.0	>30

(a) Silca concentrations in ppm; 1 ppm = 1 mg l^{-1}.
(b) Point taken before treatment and within 5 min of stated time.
(c) MF - American Cyanamide Magnifloc.

TABLE 5.10. Flocculation Experiments with Low Ca Synthetic Brine[a]

Date	Flocculant	Quantity Used	Initial SiO_2, ppm	Initial pH	Suspended SiO_2, ppm 30 min	Suspended SiO_2, ppm 40 min	Final Suspended SiO_2 ppm	Final Suspended SiO_2 at (min)
4/13/79	None	-	1094	7.24	253	179	27	>60
4/10/79	None	-	1000	7.26	356	294	32	>60
4/11/79	pH raised to 7.90	-	1000	7.29	<10		2.5	>34
4/17/79	pH raised to 7.83	-	1094	7.30	<10		3.6	>30
5/31/79	MF 572C[c]	2 ppm	1100	7.22	617[b]	243	177	>45
6/04/79	MF 572C	2 ppm	1100	7.34	530[b]	31	26	>40
6/01/79	MF 572C	2 ppm	1100	7.32	278		303	>30
4/24/79	MF 573C	2 ppm	900	7.28	388		310	65
4/18/79	MF 573C	2 ppm	900	7.27	499[b]		32	52
6/05/79	MF 577C	2 ppm	1100	7.36		79	>32	>36
4/16/79	MF 585C	2 ppm	1094	7.32	<10		31	>30
6/05/79	MF 587C	2 ppm	1100	7.32	94[b]		>32	>31
6/06/79	MF 591C	2 ppm	1100	7.31	295[b]		27	>34
5/01/79	Calgon M 570	5 ppm	1100	7.25	92		133	>31
5/02/79	Calgon M 580	5 ppm	1100	7.23	599	144	82	>45
5/02/79	Calgon M 590	5 ppm	1100	7.30	149		174	>30
4/12/79	Purifloc CM[d]	2 ppm	1000	7.27	58		30	>32
4/20/79	Separan CP7[d]	2 ppm	900	7.25	503		338	>28
4/19/79	Separan CP7	2 ppm	900	7.41	230[b]	55	0.7	>44
4/11/79	Separan CP7	2 ppm	1000	7.37	39		24	>33
5/01/79	Separan CP7	5 ppm	1100	7.30	18[b]		21	>28
4/25/79	Separan CP7	7 ppm	1000	7.27	170		>31	>35

(a) Silica concentrations in ppm; 1 ppm = 1 mg l^{-1}.
(b) Point taken from the treatment and within 5 min of stated time.
(c) MF - American Cyanamid Magnifloc.
(d) Purifloc and Separan are Dow products.

tests for both high and low Ca brines. Due to the high cost, the slow decomposition at high temperature, and probable difficulty in maintaining a convenient supply, the organic flocculants were less desirable compared with lime, which is inexpensive, readily available, and very effective for accelerating the formation of a good settling silica floc.

5.3.2 Sedimentation

Gravity Sedimentation

The four distinct phenomena that take place during sedimentation are referred to as sedimentation Types 1, 2, 3, and 4 (Figure 5.23). Type 1 sedimentation can be described mathematically by Stokes' Law, which applies to the unhindered settling velocity of discrete particles in a quiescent liquid suspension:

$$U_c = \frac{g(\rho_s - \rho)d^2}{18\,\mu} \qquad (5.3)$$

where U_c = settling velocity
g = gravitational constant
ρ_s = density of particle
ρ = density of fluid
d = particle diameter
μ = viscosity of fluid.

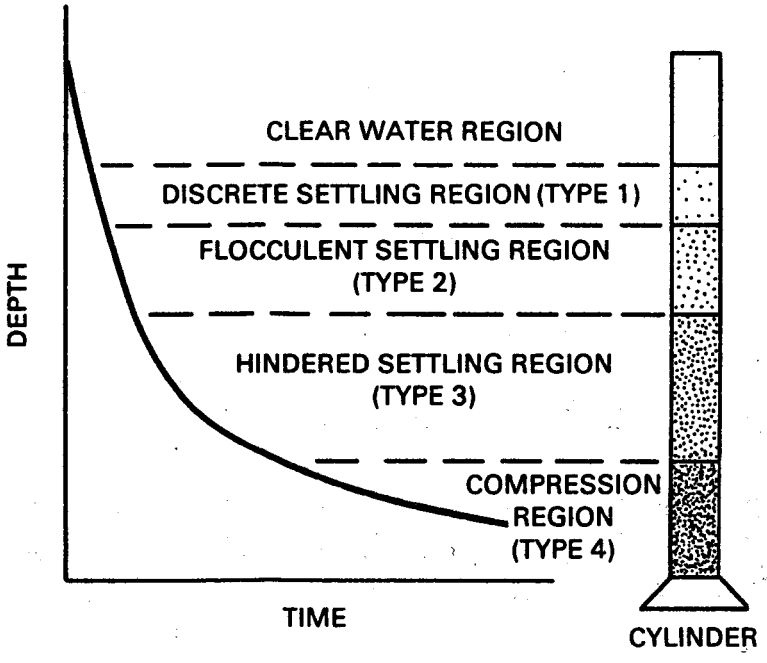

FIGURE 5.23. Sludge Settling Zones

Since the viscosity of water decreases with increasing temperature, settling velocity and hence clarifier efficiency increases with temperature (provided thermal convection currents are minimal).

In practice, a particle with a characteristic U_c value is selected and the basin is designed so that all particles with settling velocity greater than U_c are removed in the basin. The basin then produces clarified water at the rate Q:

$$Q = AU_c \tag{5.4}$$

where A is the area of the basin. Thus, Type 1 settling is independent of basin depth; however, for particles to completely settle to the tank bottom and at the same time optimize the tank size, the following relationship should be used:

$$U_c = \frac{\text{tank depth}}{\text{retention time}} \tag{5.5}$$

The actual design is more complicated than this in that nonideal factors such as inlet and outlet turbulence, short circuiting, sludge storage, and currents resulting from sludge removal must be accounted for.

Type 2 settling occurs when the particles in relatively dilute solution do not settle independently but coalesce. As this occurs, the particle mass increases and the settling occurs more rapidly. The rate at which flocculation occurs varies with opportunity for particle contact. Hence, particle concentration, size ranges, basin size, depth and overflow rates, and velocity gradients all play a part. The complexity of this system does not readily lend itself to mathematical analysis. Type 2 settling is normally studied by using a model consisting of a transparent tube that is 15 cm or more in diameter and ~3 m high (Metcalf and Eddy 1979). Sampling outlets are located ~60 cm apart along the vertical dimension (Figure 5.24). Quiescent settling in a model basin must be corrected for less than optimum conditions in actual operating units. Model detention times are therefore multiplied by a factor of 1.25 to 1.5 to obtain design settling times.

Type 3 settling (zone settling) occurs when the suspension concentration is sufficient for hydraulic characteristics and interparticle forces to cause particles to maintain the same relative position as they settle. The result is a discrete "blanket" or zone that may be observed in the settling basin or model.

Type 4 settling (compression settling) occurs when particles settle near the bottom of the sedimentation basin. Compression settling results when there is physical contact between particles and a structure is formed. The resulting mass compresses slowly under its own weight (see Figure 5.23). Type 3 and Type 4

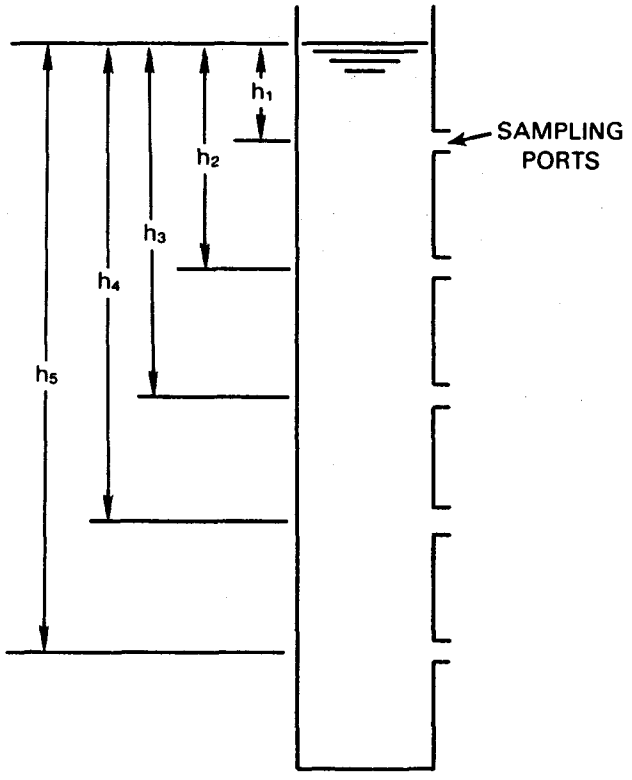

FIGURE 5.24. Laboratory Settling Model and Apparatus

settling have not been satisfactorily analyzed mathematically. The area requirement for Type 3 settling may be determined using laboratory data from a transparent tube.

Plain Sedimentation and Aging

Plain sedimentation is a well-established process that is used for removal of settleable and floatable matter from waste water. The process involves quiescent containment of waste water for a sufficient period of time to allow some or all of the suspended matter to settle out or float to the surface of the waste water. In its simplest form as a batch process, a given volume of waste water is transferred to a vessel or basin and held there until essentially all the settleable and floatable matter separates. Floating matter may then be skimmed and the clarified waste water decanted for discharge or further treatment. Sludge that collects in the vessel or basin is removed after several batches of waste water have been processed. Sludge removal may be a manual operation using shovels or front-end loaders to transfer the sludge to containers for disposal. Sludge transfer from a batch settling vessel can be facilitated by constructing the vessel with a conical bottom to route the sludge through a valve into a container or transfer line (Figure 5.25). The conical bottom could be sloped for sludge

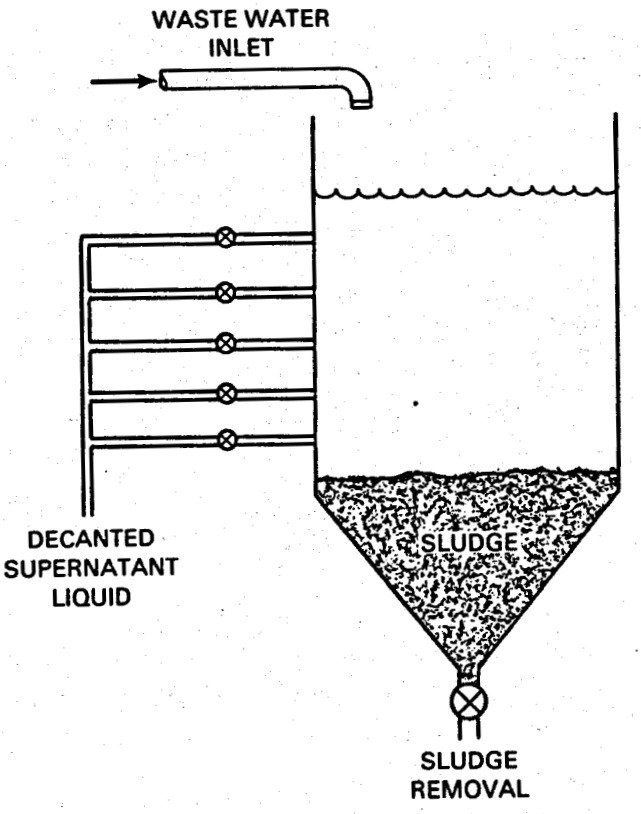

FIGURE 5.25. Batch Sedimentation Tank

drainage; however, a scraper to sweep the bottom may also be included. Outlets equipped with valves are located on the side of the vessel for decanting the supernatant liquid after settling is complete.

Large settling ponds may be constructed where sufficient land area is available. These ponds are frequently sized to contain several days output of waste water (nongeothermal practice), thereby achieving quiescent conditions for settling while waste water flows continuously into and out of the ponds. The ponds are drained periodically to remove sludge collected on the bottom of the ponds. Cooling the water in large outdoor ponds or lagoons can inflict an economic penalty by cooling the geothermal reservoir if this water is injected. Large settling (evaporation) ponds are used at Cerro Prieto; however, no solids separation is attempted.

"Aging" the brine in a pond or a tank can be done to permit silica particles to grow and take the solution closer to equilibrium. It is essentially the same process as sedimentation except that it is done at the point where particulates form. Contacting the brine with air (oxygen) seems to accelerate the formation of silica precipitates after an initial period for nucleation (Brown and McDowell 1982). Aging is an inexpensive option.

At the 10-MWe Brawley plant, Union Oil has tried ponds for aging the brine prior to injection. Although the details (temperature, residence time, etc.) are not publicly available, it is known that the overall system performance was unsatisfactory for this high-temperature, hypersaline brine; scaling and well plugging resulted. Rothbaum et al. (1979) report that ponding was unsatisfactory as a scale control technique in New Zealand; however, Yanagase, Suginohara, and Yanagase (1970) reported that tests at the Otake field showed that 1 h of pond settling reduced the silica scaling by 90%. At Otake, ponding is not practiced routinely (immediate injection is followed); however, at adjacent Hatchobaru field ponding for 1 h prior to injection is practiced, although silica separation/sedimentation is not attempted. After 1 h of aging, the gel does not adhere to pipe walls, and the suspension is injected. A 20% annual loss of injection capacity results (Yoshida, Tanaka, and Kusunoki 1983). Thermal degradation of the production wells and tracer tests indicate a fractured system that explains the fair tolerance for the minimal brine treatment process.

Tests at Cerro Prieto showed that a good process for clarifying their brine included aging for 10 to 15 min followed by lime addition and sedimentation in a clarifier (Hurtado et al. 1981). Effluent suspended solids were ~30 ppm--almost a factor of 10 less than the GLEF-type reactor clarifier.

Ponding/aging is the sole treatment for waste brine at the 3-MWe Hawaii power plant; however, injection is not practiced. Instead, the brine is allowed to percolate into the porous lava. These experiences indicate that surface ponds may have a place as a component in a brine treatment process, but it is unlikely that they will be sufficient by themselves. As described earlier, the treatment must be matched to the injecting formation (and the brine).

Conceptually comparing the plain settling tank/pond with the flash crystallizer in geothermal flows indicates why the crystallizer may yield superior results. The flash crystallizer with its recirculating crystals encourages large particulate growth, while the settling pond encourages large particulates to settle out early and perhaps lead to more smaller particles at the exit that do not have a chance to settle out.

When sufficient land area is not available and relatively large volumes of waste water with low suspended solids concentrations (for example, <1000 mg/l) must be treated, more sophisticated units (clarifiers) are usually employed. Geothermal usage would normally fit these guidelines. These clarifier units are engineered to achieve maximum settling rates for a given volume and configuration. Many configurations have been developed to increase the rate of settling per unit volume of clarifier. Figure 5.26 shows a diagram of a conventional circular clarifier. Influent flows continuously through the inlet to a well at the center of the clarifier that is baffled to prevent excessive velocities. The waste water flows radially outward from the well to a peripherally mounted

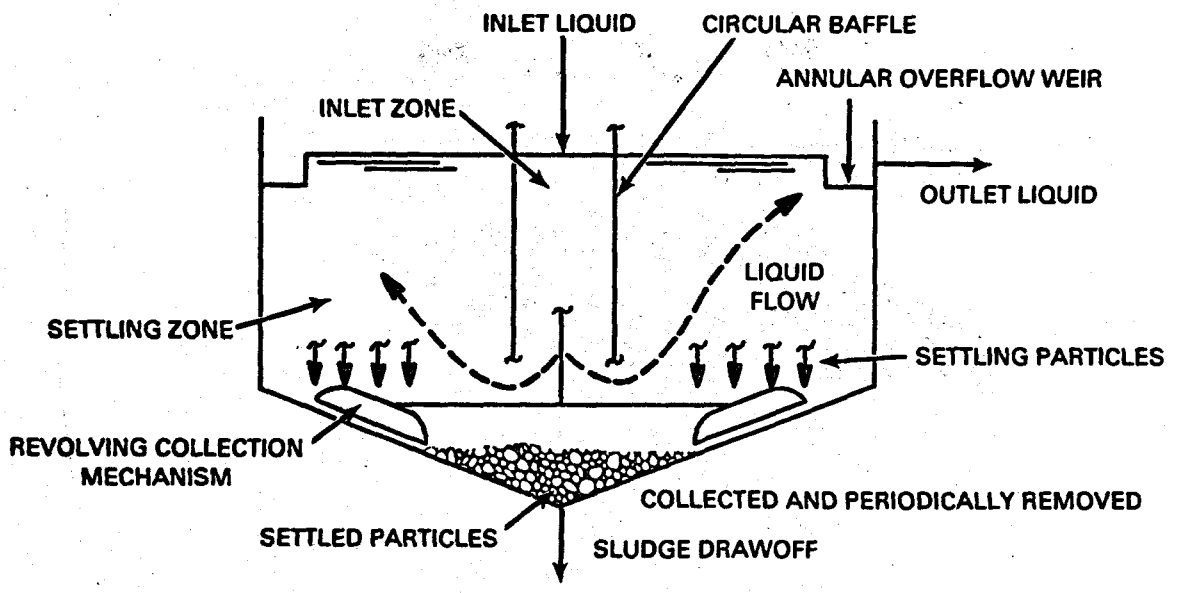

FIGURE 5.26. Circular Clarifier Design

serrated weir protected by a baffle to prevent stray currents from disturbing the quiescence of the waste water. The clarifier is equipped with radial rotating collector arms that move along the bottom to move settled sludge toward the center for continuous or periodic removal. A radial arm or skimmer can be included to sweep the surface to remove floating matter.

High-Rate Settlers

The Type 1 sedimentation process is a function of area and is independent of the depth of the clarifier. It has long been recognized that solids removal could be accomplished within a few minutes if shallow basins could be used to reduce the free fall distance of particles. Early prototypes of such equipment were unsuccessful due to problems with flow distribution and sludge removal. One such attempt involved inserting layers of horizontal plates into a settling basin, which had the effect of many shallow sedimentation basins stacked on top of each other.

Commercial high-rate clarifiers have been introduced in the past two decades. These units use the shallow depth settling concept in slightly inclined or steeply inclined tube settlers. This type of clarifier is useful where space is limited or where the capacity of an existing conventional clarifier must be increased. One type of high-rate settler--a Lamella settler--is illustrated in Figure 5.27. Experiments conducted at the Los Azufres geothermal field in Michoacon, Mexico, indicated that residence time in a settler can be reduced from 120 min to 5 min by using a Lamella settler for lime-precipitated solids in spent geothermal brine (Martinez et al. 1983). This 24-fold reduction in tank size

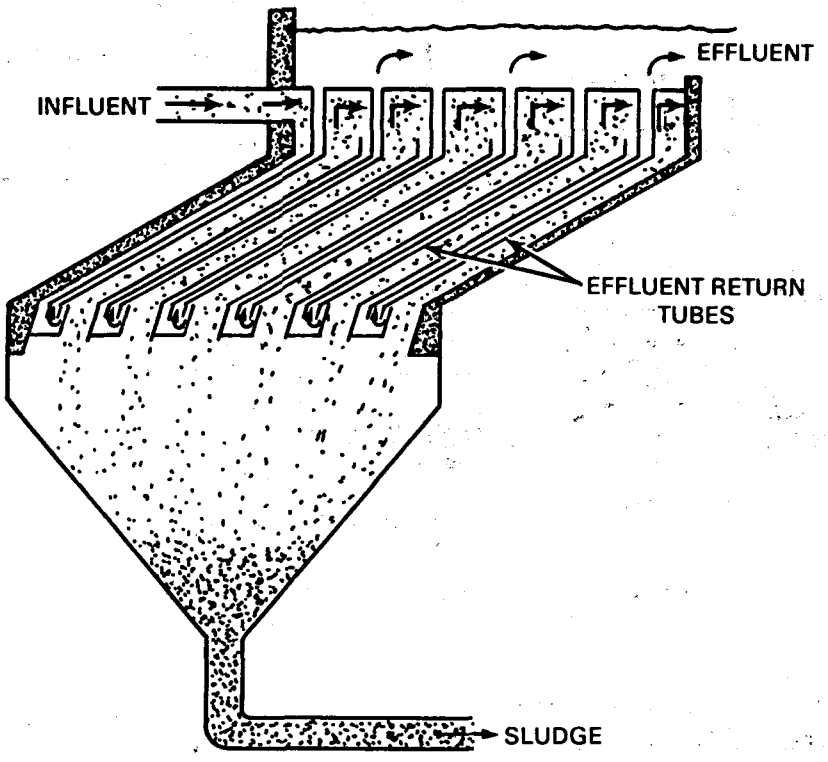

FIGURE 5.27. Lamella Settler Design (Culp, Wesner, and Culp 1978). Several variations of this design are commercially available.

could greatly reduce equipment costs. More than 95% of the suspended solid was removed with a pilot-plant Lamella separator from lime-treated brine at the Los Azufres field.

Gravity Thickeners

Gravity thickeners concentrate slurries containing large amounts of suspended solids (for example, sludge from a gravity clarifier or solids contact clarifier). A diagram of a gravity thickener used at the GLEF is shown in Figure 5.28. Gravity thickeners normally operate with Type 3 settling; therefore, a settling model (for example, graduated cylinder) must be used to obtain data for design purposes. The area required for thickening is determined by filling the settling model with a uniform suspension with a known solids concentration. The position of the interface is then recorded at various time intervals; the height of the interface is plotted on a graph as a function of time; and a line is drawn through the points as illustrated by the curve in Figure 5.29. The area required for thickening is computed from the following equation (Talmadge and Fitch 1955):

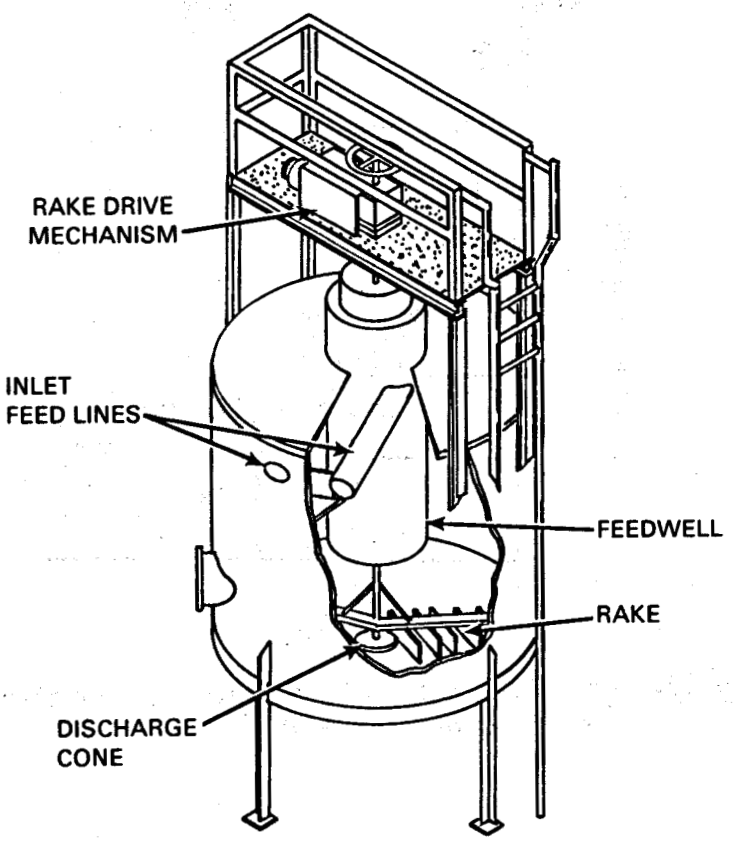

FIGURE 5.28. Gravity Thickener Used at the GLEF (San Diego Gas and Electric 1980)

$$A = \frac{Qt_u}{H_o} \tag{5.6}$$

where A = area required for sludge thickening, m^2
Q = flow rate into thickener, m^3/s
t_u = time to reach desired underflow concentration, s
H_o = original height of interface in column, m.

Tangents are drawn from the hindered settling portion of the curve and the compression portion. The critical concentration (C_2), which controls the sludge-handling capability of the thickener, is determined by dissecting the angle formed by the tangents. A horizontal line is drawn at depth H_u that corresponds to the desired sludge underflow concentration C_u. The value of H_u is computed as:

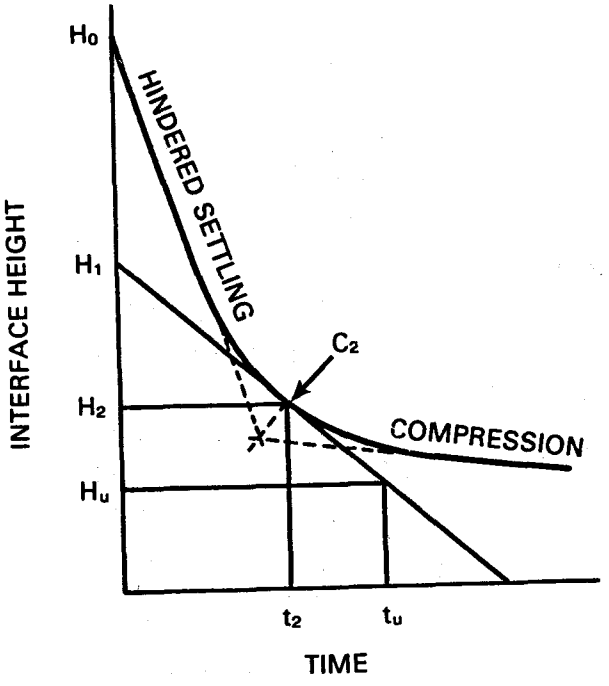

FIGURE 5.29. Graphical Analysis of Interface Settling Curve (Talmadge and Fitch 1955)

$$H_u = \frac{C_o H_o}{C_u} \tag{5.7}$$

where C_0 = the initial solids concentration.

A tangent to the settling curve at point C_2 is constructed, and a vertical line is drawn to this tangent where it intersects with line H_u. The point on the X axis where this vertical line intersects is t_u, and the value of t_u is used in Equation (5.6) to determine the area requirement.

Centrifugation

The gravity solids/liquid separation can be accelerated by increasing the force of gravity and therefore the particle settling velocity. Particle dynamics determine the relationship between particle velocity (U_p), processing rates (q), and the required area (A) perpendicular to the particle velocity.

For gravitational separation within centrifugation or settling, the following relationship applies:

$$U_p \geq \frac{q}{A} \qquad (5.8)$$

Assuming that Stoke's law can be applied, the particle velocity can be described by Equation (5.3).

Since the apparent force on the particle as determined by $P_s - P$ is linear with U, g can be interpreted as the product of N times the gravitational constant, where N is the number of g's conventionally used in centrifugation. The particle settling velocity depends on the square of the particle diameter.

Using these calculations, Figures 5.30 and 5.31 were prepared to assist in determining the minimum requirement for separation based on 100 gal (minimum geothermal fluid with the density and viscosity listed). In a practical case, hydraulic and mechanical instabilities will increase the requirements, depending on design and flow control characteristics of the system.

The relationship between the particle diameter and the required area for settling and for g parameters of 10, 100, and 1,000 is shown in Figure 5.31 The projected power requirements for a centrifuge design with radius equal to the length are presented in Figure 5.30. The power necessary for a given separation requirement can be determined from the figure.

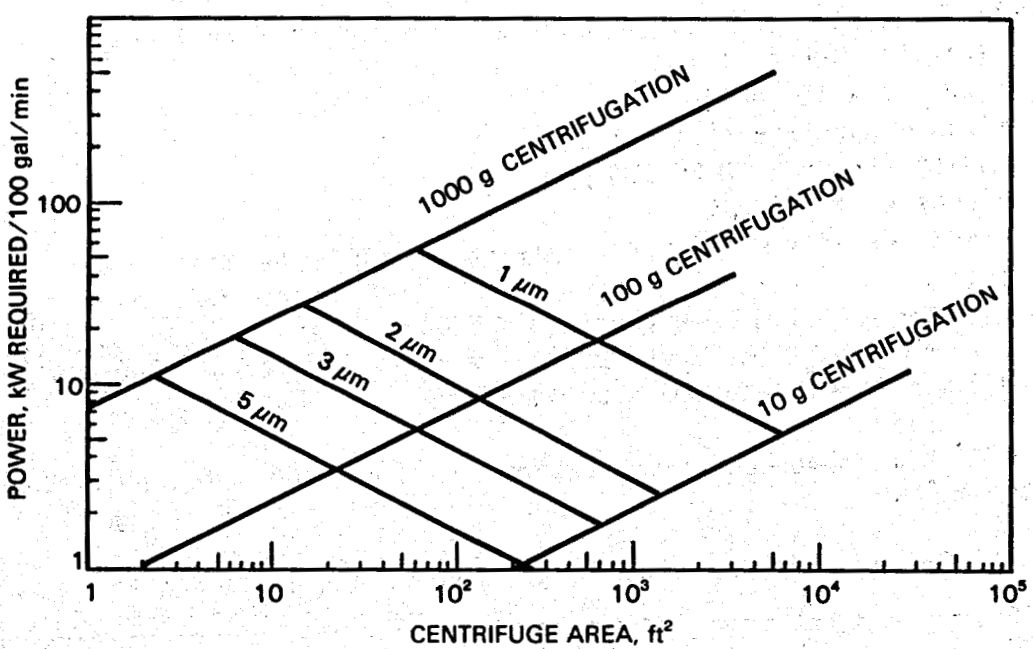

FIGURE 5.30. Centrifuge Power Requirements Versus Performance on Different-Sized Particles for a Unit with Radius Equal to Length

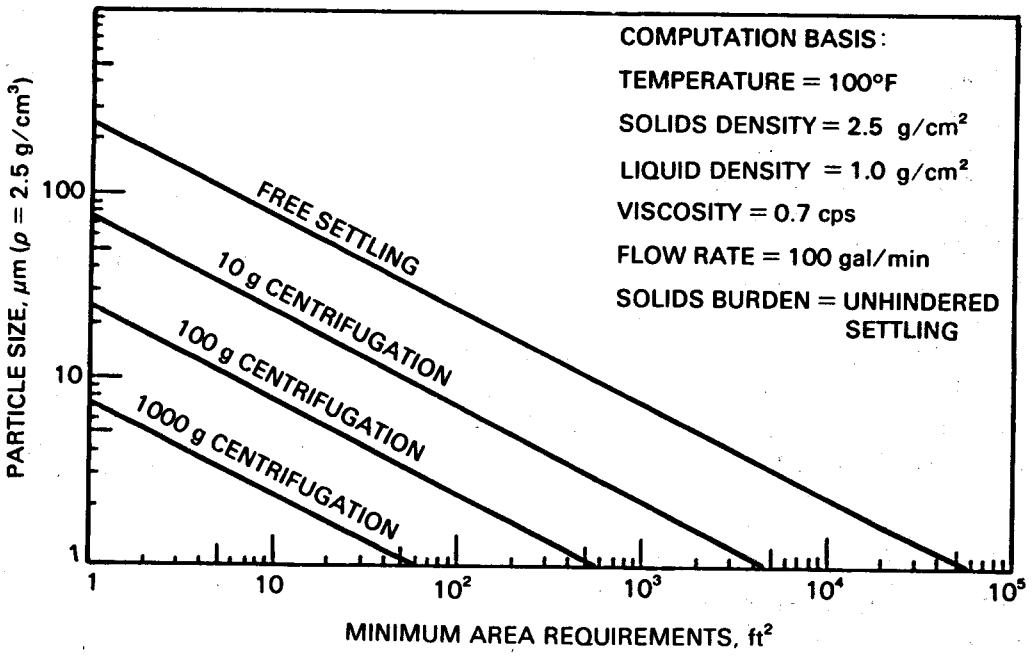

FIGURE 5.31. Centrifuge Size Versus Particle Size for 100 gal/min Geothermal Flow

- Example for application of centrifugation to a geothermal power plant injection stream:
  - Flow = 6×10^5 gal/h
  - Minimum particle size = 1 μm
  - Solids burden = 50 to 100 ppm
  - Viscosity = 0.7 cps
  - Liquid density = 1.0 g/cm^3 (may vary with brine and scale)
  - Solids density = 2.5 g/cm^3 (may vary with brine and scale)
  - Minimum settling area required = 5.8×10^6 ft^2
  - Minimum centrifuge area required = 5.8×10^3 ft^2 at 1000 g's
  - Minimum power required = 5500 kW.

Translation of the above requirements to commercially available equipment is tabulated below:

Type	Power/Unit, hp	Capacity, gpm	Unit Cost, $K	Number Required	Total Cost, $M
Dorr-Oliver HPC-30	125	450	265	24	6.36
Western Machine Slug-A-Tron	75	60	168(a)	180	30

(a) Titanium.

Obviously centrifuging the entire waste stream prior to injection requires a large capital investment and imposes significant parasitic loads on the plant output. However, if a centrifuge is considered as a component working on a sidestream with a high solids content, it appears to be a more attractive option.

- Example for application of centrifugation to a geothermal power plant thickener stream:
  - Flow = 2.4×10^4 gal/h
  - Particle size (maximum effluent) = 5 μm
  - Solids burden = 18%
  - Viscosity = 0.7 cps
  - Liquid density = 1.0 g/cm^3 (may vary with brine and scale)
  - Solids density = 2.5 g/cm^3 (may vary with brine and scale)
  - Minimum settling area required = 2.65×10^5 ft^2
  - Minimum centrifuge area required = 2.49×10^3 ft^2 at 100 g's
  - Minimum centrifuge area required = 249 ft^2 at 1000 g's
  - Power required = 27 kW.

Translation of the above requirements to commercially available equipment is tabulated below:

Type	Power/Unit, hp	Capacity, gpm	Unit Cost, $K	Number Required	Total Cost, $M
Dorr-Oliver HPC-30	125	450	265	1	0.265
Dorr-Oliver Dorrclone rmc-300		260	93	2	0.186
Western Machinery Slug-A-Tron	75	60	168[a]	7	1.78

(a) Titanium.

Although a centrifuge or a Dorrclone appear to be feasible, solids handling systems using them have not yet been demonstrated in geothermal applications.

Process Application

Information on aging or ponding at geothermal facilities was discussed earlier and will not be repeated here.

Gravity thickeners have been successfully tested at the GLEF and are currently used at the Salton Sea demonstration plant. The average suspended

solids in the sludge to the thickeners at the GLEF was 6 to 10 wt%. The thickener underflow averaged 10% to 20% and the overflow was 0.05% to 0.10% suspended solids.

Lamella settlers are currently being used at the Geysers geothermal power plant in California to remove precipitated solids from condensate produced by Units 3, 4, 5, 6, 11, and 12. The condensate from these units is treated with an iron catalyst for removal of H_2S. The precipitate produced by reaction with the iron catalyst consists mostly of sulfur. Effluent from these Lamella settlers is sufficiently free of suspended solids for direct underground injection into the porous reservior without filtration. As described earlier, Lamella settlers were successfully tested in Mexico for accelerated removal of 95% of the silica particles after lime treatment.

5.3.3 Filtration

Granular Media Deep-Bed Filtration

The mechanisms involved in the removal of suspended or colloidal material from waste water by filtration are complex and interrelated. The dominant mechanisms depend on the physical and chemical characteristics of the particulate matter and filtering medium, the rate of filtration, and the chemical characteristics of the water. The mechanisms responsible for the removal of particulate matter will vary with each treatment system.

The principal processes used to filter solids from waste water may be classified into two general categories: adhesion and straining. Adhesion involves the physical/chemical process of particle adsorption on the surface of the filtering medium. As a particle approaches the surface of the filtering medium or previously deposited solids on the medium, an attachment mechanism retains the particle. This attachment mechanism may involve electrostatic interaction, chemical bridging, or specific adsorption. The adhesion process allows removal of submicron particles during filtration by adsorption on the surfaces of the filter media.

The second process--straining--takes place in the filter media at restrictions in the pores (minute openings in the filter). All particles larger than these openings will be trapped and held back. In granular filters, straining action takes place in the filter medium at restrictions in the pores formed where several particles of the filter media come in contact. In practice, all of the suspended solids larger than the pore space between the filter medium would be removed by straining, frequently on top of the filter medium (surface removal). Smaller particles are also removed by straining in the depth of the filter (depth removal), but the fraction removed by straining decreases with the decreasing suspended solids particle size. Other mechanisms of minor importance include flocculation, sedimentation, and entrapment that occurs in

the pores of the bed. Information in Culp, Wesner, and Culp (1978), Metcalf and Eddy (1979), and Cleasby (1972) provides a thorough discussion of deep-bed filtration.

Variables Affecting Filtration Efficiency

A number of variables will affect the efficiency of the filtering operation. These variables include characteristics of the suspended solids and the filter media, the fluid properties of the waste water, and methods of filter operation. Some of the more important variables in waste water filtration include:

- media size - A higher percentage of the applied suspended matter is removed using small-sized filter media (small filter pores). The surface area of smaller media is greater for a given unit volume than the surface area of larger media, and the opportunity for the solids to attach to the media in a natural bridge-like manner across the filter pores is greater for smaller media. The rate of head loss increase is greater for small-media than for large-media filters. Consequently, with granular media filters, shorter filter runs can be expected with smaller grain size (smaller pores) than with larger grain size (larger pores). A filter run commences with the flow of water through the filter and ends when excessive head loss across the filter or solids breakthrough occurs.

- flow rate - The flow rate of waste water through the filter is a critical variable because hydraulic shearing forces tend to drag the floc particles deeper into or through the filter media. As more solids accumulate in the media, the cross-sectional flow area is reduced and the velocity of the water increases for the same flow rate. Finally, equilibrium is reached when the dragging forces of the water on the particles balance the adhesive (or attractive) force of the particle for the media and no further deposit occurs. For a given suspension and a given filter, there will be a flow rate that will result in filter breakthrough.

- desired effluent quality - The desired effluent quality of the filtered waste water can be measured by running a suspended solids or turbidity determination, which depends on discrete sampling operations and will yield particle concentration data but no size information.

- applied suspended solids characteristics - Both the nature and amount of the suspended solids applied to the filter have a major effect on filtration performance. The filtration characteristics of

the solids found in a biological treatment plant effluent are different than those resulting from chemical coagulation. Geothermal use will more closely follow that of chemical rather than biological processes.

Polymeric Filter Aids

The amount of polyelectrolyte needed to aid filtering is generally much smaller than that required for coagulation or as a flocculent in conjunction with another coagulant. Typical filtration doses are less than 0.1 mg/l while doses of 0.1 to 2.0 mg/l are commonly used as a coagulant or flocculent (Culp, Wesner, and Culp 1978). When used as a filtration aid, the polymer is added to increase the strength of the floc, thereby reducing floc shearing and prolonging the length of the filter run.

For maximum effectiveness as a filtration aid, the polymer should be added directly to the filter influent and not in an upstream settling basin or flocculator. However, if polymers are used upstream as settling aids, it may not be necessary to add any additional polymer as a filtration aid. Figure 5.32 illustrates the importance of proper dosing of polymers and the resulting effect as a filter aid on the effluent turbidity.

The condition of inadequate polymer dose represented by Figure 5.32a illustrates the results of a fragile floc shearing and then penetrating the filter. If the polymer dose is too high (Figure 5.32b), the floc is too strong to permit penetration into the filter; therefore, a rapid buildup of head loss occurs in the upper few centimeters of the filter, which causes premature termination of the filter run. The optimum polymer dose--Figure 5.32c--will permit the terminal head loss to be reached simultaneously with the first sign of increasing filter effluent turbidity. The optimum value is normally reached through trial and error since no predictive technique has been developed to give polymer dosage as a function of all the filtration variables.

Multimedia Filtration

The limitations of the single media rapid sand filter prompted the development of filters using two or three different media to attain a higher degree of in-depth filtration. A single-medium filter hydraulically grades during backflushing to place the finest grade of the medium at the top of the filter bed and the coarsest grade at the bottom. In an ideal filter, this situation would be reversed. The ideal system is approached by using two or more filter media with different mesh sizes and densities. The coarser media with lower densities remain on top of the finer, more dense media. A single-medium filter, a dual filter, and an ideal filter are compared in Figure 5.33.

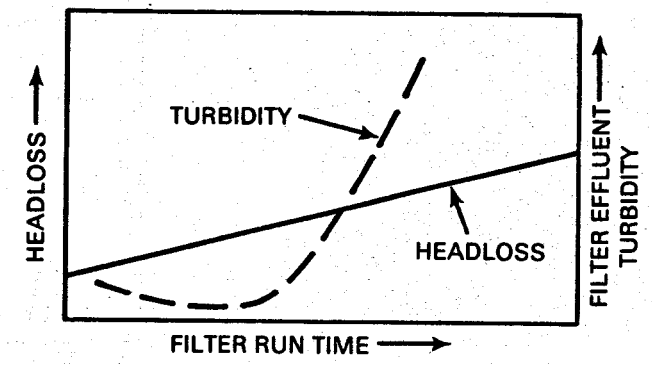

a) Polymer Dose Inadequate

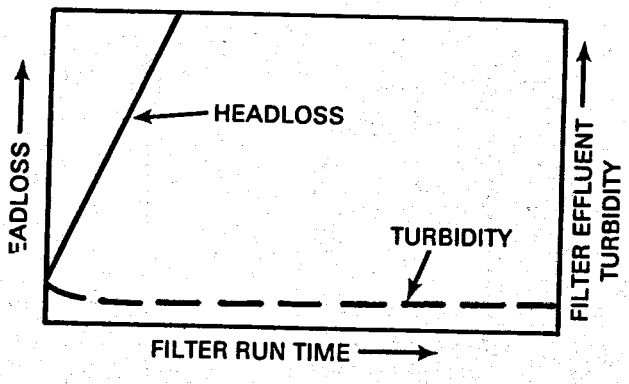

b) Polymer Dose Excessive

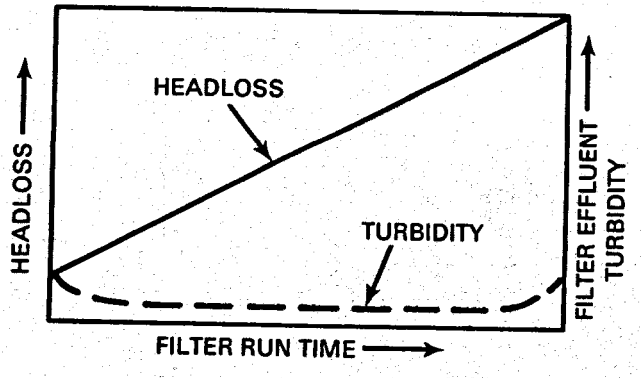

c) Optimum Polymer Dose

FIGURE 5.32. Effects of Polymer Dose on Filtration (Culp, Wesner, and Culp 1978)

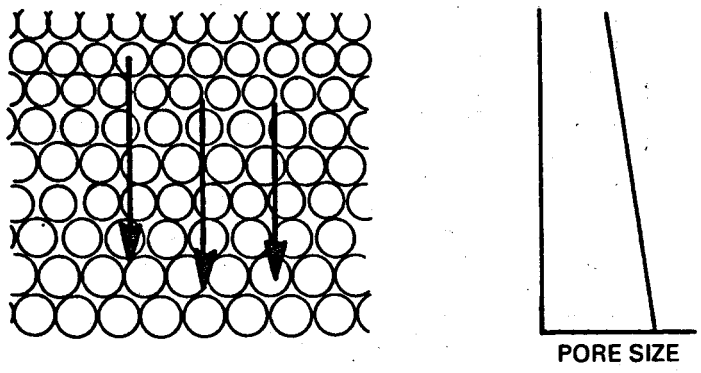

a) Single-Medium Filter

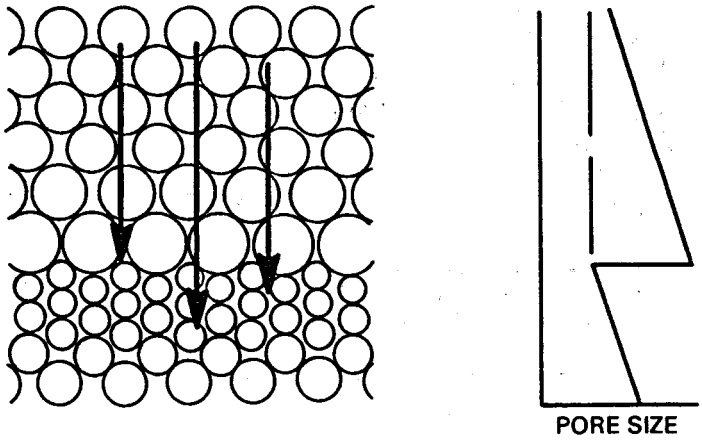

b) Dual-Media Filter

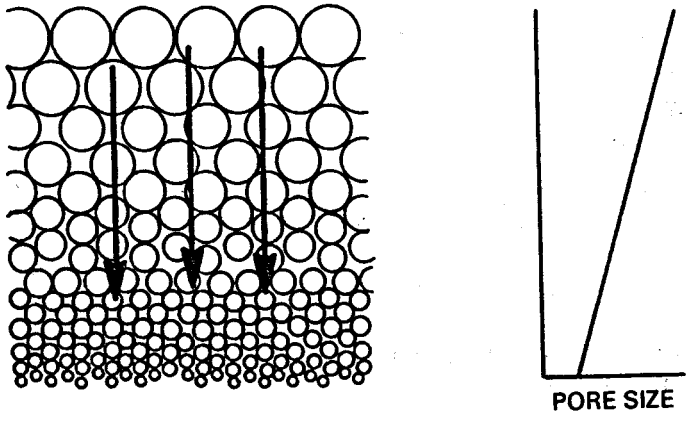

c) Ideal Filter

FIGURE 5.33. Various Media Filter Designs (Culp, Wesner, and Culp 1978)

The effective filtering depth is extended by using two media (such as coal and sand), although there is some fine-to-coarse stratification within each of the layers as shown by the graph depicting pore size. The effective size of sand in a typical dual-media filter is 0.4 to 1.0 mm with an anthracite coal size of 0.8 to 2.0 mm. The layers commonly consist of 6 to 10 in. of sand under 20 to 30 in. of coal. A dual-media filter may be pressure or gravity operated.

Dual-media filter beds composed of crushed coal and sand were originally used in pressure filters for removing particulate matter from swimming pool water. Many municipal water treatment plants subsequently adopted this type of filter bed to improve filter performance. Filter flow rates were typically in the range of 2 to 3 gpm/ft^2 of surface area. Considerable research was conducted at the Hanford Atomic Energy Works (Richland, Washington) to upgrade the performance of the dual-media filters (Conley 1961). The use of polymers was introduced at Hanford to aid in flocculation and filtration, thereby permitting flow rate increases to as high as 8 gpm/ft^2 of filter surface. The quality of the filtered water was excellent. The dual-media filters used at Hanford normally consisted of ~24 in. of 1.0-mm anthracite coal overlying 6 in. of 0.43-mm sand. This type of filter is now widely used throughout the United States with alum and polymer treatment at flow rates from 3 to 5 gpm/ft^2 of filter surface.

Proper selection of media grain size is an important consideration in the design of multimedia filters. In the case of the dual-media filter, the anthracite coal should be as coarse as is consistent with solids removal to prevent surface blinding, but the sand should be as fine as possible for maximum removal of suspended matter. However, if the sand is too fine in relationship to the coal, it will rise to the top of the filter bed during backflushing and nullify the advantages of the dual-media filter. Experience has shown that it is not feasible to use silica sand smaller than 0.4 mm because the corresponding coal grain size would be small enough to cause unacceptably high head losses at rates above 3 gpm/ft^2 of filter surface.

The mixed-media filtration concept with three filter media was introduced as an improvement over dual-media filters. In addition to silica sand, a third very heavy fine medium (garnet with a specific gravity of ~4.2 or ilmenite with a specific gravity of ~4.5) is placed under the silica sand (Culp, Wesner, and Culp 1978). The garnet (or ilmenite), silica sand, and coal particles are sized so that intermixing of these materials occurs and no discrete interface exists. This mixing eliminates the stratification that occurs in the dual-media filter (Figure 5.33) and results in a filter that closely approximates a uniform decrease in pore space with increasing filter depth.

Typically, a mixed-media filter is composed of 10% to 15% garnet or ilmenite, 25% to 30% silica sand, and 55% to 60% anthracite coal. Figure 5.34 shows how particles of different media are actually mixed throughout the bed. There

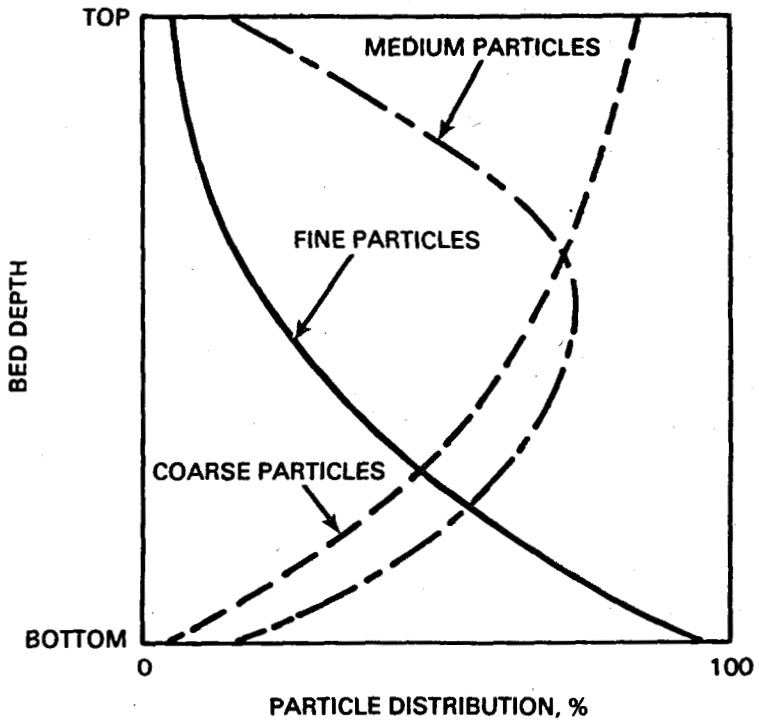

FIGURE 5.34. Distribution of Media in a Mixed-Media Filter (Culp, Wesner, and Culp 1978)

is no layer effect; the coarser, low-density coal forms the upper portion of the filter bed and the fine, high-density material forms the bottom. A typical mixed-media filter has a particle size graduation that decreases from ~2 mm at the top to ~0.15 mm at the bottom.

The construction of a mixed-media filter is very important, and the size distribution of each component must be carefully controlled. The size distribution of commercially available materials is rarely adequate for a good mixed-media filter. Failure to remove excessive amounts of fine materials is the most common construction problem. These fine materials can be removed by placing the medium in the filter bed, backflushing, draining the filter, and skimming the upper surface. These steps are repeated until sieve analysis indicates that the desired particle size distribution is reached. The procedure is then repeated for the second and third media. Sometimes 20% to 30% of the filter media may have to be skimmed and discarded to achieve the proper particle size distribution.

No one filter design is optimum for all waste water treatments. The physical and chemical characteristics of suspended solids as well as their concentrations will have a profound effect on the design of a filter bed. For example, the removal of small quantities of high-strength floc may be readily

achieved by a dual-media filter. Poorly flocculated solids, however, may require three media to remove fine solids in the bottom layer of the filter. The low physical strength of chemical flocs will usually dictate the use of a mixed-media filter for high solids removal and high productivity per filter run.

The single most important factor influencing filter performance is the effectiveness of the preceding chemical coagulation-clarifier treatment. If the treatment system is performing well, good filter performance can also be expected. Conversely, if the system is subject to frequent upsets, filtration will be much more difficult during those periods. The need for extensive pilot-plant studies intensifies with such an operation. No universally reliable measure of the filterability of different types of solids exists. The design of a filter bed must rely on pilot-plant studies using the actual waste stream to be treated (Metcalf and Eddy 1979; Kriessel 1973).

The importance of filter backflushing cannot be overemphasized. Waste water filtration usually involves a much higher degree of agglomeration of solids and media in a filter bed than does normal water filtration. As a result, a greater effort is required to break up the crust that forms on the filter and to prevent "mud ball" formation. In addition to backflushing, two methods may be used to assure that agglomerated solids break up. In the first method, a revolving distributor equipped with nozzles directs jets of water into the filter bed. This approach involves more than the surface of the filter since a good revolving surface wash actually causes mixing throughout the bed. The wash water nozzles are directed at ~30° from horizontal, and the jets of water under 50- to 100-psi water pressure cause the distributor to revolve.

In the second method, air and water are used to break up the agglomerated solids. Air is initially injected through the underdrain system while the backflush water is shut off. To avoid loss of media, the water level is lowered to within 2 to 6 in. of the surface of the filter. The bed is violently agitated for 3 to 10 min with air alone at a rate of 2 to 5 $ft^3/min\text{-}ft^2$. Backflush water is then applied at a low rate (~2 gpm/ft^2) with the air sparge continuing until the water is within 8 to 10 in. of the wash water troughs. At this point, the air sparge is discontinued and the filter bed is backflushed with water at 8 to 10 gpm/ft until the filter is clean. Backflushing mixed-media filters will ordinarily require flows of 15 to 20 gpm/ft^2. No surface washing or air sparging must take place in the final 1 to 2 min of the backflush to allow the bed to classify properly.

Precoat Filters

Precoat filtration is a form of mechanical liquid/solid separation where a layer of powdered filter aid of refined diatomaceous earth is built on a relatively loose septum (for example, wire cloth) to screen out suspended solids in

waste water (McIndre 1969; Cleasby 1972). The septum is usually fabricated of corrosion-resistant material (for example, stainless steel) with permeability characteristics that do not impart unnecessary hydraulic resistance to the flow of influent water. The septum collects the bulk of the diatomaceous earth on the surface during the precoating of the filter aid and will easily release the filter cake during cleaning operations.

The first major use of diatomite as a filtration media occurred during World War II when the U.S. armed services utilized thousands of small portable diatomite filtration units to produce safe, amoebic cyst-free drinking water for troops in the field (McIndre 1969). Precoat filtration was first used in small industrial applications prior to 1915, but it has only been in the last 45 years that this process has been used for large-scale applications. The major advantages of precoat filtration include lower capital investment, smaller space requirements, and decreased need for extensive pretreatment. Generally high operating (labor) costs are the major disadvantage.

In general, precoat filtration is a two-step operation. First, a thin protective layer of filter aid (precoat) is built up on the porous filter septum that supports the filter media throughout the filter run. Even the coarsest grades of filter aid used for filtration are usually substantially finer than the openings in the septum material. Thus, the initial precoat formation must be made by bridging. Bridges must form over the openings between the septum material for the final precoat formation to be achieved. Once established, these bridges are extremely stable due to the diverse shapes of the filter aid particles. This filter aid buildup is accomplished by recycling a diatomaceous earth slurry (~0.10 to 0.15 lb/ft^2 of filter area) through the filter. The resulting precoat protects the filter system from becoming fouled by the solids to be removed and also acts as the initial filter medium.

The second step, called body feed, involves adding small amounts of earth to the incoming waste water. By adding a predetermined amount of body feed to the influent, clogging of the precoat pores is prevented and a fresh filtering surface is formed. This action helps to maintain a higher filter porosity. The two steps are shown in Figure 5.35.

The filtering equipment can be put into two general classifications: pressure and gravity/vacuum. With pressure filters, the feed is forced by a pump in the influent line or by an available hydrostatic head. The most common types of pressure filters are cylindrical element filters (Figure 5.36) and vertical leaf filters (Figure 5.37).

The gravity-vacuum filter is similar to the pressure filter; the design of the tank is the principal difference. In a vacuum filter, filtration is performed in an open tank. The combined forces of gravity and atmospheric pressure push the water through the filter to be pumped away by a suction filtrate

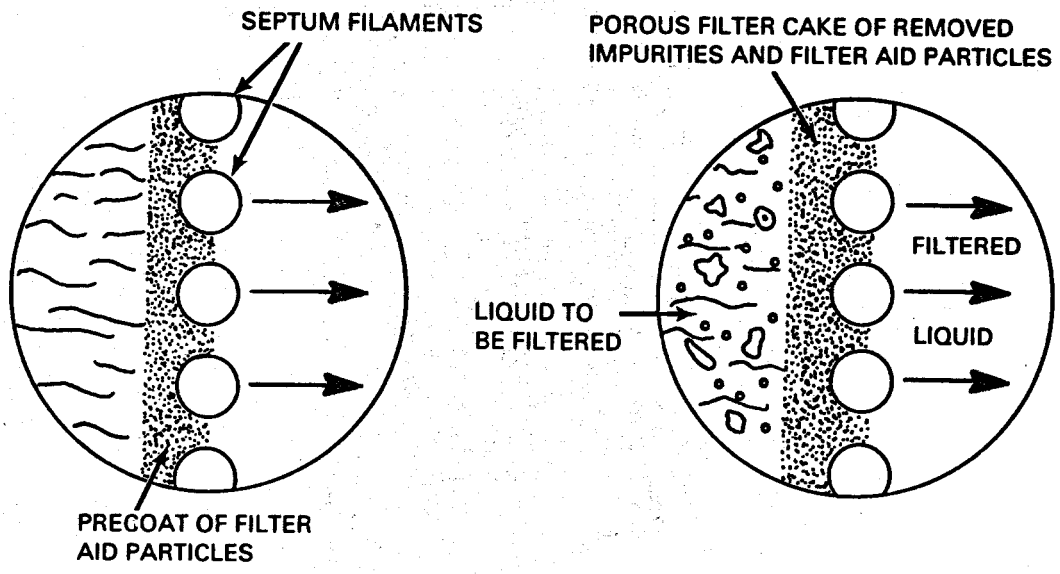

a) Precoating b) Filtering

FIGURE 5.35. Diatomaceous Earth Filtration

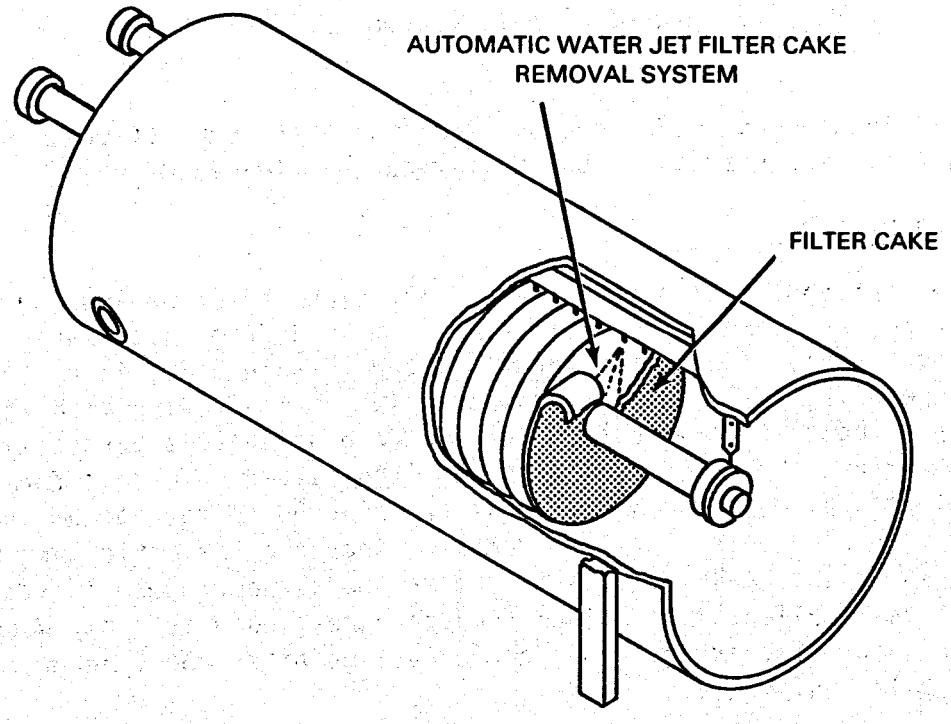

FIGURE 5.36. Cylindrical Element Pressure Filter

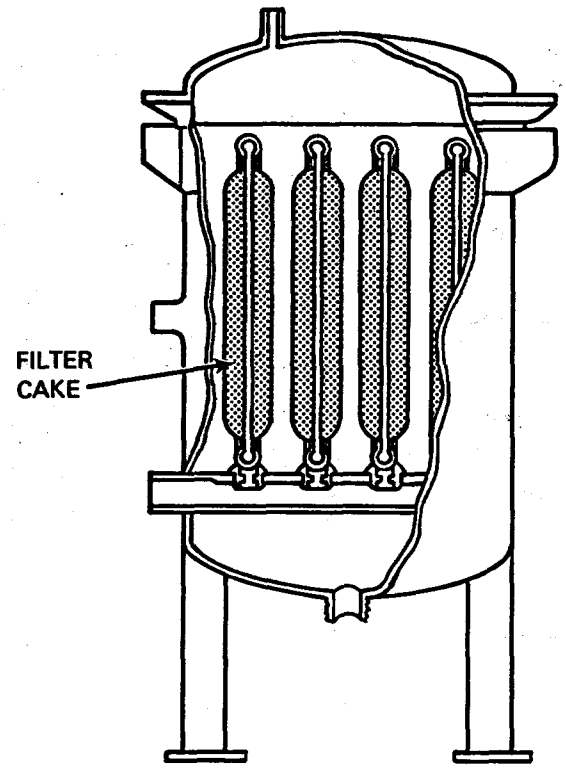

FIGURE 5.37. Vertical Leaf Pressure Filter

pump. The pump is located on the discharge side; thus, it pumps filtered water away from the filter. The gravity/vacuum filter can be cleaned manually.

Rotary Vacuum Filter

The most frequent application of surface filtration is for dewatering sludges or filtering large amounts of solids precipitated from waste water such as metal finishing wastes. The rotary vacuum filter (Figure 5.38) is representative of this type of filter. The filter medium (a fabric or wire mesh in the form of a continuous belt) rotates over a perforated drum that is partially submerged in the slurry. Water is pulled through the filter cake that forms on the belt to the inside of the drum where it is transferred to the vacuum system. The filter cake also acts as filter media to increase the efficiency of solids removed. The filter cake rotates around to the scraper where it is removed and drops to a collector. Various appurtenances, such as spray washers to rinse the cake before the scraper and remove residue after the scraper, may be included with this equipment.

Sludge characteristics are important for successful operation of rotary vacuum filters as well as other types of surface filtration devices. The sludge must be sufficiently coagulated to allow water to drain freely through the sludge. Chemical conditioning with ferric chloride or polymers may be necessary to filter a sludge effectively.

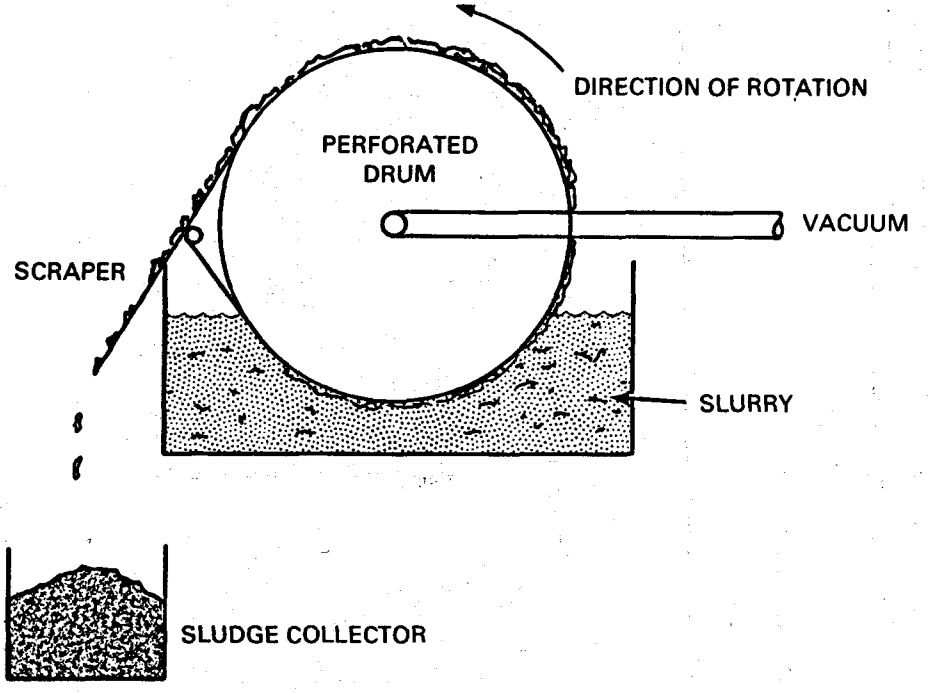

FIGURE 5.38. Rotary Vacuum Filter

Filter Presses

Filter presses are constructed of a series of plates and frames (Figure 5.39) and are primarily used for dewatering sludges. The volume provided by these filters consists of cavities lined with filter cloth between the plates as shown in Figure 5.40. Plate and frame filters operate on a batch basis. The sludge to be filtered is pumped into each of the cavities illustrated by B in Figure 5.40, the solids are retained on the filter cloth in each cavity, and filtered liquid flows into chambers next to the cavities and down through an outlet. When the filter cake builds up to a certain level, the plate and frames are separated by a hydraulic mechanism and the solids are removed mechanically.

Geothermal Process Application

A dual-media gravity filter was evaluated at the GLEF for removing residual suspended matter in the reactor clarifier effluent (San Diego Gas and Electric 1980). This filter was 26 ft in diameter, 16 ft high, and contained three cells (see Figure 5.41). The filter was operated for 500 h after stable operation of the reactor clarifier was achieved. Due to problems with the distribution nozzle, short filter runs, interrupted backflush cycles, and insufficient backflush capacity, the results of the filter tests are considered preliminary. Prior pilot-plant filter runs had been conducted for 24 h; the runs with the

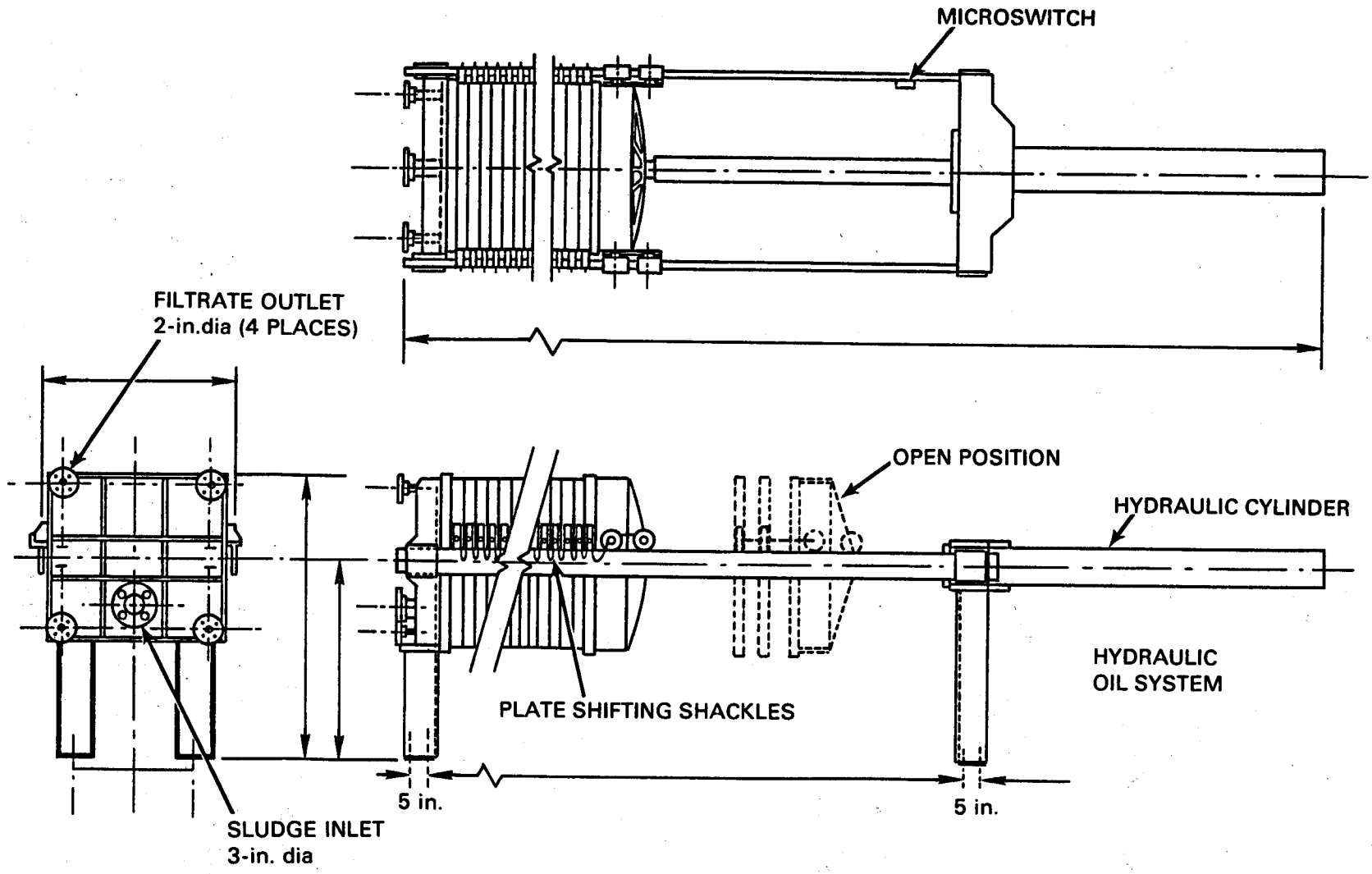

FIGURE 5.39. Plate and Frame Filter Press

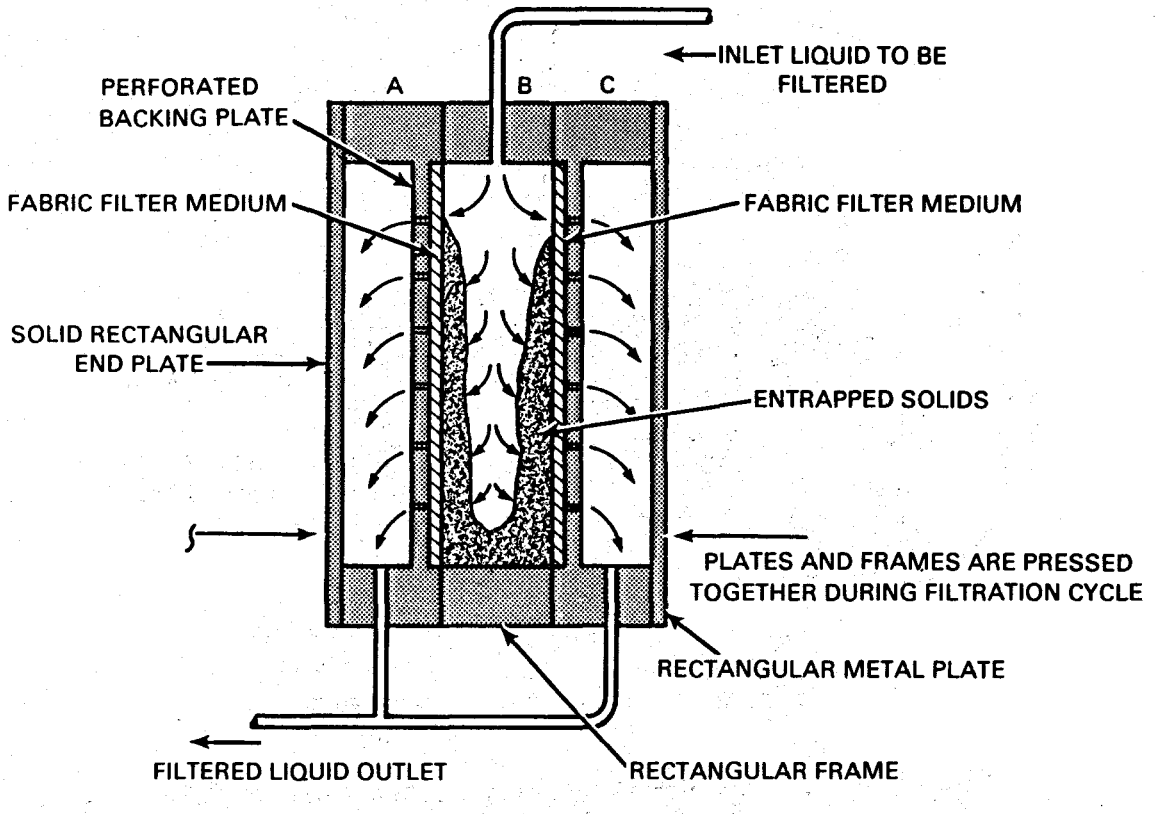

FIGURE 5.40. Cross Section of One Rectangular Chamber of a Filter Press

26-ft diameter filter were conducted for 15 h. Two possible reasons for this difference were noted: 1) The pilot-plant filter received brine with only half as much suspended solids as the 26-ft diameter filter (50 versus 100 ppm) and 2) the chemical and physical composition of the suspended matter was different. The feed to the large filters contained finer particles of ferric hydroxide, which may have caused a matting problem on the surface of the filters.

The filtration rate for the GLEF dual-media filter depicted in Figure 5.41 was 2.5 gpm/ft^2 and the backflush rate was 20 gpm/ft^2. Inspection of the filter after shutdown showed that ~25% of the sand and a lesser amount of anthracite was lost during operation of the filter. There was no evidence of scaling on the filter media. The suspended solids concentrations of the clarifier and filter effluents during operating periods are presented in Figure 5.42. Much of the suspended matter in the filter effluent contained ferric iron, which was believed to result from oxidation of soluble ferrous iron in the brine. Limiting contact of the brine with air is expected to overcome this problem.

Dual-media filters at the Salton Sea 10-MWe plant reduce the suspended solids to ~10 mg/l (from 50 to 200 mg/l) prior to injection. These filters have required some maintenance to overcome scale deposits and breakthrough that

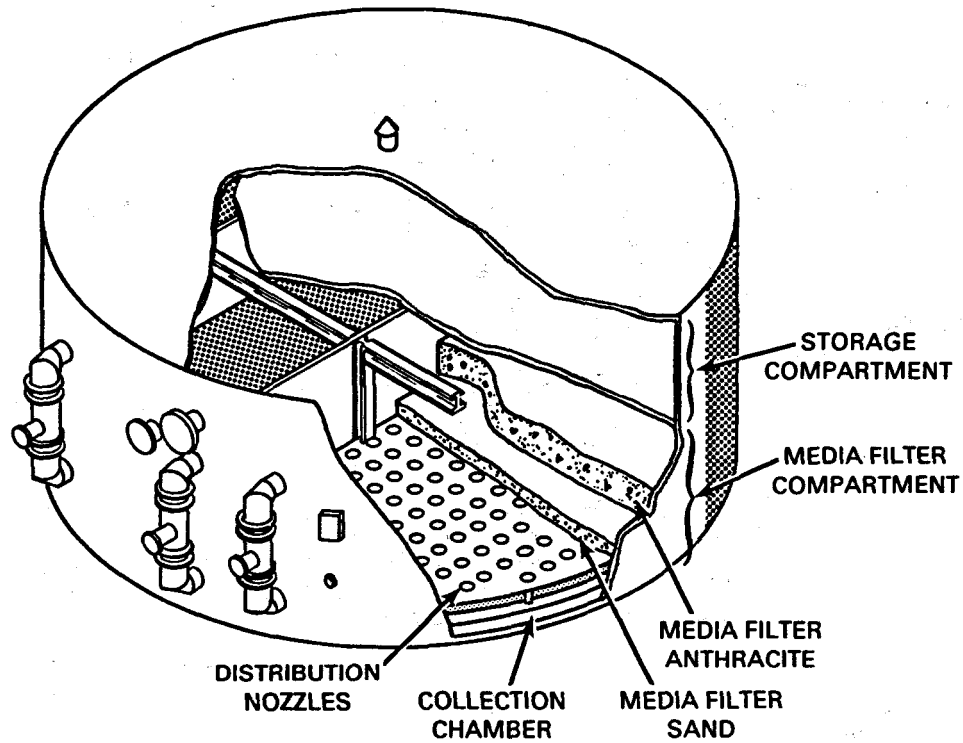

FIGURE 5.41. Dual-Media Gravity Filter Used at GLEF (San Diego Gas and Electric 1980)

occurred during the first year of operation. The new crystallizer/reactor clarifier technology was being optimized during this time, which probably resulted in more operational transients than normal.

The filter press used for the large-scale demonstration test at the GLEF processed about 100 tons of solids during the test period (San Diego Gas and Electric 1980). The cycle time for dewatering a batch of sludge from the thickener was ~45 to 50 min. The unit was generally reliable and produced a filter cake containing ~65% dry solids from thickener underflow with 10% to 20% dry solids. A filter press was also used initially at the Salton Sea plant, but it was bypassed and the slurry was disposed of directly.

A pilot-sized rotary vacuum filter was tested at Wairakei and Broadlands, New Zealand, for dewatering a calcium silicate sludge (Rothbaum and Anderton 1976). This sludge yielded a filter cake containing 30% dry solids.

5.3.4 Gas Flotation

The principles of gas flotation, its current usage (particularly in the mining industry), and the single geothermal experience are described in this

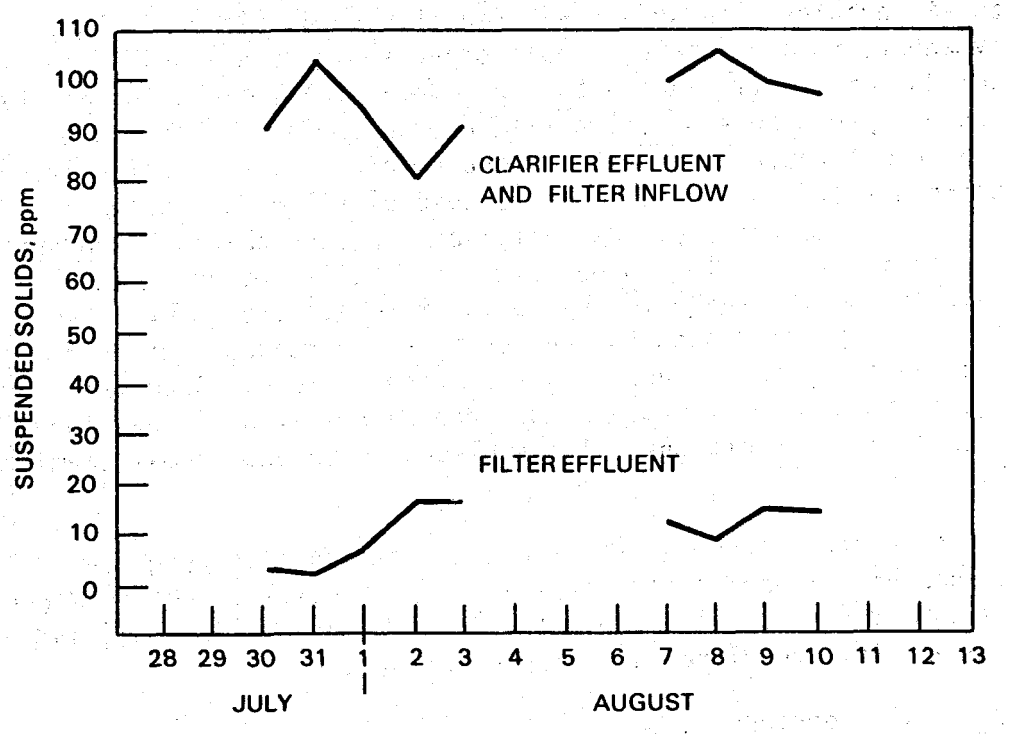

FIGURE 5.42. Suspended Solid Removal Across GLEF Filter

section. Among liquid/solid separation approaches, this technique has a conceptual advantage for geothermal applications because of the natural source of gas (the entrained/dissolved NCG). This process is therefore described in some detail even though geothermal experience is limited.

Gas (air) flotation is a method of separating particulates from liquids by levitating them with gas bubbles. The lower specific gravity of the particles/bubble aggregates causes them to rise to the surface where they can be removed by skimming or overflowing. Any gas or even liquids of low specific gravity can be used for levitation, and the method can be made selective for certain particles. Particulate material includes not only solids but also dispersed liquid phases. The flotation process is broadly applied in the mineral industry for the selective recovery of metallic and nonmetallic minerals and the rejection of undesired gangue minerals from ores; in the removal of free or emulsified oil from refinery waste water in the petroleum industry; in the removal of particulates from effluents of municipal waste treatment plants; in the recovery of potassium, lithium, and other salts from brines; and experimentally at least in the removal of particulates from geothermal fluids. The process is effective for separating small particles from liquids that are otherwise difficult to separate by sedimentation because of their low settling rates.

Flotation is based on the fact that particulate matter can be made to adhere to air bubbles with sufficient tenacity to be floated. Nonpolar solids naturally adhere to air bubbles. Most other solids and liquids are water wetted and do not readily adhere to air. Traditional flotation processes have been based on adsorbing a nonpolar film on the surface of particles to be floated to permit their strong attachment to air bubbles. Selective adsorption of hydrocarbon films on a desired solid species allows the selective flotation of that species. Conversely, adsorption of reagents that wet the surface of a particle allows that species to be rejected in a flotation process. Air flotation as applied to liquid-solid separation in water treatment depends on forces of attachment of particulates to bubbles that are tenuous but sufficient to accomplish phase separation under quiescent conditions. Such water-avid particulates as silicates or hydrated oxides are readily floated by clouds of fine bubbles under these conditions. The application to geothermal chemistry is apparent.

One test of this process has been conducted to clarify geothermal brine. Since the geothermal application of flotation is still in the research stage with many unknowns, the principles of air flotation, variations, and nongeothermal industrial experience are also described.

Geothermal Experience

Geothermal discharge water has been processed in a 6 tonne/h dissolved air flotation pilot plant in the Wairakei, New Zealand, geothermal field (Shannon, Owers, and Rothbaum 1982). The objective was to separate and remove arsenic coprecipitated with iron hydroxide flocs and to remove calcium silicate solids by flotation. The composition of typical Wairakei geothermal discharge waters is shown in Table 5.11 (Buisson, Rothbaum, and Shannon 1979). The pilot-plant layout is shown in Figure 5.43.

TABLE 5.11. Composition of Typical Wairakei Geothermal Waters (pH = 8.2)

Element	Quantity, ppm
Chlorine	2085
Silica	580
Lithium	12.5
Arsenic	4.3
Cesium	2.28
Aluminum	0.35
Iron	0.012
Manganese	0.0007
Beryllium	0.00005

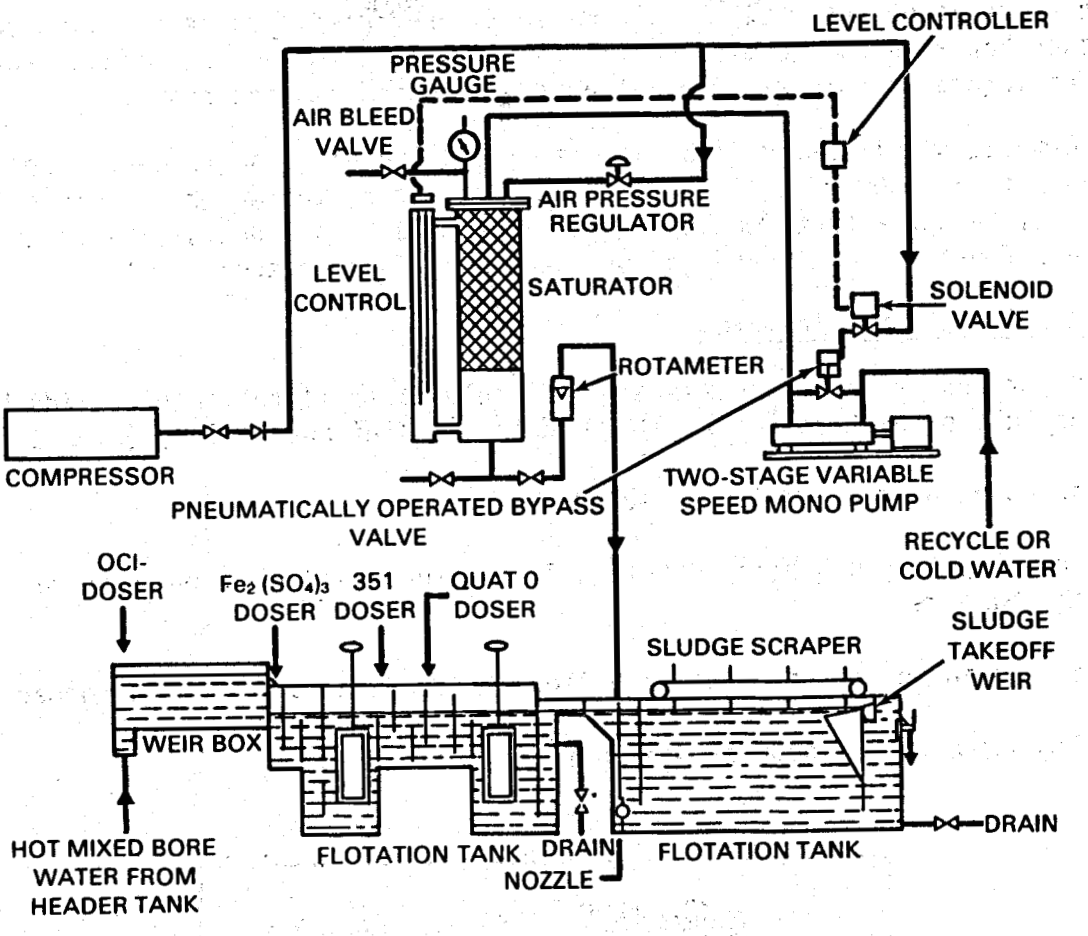

FIGURE 5.43. Geothermal Air Flotation Pilot Plant (Shannon, Owers, and Rothbaum 1982)

Geothermal water (84 to 86°C) is first dosed with sodium hypochlorite (~3.6 g/t) to oxidize As(III) to As(V) followed by this sequence of mixing and conditioning in the flocculation tank:

- add ferric sulfate (40 to 70 g/t) with 30 s mixing
- slowly stir for 100 s to produce iron floc
- add Magnafloc 351 (0.5 to 0.6 g/t) with 30 s mixing
- add Quaternary 0 surfactant (1.0 g/t) with 30 s mixing
- slowly stir for 140 s to promote and condition floc.

The conditioned water flows to the flotation tank where water (~13% of main flow) saturated with air at 200 kPa (29 psi) is injected. Up to 89% of the iron floc floated carrying with it ~89% of the arsenic in a total treatment time of 6 min. Tests were also run using about 6% to 7% addition of cold water saturated with air at 222 kPa (32 psi) for injection in the flotation tank in

place of recycled hot water. Cold water is preferred because it dissolves more air than hot water and avoids collection of silica in the saturator. The smaller volume of cold water required also reduced pumping costs.

Removal of silica by dissolved air flotation was also tested. Freshly slaked 10% CaO (500 g/t) slurry was added to geothermal water to form calcium silicate. A surfactant (Quaternary O, 4 g/t) was also added. The calcium silicate floated rapidly and 95% of the solid was recovered.

Air Flotation Principles

Major mechanisms responsible for dissolved air flotation of solids have been postulated by Vrablik (1959) and Neis and Kiefhaber (1980) (Figure 5.44):

- adhesion of gas bubbles on solid phase
- trapping of gas bubbles within a floc structure during the rise of the bubbles
- adsorption of gas bubbles in a floc structure as the floc is formed
- formation of gas bubbles within flocs.

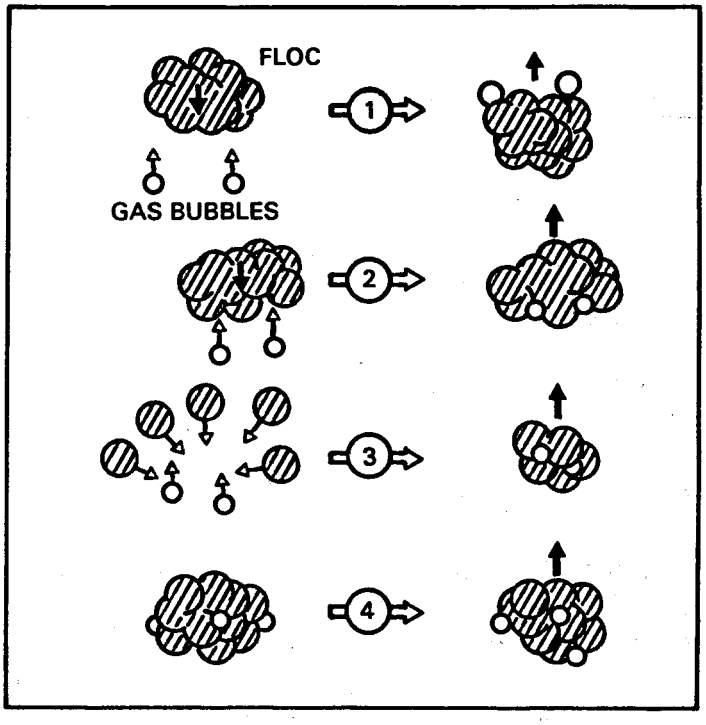

FIGURE 5.44. Major Mechanisms Responsible for Dissolved Air Flotation (Neis and Kiefhaber 1980)

Whatever the detailed mechanisms, the process depends on the generation of large numbers of very small bubbles (~80 μm diameter) and allowing the bubbles to separate under quiescent conditions. Flotation processes in the mineral industry involve violent agitation and bubble sizes are much larger (~1000 μm diameter). Because of this, conventional flotation processes have been relatively inefficient in the recovery of finer particles (<40 μm).

Dissolved Air Flotation

In dissolved air flotation, water is saturated with air; and on subsequent pressure reduction, the dissolved air comes out of solution and forms bubbles. The volume of bubbles formed depends on the solubility of air or other gases in water, on the temperature, and on the pressure of the system. The solubility of air and other gases in water at 20°C and 760-mm Hg pressure and the equivalent number of 80-μm diameter bubbles generated by complete exsolution are shown in Table 5.12.

The bubbles nucleate on particles, become entrapped in flocs, or attach to particles by collision. Water saturated with air at atmospheric pressure is subjected to a vacuum to generate bubbles (vacuum flotation). Alternatively, water saturated with air at elevated pressure is released through valves to atmospheric pressure to produce flotation bubbles. The solubility of gases in water is proportional to the pressure applied (Henry's Law); thus, a greater volume of bubbles is produced by the latter process. The theoretical and

TABLE 5.12. Solubility of Various Gases in H_2O (a,b)

Gases	Gas/ H_2O, cc	Grams of Gas/ 100 H_2O	Equivalent Number of 80-μm Diameter Bubbles Generated by Complete Exsolution/cc H_2O
Nitrogen	0.015	0.0019	56,000
Oxygen	0.031	0.0043	116,000
Hydrogen	0.018	0.00016	67,000
Carbon dioxide	0.88	0.17	3,300,000
Carbon monoxide	0.023	0.0028	86,000
Air	0.0187	1.87	70,000
Hydrogen sulfide	2.58	0.38	9,600,000
Sulfur dioxide	39.4	11.28	147,000,000
Methane (natural gas)	0.033	0.0023	123,000

(a) Conditions: 20°C and 760-mm Hg.
(b) Vrablik (1959).

actual mass of air evolved at various saturation pressures is shown in Figure 5.45. An example of the size distribution of air bubbles generated by release through a 1/8-in. needle valve of water saturated at 20 and 50 psig is shown in Figure 5.46.

In practice, air or other gas is drawn into a centrifugal pump with the water to be treated and injected into a retention tank. The mixed fluids are held under pressure for a short period (30 to 60 s) to allow time for the air to dissolve in the water. The gas-saturated water is then jetted into the flotation cell where the dissolved air precipitates in a cloud of small bubbles that rise through the liquid. The bubbles collide with and become attached to particles or are entrapped in flocs, lifting them to the surface where they are discharged by skimming or overflowing. The entire stream or only part of the stream to be treated can be pressurized, depending on the volume, the amount of solids, and the effectiveness required. Alternatively, a portion of the clean water discharged from the flotation cell can be charged with air under pressure and used to generate bubbles in the flotation cell. This latter process avoids the plugging of equipment by the solids in the feed stream. The several flow sheets described are illustrated in Figure 5.47.

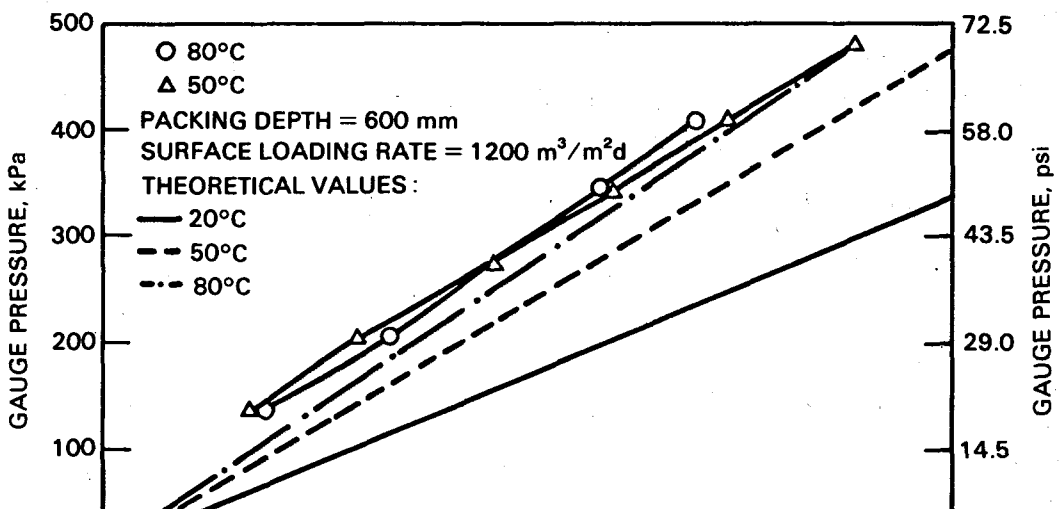

FIGURE 5.45. Mass of Air Evolved at Various Saturation Pressures for Temperatures of 50°C and 80°C at Constant Surface Loading Rate. Theoretical curves from Wilhelm et al. (1977) for 20, 50, and 80°C; Shannon and Buisson (1980).

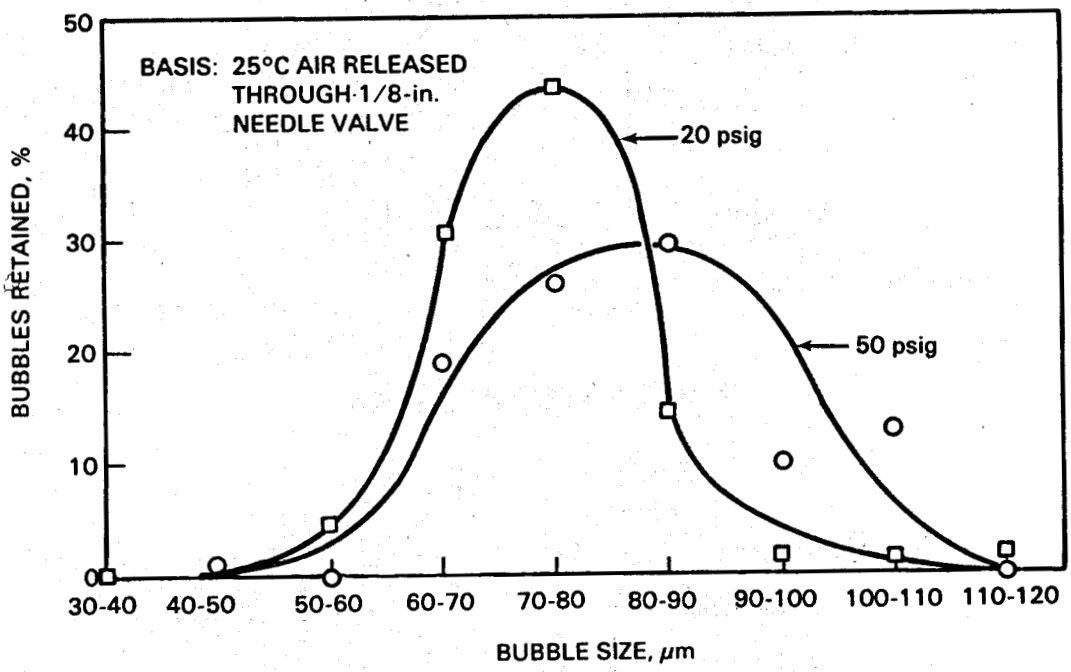

FIGURE 5.46. Size Distribution of Air Bubbles Released Into Flotation Chamber in Laboratory Tests (Vrablik 1959)

Induced Air Flotation

In induced air flotation, air is drawn into an impeller where it is speared and dispersed into the liquid as bubbles (Figure 5.48).

Pneumatic and Air Lift Flotation

Pneumatic flotation machines generate bubbles by blowing air into the liquid through a porous material like porous carbon, ceramic, or canvas (Roe 1980). Air lift machines discharge air from a pipe immersed in water in a confined channel where the air bubble/water mixture rises, creating a pumping action to circulate pulp and provide bubble/particle contact. A quiet zone allows froth to separate for removal. Bubbles formed by these methods are orders of magnitude larger than those created in the dissolved air method.

Other methods of generating bubbles that have been suggested include electrolysis of the liquid by the reaction of acid with carbonates or sulfides or by boiling the liquid forming its vapor (boiling flotation).

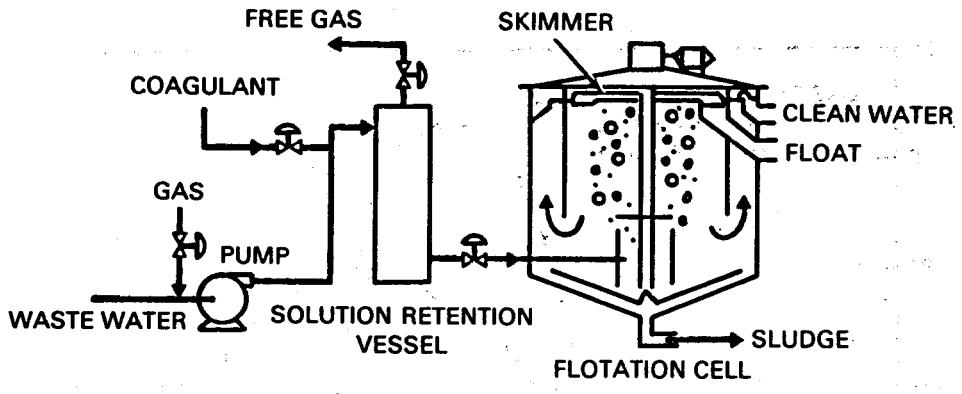

FULL-STREAM PRESSURIZATION

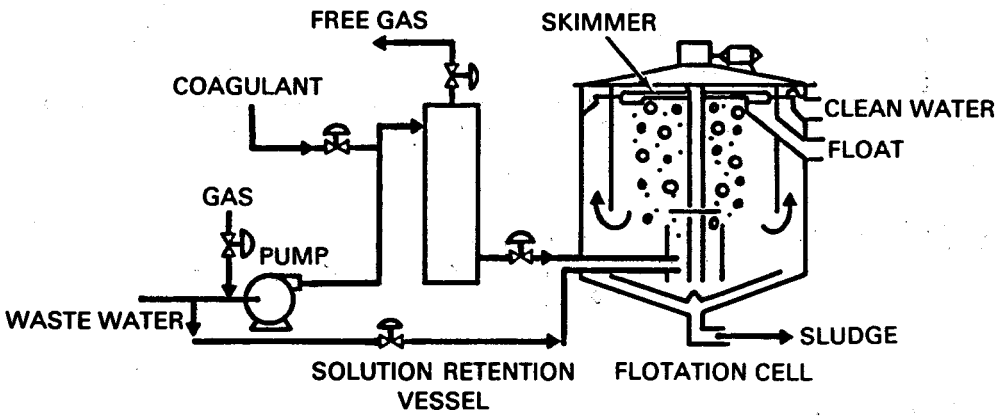

SPLIT-STREAM PARTIAL PRESSURIZATION

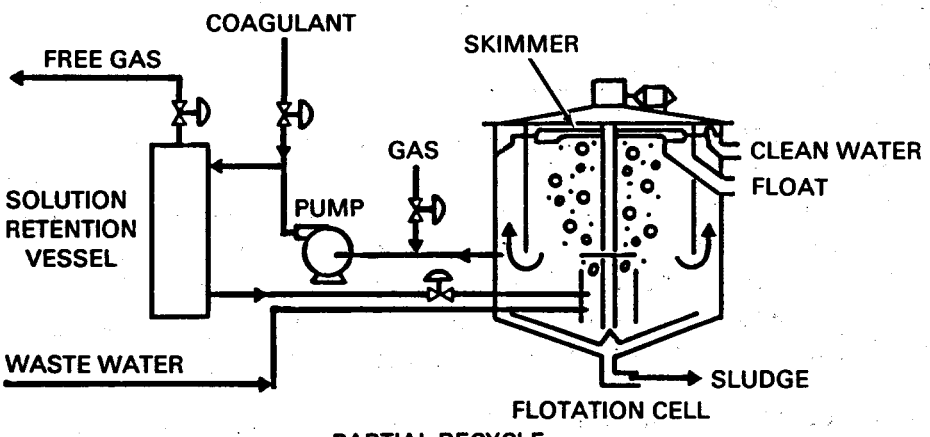

PARTIAL RECYCLE

FIGURE 5.47. Dissolved Air Flotation Variations (Churchill and Tacchi 1978)

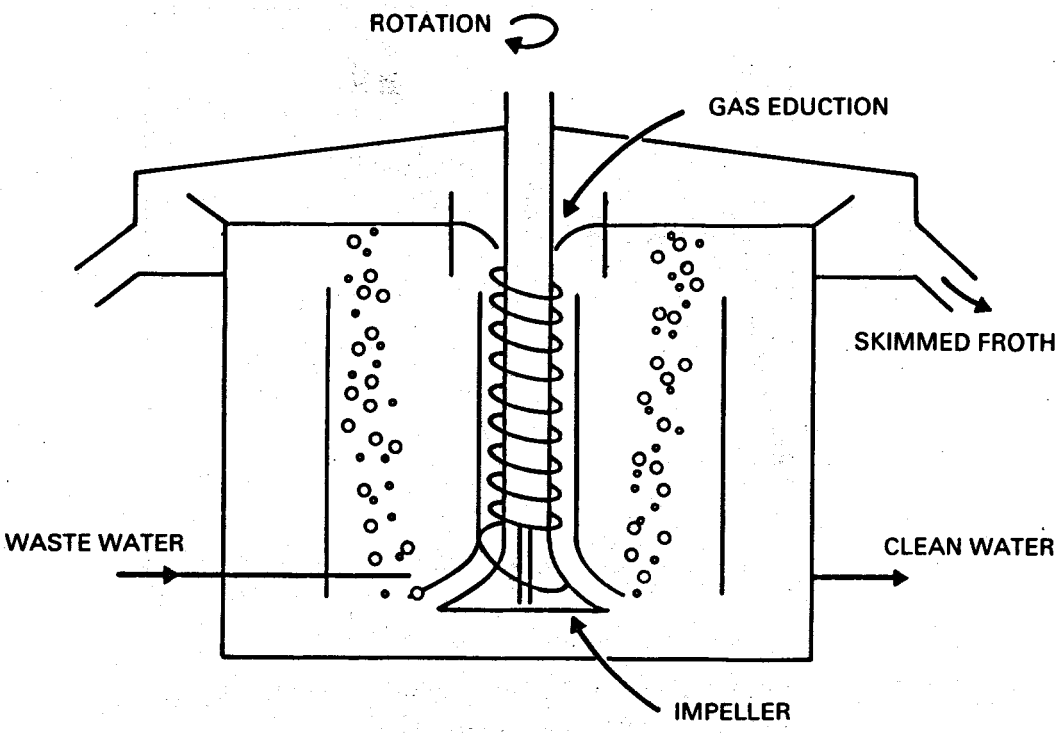

FIGURE 5.48. Induced Air Flotation Unit (Churchill and Tacchi 1978)

Bubble Rise Velocity and Buoyancy

The size of an air bubble governs its buoyancy and rise velocity, which determines hold up time and capacity of flotation cells. The terminal rise velocity of a particle/bubble aggregate is given by Stokes' equation:

$$V_t = \frac{g(\rho \text{ liquid} - \rho \text{ aggregate})D_a^2}{18\mu} \qquad (5.9)$$

where V_t = terminal rise velocity of the gas/solid agglomerate
g = acceleration of gravity
ρ liquid = density of the liquid
ρ aggregate = density of the gas-solid agglomerate
D_a = diameter of the agglomerate
μ = viscosity of the liquid.

The rise velocity of various diameter bubbles is shown in Figure 5.49. Gaudin (1932) cites desirable bubble velocities as 12 cm/s or more; dissolved air flotation velocities are much less. The Nagahama flotation cell rise rate is 3 cm/s (Nagahama 1974). Shannon and Buisson (1980) report a rise rate in hot water (80°C) of 0.5 cm/s.

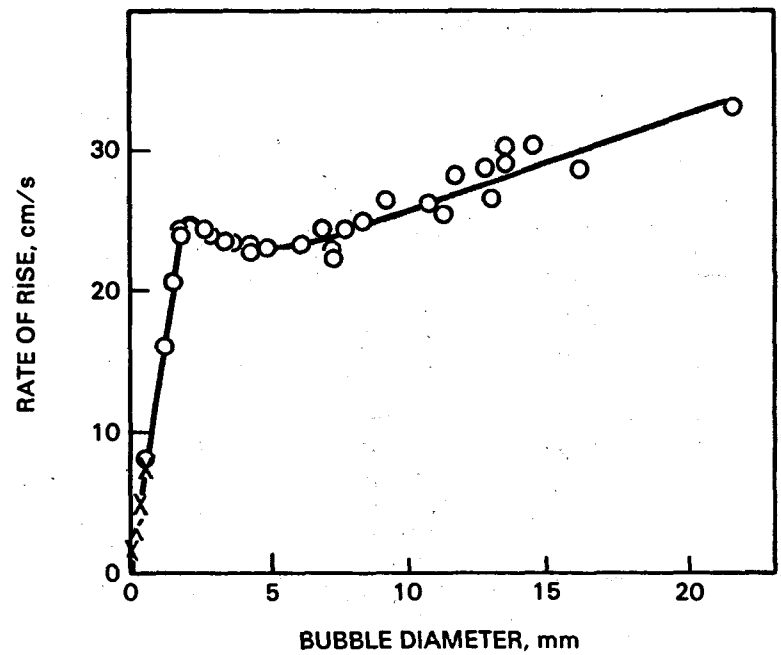

FIGURE 5.49. Rise Rates of Single Bubbles of Different Sizes (Klassen and Mokrousov 1963)

The size of particles that can be levitated by a given size air bubble is illustrated in Figure 5.50. The bulk specific gravity of the bubble/particle aggregate must be less than the specific gravity of the fluid (less than 1 in the case of water) for flotation to occur. An 80-μm diameter bubble would be unable to float a silica particle as large as 68 μm in diameter or a pyrite (FeS_2) or hematite (Fe_2O_3) particle as large as 50 μm in diameter.

Industrial Use and Experience

Vrablik (1959) lists some known applications of dissolved air flotation for industrial waste treatment:

- canneries - Citrus, fish, fruit, and vegetable canning produce waste streams containing organic suspended solids that may be removed by flotation.

- chemicals - Dissolved air flotation is being used for recovering fines during the copolymerization of synthetic rubber. It also may be used to recover fines from polyethylene production processes. Carbon, colloidal metals, calcium sulfate, hydroxides, etc., have illustrated excellent tendencies toward concentration by flotation.

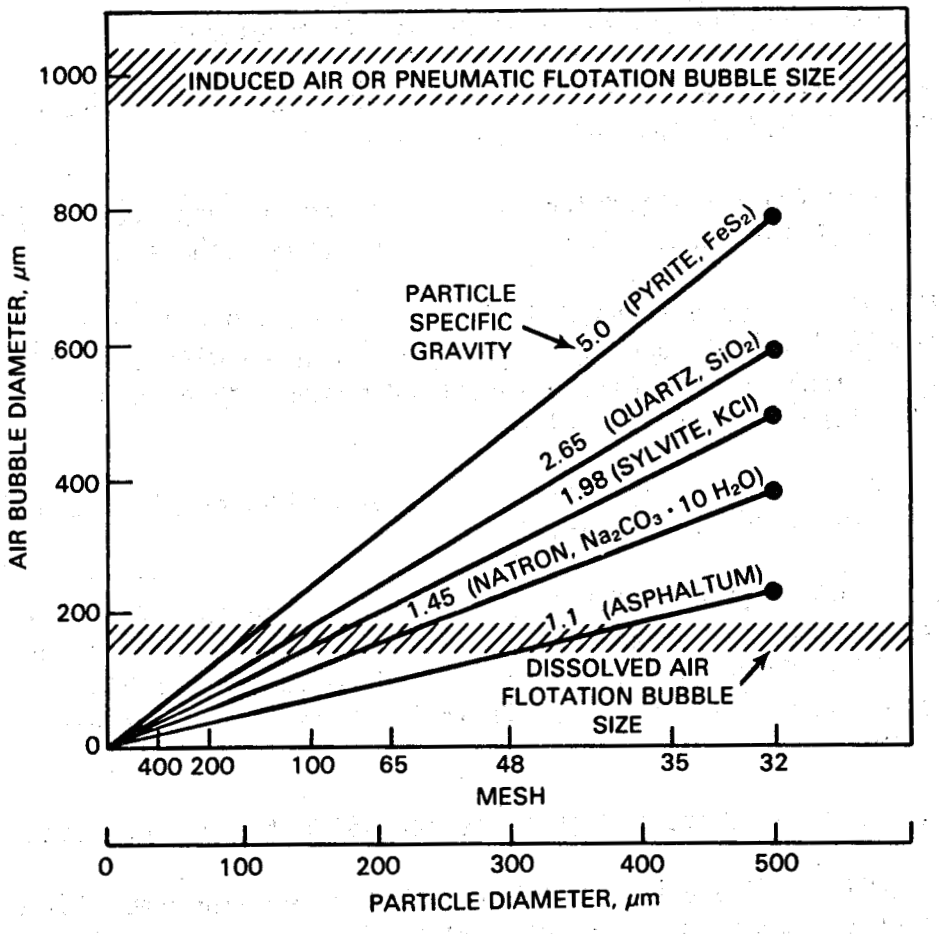

FIGURE 5.50. Air Flotation Effectiveness on Various Size Mineral Particles. The diameter of an air bubble that will just suspend a single particle of a given size and specific gravity in water is indicated by the diagonal lines. Larger bubbles will cause flotation. The shaded bands indicate typical bubble size characteristics of dissolved air flotation and induced air or pneumatic flotation. Other mineral densities include $CaCO_3 \cdot 6H_2O$ - 1.8, $CaCO_3$ - 2.7, and SiO_2 gel - 1.4 (presumed).

- coal - Finely divided coal has been successfully floated by a dissolved air process; CO_2 is the gas usually incorporated. The process is used when the size range precludes the use of dispersed air flotation. A specific application would be the separation of coal and pyrite from slate. The coal and pyrite are easily floated, whereas the slate settles out. Flotation may be applicable for closing a coal-washing circuit in place of settling basins.

- iron and steel - Scale and oil present in iron and steel mill waste water as a result of manufacturing may be removed by flotation.

- laundry waste - Solids and fatty acids may be recovered.

- meat products - Valuable grease is recovered, and BOD is reduced sufficiently to allow reuse of process water.

- mining - dissolved air flotation is used to remove suspended solids present in overflows from dispersed air flotation machines.

- metal finishing - Coolants used during machining and oils used to wash castings result in a waste stream contaminated with suspended solids and soluble oils. Aircraft-washing wastes may also be treated by dissolved air flotation.

- oil industry - Free or emulsified oil in refineries or oil fields is removed by dissolved air flotation.

- pulp, paper, and allied products - This field represents the historical application of dissolved air flotation; the technique has been used since World War I. The suspended solids in a typical paper waste stream are extremely difficult to recover by gravity sedimentation.

- soap manufacturing - Fats and oils are recovered for reprocessing.

- sugar refineries - Flotation is applicable for removing impurities and nonsugar solids from a raw sugar melt.

Examples of the recovery of lithium salts from brines, the removal of precipitates and fine particulates from mineral plant effluents, and oil and suspended particle removal from petroleum refinery waters are described below.

Lithium Salt Flotation. Dilithium sodium phosphate in the form of 2.5-μm diameter particles was floated from hot brine solutions in the Trona, California, plant of the American Potash and Chemical Corporation (Ryan 1951; Roe 1980; Meinhold and Walker 1968). The plant was closed in 1978 after 34 years of operation (Roe 1980). The slurry of hot brine and dilithium sodium phosphate particles was aerated by spraying downward in upward rising air currents in cooling towers and then pumped to flotation tanks. The lithium salt particulates coated with a soap residue from earlier process steps combined with fine bubbles and floated to the top of the tank under quiescent conditions where they were discharged over a froth overflow lip. A second-stage dissolved air flotation unit processed the tailings from the first stage. Second-stage recycle brine was pressurized with air at 90 psi, held for 2 min in a 1500-gal

pressurized retention tank, and then released into the flotation tank where residual particulates floated with the air bubbles for recovery. Flow through the recovery system was about 1000 gpm.

Mineral Plant Effluent Flotation. Effluent from the Kamioka, Japan, zinc concentrate thickener contains copper and other heavy metal ions and cyanide. A process was developed to reduce the concentration of these contaminants for environmental and other reasons (Nagahama 1974). The process is of interest because of the combination of ion flotation, precipitate flotation, and ultrafine particle flotation using a specifically designed induced air flotation machine that generates a large volume of fine bubbles in nonturbulent conditions. The composition of the thickener overflow is shown in Table 5.13. The pH of the effluent was adjusted from 11.6 to 3 with sulfuric acid, which decomposed the soluble $Cu(CN)_3^{=}$ ion into insoluble CuCN and Cu^{++} and CN^- ions. The copper ions form a precipitate with residual ethyl xanthate ion from the concentrator process and cyanide ion remains in solution. Sodium sulfide was added to precipitate any remaining copper, zinc, cadmium, and iron ions. An anionic polyacrylamide flocculent (Accofloc 305) and a frother (MIBC-methyl isobutyl carbinol) was added, agitated for 7 min, followed by 10-min flotation: 97.7% of the copper, 98.3% of the zinc, and 98.3% of the cadium were recovered in the flotation froth.

Petroleum Refinery Wastewater Flotation. Dissolved air flotation and induced air flotation are used in the petroleum industry for the removal of oil and suspended solids from wastewater. A summary of a number of refinery systems is presented in Table 5.14 (Churchill and Tacchi 1978).

TABLE 5.13. Contaminants in Zinc Thickener Overflow[a]

Elements and Radicals, ppm	Chemical Species	Concentration of Chemical Species, ppm
Cu, 30	$Cu(CN_3)^-$	67[b]
CN, 51	Free CN^-	14[c]
Zn, 203.43	ZnS + soluble Zn	301, 0.43
Cd, 1.09	CdS + soluble Cd	1.29, 0.01
Fe, 3.36	FeS	4.9
	Soluble Fe^{++}	0.08
	Soluble Fe^{+++}	0.20
Xanthate	$C_2H_5OCSS^-$	16.8
	Frother	18.0[d]

(a) Nagahama (1974).
(b) Zt pH = 11.6 with excess CN^-, Cu becomes completely complexed as $Cu(CN)_3^{=}$.
(c) CN^- concentration excluding $Cu(CN)_3^{=}$.
(d) Determined using calibration curve of "frother power tests."

TABLE 5.14. Summary of Dissolved Air Flotation Systems

Design Parameter	Refinery No. 1	No. 2	No. 3	No. 4	No. 5	API[a]
Inlet oil content, mg/l	---	270	70	112	---	---
Flocculation prior to flotation	Yes	No	Yes	Yes	Yes	Yes
Overflow rate, gpm/ft^2	3.45	2.3	2.9	2.3	4.0	2.0 to 2.5
Detention time, min						
Flotation chamber	19.5	23	27	20	10	10 to 40
Contact tank	18	1 to 2	1 to 2	---	---	1 to 2
Recycle pressure, psig	50	40	40	40 to 50	40	40
Recycle, % of feed	25	33	33	---	50	20 to 50
Air/water ratio, SCF/100 gal	0.8	1.0	1.0	0.36	---	0.05 to 1.0
Removal efficiency						
Oil, %	70 to 85	60	92	66	75	---
Suspended solids, %	30 to 50	---	72	---	---	---
Designed flow, mgd	30	4.3	5.7	2.5	2.5	---

(a) API refers to general criteria specified by the American Petroleum Institute.

5.4 PURIFICATION TREATMENTS: REVERSE OSMOSIS AND ION EXCHANGE

Other possible water treatment approaches have been tested in geothermal applications but are almost certainly inappropriate for main flow treatment prior to injection. Reverse osmosis is an energy-intensive method to remove essentially all dissolved solids from solution. This is more than is needed for geothermal injection treatment because there are only a few chemicals that cause particulate/scale problems; removing dissolved NaCl is of little interest in geothermal applications. The membrane involved in the reverse osmosis process must be kept clean from scale, which requires the use of inhibitors and backflushing. Mickley and Coury (1982) reported a study of silica scaling from brines undergoing reverse osmosis treatment. One geothermal application of reverse osmosis was a unit to provide domestic and process cleanup water for a geothermally heated food processing plant at Brady Hot Springs in Nevada

(2800 ppm dissolved solids, 131°C). As of 1982, the unit was unused because it reportedly failed to deliver the volume and purity of water expected and required more maintenance than was desired.

Ion exchange is not considered feasible for treating the main flow at a geothermal power plant because the ion-exchange media are not selective enough for the scaling species in the midst of an overwhelming concentration of innocuous salts. In addition, the ion-exchange media might form scale. Ion exchange might very well play a part in water conditioning for a specific plant use (pump bearing lubrication or cooling water) but not for main flow treatment prior to disposal. Anderson (1981) describes the application of ion exchange to concentrated solutions.

5.5 CURRENT BRINE PROCESSING EXPERIENCE

Specific treatment tests have been described under the particular technology heading in this chapter. On a geographic basis, the experiences are summarized in Section 8. In the United States, there are six instances in which several different components or approaches have been combined into a single treatment process. These are described to emphasize these processes, which combine several technologies.

5.5.1 Salton Sea Geothermal Demonstration Unit 1

A simplified process flow sheet for the steam production and brine treatment systems for the Union Oil 10-MWe Salton Sea Unit 1 facility is illustrated in Figures 5.51 and 5.52. This unit began operation in 1982 to supply steam to a companion Southern California Edison 10-MWe steam generator.[a] Production wells at this facility supply up to 1,416,000 lb/h of hot brine (475 to 500°F) to the steam production system. The two-phase flow from each production well is processed through a wellhead separator (~420°F) where steam flashed from the brine is collected and routed into the main steam line to the power plant. Hot brine from the separators is collected in a common header and directed to the first-stage flash crystallizer, which operates at ~125 psia. Sludge is recycled from the thickener to the first-stage crystallizer to provide seed particles for deposition of silica and other supersaturated constituents in the brine. Steam separated in the first-stage crystallizer is routed to the main steam line, and the spent brine slurry is sent to the second-stage flash crystallizer that operates slightly above atmospheric pressure. Steam from the

(a) This large-scale pilot plant uses hypersaline brine, ~250,000-ppm TDS, and incorporates the following techniques in its brine treatment process: flash crystallizers, reactor clarifier, gravity thickener, and dual-media filters.

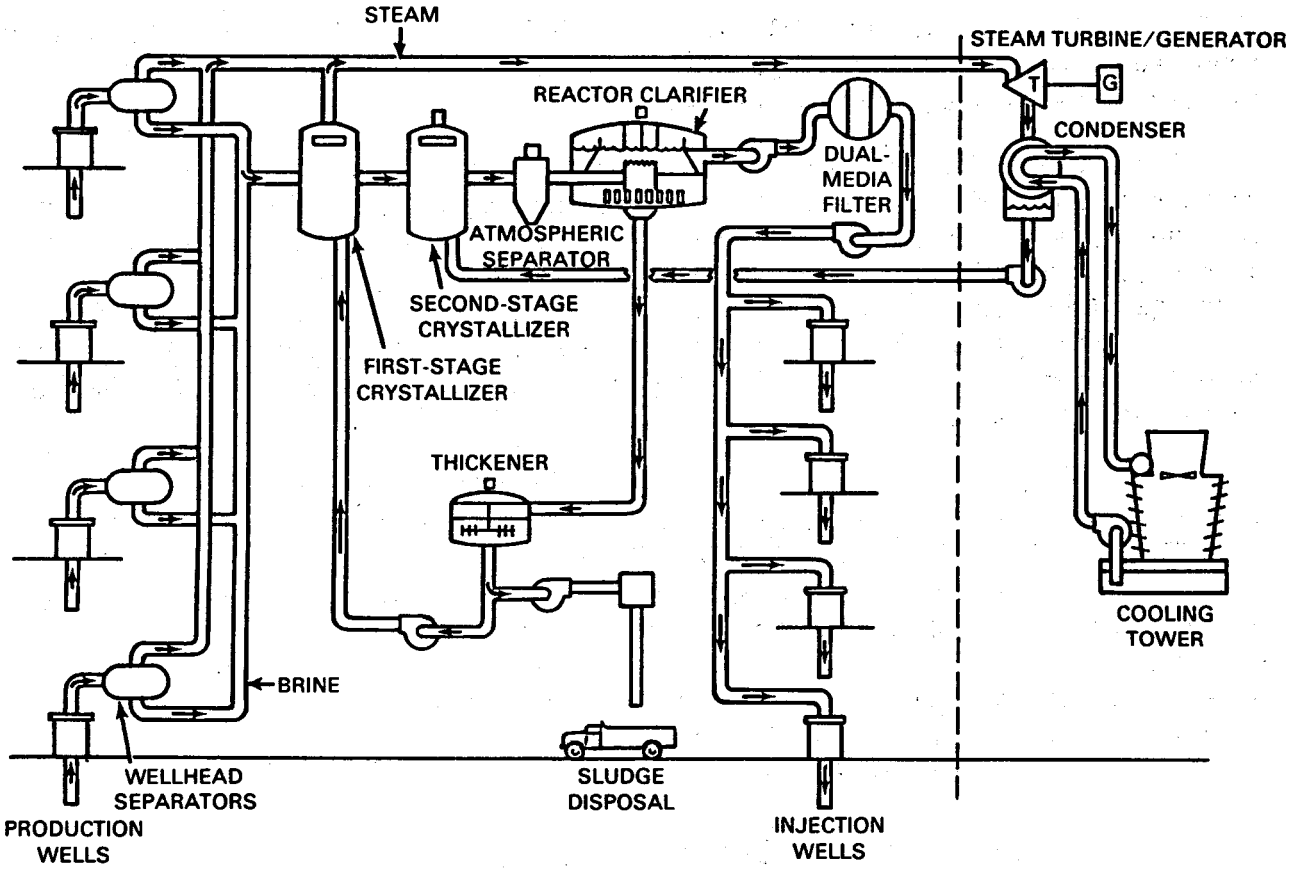

FIGURE 5.51. Flow Diagram for Salton Sea Unit No. 1 (Moss, Whitescarver, and Yamasaki 1982). The duplicate crystallizer separator train is omitted for clarity.

second-stage flash crystallizer is currently vented to the atmosphere, and the brine slurry flows to an atmospheric separator for final separation of the steam from the brine. Two separate trains of flash crystallizers and atmospheric separators are available; each is capable of processing 100% of the flow. This arrangement allows one train to be shut down for maintenance without interrupting power generation and also provides a greater degree of control for balancing brine flow and stabilizing vessel operating conditions. Additional surge capacity is available in the system by using second-stage crystallizers.

Spent brine flows from the atmospheric separators (suspended solids content believed to be 1% to 2%) to a reactor clarifier where precipitation or crystallization of supersaturated constituents is essentially completed and much of the particulate matter is separated from the brine. Postclarifier residual particulate matter (believed to be 50 to 200 ppm suspended solids) in

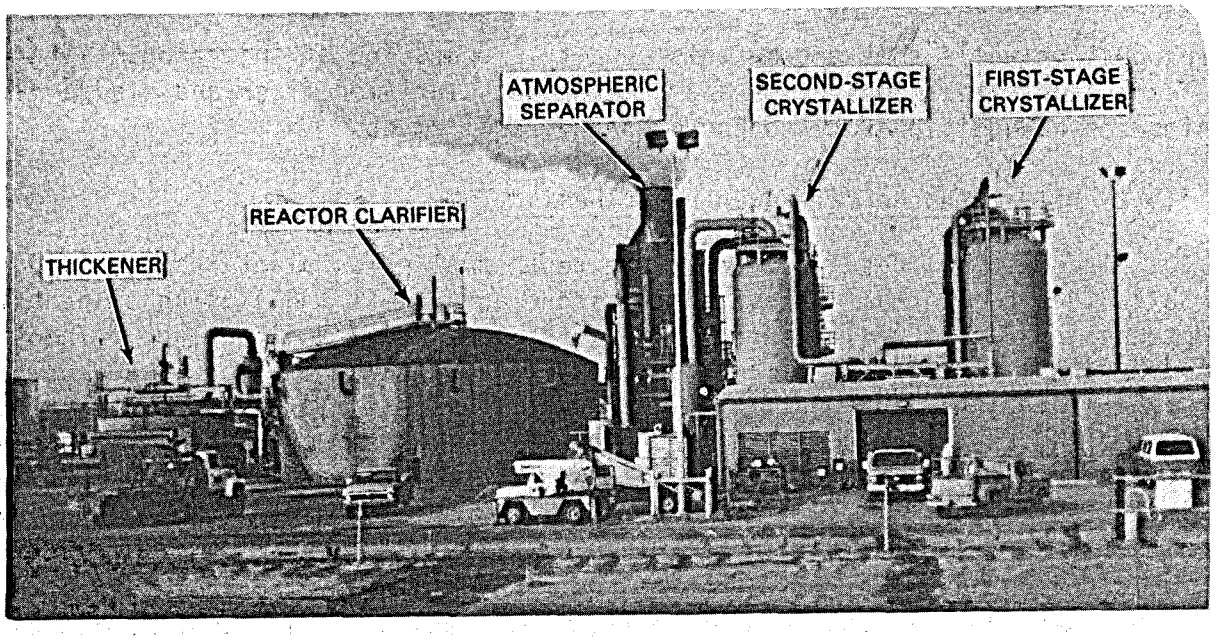

FIGURE 5.52. Brine Treatment Facilities at Salton Sea 10-MWe Plant (1983)

the brine is lowered to ~10 ppm by the dual-media filters that receive the brine effluent from the reactor clarifier. Four injection wells discharge the 190°F filtered brine to underground receiving formations.

Sludge from the reactor clarifier (believed to be 5% to 8% solids) is routed to a thickener to remove water that can be separated by gravity sedimentation. The sludge from the thickeners (believed to be 15% to 18% solids) is pumped to a filter press for final dewatering; it is designated as a hazardous waste due to its relatively high heavy metal content (for example, Ba, Pb, and Cu) and must be transported a considerable distance to an approved burial site near San Diego. A local disposal site is planned when the quantity of hazardous waste produced becomes large enough to justify building the site. An alternative tested at the plant is to bypass the filter press and dispose of the slurry directly.

The Salton Sea Unit 1 facility has operated well within expectations for a demonstration plant. Some minor difficulty has been experienced with plugging and loss of efficiency in the dual-media filters, probably resulting from overloads caused by occasional upsets of the reactor clarifier.

Recycling sludge from the thickener to the first-stage crystallizers imposes an energy penalty on the system because of the cooling effect of the recycled sludge. Additional brine (~3%) must be added to the flow from the

production wells to overcome this penalty. Operation of injection, filter feed, and filter press pumps and the reactor clarifier mixer and sludge rake imposes an additional but unknown energy requirement.

5.5.2 Niland Geothermal Power Plant Design

A conceptual design for a 49-MWe geothermal power plant was developed for Salton Sea geothermal waters (Featherstone and Powell 1981) using a spent brine processing facility similar to that of the 10-MWe Salton Sea plant. The steam-gathering system of the Niland design differed in that only one stage of flash crystallization is used and high-pressure steam is collected separately from low-pressure steam and each is routed separately to a dual-pressure turbine. High-pressure steam is collected in centrifugal separators; low-pressure steam is collected in flash crystallizers that operate at 22 psia. The energy penalty for recycling sludge to the flash crystallizer in this design requires ~1% additional production. Eliminating the second-stage flash crystallizer would reduce the capital cost of a brine treatment facility. The plant would probably be operated with a first-stage high-pressure, high-temperature system (200 psia) to minimize scale formation.

5.5.3 Flash Crystallizer Separator Design

The conceptual flow sheet for using the FCS in the dual-flash system is illustrated in Figure 5.53 (Awerbuck, Van der Mast, and Rogers 1982). Feed is introduced to FCS No. 1, which produces high-pressure steam for a dual-pressure turbine. The clarified brine from FCS No. 1 flows to FCS No. 2, which produces low-pressure steam for the turbine. Clarified brine from FCS No. 2 (now separated with silica) is diluted with a portion of the steam condensate and is heated by compressing a portion of the low-pressure steam produced by FCS No. 2. Dilution and heating of the brine reduces silica and other constituents below their respective saturation limits, thus preparing a clear brine for underground injection. Sludges produced by the FCS units are routed through small flash tanks to permit the sludges to reach thermal equilibrium at atmospheric pressure prior to further processing (e.g., dewatering by gravity thickening and filter press). The major advantage of this design is a substantial reduction in equipment requirements for brine treatment (eliminates reactor clarifiers and brine filters). The FCS units are estimated to be about the same cost as the flash crystallizers; however, they have not been constructed. The clarification sections of the FCS units require a longer residence time than the flash crystallizers and therefore a larger volume. It is important to minimize the size of the FCS units, however, due to the high cost of building large high-pressure vessels. Therefore, as indicated earlier, it is planned that only 80% of the supersaturation will be relieved, which substantially reduces the time requirement. A 6% energy penalty is imposed to reheat the brine.

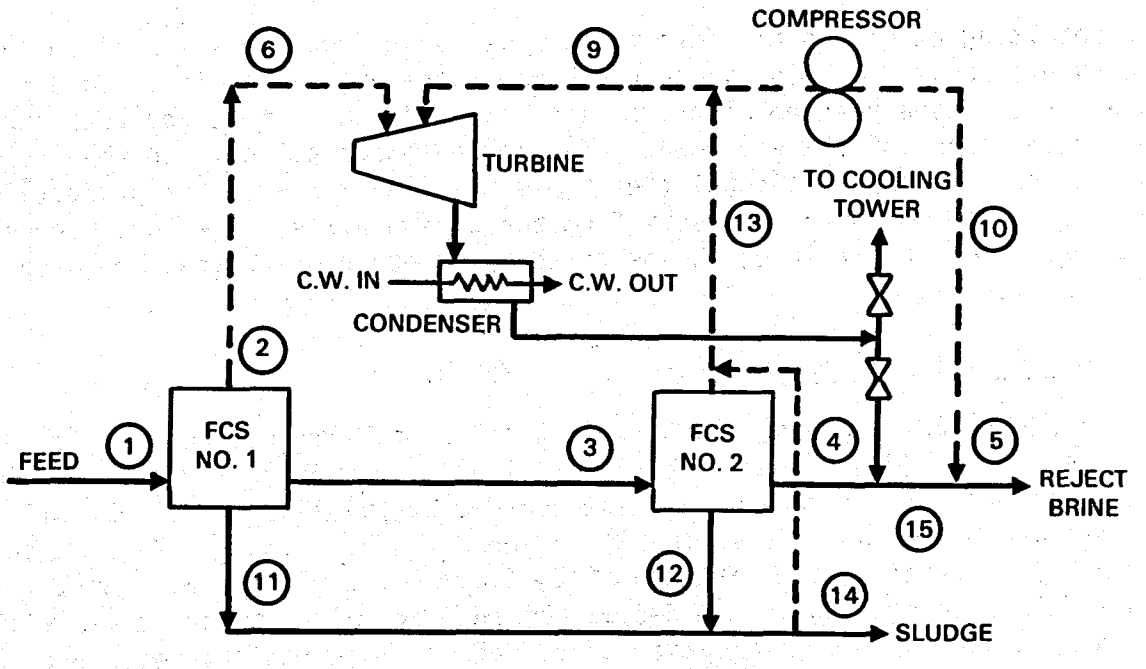

FIGURE 5.53. Conceptual Flow Diagram for Power Plant Using FCS Units (Awerbuck, Van der Mast, and Rogers 1982)

5.5.4 Brawley Demonstration Plant

This 10-MWe plant was the first to operate on the hypersaline brines from the Salton Sea area of the Imperial Valley. Silica and sulfide scaling are problems at this location. The brine treatment approach consisted initially of ponding/aging only and was unsuccessful at controlling equipment and injection well plugging. This has been modified to include acidification. The owner/operator of the steam supply/brine supply for this plant, Union Oil Company, has retained the details of the Brawley experience as proprietary information. The dose rate and location of the acid addition are unavailable. Since this plant is operating on a kinetics-based precipitation avoidance treatment scheme (in contrast to Union Oil's Salton Sea Plant with its controlled precipitation approach), other consistent actions would be maintaining temperature, avoiding oxygen contact, and minimizing delay prior to injection. Whether these activities are being done is not known.

5.5.5 Magma Power Binary Cycle Plant

This 11-MWe plant was the first long-lived plant to operate in the Imperial Valley and the first binary cycle plant in the United States. It operates on a moderate-temperature (377°F) brine that has a pronounced tendency to form calcite scale. The brine treatment consists of maintaining pressure and controlling the temperature decline of the brine upon energy extraction. Pressure is maintained by downhole and surface pumping to prevent flashing and

the resulting calcite scale formation. The design and operation of the heat exchangers keeps the brine above the temperature at which silica could precipitate. There have been no problems with this brine treatment approach other than maintenance of the equipment. Scaling has been slight, and the suspended solids that are injected consist of fines carried over from the production wells and some corrosion products from the piping walls. The total concentration of suspended particles is low relative to other brine treatment approaches (see Section 6).

5.5.6 Roosevelt Hot Springs

A 20-MW (23-MW gross) flash cycle plant near Milford, Utah, is scheduled to come on-line (June 1984). The power plant is operated by Utah Power and Light, and the brine/steam supply is operated by Phillips Petroleum. The approximate brine conditions are 18% wellhead flash to 350°F resulting in a 790-ppm SiO_2 level in the flashed brine; fluoride levels are high at 1 to 3 ppm. Calcite scaling is avoided by the addition of a few parts per million of phosphonate inhibitor (believed to be Dequest 2060) at the wellhead. Silica scaling is controlled by maintaining the temperature at ~350°F in a totally pressurized and insulated injection system. The brine residence time from flash to injection is on the order of 45 min. Some silica scaling is observed; but because injection is into a 3- to 5-ft wide fracture, it is hoped that long-term injectivity will remain good. The field has produced low volumes of flow for over two years during a test of a new turbine concept. Presumably this permitted Phillips the opportunity to match their treatment to the particular production and injection characteristics. The use of an inhibitor (calcite), temperature maintenance, and oxygen avoidance combine to make an operational system at this site.

6.0 OPERATIONAL ASPECTS

The design of an injection treatment process will determine specific operational procedures; however, there are several aspects that deserve highlighting for all processes. Although pursuing each activity that is described may not be achievable for a given installation, they are all available for consideration during the design or operational phases.

6.1 TREATMENT PROCESS MONITORING

The maintenance of injectability is necessary to preserve the capital investment in the injection system and ultimately in the entire plant. Since the treatment process works on a complex chemical equilibria/kinetics problem, it is prudent to monitor chemically related parameters in addition to normal process measurements (pressure, pressure drop, temperature, liquid level, flow rate). These additional parameters include fluid chemistry, particulate content in fluid, and gas content (for pressure maintained systems).

On-line particulate monitoring assures rapid detection of operating upsets that might go unnoticed by normal process measurements. On-line monitoring provides a mechanism to optimize the process. PNL (Shannon, Elmore, and Pierce 1981) and Vetter Research (Kandarpa et al. 1981) have tried on-line particle monitoring under geothermal conditions. PNL found that high concentrations of suspended particles resulted from thermal cycling during up and down operation of a binary cycle plant. Vetter Research found that increased residence time in a reactor resulted in both increased sizes and concentrations of particles. Both groups found limitations on using existing instrumentation for on-line geothermal applications. PNL is undertaking additional research of particle instruments designed for on-line geothermal applications.

Since the purpose of injection treatment is to avoid the injection of suspended particles, or a solution that may yet precipitate them, the establishment of the solids flow through the process is a direct measure of its success. Table 6.1 illustrates particulate distributions through four examples: one pumped binary cycle plant and three reactor clarifier processes. If more information were available, particularly relating to the size of the particles, it would fill in the gaps and aid in the selection of subsystems to separate the solids from the brine. If a conclusion can be drawn from this limited data base on different reservoirs, it would have to be: if the receiving formation is porosity controlled to avoid plugging the formation, then the pumped binary cycle will deliver cleaner brine whose particulates are sized larger. The larger particulates, when they do accumulate to affect injectivity, will be easier to remove by backflushing. Smaller particulates can invade the formation and cause more serious damage. Unfortunately, we have no operating geothermal

TABLE 6.1. Particle Distribution in Brine Treatments (μm/ppm)

	Magma Binary Plant[a]	GLEF Test[b]	MCR (Mercer-2) 42-Day Test[c]	Salton Sea Plant[d]
Production flow	(<0.4 and ≥5 to 13/0.7)			
Power extraction step; output to injection (Hx or flash crystallizer)	(≥5/1.1)			
Reactor clarifier inflow		(/180)		(/1-2%)
Reactor clarifier brine output		(/100)		(≤10/50-100)
Reactor output Fluidized bed output Settling area			(5-10/) (5-10/) (5-7/360)	
Reactor clarifier sludge output		(/6-10%)		(/5-8%)
Media filtration brine output		(/4-10)	(<2/28)[e]	(/~10)
Thickener brine output		(/500-1000)		
Thickener sludge output		(/10-20%)		(/15-18%)
Filter press brine output		(/100)		
Filter press sludge output		(/65%)		

(a) Shannon, Elmore, and Pierce 1981.
(b) San Diego Gas and Electric 1980.
(c) Vetter et al. 1981; Kandarpa et al. 1981.
(d) Not confirmed by operator.
(e) Conflicting data (see text).

information on particle sizes of filter effluent other than <2 μm (and even this is unsure since the same researcher, using other instruments, reported fair numbers of 5- to 9-μm particles). The available data are too limited to make a good interpretation.

Fluid chemistry is an effective monitoring tool for a geothermal plant because small differences in composition between entering and leaving fluids can detect corrosion, scale deposition, or scale dissolution. The basic sampling equipment (described in Section 3) was adopted as ASTM Specification E947 in 1983. The use of the sampling probe inserted into the main flow is especially important in situations where scale is deposited inside the piping. The scale would tend to filter or precipitate out components as a sample is withdrawn unless a probe is pushed through the scale into the main flow. This monitoring principle was used at the Salton Sea GLEF to detect major scaling in the equipment (Needham, Murphy, and McCawley 1976). PNL used concentration increases of 2 ppm iron to detect corrosion in a geothermal binary cycle plant (Shannon, Elmore, and Pierce 1981). The small concentration increase becomes significant when the large flow rates are evaluated (Table 6.2).

Monitoring the gas content of the brine is useful in binary cycle geothermal plants, although it may be of little interest in flash cycles. The pressurized binary cycle has two concerns for gas detection: NCG breakout can change the pH enough to cause $CaCO_3$ scaling and leaks of highly pressurized organic working fluid into the brine can be indicative of corrosive perforation of the heat exchanger. On-line instrumentation can detect both conditions (Shannon, Elmore, and Pierce 1981). PNL is developing improved instrumentation to detect both gas breakout (Robertus, Shannon, and Sullivan 1984) and working fluid leaks into the brine flow (Kindle 1983).

TABLE 6.2. Chemical Indications of Corrosion in a Binary Cycle Geothermal Power Plant[a]

Date	Iron in Incoming Brine, mg/l	Iron in Outgoing Brine, mg/l	Iron Increase, mg/l	Flow, 10^3 kg/h	Iron Loss, kg/day
11/6/79	0.5	3.1	2.6	215	14
11/10/79	0.7	1.7	1.0	355	9
1/30/80	0.2	2.2	2.0	277	13
1/31/80	0.2	2.1	1.9	277	13
9/15/80	0.3	1.9	1.6	300	11
10/22/80	0.5	2.1	1.6	273	11

(a) Samples were stabilized with nonoxidizing acid (HCl) before analysis. The usefulness of precise chemistry in monitoring the process is shown (Kindle and Shannon 1982).

6.2 CORROSION

Produced brines are oxygen free and chemically compatible with the rock of the production formation. Many metals are not compatible with these brines, even as produced, and undergo a corrosion deterioration process. Subsequent to utilization and brine treatment, these brines may have been changed to: lose dissolved gases, lose precipitated minerals, add scale inhibitors, and add atmospheric gases. The effect of these changes on metal durability should be included in the design of a brine treatment process. The loss of dissolved gases is usually beneficial from a corrosion standpoint since the loss of CO_2 will tend to raise the pH in many waters. Corrosive attack on steels is reduced as the pH rises.

Duhalt, Mendoza, and Cortes (1970) looked at the corrosiveness of low-temperature (80°C) oil field brines and concluded that the aggressiveness did not vary significantly between pH 5 and 7. Similar results were found by Posey and Palko (1979) in their study of hypersaline corrosion rates as a function of pH and temperature. Their data, Figure 6.1, indicate little significant pH dependence between pH 4 to 7 above 100°C.

A uniform scale deposition inhibits corrosive attack on the underlying surface. The effect of scale inhibition on corrosion rate is much more varied

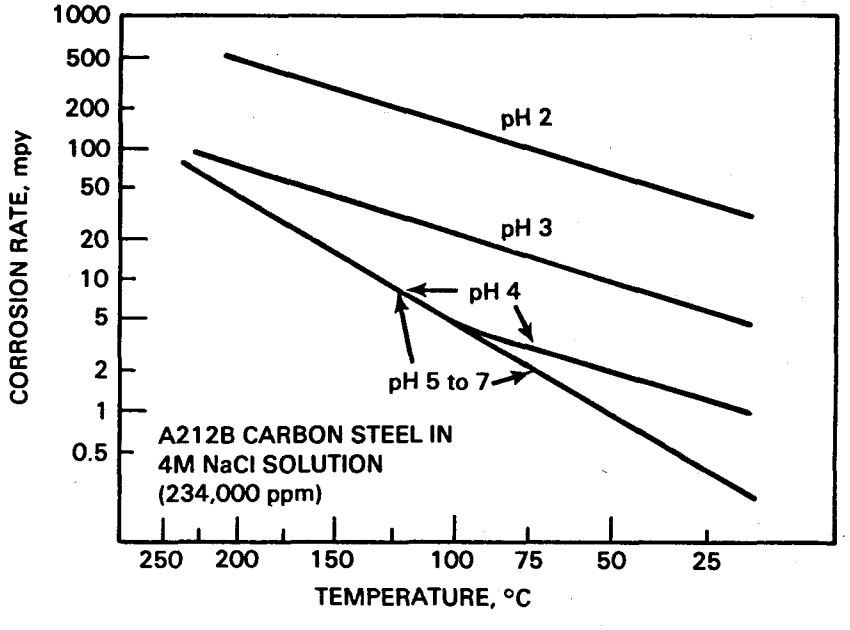

FIGURE 6.1. Electrochemical Corrosion Rates in Deaerated Hypersaline Brine as a Function of pH and Temperature. Data points omitted (Posey and Palko 1979). Note lack of pH dependence in pH 4 to 7 range above 100°C in this study.

and is frequently untested. Harrar tested the relative effect of some scale inhibitors on corrosion during silica inhibition studies (Harrar et al. 1982). The scale inhibitor that showed the best corrosion protection was Corcat P-18 (see Figure 6.2). Not all scale inhibitors performed as corrosion inhibitors at 125°C (Table 6.3); a few were accelerators. In a 45-day Italian field test (Corsi 1984) of Monsanto Dequest 2066 inhibitor (250 ppm in a brine with high scaling tendencies) the corrosion of the Incoloy 800 piping was attributed to the presence of the inhibitor.

Atmospheric gases can dissolve in the brine if it is exposed to the atmosphere. The only gas of any corrosion consequence is oxygen. Although the solubility of oxygen decreases to a minimum as the temperature rises near 100°C (Figure 6.3), it is very important to exclude oxygen contact with brine. Above 100°C, the solubility increases with temperature. In addition to uniform corrosion, oxygen in brine causes pitting attack on some steels and can lead to perforation of the metal at rates faster than predicted, based on uniform corrosion rates. Corrosion inhibitors do not prevent pitting, which proceeds at 5 to 20 times the uniform corrosion rate (Annand, Hilliard, and Tait 1977). Since the injection well and brine treatment equipment represent a substantial investment, the corrosive lifetime should be established, particularly if the

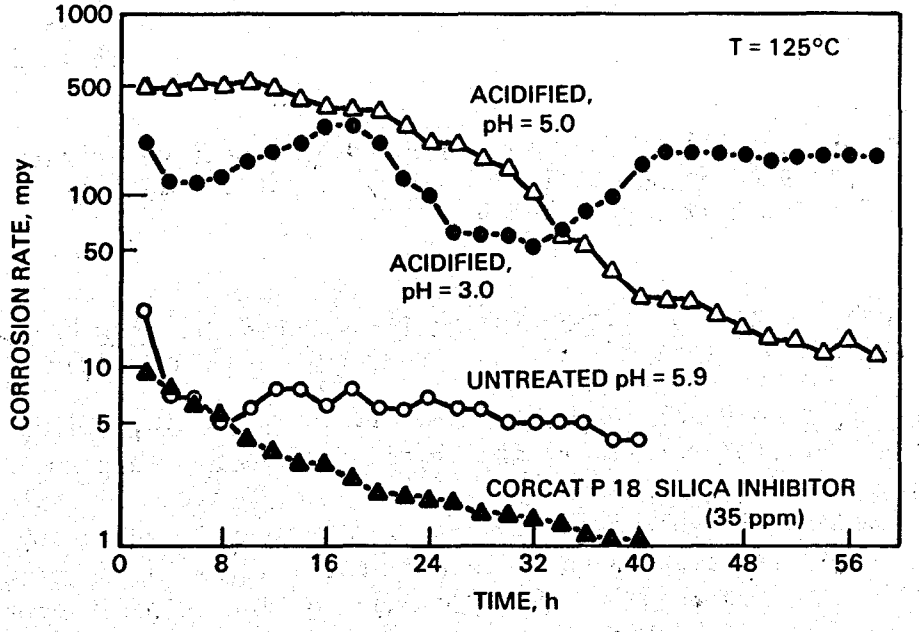

FIGURE 6.2. Corrosion Rate of Mild Steel (AISI 1018) in Hypersaline Magmamax 1 Brine. Petrolite instrumentation; Harrar et al. 1982. Note beneficial effect of chemical inhibitor at high concentrations.

TABLE 6.3. Silica Scale Inhibitor Effect on Corrosion Rate.[a]

Additive	Corrosion Rate, mpy (0.001 in./yr)
Group A	
None, control	5
Mirapol A-15 and Cycloryl MA (20/20 ppm)	2.4
PAE-HCl (35 ppm)	2.0
Corcat P-18 (35 ppm)	1.0
Ethoquad 18/25 and HCl (27/100 ppm)	20
Ethoquad 18/25 and Duomac T (25/7 ppm)	2.0
Ethoquad 18/25 (325 ppm)	1.2
Group B	
None, control	15
Calgon CL-165	2
Natco S-404	3
Betz 419	4
Thermosol APS	5
Geomate 256	15
Drewsperse 747	15
Cortron R-16	25
SW Chem SC-210	25 to 60

(a) Mild steel (AISI 1018) rates measured by linear polarization resistance technique at 125°C (after Harrar). Magmamax 1 hypersaline brine; pH 5.7-5.9.

brine treatment includes a pathway for oxygen contact with the brine. Figure 6.4 shows the result of pitting in downhole well materials.

Corrosion data may not be readily transferrable to other situations due to the local test variations that affect the environment surrounding the metal test coupon. In addition, shorter term (less than 30 days) corrosion tests frequently overestimate the corrosion rate when extrapolated to longer term exposures. Partly in response to these concerns, Radian Corporation and DOE have published two comprehensive survey manuals on corrosion in geothermal environments (Ellis et al. 1983; Ellis and Conover 1981).

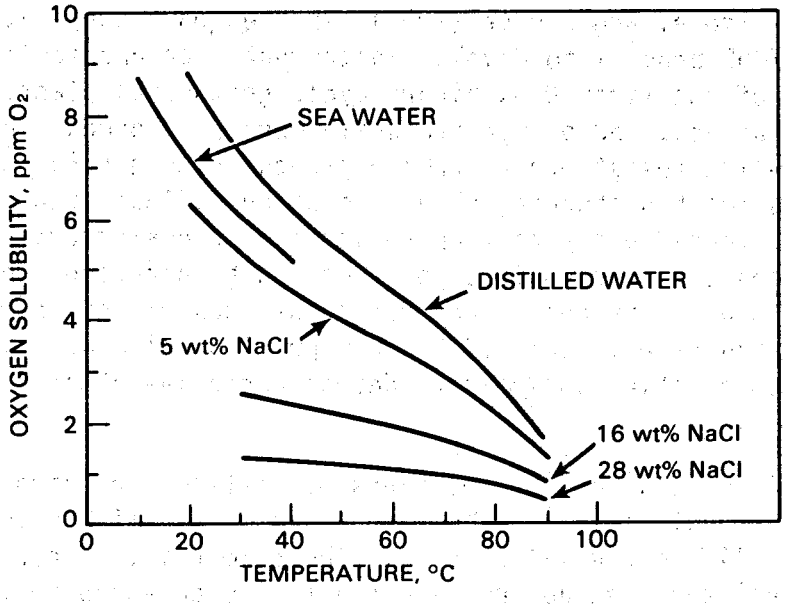

FIGURE 6.3. Solubility of Oxygen in Brines. Air saturated with water vapor at a total pressure of 760 mm Hg (Cramer 1974).

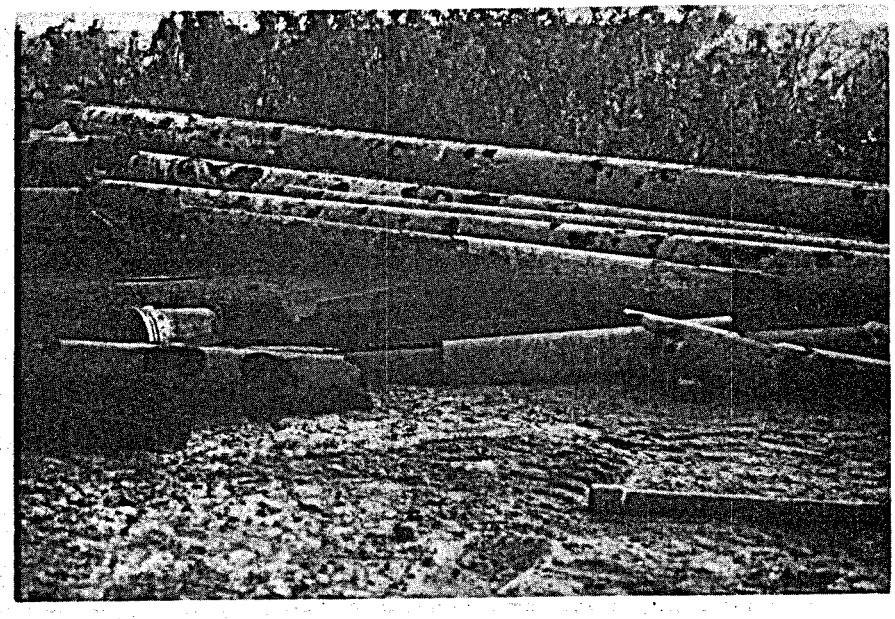

FIGURE 6.4. Results of Pitting Attack on Well Casing; 1983 Photograph at Hypersaline Salton Sea Geothermal Field

Shannon, Elmore, and Pierce (1981) reported on a cooperative PNL/Magma Power Company/DOE program to develop instrumentation and monitor the chemistry and materials of the first U.S. binary cycle geothermal plant. Uniform corrosion, pitting attack, and protective scale were all noted. Through the use of insertable on-line resistance corrosion probes (Figure 6.5), permitting removal installation without disturbing plant operations (Figure 6.6), the corrosion rate changes detected unexpected operating conditions/errors before damage was done to components. In the first years of plant operation, which experienced a lot of up and down plant operations during startup of this new technology, the typical corrosion rate in this 177°C 8000-ppm TDS brine was 5 to 10 mpy. The use of brine composition analysis to detect corrosive attack is illustrated in Table 6.2.

Shannon found that of the two types of on-line corrosion monitors, resistance and linear polarization, the former was more reliable in pressure and temperature cyclic geothermal service. The commercial linear polarization probe had a seal that leaked and resulted in indicated corrosion rates below what was actually being experienced. All probes need to be placed to protect them from the erosion potential of the center part of the brine flow.

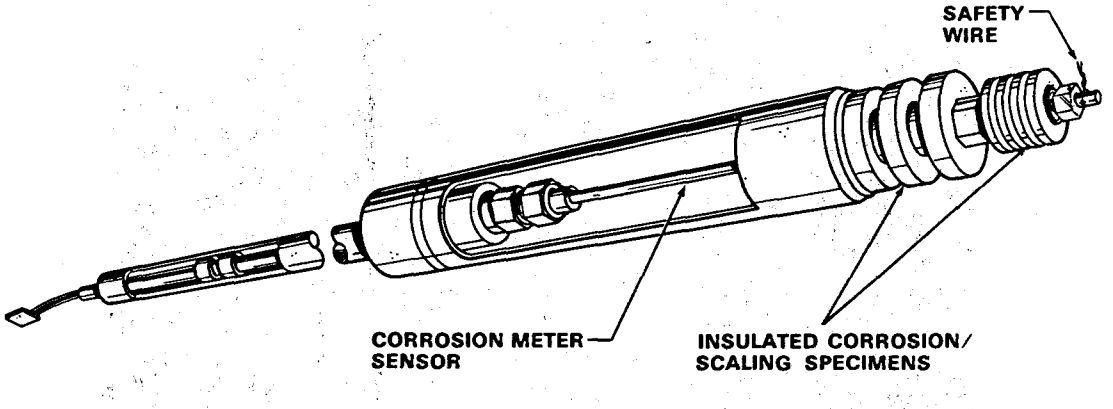

FIGURE 6.5. Insertable Corrosion Monitoring Probe. PNL used this device and variations of it to provide combined on-line and historical corrosion data (Shannon, Elmore, and Pierce 1981). This insertable probe is referred to in the following figure. The specimens and the sensor must be protected from atypical velocity-based erosion.

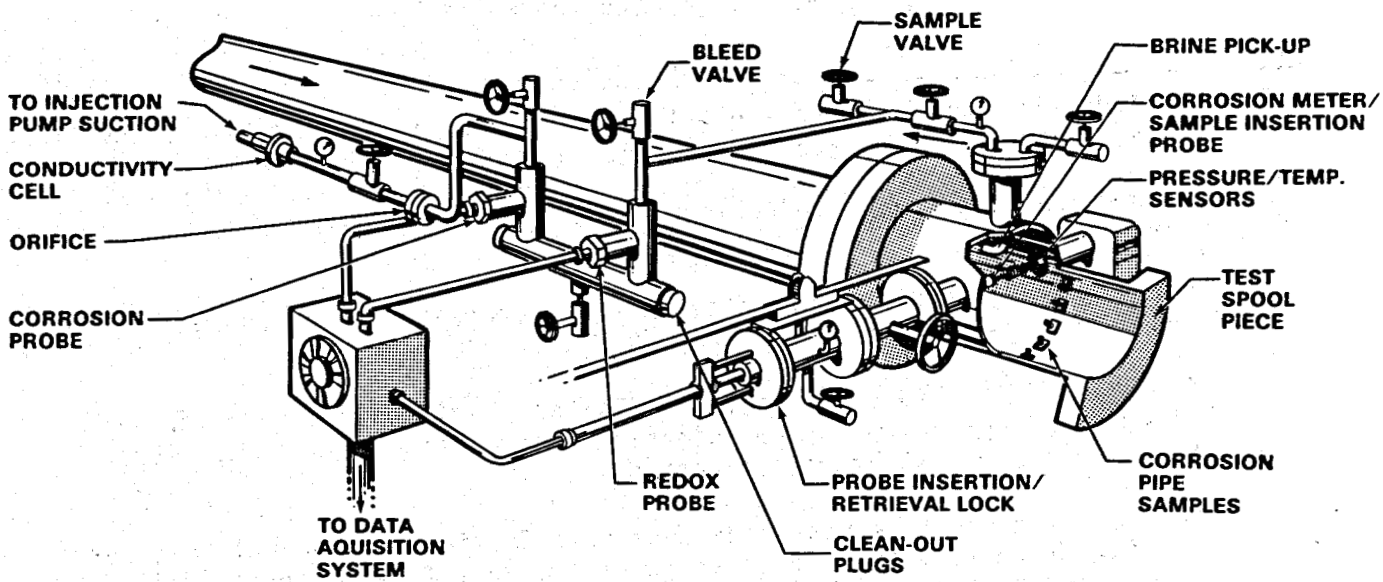

FIGURE 6.6. Monitoring Station After Injection Pump. This station monitored corrosion changes and test instruments at the Magma East Mesa Plant. The difference in pressure before and after the injection pump permits a controlled flow through the station (Shannon, Elmore, and Pierce 1981).

6.3 INJECTION WELL MONITORING

The life span of an injection well is often a reflection of how the well is operated. One of the key operations that aid in maintaining capacity is periodic backflushing. It is essential that the injection system be designed for periodic backflushing. It is advantageous to have multiple injection zones so that as a zone becomes ineffective it can be abandoned in favor of more permeable zones if it cannot be restored.

Besides periodic backflushing and abandoning ineffective zones, there are several operational aspects that can aid in maintaining the capacity of a well. As mentioned by Knutson and Boardman (1978), the life span of an injection well increases as the injection flow rate decreases. Thus, it might be prudent to use all the available injection wells simultaneously for disposal, which would minimize the disposal flow rate per well. It was also noted that injection wells lose capacity more rapidly if they are used intermittently.

Careful monitoring and record keeping are essential for each injection well to establish the magnitude of well impairment, its potential cause, and the percent of recovery after well rehabilitation. Data that should be collected during the life of an injection well are listed on Table 6.4. All the items listed are not needed at any one time; and, in many cases, some of the

TABLE 6.4. Suggested Field Investigations for Monitoring Injection Wells

Item	Procedure
1	Periodically sample the brine before treatment, after treatment, and just before injecting for water chemistry, suspended solids, and gas bubbles.
2	Record injection rate, injection pressure, and injected fluid temperature.
3	From recorded data (Item 2) determine the conductivity of the well (Kh) from a reinjection impairment map (RIM).
4	Run periodic membrane filter tests (Barkman-Davidson) to coincide with fluid sampling on samples of injection fluid before treatment, after treatment, and just before injection.
5	Run flow and pressure tests (discussed in Section 3); downhole pressure profile of well, transient pressure tests, interference tests, drill stem tests, and falloff tests.
6	Re-perform geophysical logging, caliper, gamma density, temperature, and natural gamma.
7	Record injection pump performance.
8	Collect samples of scale in the injection system.
9	Collect corrosion data from coupons and corrosion rate meters.
10	Keep a well log, record times of injecting, any problems, maintenance, and well recovery operations.

items will never be required, depending on well performance. At the minimum, Items 1, 2, 3, 4, and 10 are recommended. Since most of the injection performance tests were discussed in Section 3 for establishing a preoperational base line, these tests will only be briefly reviewed here as they apply to well monitoring.

6.3.1 Item 1 - Suspended Solids

Particulate plugging is one of the major causes of well impairment; thus, it is essential that particulates be monitored. Monitoring the particulates at key locations in the stream[a] can help determine where the particulates are produced. These data along with their chemistry, quantity, size ranges, and

(a) For example, at each production well, after mixing of the production fluids, after heat extraction or steam flashing, after waste treatment, and just before injection.

physical characteristics provide the necessary information for establishing treatment methods and for monitoring the success of these methods. Sudden changes in the particulate content can occur due to changes in the plant operation. By frequent monitoring, these changes can be identified and corresponding changes in the waste treatment can be made to offset these peak periods. Methodology for sampling and analyzing the brine chemistry and suspended particulates was discussed in Section 3.

6.3.2 Item 2 - Injection Wellhead Data

Recording the flow rate at each injector well, the corresponding injector well pressure, and injected fluid temperature provides a low-cost picture of the injector performance. Because of the simplicity and low cost, it is highly recommended that Item 2 be included in a well monitoring program. Plotting the injection pressure versus the injection rate provides a good visualization of the injection performance. Table 6.5 contains data from Magma Power Company's injection well 46-7 and shows that the injectivity of the well decreased from 1.81 to 0.93 as the well became impaired. After backflushing, the injectivity increased to 2.53.

6.3.3 Item 3 - Reinjection Impairment Map

A RIM plots injection well surface pressure against water injection rate for a family of kh (millidarcy-feet) values. By plotting the pressure versus flow data obtained at the well, an estimate can be made of the well's current conductivity (kh). The RIM is an improvement over just injectivity (Item 2) because it encompasses the total system hydraulics, including reservoir hydrodynamics, tubing friction, and hydrostatic driving forces. One disadvantage is

TABLE 6.5. Excerpt from Magma Power's Operational Log for Injection Well 46-7

Date	Flow, gpm	Pressure, psig	Injectivity (flow/pressure)
3/3/78	763	470	1.81
3/6/78	749	530	1.41
5/23/78	646	515	1.25
5/25/78	656	541	1.21
5/26/78	721	645	1.12
5/31/78	506	540	0.93
	Well impaired; backflushed		
8/9/78	647	255	2.53

that a separate map must be constructed for each water injection temperature and probably for each injection well. Despite the initial time for construction of the RIMs, they are recommended as a valuable tool to evaluate the current state of the injector. For more details on the construction of a RIM, see Jorda (1978). Figure 6.7 is an example of a RIM for Magma Power Company's injection well 46-7.

6.3.4 Item 4 - Membrane Filter Tests

The membrane filter test is a relatively quick and inexpensive test and is recommended for a well monitoring program. By comparing the permeability (md) of the filter cake from a current test with previous tests, a relative guide to the potential for the current waste to impair the injection system can be made. By using the filter cake md and the estimated formation md, the mode of impairment can be estimated.

6.3.5 Item 5 - Flow and Pressure Tests

Flow and pressure tests provide many well and reservoir data such as porosity and permeability of reservoir rock around the well, skin factor, the number of aquifers, and changes in pressure with depth. Monitoring changes in these parameters would provide insight as to the acceptability of the injection system to the injected waste. Although these tests do require more elaborate equipment than the tests listed under the first four items, they also provide more detailed information. Thus, it depends on the performance of the injection system how often these tests should be performed, if at all. Both downhole pressure profiles of the well and transient pressure testing can be performed during normal plant operations, so they are more convenient than the other tests. An example of estimated reservoir parameters obtained from pressure and flow tests is presented in Table 6.6.

Briefly, the two production tests demonstrated in Table 6.6 provide a measure of the average formation permeability throughout the well depth (kh) and a measure of average reservoir compressibility throughout the well's depth (ϕch). Besides obtaining base-line well data for later comparisons, inferences about the area hydrology can often be made. Since the production tests with Well 38-30 and then Well 25-20 producing resulted in similar kh and ϕch values in Wells 56-30 and 31-1, there appears to be open communication between these wells.

6.3.6 Item 6 - Geophysical Logging

By repeating the geophysical logs and then comparing them with the preoperational logs, a basis can be derived for determining what damage has occurred to the injection system during plant operations or the effectiveness of well recovery methods. The disadvantages of geophysical logging for well monitoring are that the well must be temporarily shut down and the test is more

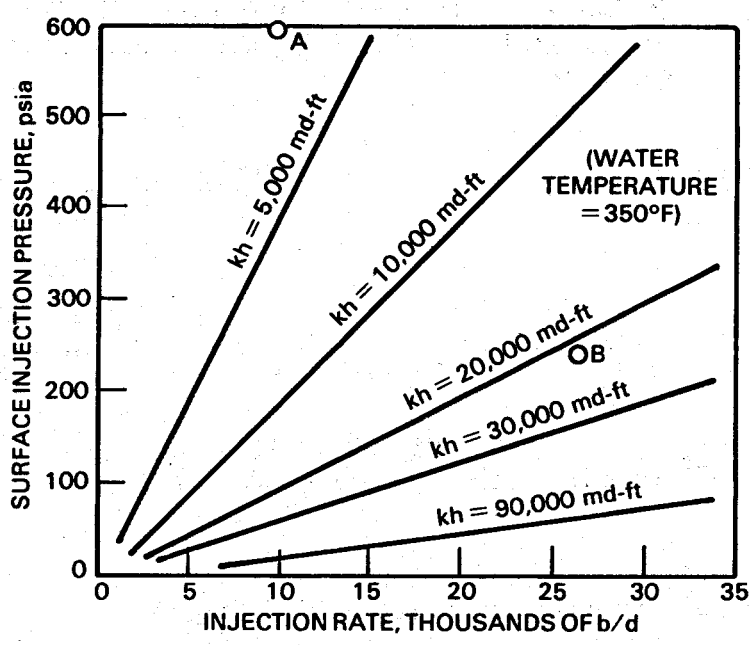

FIGURE 6.7. RIM for Well 46-7. Based on: water viscosity = 0.185 cp; Re = 1000 ft; R_w = 6 in. Fracture pressure is just under 700 psi (Jorda 1980).

expensive than most of the other listed items. Of course, if problems are implied from surface data, these disadvantages are outweighed by the precise information that they can provide, such as borehole diameter profile, porosity of injection intervals, temperature profile, and location of and fraction of clay mineral zones.

6.3.7 Record Keeping and Sample Collection

The first six items are tests to obtain current data on the injectability of the system. The next four items are more of a cataloging nature. Besides such data as the permeability of the receiving formation, it is advantageous to record and collect the information listed in Items 7 through 10. Without that data, a full picture of the history and the current state of the injection system cannot be drawn. Background data include: Item 7, a record of injection pump performance; Item 8, a collection of scale samples from the injection system; Item 9, corrosion data of the injection system obtained from coupons and/or corrosion rate meters; and Item 10, a well log record of all events including shutdown and injection times, any problems, and well recovery operations.

TABLE 6.6. Estimates of Reservoir Parameters Obtained from Pressure/Flow Tests at Republic Geothermal Wells[a]

Well	Test 1 (38-30 producing)	Test 3 (25-20 producing)	Previous Estimates
36-30	kh = 24,800 md-ft	---	Borehole logs (Republic): kh = 44,000 md-ft Buildup test (Republic): kh = 41,700 md-ft Interference test (LSL): kh = 29,500 md-ft
56-30	kh = 26,300 md-ft $\phi ch = 4.5 \times 10^{-4}$ ft/psi	kh = 23,600 md-ft $\phi ch = 7.89 \times 10^{-4}$ ft/psi	
31-1	kh = 35,400 md-ft $\phi ch = 2.07 \times 10^{-3}$ ft/psi	kh = 31,700 md-ft $\phi ch = 2.4 \times 10^{-3}$ ft/psi	
16-29	kh = 21,800 md-ft $\phi ch = 2.35 \times 10^{-3}$ ft/psi	---	Borehole logs (Republic): kh = 30,000 md-ft Buildup test (Republic): kh = 34,700 md-ft
78-30	---	kh = 10,400 md-ft $\phi ch = 6.68 \times 10^{-3}$ ft/psi	

(a) Narasimhan et al. 1977
(b) kh = reservoir transmissivity and ϕch = reservoir compressibility.

Collecting and logging the information is not expensive or time consuming; thus, the monitoring plan for every injection well should include Items 7 through 10.

6.4 IMPAIRED INJECTION SYSTEMS

Despite the impairments that are discussed in this section, many injection systems operate with minimal difficulty. Their success is a combination of careful planning to avoid or easily recover from impairments and favorable receiving systems. Owen et al. (1979) discuss testing of clarified geothermal brines for injectability. Some examples of geothermal injection systems that have operated without difficulty are listed in Table 6.7. More detail on these geothermal systems can be found in Section 8.

TABLE 6.7. Geothermal Injection Systems That Have Operated Without Difficulty

Location	Problem Avoided
Ahuachapan, El Salvador	Silica scaling by injecting above amorphous silica saturation
Onikobe, Japan	Thermal breakthrough; successful injection configuration
Salton Sea, California	Aggressive brine treatment process results in silica and metal sulfide deposition in surface facilities rather than downhole

Several injection system impairments and several possible solutions and preventions are listed in Table 6.8. The impairments include vapor loading, formation clay swelling, formation permeability reduction, wellbore fill and scaling, thermal breakthrough and unwanted fluid migration, and mechanical problems. The solutions to these impairments most often call for backflushing, the use of additives, hydrocracking the formation, mechanical treating or cleaning of the injection well, changing operational procedures (such as closing off the system to oxygen), and relocation to another injection horizon.

The success rate for recovery from injection system impairment is good; examples of recovered geothermal sites are listed in Table 6.9. The four injection system problems that have been successfully treated are: 1) thermal breakthrough by changing the strata that receives the injected fluid by redrilling or cessation of problem wells; 2) impairment due to wellbore fill by backflushing; 3) impairment due to amorphous silica deposition by acid treatment or hydrocracking; and 4) impairment due to heavy metal oxide buildup by sealing injection systems from air intrusion.

6.4.1 Vapor Loading

Vapor loading occurs when undissolved air in the liquid is injected into the reservoir and remains a gas. The air will then produce vapor-filled "tubes" that provide a barrier to liquid flow. Vapor loading could also theoretically happen when acidizing an injection well that transects carbonate formations. There are a number of solutions for a vapor-loaded injector. These include backflushing and resolubilizing the gas by increasing the pressure. Vapor loading has not been a problem in geothermal injection systems.

TABLE 6.8. Common Tactics for Recovery and Prevention of Injector Decline

Injection System Problems	Possible Solutions and Preventions
Vapor loading	Backflushing. Resolution with higher pressure.
Formation clay swelling	Additives to reduce (alcohols, ketones) or prevent (hydroxy aluminum) swelling. Hydrocrack formation. Preoperational study to prevent swelling.
Formation permeability reduction; other causes	Backflushing. Hydrocrack formation. Additives for dissolution. Dissolving by reheating formation during shut-in. Preoperational study of injection on the injector formations. Proper injection treatment process.
Wellbore fill and scaling	Backflushing. Redissolving by reheating during shut-in. Redissolving by additives, including CO_2. Close off system from oxygen; prevent metal oxide compounds. Maintain a CO_2 pressure; prevent carbonates. Maintain an injection temperature and pressure to prevent preparation of amorphous silica or carbonates. Clean out well mechanically. Reperforate liner. Proper well design to prevent sand infiltration. Proper injection treatment process.
Thermal breakthrough and unwanted fluid migration	Relocate injection wells/cessation of particular wells. Change injection depth by reperforating/sealing. Induce formation scaling to retard migration. Perform initial study to determine best locations for injection/production wells.
Mechanical problems	Replace or repair.
Subsidence	Increase injection volume.

TABLE 6.9. Successful Recoveries from Geothermal Injection Problems

Injection System Problem	Location	Solution
Thermal breakthrough	The Geysers, California	Redrilled injection wells deeper than production wells.
	Kakkonda, Japan	Cessation of injection at four wells.
	Onikobe, Japan	Redrilled new injection wells further apart.
Wellbore fill	Magma, California	Backflushing.
	Magmamax 2, California	Backflushing.
	Iceland	Backflushing.
Amorphous silica deposition	Niland (GLEF), California	Produced formation fractures, later employed a treatment system.
	Otake and Hatchobaru, Japan	Drilled additional wells; used acid cleaning (HCl) and testing water treatment methods
	North Brawley, California	Acid treatment (HCl-HF).
	Magmamax 3, California	Acid treatment (HF).
	Veysey Well 1, California	Acid treatment (HCl-HF).
	Beowawe, Nevada	Acid treatment (HCl-HF).
Heavy metal oxide deposits	Niland (GLEF), California	Sealing system from air intrusion.

6.4.2 Formation Clay Swelling

If clay minerals, especially montmorillonite, are contacted by a foreign water with a lower salinity, they will undergo some expansion. Clay swelling reduces the pore space and thus lowers the permeability of the formation. For most geothermal sites, a fluid with higher salinity than the connate water may be injected. In addition, the clay content of current injection sites happens to be low. For these two reasons, formation clay swelling has not been troublesome.

If clay swelling does occur, recovery is generally successful; strong acids, alcohols, and some ketones can remove the effects of clay swelling within a few hours. Replacing the foreign water, which caused the swelling, with water of equal pH and ionic strength to the original connate water will cause the clays to slowly return to their original state. The foreign water can be replaced by backflushing. Hydrocracking the impaired formation might also be an alternative.

Formation clay swelling can be prevented by performing initial tests on the receiving formations prior to injection to determine their swelling potential. Potentially troublesome formations can be flushed with chemicals that are easily absorbed on the clay surfaces to prevent swelling, such as the widely used hydroxy aluminum series of retardants.

6.4.3 Formation Permeability Reduction

The operational signs that formation permeability reduction is taking place can be the same as for wellbore fill and scaling. Increased injection pressure is required to maintain flow. When this happens, the well system should be tested to determine what is causing the impairment.

Inducing formation fracturing is one of several techniques to rehabilitate plugged formations. Other techniques include backflushing the injection wells to remove the solids, introducing additives to the injected brine to dissolve the plugs, or dissolving by reheating the formation during shut-in. Neither backflushing nor the use of additives will be successful if the formations are extensively plugged because not enough flow will be available to either push the solids out or to distribute the acid to the effective areas. The additives for dissolving the plugs are discussed in the following section.

Reservoir fracturing has long been used by the petroleum industry to stimulate production wells. The process entails pumping water and sand under high pressure into the strata near a well. The hydraulic pressure opens cracks and bedding planes and the sand keeps the fractures open when pressure is reduced. Formation permeability reduction occurred at the GLEF facility at Niland,

California. As the injection became progressively more difficult, the injection pressures were raised and formation fractures were opened. Formation fracturing was required several times.

Current well stimulation techniques by reservoir fracturing and how they apply to geothermal systems have been studied by the Geothermal Reservoir Well Stimulation Program (Republic Geothermal 1980) (Table 6.10). Comments apply to formation fracturing to enhance production, but these same techniques can be used to fracture formations to increase their injectability.

Another method to produce formation fracturing is to detonate explosives in the borehole. McKee and Hanson (1976) have developed theoretical expressions to aid in predicting the effects of explosives on permeability enhancement.

6.4.4 Wellbore Fill and Scaling

For the purpose of this section, the term "wellbore" also includes the area immediately around the well. Wellbore fill and scaling is a major cause of geothermal injection system impairment. It has occurred at a number of sites; for example, Magma Well 46-7A, Magmamax 2 and 3, North Brawley, Veysey Well No. 1, California; Iceland; and Otake and Hatchobaru, Japan. As the wellbore area becomes plugged, injection pressure must be increased to maintain flow. Eventually, either the additional cost of increased pumping or the limit on pumping pressure will require rehabilitation or abandonment of the well.

The method of injection well rehabilitation depends on the cause or causes of the impairment. Frequent causes of well impairment are listed below:

- During shut-in periods, sand grains infiltrate into the well due to poor well completion techniques.
- During operation, nonscaling causes might include
  - particulates from production wells or plant and treatment systems may plug the well
  - well casing and fluid corrosion products may cause filling
  - introduction of oxygen into injection system may cause plugging due to metal oxides
- During operation, scaling causes, as explained earlier, might include

TABLE 6.10. Examples of Formation Fracturing Techniques and Their Application to Geothermal Systems

Potential Type of Stimulation Technique	Removes Wellbore Damage	Provides Reservoir Stimulation	Type of Proppant	Chemical Effects	Fluid Compatibility	Formation Damage	Application to Geothermal Reservoirs
Water fracturing	Yes	Slight, because fractures are too short	Usually sand at low concentrations up to 1 lb/gal	Minimal	Water has to be compatible	Minimal if water is compatible with formation	Yes; in certain areas to overcome wellbore damage by scale and to reduce pressure drop
Pressure cycling fracturing	Yes	Yes	Usually sand at low to medium concentrations, may be slugs of sand	Minimal	Water has to be compatible	Minimal if water is compatible with formation	Yes; for increased production fractures and fractured zones
Super sand flux	Yes	Yes	Super sand - a cohesive proppant retains permeability under high closure	Minimal	Water has to be compatible	Minimal because no fines, more input	Yes; no sand flow back; permanent stimulation

Source: Republic Geothermal 1980.

- amorphous silica deposition

- various mineral precipitation caused by injecting water that is incompatible with the connate water

- carbonate precipitation (due to retrograde solubility) as the water is reheated to downhole temperature.

Sand grain infiltration results from poor well completion techniques that allow sand grains to infiltrate into the well during shut-in periods. The injectability of the well decreases as the well is filled and injection aquifers are buried. The well can be periodically rehabilitated by backflushing. Backflushing is probably the most successful technique to recover from sand grain infiltration as long as the grains are not significantly cemented. If they are, chemical treatment or mechanical cleaning methods will probably be required. The petroleum industry has developed many tools for mechanical cleaning; for example, the McGaffey-Taylor and the Chevron Hyperjet tools.

Backflushing consists of bringing up, with a sudden flow, the fluid or fluid/gas that was injected into the well. Hopefully, the particulates and scale that plugged the pore spaces will be washed up with the fluid. Care must be taken during backflushing not to damage the wellbore. One of the potential damages could be the development of carbonate scale resulting from too great a pressure drop across the sand face. Formation fracturing and backflushing are relatively less expensive than using additives if there is already sufficient pumping pressure.

Acidizing wells to improve their permeability has long been used as a recovery tool by the oil industry. Typically, either HCl or HF is pumped into the wells to dissolve wellbore scale or small fines that would otherwise be free to move during well flow and cause pore blockage. Using HF to improve injectability in sandstone formations can lead to near-wellbore formation changes, although development of self-generating, low-strength HF acids has lessened this possibility. All major oil field acidizing companies now supply self-generating acids.

Injectability can also decrease due to plugging of the injection well or the near-well area from introduced solids during injection. These solids plug pore spaces and thus limit the flow of fluid. These particulates can originate anywhere from the production wells throughout the plant to the treatment system just prior to injection. The best prevention for this problem is a proper treatment system containing filters as the final step. Otherwise, backflushing can generally recover injectability. Acid treatment or cleaning tools might be required, especially if the impairment is extensive. Wellbore fill from introduced solids has occurred at several geothermal sites: Magma and Magmamax 2, California; and Iceland. In each case, backflushing increased injectability.

Wellbore silica scaling can result from lowering the geothermal fluid temperature during heat extraction. Maintaining the fluid at a temperature above amorphous silica solubility will avoid this problem. However, once an injection well is impaired with amorphous silica scale, backflushing to regain injectability will generally not be successful. A more rigorous approach is required; for example, formation fracturing, acid treatment, and mechanical cleaning. Another possible method suggested by experiments at Niland is to redissolve the silica by reheating the injected fluid containing the silica in the well during shut-in periods, possibly by using two widely spaced injection wells in an alternating mode (Jorda 1978).

There is at least one successful Japanese experience using concentrated base to clean out a well. Two base treatments were used alternately with flushes in a 30-min period. Whether this cleaned out any formation damage is unknown; the base was 125 kg of NaOH and 300 l of water (Ozawa and Fujii 1970). Depending on the brine, however, a base treatment can initiate the precipitation of carbonates, sulfides, sulfates, or metal hydroxides.

Well impairment can also occur when the wellbore becomes filled with corrosion products produced by the interaction of the injected fluid and the well casing, although this has not yet been reported to be a major concern in the geothermal industry. There are a number of corrosion inhibitors that would probably control this problem. If this problem does develop, any combination of the rehabilitation methods discussed could apply to recover injectability. The fluids potential for scaling or corrosion can be estimated by using the Ryzner stability index or the Langelier index. These indexes relate to water pH, alkalinite, calcium hardness, TDS, and temperature.

6.4.5 Thermal Breakthrough and Unwanted Fluid Migration

Thermal breakthrough occurs when the relatively cold water that was injected migrates faster than the reservoir rock can heat it. This relatively cold water then cools the hot production water. Unwanted fluid migration can also occur when the injected water migrates into drinking or irrigation aquifers.

These two problems usually occur in geothermal systems that are permeable due to highly fractured formations (such as Raft Valley, Idaho, and Japanese fields) rather than systems that are permeable due to porosity (such as Imperial Valley, California). Fluid migration in fractured systems is much faster than in porous systems. For example, at Hatchobaru, Japan (a fractured system) actual tracer speeds in the reservoir were as high as 80 m/h. The presence of a fractured system does not necessarily imply a reduced reservoir lifetime due to thermal drawdown of the production wells. Initial testing to determine the underground flow paths can guide in the location and depths of injection wells to minimize thermal interference or unwanted fluid migration.

Lippman, Tsang, and Witherspoon (1977) developed a code (conduction-convection and compaction or CCC) to aid in establishing the best production/injection well placement.

Thermal breakthrough has occurred are Kakkonda, Onuma, Hatchobaru, Japan; the Geyers, California; Larderello, Italy; and to a small degree at Broadlands, New Zealand. At Raft River, Idaho, injected fluid migrated up into irrigation aquifers. At the Geyers, thermal breakthrough was stopped by redrilling the injection wells deeper than the production wells. At Kakkonda, thermal breakthrough was stopped by abandoning four injection wells. Both of these solutions were expensive. The cost of establishing the underground flow paths, especially for a highly fractured reservoir, is highly justified.

Another solution for correcting thermal breakthrough has been proposed by Vetter et al. (1982), who suggested selectively scaling the receiving formation at high permeability streaks or fractures to retard the flow of injected fluids through these flow channels. Such flow retardation will increase the residence time of the injected fluids and thus enable them to heat up to the production fluid temperature. Three methods of selective scaling were proposed: injection of a thermodynamically unstable brine, injection of a slug of dirty brine, and mixing a reservoir brine with an incompatible injection brine.

6.5 IMPAIRED WELL RECOVERY EXAMPLE

Magma Power has an operating power plant at the East Mesa Reservoir. This moderate-temperature (~360°F) reservoir produces brines of 7500 ppm dissolved solids having a large calcite scaling potential. The plant pumps the wells and maintains sufficient pressure to prevent flashing and calcite plugging. A minimum brine temperature (~160°F) is maintained to avoid supersaturating silica and plugging the injection wells. Despite using these proper techniques, some injection impairment has occurred that has necessitated corrective actions to restore injectivity. Reviewing this experience is an example of: 1) how to apply monitoring techniques to the real world, 2) the need for monitoring these wells even when the treatment process is properly designed, and 3) that injection impairments can be overcome.

6.5.1 Magma Power Plant

This 10-MWe geothermal power plant has been the site of many tests performed by PNL under a cooperative program with Magma Power. A history of the plant and its primary injection well offers a good example of a working geothermal injection system. The typical chemistry of the plant effluent just before injection is presented in Table 6.11. Chemical variations were minor, especially considering the many flow combinations of the five production wells. The typical effluent was a brackish fluid with nominal 2-mg/l particulates

TABLE 6.11. Typical Effluent Chemistry Before Injection with Both Magma Power Wells Flowing

Sampling Conditions: Date - September 15, 1980
Well No. 1 - 810,000 lb/h
Well No. 2 - 675,000 lb/h

Pressure	370 psi	Total CO_3	1,900 mg/l
Temperature	160°F	Al	<0.5 mg/l
pH	5.66	As	0.9 mg/l
O_2	<5 ppb	B	8.8 mg/l
Conductivity	12,200 µmho	Ba	1.0 mg/l
TDS	7,470 mg/l	Ca	32 mg/l
Turbidity	<5 FTU	Fe	1.9 mg/l
HCO_3^-	434 mg/l	K	234 mg/l
H_2S	2.1 mg/l	Li	9.0 mg/l
$SO_4^=$	91 mg/l	Mg	1.6 mg/l
F^-	3 mg/l	Na	2,610 mg/l
Cl^-	4,050 mg/l	P	<0.5 mg/l
SiO_2	252 mg/l	Si	118 mg/l
NH_3	18 mg/l	Sr	7.0 mg/l

injected at a temperature above amorphous solubility of silica and a pressure above the breakout of CO_2. Thus, well or formation impairment due to silica or carbonate deposits theoretically should not occur; and observations from the fall of 1979 to the fall of 1982 confirmed that the treatment process operated as designed.

Despite this success, injection well impairment has repeatedly occurred. Injection well 46-7A has been the primary injection well, and it has been rehabilitated by backflushing at least four times (Table 6.12 and Figure 6.8). Each time, backflushing significantly recovered the injectability of the well. Figure 6.9 graphically demonstrates the decline of the well; injection wellhead data are plotted as recommended. It is easier to graphically locate the well impairment if the injectivity ratio is plotted rather than just the pressure and flow data. The backflushed slurry was examined for a clue into the cause of the impairment.

TABLE 6.12. Data Used to Calculate kh Values in Injection Well 46-7A Before and After Backflushing

Condition	Data Point	Date	Injection Pressure, psig	Injection Rate, b/d	Brine Temperature, °F	kh
Well impaired[a]	A	6/13-14/78	600	9,500	350	2,880
After backflushing[a]	B	6/78	600	26,000	350	21,600
Well impaired	C	5/3/78	540	17,349	338	6,000
After backflushing	D	8/3/78	245	25,371	-	19,800
Well impaired	E	5/19/80	353	16,107	145	9,000
After backflushing	F	8/28/80	335	29,130	255	18,000
Well impaired	G	7/31/81	365	29,300	-	15,000

(a) Estimated from Figure 6.9.

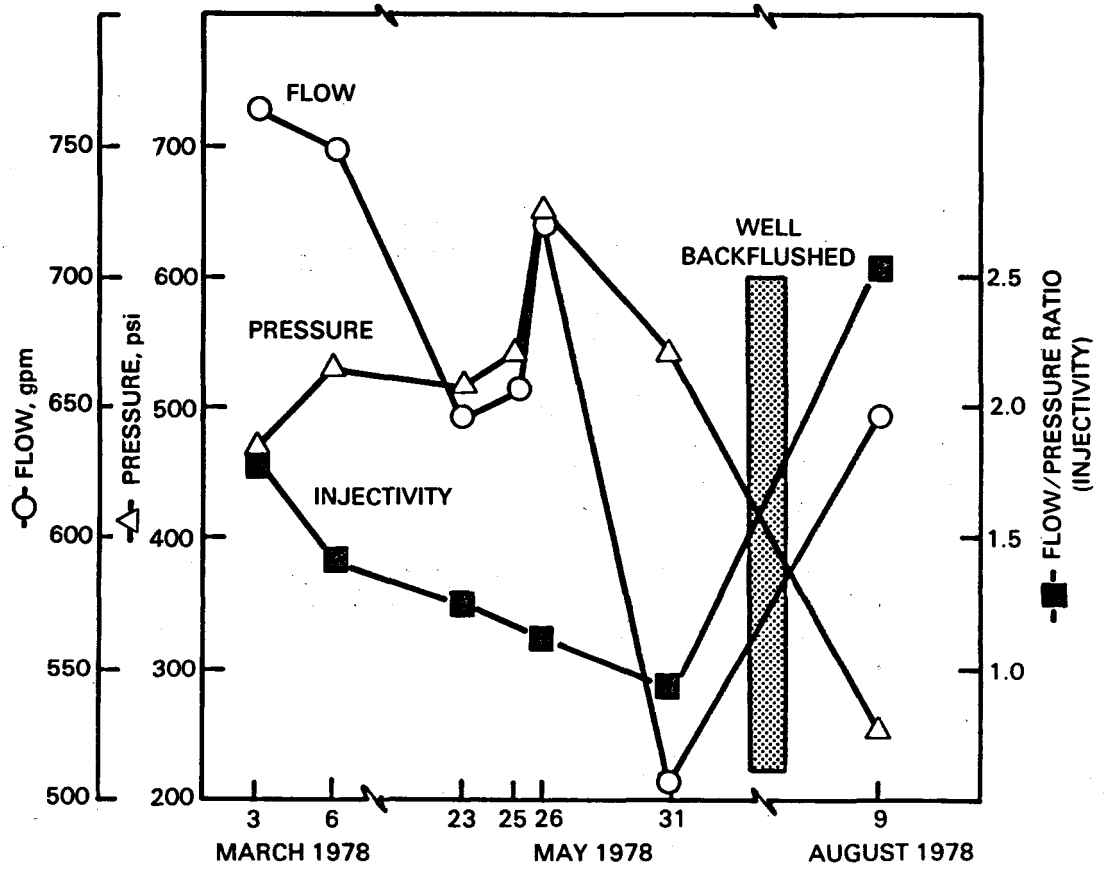

FIGURE 6.8. Selected Injectivity Data from Injection Well 46-7 (courtesy Magma Power Company). The effectiveness of backflushing at restoring injectivity lost over time is shown. Note the graphical clarity from plotting the injectivity ratio rather than pressure data.

Injection well 46-7A was backflushed during June 1980, and the slurry that was being flushed from the well was sampled. The chemical analysis of the particles in the slurry are reported in Table 6.13. The predominant elements in order of concentration were Si, Al, Fe, S, and Ca. The mineral phases identified by XRD were quartz, feldspar, pyrite, and a trace of mica. This composition differs from the suspended solids sampled in the brine line before entering the injection well. The slurry obtained during backflushing was higher in silicate minerals and much lower in scale particles (Fe + S).

Several important conclusions can be drawn from the chemistry of the slurry. First, a significant portion of the suspended solids that are being injected into the injection well appear to be remaining in the wellbore itself. This is verified by the presence of scale particles (pyrite or identified by Fe + S) that originated on the heat exchanger surfaces and are present in the

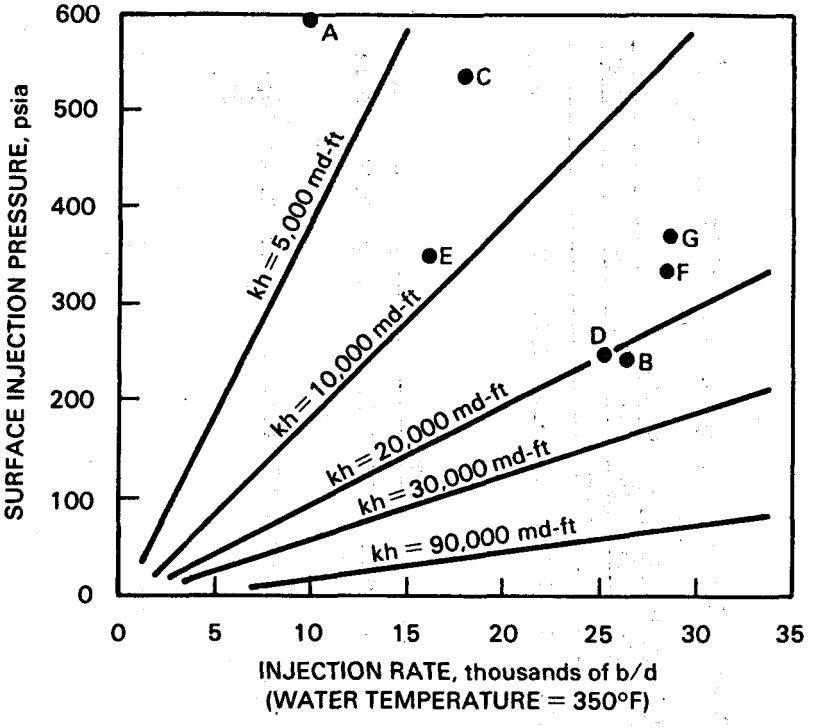

FIGURE 6.9. Injection Impairment Map for Well 46-7A. The RIM is based on a water viscosity of 0.185 cp, R_e = 1000 ft, and R_w = 6 in. Fracture pressure is just under 700 psi (Jorda 1980).

backflushed slurry. Pyrite is not identified as a major mineral in the underground formations. Second, the higher rate of mineral grains to scale particles in the slurry suggests that additional minerals are infiltrated through the slotted liner of the injection well, most likely during well inactivity. It should be noted that the effluent is not treated before injection, except for maintaining temperature and pressure.

As suspected, the particulate content was the most important quantity of the effluent chemistry in respect to injection well performance. If the source of the suspended solids (grains from producing formation, grains produced due to changes in brine chemistry, or scale fragments) and their chemistry and size distribution is known, then methods to prevent, control, or eliminate the particles can be chosen. Several monitoring schemes were used at Magma by PNL to measure and then study these particulates.

Locations at the Magma plant where suspended solids were collected for sizing and chemical analysis are shown in Figure 6.10. Suspended solids were determined at each production well after the sand separator, at the inlet to

TABLE 6.13. Comparison of Particulate Chemistry During Backflushing and Normal Activity[a]

Sampling Location	Plant Conditions	Total Particulates, mg/l	Chemical Composition of Particulates											
			Al	Si	S	Ca	Fe	Cu	Zn	As	Sr	Ag	Sb	Ba
			μg/cm²											
Port PC-2 before injection	Normal	0.34	NA[b]	<16	32	0.44	16	0.69	3.6	1.3	0.11	NA	<1.1	<0.5
			wt%											
Injection Well 46-7A	Backflushing	1.82	5.5	23	0.74	0.57	4.4	0.20	0.10	0.05	0.04	0.04	0.06	0.48
Production Well SW3	Backflushing	2.33	5.0	24	0.69	6.6	5.6	0.09	0.57	0.03	0.27	0.01	0.004	0.5

(a) Shannon, Elmore, and Pierce 1981.
(b) NA - not analyzed.

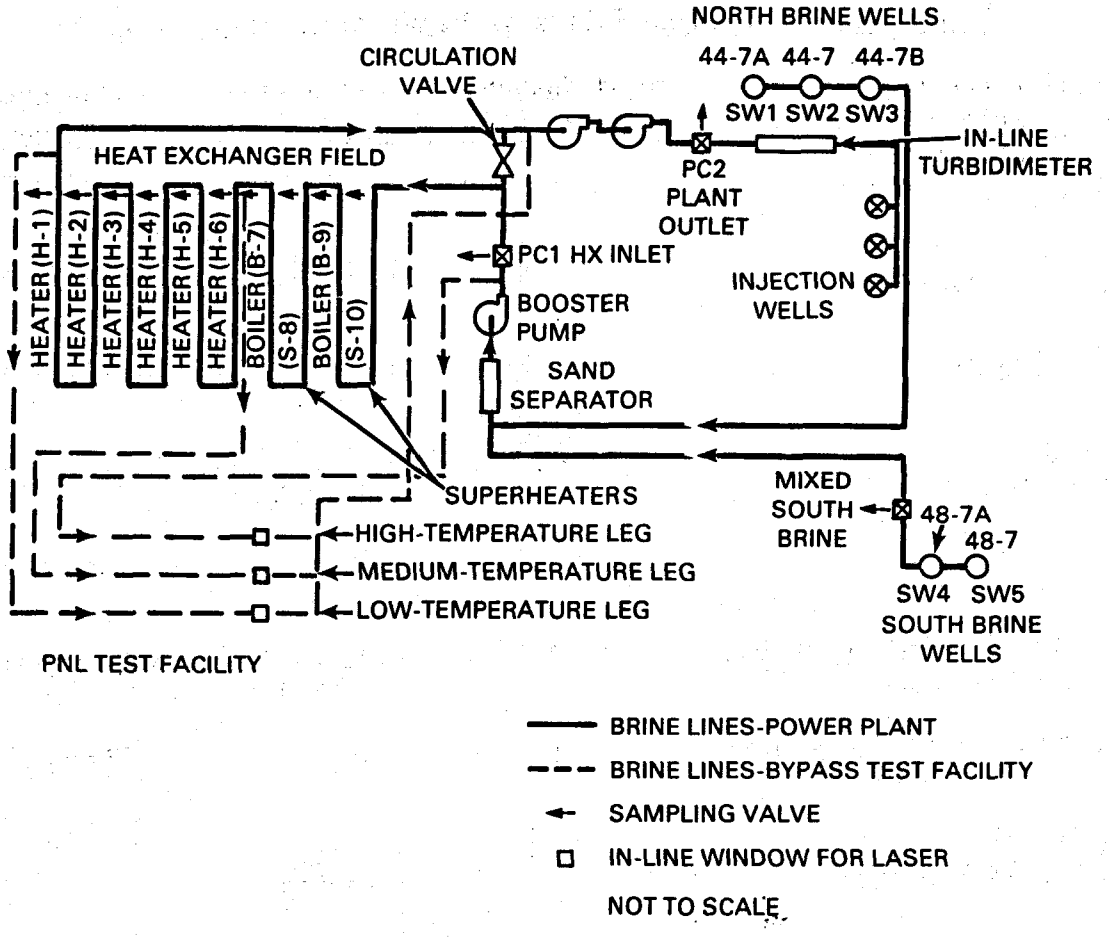

FIGURE 6.10. Monitoring Locations at Magma Power Plant (Shannon, Elmore, and Pierce 1981)

the heat exchanger, after each leg of the heat exchanger, and finally downstream of the booster pumps before injection. The quantity and the size distribution of suspended solids in the brine at each sampling port are constant during steady-state plant operation. All five production wells typically produce up to 2 mg of particulates per liter of brine. As the brine flows through the sand separator, the particulate content is reduced only very slightly. The sand separator does separate large suspended grains from the brine and may provide a service when large slugs of sand are produced during well startups. Typically, total suspended solids in the brine are increased slightly after passage through the heat exchanger.

Plant operations that produce unusually large particulate contents include recirculation of brine through the heat exchangers (which occurs during warmup) and the first few hours of brine production just after a well is started. These observations are documented on Table 6.14, which lists total suspended solids at various locations under varying plant conditions. In Figure 6.11,

TABLE 6.14. Suspended Solids in Magma Power Plant Brine[a]

Filter Location and Sample History	Total Suspended Solids, mg/l	Major Size Ranges, μm	Major Chemical Components
Supply well SW2 (well just turned on)	11.0	--	Silicate minerals
Supply well SW2 (flow stabilized)	1.4	1 to 10	Silicate minerals
Supply well SW3 (flow stabilized)	2.2	3 to 15	Silicate minerals
Supply well SW4 (flow stabilized)	1.9	0.22 to 0.45; and ≥8.0	Silicate minerals
Supply well SW5 (flow stabilized)	0.8	1 to 10	Silicate minerals
Plant inlet/normal operation (pre-heat exchanger)	0.7	0.22 to 0.45; and ≥5.0	Silicate minerals
Plant outlet/normal operation (post-heat exchanger)	1.1	≥5.0	Silicates/Fe-S
Plant outlet (recirculating brine)	180.0	Slightly favoring ≥5.0	Fe-S

(a) Shannon, Elmore, and Pierce 1981.

the output of the inline turbidity meter is shown. It can be seen that plant startups and temperature transients produced "bursts" of solids much higher than the normal level. Unfortunately, this instrument could not be kept operational due to deposits on the optical window. However, intermittent sampling of the brine clearly underestimates the average solids content during these operational modes because the "spikes" are usually missed.

At the bypass inlet, while the south supply wells were flowing, a size distribution of the suspended solids in the brine was determined using a filter chain. These filters were then analyzed to determine the composition of the suspended solids for various sizes. Fe, As, Sb, and S became more common as the pore diameter of the filter increased, which implies that they are metallic sulfides, most likely the source of the yellow color observed on the filters. Silicon was the most common element on the largest filter (8.0 μm), suggesting

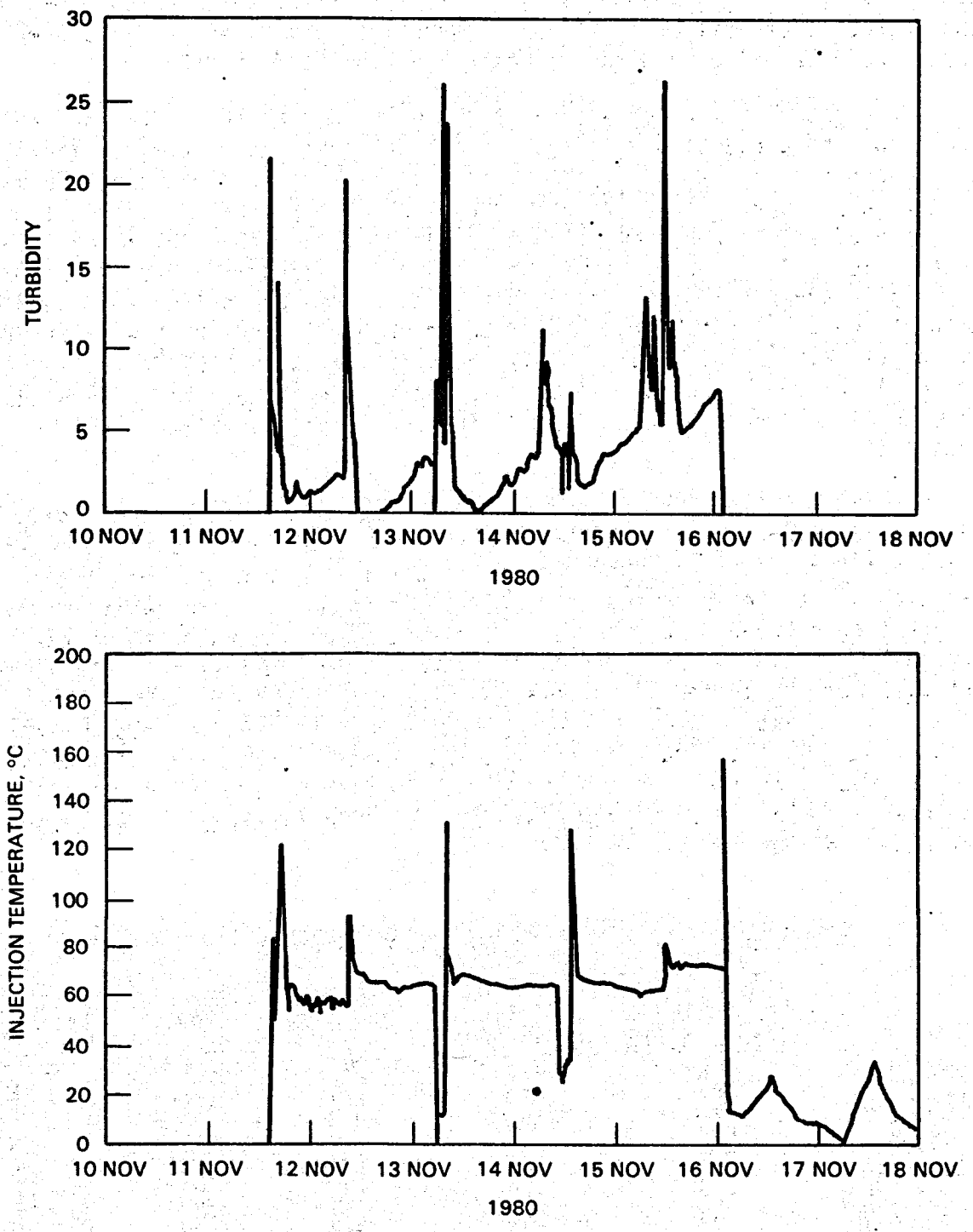

FIGURE 6.11. Brine Turbidity and Injection Temperature at Plant Outlet. Strong correlation between suspended particulates and temperature transients is evident (Shannon, Elmore, and Pierce 1981).

that Si exists in a compound that is >8.0 μm. Barium was the most common element on the finest filter (0.22 μm), suggesting that Ba exists as a compound (most likely $BaSO_4$) within the diameter range of 0.45 to 0.22 μm.

After establishing the nature of the particulates that enter the power plant from the production wells, the brine particulates were again studied at the plant outlet (PC-2) to establish to what extent the particulate population was altered by heat extraction from the brine during power production. Samples of suspended solids were collected simultaneously at the plant inlet (PC-1) and plant outlet (PC-2) during normal heat exchanger operation, and an increase in Fe and S in the particulate matter occurred. Suspended solids were sampled again at PC-2, but during recirculation while warming up the heat exchangers. The individual particles were mostly iron sulfides with very few silicates. Apparently as the brine is recirculated many times through the heat exchangers, the mineral fragments become diluted with the larger quantity of scale particles.

Suspended solids were also measured during normal plant operating conditions using laser light-scattering techniques. There appears to be an increase in the total quantity of suspended solids after the brine passes through the heat exchangers, which agrees with the filter data. In each case, the quantity of particles between 1 μm and 5 μm decreased, while the quantity of particles between 5 μm to 10 μm and 10 μm to 15 μm generally increased. These larger particles were collected on filters and were determined to be Fe-S scale fragments. These particulates were not the only iron in the injection brine; Table 6.15 shows the amount of soluble iron (passed through a 0.45-μm filter) added to the brine from the plant. Corrosive loss of iron from the heat exchanger is believed to be responsible. The heat exchanger later became perforated and was rebuilt in 1982.

TABLE 6.15. Soluble Iron Loss from Binary Cycle Plant[a]

Date	Iron in Production Brine, mg/l	Iron in Injection Brine, mg/l	Iron Increase, (mg/l)	Flow, 10^3 kg/h	Iron Loss, kg/day
11/6/79	0.5	3.1	2.6	215	14
11/10/79	0.7	1.7	1.0	355	9
1/30/80	0.2	2.2	2.0	277	13
1/31/80	0.2	2.1	1.9	277	13
9/15/80	0.3	1.9	1.6	300	11
10/22/80	0.5	2.1	1.6	273	11

(a) Kindle and Shannon (1982); particulates larger than 0.5 μm have been filtered out.

Suspended solids from four of the five producing wells were also studied to determine what particulates they each contributed. It was not surprising that the four wells are very similar in the kinds of mineral fragments they produce.

Several Barkman-Davidson filter plugging tests have been conducted to determine the plugging potential of the spent brine to the injector formations. These simulation injector tests were performed during typical heat extraction from the brine on two different occasions by PNL and on brine that was cooled and then aged by Jorda (1980). The data from these tests were plotted as cumulative filtrate volume against the square root of time to determine the slope. Once the slope is known, the filter cake permeability (K_c) can be calculated from the water quality ratio. For this example, K_c was calculated to be 0.016 md. K_c values ranged from 0.003 to 0.078 md during testing conducted by Jorda in 1978 (Jorda 1980). The two simulated injector tests by PNL in May and October 1980 resulted in similar K_c values (0.014 and 0.015 md).

Assuming a formation permeability between 10 and 1000 md with a filter cake permeability measured around 0.014, Figure 6.12 predicts that the suspended solids in the injected fluid will not be retained on the surface of the formation but will pass through. Thus, injection well degradation should not occur due to the normal state of fine particulates. However, well injectability does decrease with time and backflushing is necessary to restore the performance of the well, suggesting that the particulate concentration spikes detected by the on-line turbidity monitor (Figure 6.9) may contribute significantly to injection well impairment.

Another method to view the acceptability of the spent brine to the receiving formation is to compare the diameter range of suspended solids with the typical formation particle diameter. By microscopic examination of rock chips from the receiving formations, the grain size was determined to be between 5 μm and 50 μm. Locating the area bounded by 5- to 50-μm diameter (d_1) in Figure 6.13, surface retention (Region 1) and deep-bed filtration (Region 2) should both occur from injecting particles with diameters greater than 0.4 μm. Particles smaller than 0.4 μm in diameter should pass through the formation without forming a filter cake.

A typical amount of suspended particles with diameter >1 μm at the plant outlet is 1300 particles/ml of brine. It appears (by the method of diameter comparison) that well degradation and deep-bed infiltration should both occur due to suspended particles being retained on the surface of the formations and particles embedding in formation pores.

The discrepancy between the two predictions may be due to not collecting all the suspended solids during sampling. Larger particles (10 to 300 μm) may

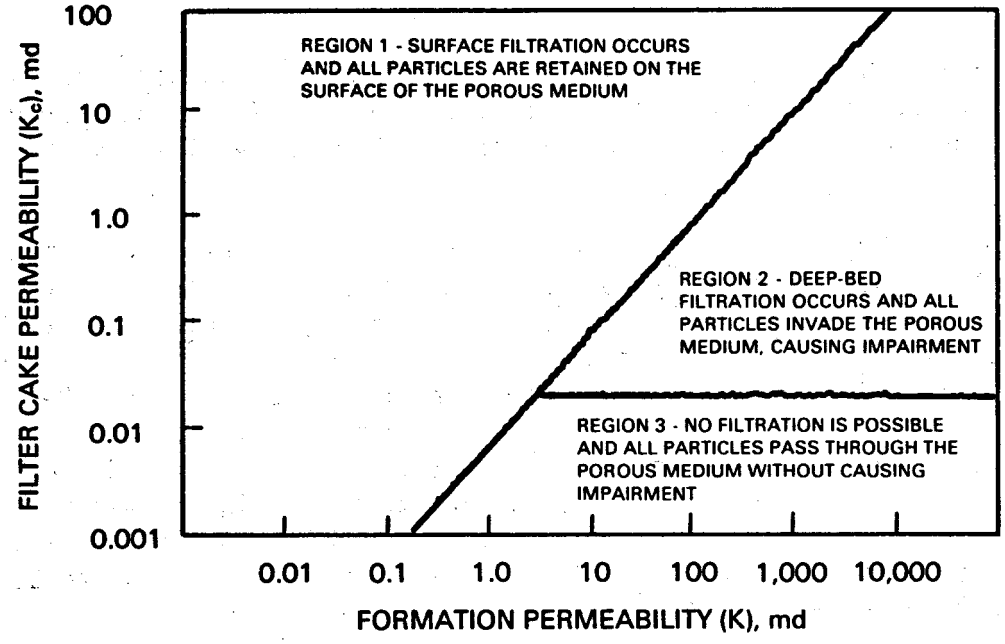

FIGURE 6.12. Relationship Between Filter Cake and Formation Permeabilities in Flow or Particle-Laden Fluid Through Porous Media (Jorda 1978)

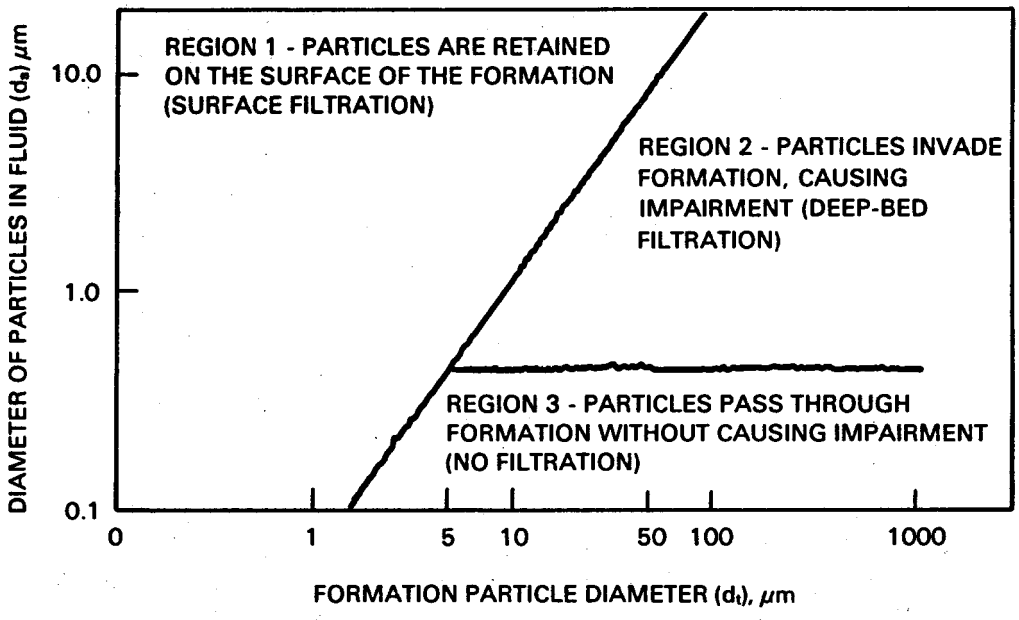

FIGURE 6.13. Particle Distribution in Systems Where Particles in Fluid and Reservoir Particles Are Spheroids (Jorda 1978)

have collected in low points in the plant or sample line, missed the sample collection, but entered the injection wells. If these larger particles are not represented in the sampling fluid, the filter cake would be more compact (thus lower permeability) than the potential filter cake in the wellbore. The lower permeability value of the filter cake results in the conclusion that the particles will pass through the formation. The predictions from the second method, diameter comparisons, appear to correspond with our observations; surface retention (as wellbore fill) occurs and injectability is improved by backflushing. Deep-bed infiltration has not been positively identified, but it may be occurring at such a slow rate that it has not been diagnosed.

6.5.2 Summary

Mineral fragments with minor amounts of pipe corrosion products enter the plant as the brine cools in the heat exchangers; insoluble sulfides form on the pipe wall as scale and deposit on the mineral fragments. The scale can break loose and become suspended during thermal expansion/contraction cycles of the plant. Thus, the injected particles are a mixture of the initial particles (mineral fragments, corrosion products) plus mineral and scale fragments. The total concentration of these particulates is greatest during well or plant startup and times of thermal transients. These particles contribute substantially to injection well impairment by surface retention or wellbore filling. Injectivity can be largely restored with backflushing.

A possible (partial) solution to prevent injection impairment in this particular situation would be to either filter the brine or use a settling tank before injection during the peak particulate production operations (recirculating warmup and the first few hours of brine production just after a well is started).

This study at a working geothermal power plant provides an excellent summary of the monitoring techniques discussed in this chapter. As listed on Table 6.16, Items 1 through 4 and 7 through 10 were periodically performed. For Item 1, brine sampling and analysis, the most important quantity of the effluent chemistry in respect to injection well performance was the suspended solids. The data collected under Item 2 clearly showed the injector decline with time and the success of backflushing to rehabilitate the injector. The RIM map, Item 3, provided a more accurate picture of the injector decline and rehabilitation; but, for this study, it could have been deleted. Item 4, membrane tests, did not aid in determining the cause of impairment, even though they are important in cataloging the characteristic of the effluent. Items 5 and 6 (flow/pressure tests and geophysical logging) were not performed due to their cost and proved unnecessary in arriving at a basic understanding of the injector history. Items 7 through 10 are basically record keeping and aided in

TABLE 6.16. Simulated Injection Test/Membrane Filter Test at Magma Power Company's Well 46-7 (Jorda 1980). This table shows how to arrive at a filter cake permeability (K_c) from filter test data.

Date 6/14/78 Water Temp. 110 °F
Differential Pressure 40 psi
Filter Size 0.45 μm
Sample Point Injection wellhead

Time, min	Cumulative Volume, ml
1	1060
2	1600
4	2180
6	2590
9	3100
12	3530

CALCULATION

1. Volume at 12 min 3530 ml
2. Volume at 6 min 2590 ml
3. Difference (slope) 926 ml/(min) 1/2
4. Water quality ratio 210 ppm/md (from graph)
5. Suspended solids content 3.29 ppm
6. Cake permeability 0.016 md (5 + 4)

obtaining a clearer picture of the injection decline and recovery. In conclusion, for this particular injection system during this monitoring period, not all of the monitoring tests were necessary to obtain an understanding of the injector performance. This will most likely be true with other injector systems. They will each require a different combination of monitoring tests.

7.0 COMPARATIVE ECONOMICS

The treatment that has been demonstrated to function in the most hostile treatment/injection location and the life-cycle costs of the treatment (crystallization/clarification) versus no fluid treatment prior to injection are discussed in this section. Wells et al. (1981) developed generic treatment cost functions that could be used to estimate the costs when treating geothermal liquid effluents at different-sized plants.

7.1 COST OF NO FLUID TREATMENT PRIOR TO INJECTION

No fluid treatment prior to injection is a base case against which the cost of crystallization/clarification can be compared. This base case involves cleaning the injection wells when plugging occurs and switching to spare injection wells during cleaning. The number of spare injection wells depends on the length of the cleaning cycle plus a safety margin. Life-cycle costs are calculated for two periods between well cleanings (1 month and 3 months), although the 1-month period seems too frequent.

Financial assumptions used in the life-cycle cost analysis include:

- debt fraction = 0.28
- equity fraction = 0.72
- bond interest rate = 5% (real)
- return on equity = 12% (real)
- federal tax rate = 48%
- 10% investment tax credit
- weighted-average after-tax cost of capital = 9%
- all costs in January 1983 dollars
- cost per injection well = $1,000,000
- well costs are 15% tangible and 85% intangible.

The following technical assumptions were used to determine the base case costs:

- 6×10^5 gal/h of geothermal fluid from the production wells
- 10 injection wells with a capacity of 1000 gpm each
- five spare injection wells
- injection well life = 10 years
- well cleaning consists of backflushing and acid treatment.

Backflushing may be accomplished through artesian flow at certain sites. However, to be conservative, this analysis includes one surface pump per well to be used for backflushing at a cost of $10,000 per pump.

Based on experience at North Brawley in the Imperial Valley, the following procedure for acid treatment was assumed:

- preflush with 5% HCl
- flush with 5% HCl and 5% HF
- postflush with 5% HCl.

Each flush is assumed to require 75 gal/ft of zone to be flushed. Since injection wells are typically slotted to a depth of 1000 ft, each flush would cover this 1000-ft zone; therefore, each flush would require 75,000 gal of acid.

Two cases were analyzed for the no-treatment option:

- Case 1 - 1 month between well cleanings
- Case 2 - 3 months between well cleanings.

7.2 COST OF CRYSTALLIZATION/CLARIFICATION

This treatment option is based on a scaled-up version (6×10^5 gal/h of geothermal fluid from the production wells) of the Salton Sea Unit No. 1 demonstration plant. Life-cycle costs are estimated for two residence times of the fluid in the crystallizers and for two recycle rates of "seed crystals." The pieces of equipment analyzed and costed were the crystallizers, the reactor clarifier, the dual-media filter, the thickener, and the filter press. In addition, the cost of sludge disposal at an offsite landfill was determined. The capital costs of the major pieces of equipment were obtained from vendor contacts.[a] Most of the operating costs were obtained from cost functions developed by Wells et al. (1981).

To properly size and cost the equipment, a material balance was done for the geothermal fluid and solids flow throughout the system. At the wellhead separator, 34% of the fluid is flashed to steam, while the remaining 66% (6700 gpm) is sent to the crystallizers. Seed crystals or recycled sludge from the thickener are also added to the crystallizers. At a recycle rate of 1%, the amount of sludge entering the crystallizers is ~59,000 lb/h. The 4% recycle rate corresponds to ~236,000 lb/h.

The crystallizers are installed in two stages in series, with backup units available. In the first crystallizer stage, the pressure of the brine is reduced from ~170 to ~125 psi, and the resultant steam is sent to the turbine. The second crystallizer stage reduces the brine pressure to near atmospheric conditions, and the small amount of low-grade steam that flashes is simply vented to the atmosphere.

The residence time of the fluid in the crystallizers was also varied. The optimum unit size for the crystallizers is 13 ft in diameter. With a flow rate

(a) Goslin-Birmingham, Inc., and Eimco Process Equipment Co.

of 6700 gpm, the optimum residence time is 8 min in each stage.[a] This process requires three units in parallel for each stage or a total of six units for both. A backup unit for each stage raises the total number of units to eight at a capital cost of $1,100,000. A 6-min residence time in each stage was also examined; resulting in four on-line units (two for each stage) and a backup unit for each stage (total of six units). The capital cost of these six units is $840,000. The operating costs for the crystallizer are minimal because there are no power requirements for the units.

The reactor clarifier is sized to accept 10,000 gpm, including ~61,800 lb/h of solids. With an upflow rate of 1 gpm/ft^2, a clarifier 120 ft in diameter is required. The cost of the reactor clarifier, which includes the internals, the tank and cover, and the concrete floor and piping, is about $1 million. The operating cost was estimated at $163,000/yr. The clarifier effluent, which is sent to the dual-media gravity filter system, contains 90 ppm of suspended solids and 200 ppm of silica in solution. The underflow, which is sent to the thickener, contains 10% suspended solids by weight.

The dual-media gravity filter system uses coal and sand as filtering agents. The system reduces the suspended solids content from 90 to 10 ppm, while depositing solids at a rate of 400 lb/h. The filter effluent is then sent to the injection wells for final disposal at a rate of 9000 gpm. The solids that are removed from the filters by backflushing are recycled to the reactor clarifier. The total cost of the dual-media gravity filtration system, including the water backflush and air-scouring subsystems, is about $1,5000,000 and would cost about $123,000/yr to operate.

The underflow from the reactor clarifier is sent to the thickener, where the solids are concentrated from 10 wt% to 20 wt%. For the 1% seed crystal recycle rate, the total amount of solids passing through the thickener is 61,500 lb/h at a flow rate of 490 gpm. A 50-ft diameter thickener (capital cost of ~$75,000) would be needed to handle the 1% recycled sludge, while a thickener capable of handling the 4% recycled sludge would cost ~$95,000. The operating costs for the thickener range from $7,500 to $9,500/yr. The underflow from the thickener is split into two streams: 2363 lb/h of solids in a 19-gpm stream goes to the filter press for final disposal and the remainder is recycled to the crystallizers.

The filter press is a plate-and-frame filter that takes the 20% solids stream and concentrates it into a 65 wt% cake. The rate of cake production is 2363 lb/h; the cake is loaded into trucks for final disposal. The capital cost of the plate-and-frame filter is ~$250,000; operating costs are ~$2500/yr.

(a) Goslin-Birmingham, Inc.

The sludge is assumed to be disposed in an offsite landfill at a cost of $25/ton of dry solids--$5/ton for transportation and $20/ton for landfill cost. The annual cost of sludge disposal is $259,000. If onsite disposal were feasible, a substantial savings would result.

Table 7.1 lists the capital and operating costs for the major purchased equipment. The effect on the purchased equipment cost of increasing the seed crystal recycle rate from 1% to 4% is negligible (~$25,000) and is not included as a variable.

The total investment cost is derived by multiplying the purchased equipment capital cost by factors accounting for installation, balance-of-plant, and indirect costs. Table 7.2 lists some average cost factors from the literature (Peters and Timmerhaus 1968; Gerlaugh et al. 1979). For an installation cost factor of 1.45, a balance-of-plant cost factor of 2.6, and an indirect cost

TABLE 7.1. Purchased Equipment Capital and Operating Costs

Equipment	Capital Cost, $	Operating Cost, $/yr
Crystallizers[(a)]	1,100,000	-
Reactor clarifier	1,000,000	163,000
Dual-media gravity filter	1,500,000	123,000
Thickener	75,000	7,500
Filter press	250,000	2,500
Sludge disposal	-	259,000
Total	$3,925,000	$555,000

(a) Crystallizer capital costs would be decreased $260,000 if the retention period were decreased from 8 to 6 min per stage.

TABLE 7.2. Average Cost Factors

Item	Cost Factor
Installation	1.4 to 1.5
Balance-of-plant	2.2 to 3.0
Indirect costs	1.25 to 1.4

factor of 1.32, the total investment cost is $19,532,000 for the 8-min retention time and $18,239,000 for the 6-min retention time. These total investment costs are used in the life-cycle cost analysis.

7.3 COST COMPARISON

Two cases were analyzed for the fluid treatment option:

- Case 3 - 8-min fluid residence time in the crystallizers
- Case 4 - 6-min fluid residence time in the crystallizers.

The life-cycle unit costs and the differential savings are shown below:

Treatment Process	Frequency/ Residence Time	Life-Cycle Unit Cost, $/10^3 gal	Differential Savings, $/10^3 gal	Differential Savings, $/yr
None	(1) Clean well/ 1 month	4.11	-	-
None	(2) Clean well/ 3 months	3.49	0.62	2,600,000
Crystallizer and clarifier	(3) 8 min	2.47	1.64	6,890,000
Crystallizer and clarifier	(4) 6 min	2.45	1.66	6,960,000

Case 4 has the highest differential savings, although the differential savings of Case 3 are only ~1% less. A crystallizer manufacturer (Goslin-Birmingham, Inc.) indicates that the optimum residence time in the crystallizers is 8 min; therefore, Case 3 represents the most realistic geothermal injection treatment alternative.

8.0 WORLDWIDE INJECTION EXPERIENCE

In this section, the current status of geothermal injection practice is discussed. It is within this patchwork of successful injection, lost injectivity, and reservoir hydrodynamics that injection and preinjection treatment processes are evolving as workable solutions to site-specific problems. It is helpful to understand the diversity in the history of injection practices before trying to evaluate a process for a particular plant or site.

8.1 UNITED STATES

The United States has demonstrated the widest range of produced/injected salinities of any geothermal user in the world, ranging from steam condensate to brines containing more than 250,000 ppm dissolved solids. Profiles are presented in the following sections.

8.1.1 The Geysers, California[a]

The Geysers is a steam-dominated reservoir. In 1983, in excess of 1240 MWe was on-line. This field contains more than 200 wells (~15 wells are needed to support a 110-MW unit). Turbine inlet conditions include temperatures from ~170 to 180°C and pressures from 80 to 115 psig. Contaminant concentrations in the produced steam are given in Table 8.1.

TABLE 8.1. Contaminant Composition of Produced Steam at the Geysers

Species	Concentration, ppm	Average Flow Into 110-MW Unit, kg/h
CO_2	290 to 30,600	2700
H_2S	5 to 1,600	180
CH_4	13 to 1,447	160
NH_3	9 to 1,060	160
H_3BO_3	12 to 233	75
H_2	11 to 218	46
N_2	6 to 638	43
C_2H_6	3 to 19	6.6
As	0.002 to 0.050	0.016
Hg	0.00031 to 0.018	0.004

(a) See DiPippo (1984, 1980); Defferding (1980); Kestin (1980).

The Geysers steam condensate contains boron and ammonia concentrations that exceed California standards for surface disposal; hence, injection has become a standard procedure at this site. About 20% of the mass of the geothermal fluid produced must be disposed of as excess liquid from cooling tower basins. Beginning with Units 5 and 6 in 1970, this excess liquid has been injected. By 1975, over 15×10^9 l had been injected, with about 18×10^6 l/day being injected by six wells. Because of the low pressure of the steam reservoir, pumping is used only to transfer injected liquid to the wells; actual injection is done by gravity feed. To prevent contamination and plugging of the injection wells, settling basins are used to remove solids before injection. Deaerating vessels remove oxygen and air from the injection system to control corrosion and oxidation, which would contribute to the solids burden of the injected fluid.

During early injection, some cooling of adjacent production wells was experienced. Injection wells are now drilled deeper than nearby production wells and are as far away as possible from the major producing regions. A tracer test on a injection well in 1973-1977 indicated that about 18% of the injected fluid is vented as steam at nearby production wells.

Subsidence and microseismic activity are carefully monitored at the Geysers. Some increase in microseismic activity was observed in 1980.

8.1.2 Niland (GLEF), Imperial Valley, California[a]

The Niland reservoir geothermal fluid is a hypersaline brine of 200,000 ppm TDS and above. Wellhead conditions for the Salton Sea GLEF were: 190°C (375°F); 150 psig; 146,934 kg/h of liquid; 29,024 kg/h vapor; 5442 kg/h NCG. The GLEF testing was completed in 1979 after 3-1/2 years of operation. This facility was jointly funded by San Diego Gas and Electric and DOE to test production options in high-salinity brine fields.

From 1976 to 1977, the GLEF was operated as a four-stage flash binary cycle system. Due to severe scaling and corrosion problems, the system was converted to a two-stage flash binary cycle system in 1978-1979, using distilled water as the working fluid. Under the four-stage flash system, the nonvaporized geothermal fluid was injected. The injection became progressively more difficult. To maintain the desired flow, injection pressures were raised and formation fractures were opened to reduce injection pressures. A number of cycles of pressure increase and formation fracture were experienced. Scaling analysis showed that the front of the plant contained heavy metal sulfides (FeS and PbS), some metal oxides (Fe_2O_3, Fe_3O_4), and NaCl. Toward the injection end of the plant, the scale was predominantly SiO_2 and NaCl.

(a) See Anastas (1980); Aducci (1980).

Following conversion to the two-stage flash binary system (Figure 8.1), plant availability increased to 60% (compared with 40% with the four-stage system). This increase was largely due to fewer equipment scaling and corrosion problems. The SiO_2 deposition was determined to be the principal cause of erratic injection performance, which occasionally necessitated rerouting fluid to holding basins while the injection well was reworked. Under the plant conditions, the sluggish SiO_2 precipitation kinetics postponed much of the SiO_2 precipitation until the fluid had entered the reservoir.

Based on tests by Magma Power Co. and Envirotech Corp., a treatment system for injected fluid evolved using a reactor clarifier, a thickener, a dual-media sand filter, a filter press, and a holding tanking for filter backwash. This system operated from June 1979 until September 1979. Pilot tests with this equipment indicated that the total suspended solids level dropped from 180 to 100 ppm and dissolved SiO_2 dropped from 390 to 200 ppm in the reactor clarifier. Following the dual-media sand filter, the fluid contained 4 to 10 ppm suspended solids and a dissolved SiO_2 content of 192 ppm.

The heavy metal oxides were another problem in the injected fluid. The principal cause of the formation of these oxides was air leakage into the reactor clarifier. Points where air entered to the system were sealed, thus remedying this problem.

Following the September 1979 shutdown, the reactor clarifier system was examined. There was no scale of any type on any of the system parts. Some corrosion was noted on interior walls of the clarifier. Methods to accelerate the precipitation of SiO_2 using flocculating agents have shown some promise. If successful, such agents could markedly reduce the size of the reactor clarifier for a given injection flow.

The duration of the injection tests using the fluid treatment system noted above was too short to permit any significant conclusions concerning the effects on the injection system and the reservoir. The results do, however, support the use of the reactor clarifier/sand filter concept for preinjection treatment of fluid for a silica-dominated geothermal reservoir. This research was the predecessor to the Union Oil Salton Sea plant, which uses a flash crystallizer, reactor clarifier, and media filter flow system.

8.1.3 Salton Sea Geothermal Demonstration Unit 1

A simplified process flow sheet for the steam production and brine treatment systems for the Union Oil 10-MWe Salton Sea Unit 1 facility is illustrated

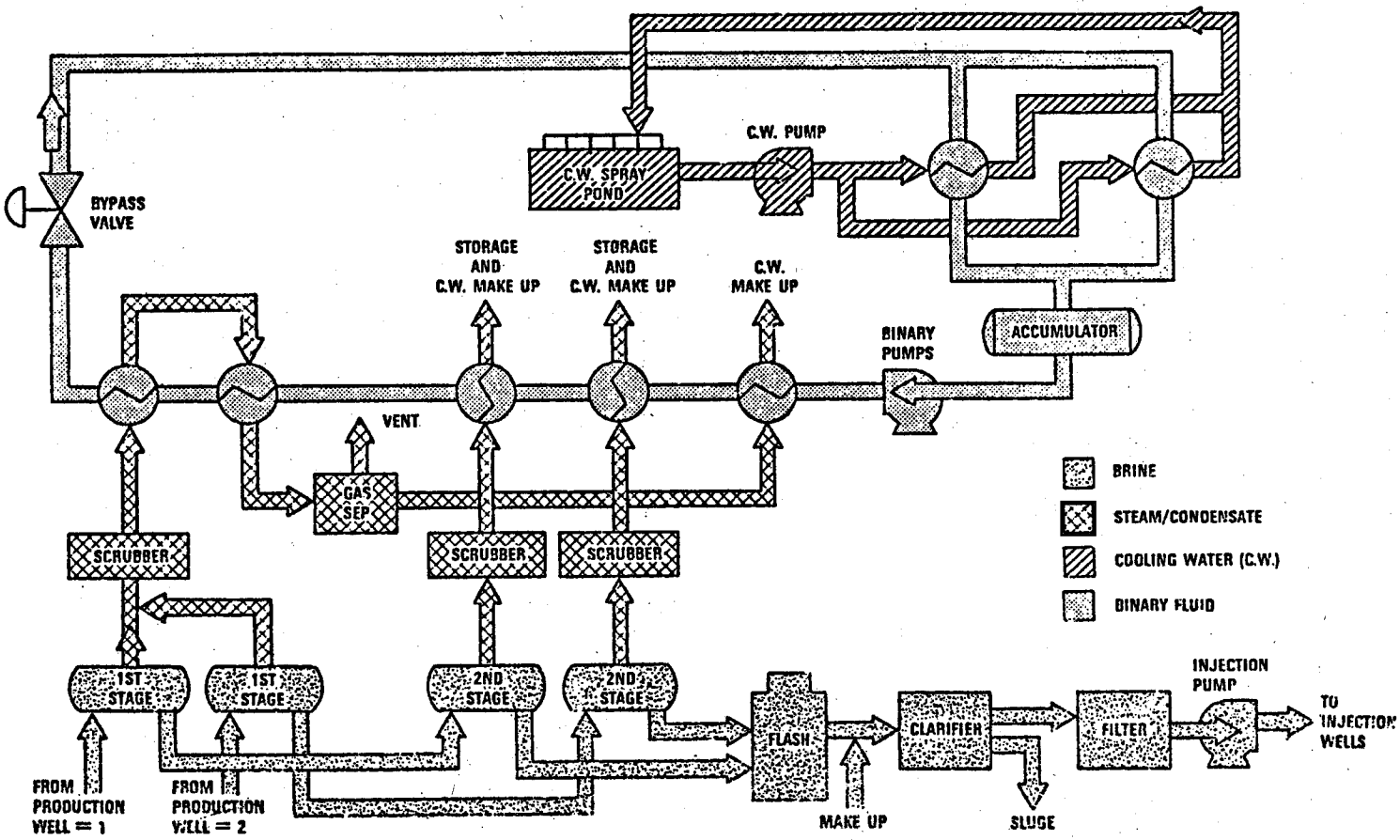

FIGURE 8.1. Process Flow Diagram for GLEF (Anastas 1980)

in Figure 8.2 (Moss, Whitescarver, and Yamasaki 1982).[a] This unit began operation in 1982 to supply steam to a companion Southern California Edison 10-MWe steam generator. Four production wells at this facility supply up to 1,416,000 lb/h of hot brine to the steam production system. The two-phase flow from each production well is processed through a wellhead separator where steam flashed from the brine is collected and routed into the main steam line to the power plant. Hot brine from the separators is collected in a common header and directed to the first-stage flash crystallizer, which operates at ~125 psia. Sludge is recycled from the thickener to the first-stage crystallizer to provide seed particles for deposition of silica and other supersaturated constituents in the brine. Steam separated in the first-stage crystallizer is routed to the main steam line, and the spent brine slurry is sent to the second-stage flash crystallizer, which operates slightly above atmospheric pressure. Steam from the second-stage flash crystallizer is vented to the atmosphere, and the

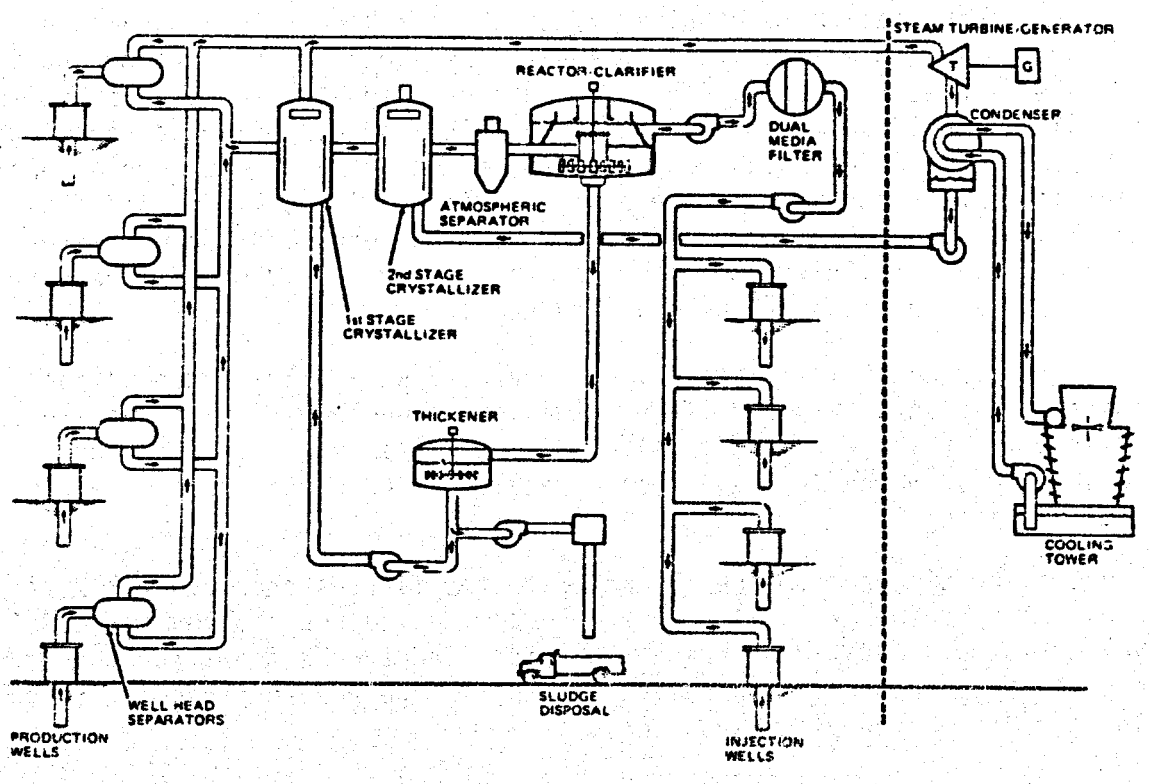

FIGURE 8.2. Flow Diagram for Salton Sea Unit 1 (Moss, Whitescarver, and Yamasaki 1982)

(a) This large-scale pilot plant uses hypersaline brine, ~250,000-ppm TDS, and incorporates the following techniques in its brine treatment process: flash crystallizers, reactor clarifier, gravity thickener, and dual-media filters.

brine slurry flows to an atmospheric separator for final separation of steam from brine. Two separate trains of flash crystallizers and atmospheric separators are available; each is capable of processing 100% of the flow. This arrangement allows one train to be shut down for maintenance without interrupting power generation and also provides a greater degree of control for balancing brine flow and stabilizing vessel operating conditions. Additional surge capacity is available in the system through the use of the second-stage crystallizers.

Spent brine flows from the atmospheric separators to a reactor clarifier where precipitation or crystallization of supersaturated constituents is essentially completed and much of the particulate matter is separated from the brine. Postclarifier residual particulate matter in the brine is reduced by dual-media filters. Four injection wells discharge the filtered brine to underground receiving formations.

Sludge from the reactor clarifier is routed to a thickener to remove water by gravity sedimentation. The sludge from the thickeners is pumped to a filter press for final dewatering; it is designated as a hazardous waste due to its relatively high heavy metal content and must be disposed of at an authorized burial site. In 1982, the daily cost of hauling and disposing of the sludge was about $800, much of which resulted from transporting the sludge a considerable distance to the burial site near San Diego. A local disposal site is being planned when the quantity of hazardous waste produced becomes large enough to justify building the site. An alternative would be to bypass the filter press and dispose of the slurry directly.

The Salton Sea Unit 1 facility has operated well within expectations for a demonstration plant. Minor difficulty was experienced with plugging and loss of efficiency in the dual-media filters in the first year of operation (Yamasaki 1983), which may have been a result of occasional upsets in the reactor clarifier.

Recycling sludge from the thickener to the first-stage crystallizers imposes a slight energy penalty on the system due to the cooling effect of the recycled sludge. Additional brine (~3%) is added to the flow from the production wells to overcome this penalty. If the sludge were not recycled, scaling would result, causing plant shutdown.

8.1.4 North Brawley, Imperial Valley, California[a]

Six wells were completed at this site in 1976-1978 by Union Oil Company. The chemical characteristics of the geothermal fluid at this site are similar

(a) See Messer, Pye, and Gallus (1978).

to those of the GLEF. Unconsolidated sediment composed of sand, gravel, and soft clay were encountered at shallow depths. At greater depths, the sediment became progressively harder.

There is little information on injection of concentrated brines into a porous formation similar to that found in the Imperial Valley. The Veysey Well No. 1 was tested for productivity and then converted to a injection well to dispose of brine from other wells. The cemented wellbore was perforated to a depth of ~4670 ft, and 775,000 barrels of brine were injected during a 16-month period. The injected brine was single phase, and the wellbore was always full of brine during the injection. Compatible brines from various producing wells were injected under the same surface conditions. The brines were supersaturated with SiO_2 and contained low concentrations of suspended colloidal SiO_2 (2 to 15 μm in size).

During the injection period, well surveys showed no evidence of bridging above the fluid entry points from the wellbore. The wellbore scale accumulation during the injection period was uniform and did not cause a major restriction or a measurable pressure increase at the wellhead (the velocity of the brine in the wellbore was generally greater than 3 ft/s). Static formation pressure surveys between injection periods showed no change in the static reservoir pressure during the 16-month test. It was concluded that most of the wellhead injection loss was caused by damage starting at the sand face. Samples of scale collected during mechanical cleaning of the wellbore revealed the following two major scale constituents: a light-colored material composed of silica and silicates and a dark-colored material composed of iron, silica, and silicates. Both constituents contained small amounts of carbonates.

The loss of injection capability was believed to be caused by particle invasion and subsequent plugging of the sand matrix along with precipitation of SiO_2 within the matrix. Significant damage occurred at depths ranging from 2 in. to 2 ft. Colloidal SiO_2 particle precipitation and plugging caused negligible damage beyond ~4 ft from the wellbore. Testing in this field revealed that severe injection damage can result if hypersaline brines are not properly treated before injection into sedimentary formations.

An acid stimulation treatment was devised to restore injection ability for the one well used in the above tests. This acid treatment consisted of:

- Before acidizing, the wellbore was cleaned by mechanical scraping and brushing the total depth of the well. This treatment, by itself, did not significantly affect the injection capability.

- A selective acid injection treatment was used. Each zone was treated in immediate succession with a 5% HCl preflush, a 5% HCl-5% HF acid treatment, and a 5% HCl acid postflush. Each stage was inhibited and designed for 75 gal/ft of zone. The acid was injected by an acid wash tool, with the acid confined to a given zone by opposing swab cups. Each zone was 8 ft long, and the injection rate was 3 to 4 barrels/min. After the acid treatment, a 2% solution of ammonium chloride was injected to minimize precipitation reactions that could form excess acid in the wellbore.

- The 3 to 4 barrels/min injection rate removed scale deposits in the perforation and also resulted in enough acid displacement to obtain the necessary penetration into the formation.

- Since the acid injection required a pressure above the formation fracture pressure, the effective acid penetration was estimated to be 2 to 4 ft along the fracture wall and 3 in. into the matrix adjacent to the fracture wall. This rate also minimized acid exposure time in the tubing to reduce corrosion.

The results and conclusions of the acid stimulation treatment are summarized below:

- Injectivity loss from SiO_2 particle plugging of the formation matrix can be restored by a properly designed HCl-HF acid treatment.

- SiO_2 particle buildup at the sand face and accumulation in the sand matrix near the wellbore were the primary causes of the injection loss at this well.

- The major injection loss was caused by total plugging of some injection intervals, rather than a general reduction in permeability.

- SiO_2 precipitation resulted from supersaturation conditions imposed on the brine when flashing the effluent before injection.

- The amount of acid treatment should be based on how much brine individual injection zones will accept.

8.1.5 Heber, Imperial Valley, California[a]

Geothermal waters at Heber are found at depths ranging from 600 to 3000 m. NaCl is the main dissolved constituent (TDS = 14,000 to 16,000 ppm), and SiO_2

(a) See Defferding (1980).

is low enough (~270 ppm) that scaling is not expected to be a problem at this site as long as injection temperatures are kept above ~150°F. Wellhead brine temperatures of 350 to 380°F are expected.

Six wells have been drilled (up to 1980) ranging in depth from 1220 to 1830 m. When the wells were flowed, all brine injected, with the exception of a small amount that was flashed to steam in an experimental facility. Blowdown from cooling towers is combined with recycled, cooled brine. The nominal injection pressure is 315 psi. With deep well pumps, injection flow rates could be from 6 to 8 x 10^6 l/day.

Currently (1984), Heber is undergoing development to supply 8 million lb of brine per hour to a San Diego Gas and Electric binary cycle plant (65 MWe gross/45 MWe net). Because this is a pumped design (note the parasitic load without flashing), all of the produced brine will be disposed of via injection. Brine temperatures are to be kept above 165°F to avoid silica precipitation, and the pressure will keep the CO_2 in solution and prevent $CaCO_3$ scaling.

8.1.6 Valles Caldera, New Mexico[a]

The Valles Caldera reservoir is believed to be liquid dominated with an overlying vapor-dominated zone. The geothermal power potential of this site had been estimated as 2700 MW sustained over ~30 years. The mean reservoir temperature is expected to be ~273°C. As of 1980, 17 wells had been drilled in the southwest quadrant of the field, at depths ranging from 1525 to 2745 m.

Union Oil Company has been conducting injection tests at this site since 1973. Injection is considered to be a viable option for this field based on the persistence of the injection ability and the lack of seismic effects from the injection. The complex geology of the Valles Caldera site, however, required substantially more drilling to establish the commercial value of the site. As of 1982, site development was suspended because of insufficient production flow despite satisfactory resource temperatures.

8.1.7 Raft River, Idaho[b]

The Raft River geothermal site is located in a closed groundwater basin in south-central Idaho. The 1982 installed capacity was 5 MWe; this experimental binary cycle plant was closed after a brief run because of high cost. Chemical analyses indicate the existence of natural communication between the geothermal reservoir and the shallower aquifers used for irrigation. Injection of geothermal fluids may result in further degradation of irrigation water.

(a) See DiPippo (1980); Defferding (1980).
(b) See Spencer (1980).

Seven monitoring wells, ranging in depth from 150 to 400 m, were drilled to evaluate injection effects. These wells were monitored over a span of 1 year, including two 21-day injection tests in 1979. Well RRG-1 (drilled to a depth of 1160 m) was used for the injection. The monitoring wells were distributed at various distances from the injection well, ranging from ~2.6 km to ~0.3 km.

The injection tests were not long enough to permit any generalizations concerning the interaction between injection of geothermal fluid and the irrigation reservoir. Specific test results included the following. The water level in the well ~0.8 km from the injection well increased an average of 0.4 m/week during the injection, indicating direct fracture connection between the injection zone and the aquifer penetrated by the monitoring well. The water levels in wells ~0.3 km, ~0.6 km, and ~0.4 km from the injection well showed a step function decrease that coincided with the period of the injection tests. This response may be caused by elastic deformation of the irrigation aquifer matrix. The Raft River experience illustrates injecting a low salinity brine into a fractured reservoir.

8.1.8 Brawley 10-MW Demonstration Plant

Brawley began operation in July 1980 and was the first plant to actually produce power using the hypersaline brines from the reservoirs in the north-central part of the Imperial Valley. The power plant is a partnership between Southern California Edison and the Los Angeles Water and Power Department. The brine production/treatment/injection and steam delivery systems are owned and operated by Union Oil Company.

The resource is high temperature (+475°F) and highly saline (>200,000 ppm TDS) with a significant NCG content. Steam is delivered at a pressure of approximately 100 psig from a flash separator at 170°C (340°F). Brine treatment initially consisted of ponding/aging, perhaps trying to duplicate the experience at the Japanese Hatchobaru field. Well and equipment plugging have resulted. As of 1984, brine acidification has been added to the treatment process with some improvement in results. Operating specifics, even the type of acid used, are unknown. Since this plant is operating on a kinetics-based precipitation avoidance treatment scheme (in contrast to Union Oil's Salton Sea Plant with its controlled precipitation approach), other consistent actions would be maintaining temperature, avoiding oxygen contact, and minimizing delay prior to injection. Whether these actions are being done is not known.

8.1.9 Roosevelt Hot Springs

A 20-MW net (23 gross) flash cycle plant is scheduled to come on-line in June 1984. The power plant is operated by Utah Power and Light, and the brine/steam supply is operated by Phillips Petroleum. The approximate brine conditions are 18% wellhead flash to 350°F resulting in a 790 ppm SiO_2 level in the flashed brine; fluoride levels are high at 1 to 3 ppm. Calcite scaling is avoided by the addition of a few parts per million of phosphonate inhibitor (believed to be Dequest 2060) at the wellhead. Silica scaling is controlled by maintaining the temperature at ~350°F in a totally pressurized and insulated injection system. The brine residence time from flash to injection is on the order of 45 min. Some silica scaling is observed, but because injection is into a 3- to 5-ft wide fracture it is hoped that long-term injectivity will remain good. The field has produced low volumes of flow for over two years during a test of a new turbine concept, and presumably this permitted Phillips the opportunity to match their treatment to their particular production and easy injection characteristics.

8.2 MEXICO - CERRO PRIETO[a]

The liquid-dominated Cerro Prieto reservoir produces a two-phase mixture at the wellhead. The chemical composition of separated water samples from 12 wells is given in Table 8.2. The geothermal steam contains ~1 wt% NCG,

TABLE 8.2. Composition of Separated Water from 12 Wells at Cerro Prieto[a]

Constituent	Concentration, ppm
Cl	14,370
Na	7,760
K	1,660
SiO_2	850
Ca	545
HCO_3	50
Li	18
B	18
SO_4	17
Mg	1.4
pH (25°C)	8.2

(a) DiPippo (1980).

(a) See Goyal, Lippmann, and Tsang (1982); Tsang et al. (1981); DiPippo (1980).

mainly CO_2 and H_2S. For eight wells, the average CO_2 and H_2S concentrations are 7320 and 1564 ppm, respectively. These samples were taken from an average steam flow of 120,000 lb/h and an average separator pressure of 114.6 psig.

Engineering studies began in 1978 under a 5-year cooperative agreement between the U.S. DOE and the Comision Federal de Electricidad de Mexico (CFE). In general, it has been observed that the mass flow produced by a given production well at Cerro Prieto has decreased with time from 1973 to 1980. This reduction is attributed to: SiO_2 precipitation in the reservoir pores; relative permeability effects in the two-phase region near and around the wellbore; and reduced pressure gradients due to field exploitation.

Since 1979, CFE has been conducting injection tests using Cerro Prieto well M-9. The injection conditions are: 165°C untreated brine, 80 tonnes/h maximum injection rate; 721 to 846 m depth of injection.

Monitoring of neighboring production wells has not shown any significant change in the wellhead temperature, pressure, or enthalpy of the geothermal fluid. Inasmuch as the production wells (>1100 m) are substantially deeper than the injection wells (721 to 864 m), this independence is not surprising. This result was corroborated by computerized modeling studies of the Cerro Prieto reservoir using injection parameters corresponding to the actual test case and geological assumptions appropriate to the Cerro Prieto field. Since Cerro Prieto is plagued with silica scaling problems, it is expected that any substantial injection will have to include a silica brine treatment process. Current spent brine disposal is accomplished by evaporation from large ponds.

Silica treatment approaches tested at Cerro Prieto include the GLEF-style reactor clarifier and an aging/lime addition/sedimentation process (Hurtado et al. 1981) tested on brines of ~30,000 ppm TDS and 1000 ppm SiO_2. The reactor clarifier operating with 0.9% solids in the reaction zone had (overflow) effluent that contained 250 ppm particulates and 300 ppm dissolved SiO_2; its performance was unsatisfactory when compared with the second process. This second process consisted of 10 to 15 min aging, 20 to 40 ppm lime addition, and sedimentation in a clarifier. This process yielded an effluent of ~30 ppm particulates at a calculated cost of 25% less than a reactor clarifier process.

8.3 EL SALVADOR - AHUACHAPAN[a]

This liquid-dominated field has an installed capacity of 95 MWe (1981). As of 1981, 28 wells, both production and injection, had been drilled; well depths range from 600 to 1000 m. Some characteristics of the Ahuachapan geothermal fluid are given in Table 8.3. The main turbine steam temperature is

(a) See DiPippo (1980); Kestin (1980); Horne (1982a); Horne (1982b).

TABLE 8.3. Characteristics of Ahuachapan Geothermal Fluid

Species	Average Chemical Composition, ppm
Cl	10,430
Na	5,690
K	950
SiO_2	537
Ca	443
B	151
Br	43.9
HCO_3	34.2
SO_4	34.0
Li	17.5
As	11.3
I	8.1
Rb	7.1
Cs	5.5
Sr	4.7
Sb	2.1
F	1.5
Mg	0.13

Gas	Composition of NCG in Steam, vol%
CO_2	86.8
H_2S	12.1
H_2	0.126
N_2	0.05
NH_3 and CH_4	1.0

reported to be 313°F; pressure, 80 psig. It is understood that this plant has continued to operate despite the military actions that have taken place in El Salvador.

Four injection wells were sited on the periphery of the field. The inner casings of the wells were not cemented to allow for easy conversion to production wells. To support 60 MWe, a liquid injection rate of ~368 kg/s (5800 gpm) is required. The injected liquid is taken directly from the wellhead separators at separator pressure and injected without booster pumps. There is no atmospheric exposure of the fluid and no chemical treatment. About 13×10^6 Mg (29×10^9 lb) of fluid has been injected since 1975. Large-scale injection experiments were carried out in 1970 and 1971; 2×10^6 m^3 of water at 150°C was injected. The combined forces of gravity and vapor pressure were used. A dual-purpose well was drilled in the production area and finished with a slotted liner to a depth of 952 m, somewhat below the depth of the producing wells. Injection was successful with this well as long as the injection temperature was held above 150°C. This high temperature is necessary to prevent silica polymerization. The use of separator and gravity drive for injection indicates that the formation has good permeability.

Using a tritium tracer, some connection was noted between an injection well and a production well ~500 m away. No connection was noted between the injection well and nearby surface springs. With proper spacing, injection can probably be successfully managed in this field. Tests have shown that injection is important to maintaining reservoir pressure. Because the temperature of the injected fluid has been maintained above 150°C (302°F), there has been no mineral deposition in the liner of the injection wells. The balance of the waste water is transported to the ocean via a 75-km long covered concrete channel.

8.4 JAPAN

Data summarizing geothermal production and injection in Japan as of September 1980 are given in Table 8.4.

8.4.1 Otake[a]

There are two geothermal zones at the Otake site. The upper zone starts at a depth of ~250 m and continues to ~550 m. The top of the lower reservoir is ~1000 m below the surface and extends to an unknown depth. This liquid-dominated field taps only the upper reservoir at a temperature of ~200°C. The NCG and TDS content of the geothermal fluid is indicated in Table 8.5. Waste fluid is injected immediately at Otake because tests indicated that it took 1 h for the silica to start polymerizing.

Injection began at Otake in 1972 to dispose of waste liquid from wellhead separators and excess steam condensate from the cold well of cooling towers. As a result of tracer tests using fluorescein dye (sodium salt), the three injection wells drilled at Otake in 1972 were located 150, 350, and 500 m from the nearest production well, respectively. The casing for the injection wells was identical to that for the production wells. Injection is done at atmospheric pressure to avoid triggering seismic activity. It has been noted that pressure injection is periodically used to overcome injection resistance. To date, no seismic effects from the geothermal activity have been noted.

After injection tests began in 1972, recovery was improved, indicating that injection was supporting the reservoir pressure. By 1975, the improvement ceased and one well ceased production due to the loss in enthalpy of the geothermal fluid, indicating thermal interference from the injection. Since that time, reservoir output has been reducing at ~6%/yr. In 1979 and 1980, production was raised to 12.5 MWe by drilling two new production wells and injection

(a) DiPippo (1980); Kestin (1980); Horne (1982a); Yoshida, Tanaka, and Kusunoki (1983).

TABLE 8.4. Summary of Geothermal Production and Injection in Japan[a]

	Otake	Hatchobaru	Onuma	Kakkonda	Onikobe
Capacity, MW	12	55	10	50	25
1980 production, MW	12	55	7	40	7.5
Production:					
No. of wells	4	8	5	11	12
Average depth, m	500	1000	1600	1000	300
Total steam, t/h	120	400	91	380	75
Wellhead pressure, kPa	304	481	300	686	200
Injection:					
No. of wells	8	14	4	15	1
Average depth, m	500	1000	800	700	1000
Total flow, t/h	680	400	360	2700	115
Temperature, °C	95	60 to 95	95	160	95
Pressure, kPa	0	0	0	540	0
Configuration	Side/equal	Side/above	Side/above	Mixed/above	Side/below
Tracer flow, m/h	~0.3	Up to 80	Up to 4	--	--
Comments	Accepts water from Hatchobaru (175 t/h)	SiO_2 scaling	--	--	Gas interference

(a) As of September 1980.

TABLE 8.5. NCG and TDS Content of Otake Geothermal Fluid

Gas	NCG, wt%
CO_2	96
H_2S	1.4
Other (O_2, N_2)	2.6

Species	TDS Content, ppm
Cl	1630
SiO_2	668
Ca	29
Mg	17
Na	940
K	110
SO_4	145
pH	6.7 to 8.4

was increased to a total of 663 t/h, including 175 t/h piped from Hatchobaru. The current practice is to inject the produced brines immediately following steam separation.

Despite the demise of one well, injection at Otake appears to be successful from a reservoir standpoint. Tracer tests in 1976 showed permeation velocities of ~0.3 m/h--two to three orders of magnitude smaller than those observed at Hatchobaru, probably due to supersaturated SiO_2 conditions at atmospheric pressure. Some scale buildup was experienced at injection wells, causing a substantial flow reduction (310 to 120 t/h in about 3 years); corresponding scale thickness was ~25 mm on the casing at the wellhead. Kyusha Electric Power Co. is presently conducting waste water treatment studies in an attempt to control or remove SiO_2 and arsenic from Otake waste water.

8.4.2 Hatchobaru[a]

The Hatchobaru field is similar to nearby Otake; both sites are over a dual geothermal reservoir. While Otake taps the upper reservoir, Hatchobaru taps the lower one at a temperature of 230°C. NCG and TDS compositions for the geothermal fluid at this liquid-dominated field are given in Table 8.6. Hatchobaru has a double flash-type power plant with a capacity of 55 MWe. Geothermal waste fluid is aged for 1 h in a tank prior to injection to permit silica polymerization. After aging, the silica adheres less to piping and the

TABLE 8.6. Characteristics of Hatchobaru Geothermal Fluid

Gas	Total NCG Burden, vol%	Species	Contaminant Concentration, ppm
CO_2	40 to 84	Na	2200 to 2860
H_2S	3 to 15	K	243 to 383
O_2, N_2, etc.	10 to 57	Ca	34 to 108
		Cl	3850 to 5150
		SiO_2	620 to 922
		As	2.9 to 3.2
		pH	4.7 to 6.5

NCG content of steam: 0.05 to 0.59 wt% of steam

(a) See DiPippo (1980); Kestin (1980); Horne (1982a); Yoshida, Tanaka, and Kusunoki (1983).

water is injected without attempting a total separation of the solid particles. Fluid channeled through heat exchangers for low-grade heat recovery is injected over a temperature range of 60 to 70°C.

Injection wells at Hatchobaru are drilled in the side/equal configuration, meaning that drilling is on the side of the production field at roughly the same depth as the production wells (see Table 8.4). Tracer tests have indicated a strong connection between some wells as high as 80 m/h, with strong returns over distances as great as 600 m. Injection has lowered the enthalpy of all production wells. An annual loss of injection capacity (approaching 20%) has been experienced due to SiO_2 plugging. To maintain injection capability, 25% of the waste water is exported to Otake and injected there.

Possible reservoir short-circuiting problems have been identified at Hatchobaru using fluorescein dye. This agent has proved as satisfactory as the more expensive KI tracer in identifying first arrival times of the tracer fluid at production wells.

8.4.3 Onuma[a]

At the liquid-dominated Onuma field, one injection well and all the production wells have been slant drilled. The injection wells receive liquid at atmospheric pressure immediately after the pressure is let down in cyclonic silencers. Waste water is injected from the periphery of the field and at a somewhat shallower depth than the production wells (a side/above configuration; see Table 8.4).

There is some evidence that short-circuiting occurs during injection, although to a lesser extent than at Kakkonda. Tracer return rates are an order of magnitude slower than at Kakkonda. It appears that injection and production can coexist fairly successfully at Onuma, provided that injection wells are not sited too close to production wells.

8.4.4 Kakkonda[b]

This liquid-dominated field is the newest geothermal plant complex in Japan. The average depth of the injection wells is 754 m; production wells, 1000 m. Injection wells are sited in between the production wells; hence, this is an intermixed/above injection configuration (see Table 8.4).

Injection is done at separator pressure (~550 kPa), unlike all other Japanese geothermal plants where injection is done at atmospheric pressure to

---

(a) See DiPippo (1980); Kestin (1980); Horne (1982a).
(b) See DiPippo (1980); Kestin (1980); Horne (1982a).

minimize seismic effects. Extensive injection has not caused noticeable seismic action. The injection temperature is ~160°C, which prevents SiO_2 deposition in the injection wells.

The very large injection rate for Kakkonda (3000 t/h per 500 t/h of produced steam) represents a worst-case for reservoir short-circuiting. Such short-circuiting has been identified by tracer studies. Wells that have had rapid tracer arrival times from four particular injection wells declined significantly in output from the start of production. Cessation of injection from these wells resulted in a recovery of production from the affected wells. Injection at separator pressure and temperature appears to have avoided many of the deposition problems that have lessened injection capability in wells using atmospheric injection conditions.

8.4.5 Onikobe[a]

Onikobe lies over a dual geothermal reservoir; the shallow zone is vapor dominated and the deep zone is liquid dominated. The acid nature of the deep zone prevented its exploitation until 1980. NCG and TDS compositions for the Onikobe reservoir are given in Table 8.7 (see Table 8.4 for additional details on production and injection at Onikobe).

All waste liquid (drawn from separators, turbines, etc.) and the overflow from cooling tower basins are collected in drain ponds and then injected, which is a relatively small fraction of the geothermal fluid because of the high dryness fraction of the fluid at the wellhead. The high H_2S burden is released to the atmosphere without controls. Spent produced brine is combined with waste water to make a total of ~115 t/h that is injected into a single well at

TABLE 8.7. NCG and TDS Content of Onikobe Geothermal Fluid

Gas	Concentration, wt%	Species	TDS of liquid, ppm
CO_2	58.4	Cl	7590
H_2S	36.0[a]	Ca	930
H_2, CH_4, NH_3	5.6	SiO_2	550
		Mg	340
		SO_4	24

(a) Highest of any geothermal plant in the world.

(a) See DiPippo (1980); Kestin (1980); Horne (1982a).

atmospheric pressure. This single well is located at one end of the field and injects at 1000 m into the acidic portion of the reservoir (side/below injection configuration; see Table 8.4).

The Onikobe field experienced a decrease in steam output between 1975 and 1980, which may be due to an influx of cold surface water or to injection. There has been no noticeable alteration in the thermal or pressure behavior of the field since injection began in 1978.

There was a distinct rise in nitrogen content of the NCG in the months following injection. This rise (accompanied by a decrease in the CO_2 content) was attributed to entrainment of air in the injection well. The injection well was enclosed in 1980 to prevent air entrainment, and the nitrogen content of the producing wells has since declined. Similar transport of nitrogen has been observed at Hatchobaru. Injection tests have demonstrated a connectivity for NCG between the two reservoirs under the Otake site but not for the waters.

8.4.6 Summary of Japanese Injection Experience[a]

In cases where interwell flow occurs, the resulting thermal interference can be very detrimental to production. Such interference has occurred at Otake, Hatchobaru, Onuma, and Kakkonda. Hydraulic interference, however, may be beneficial in providing pressure support for the reservoir. The problem is one of sufficient separation between the injection and production wells so that injection fluid is heated to production levels before reaching the production wells. Previous estimates of safe distance have varied and appear to be quite site specific; for example, the suggested distance of 150 m for Otake is not sufficient for Hatchobaru.

Reduced performance resulting from injection has been observed at Hatchobaru, Kakkonda, and Onuma. In highly fractured systems, it appears to be expedient to avoid thermal interaction even at the cost of losing hydraulic support. One attractive method of doing this is to inject at a neighboring, but separate site.

Tracer studies have been used to great advantage in Japan to identify and overcome some of the injection breakthrough problems, particularly at Kakkonda. The Japanese have emphasized the use of chemical instead of radioactive tracers.

Loss of injection capability has presented operational difficulties at Otake and Hatchobaru. Kakkonda has had fewer injection problems with its pressurized high-temperature practice.

(a) See Horne (1982a).

8.5 ITALY - LARDERELLO[a]

As of 1979-1980, the vapor-dominated Larderello field had ~190 producing wells, involving various types of utilization systems. The Cycle 1 system is the simplest and involves no treatment of the geothermal fluid. In the mainstay Cycle 3 system, impurities and corrosive substances are removed by scrubbers upstream of the turbine inlet. Pure water and alkaline solutions wash the stream, and axial separators remove liquid prior to turbine entry.

Wellhead steam temperatures at Larderello range from 140 to 220°C (285 to 430°F); pressures, from 200 to 700 kPa (29 to 102 psig). NCG in the steam phase contains ~5 wt% CO_2 and ~0.5 wt% H_2S. The NCG content of the liquid and vapor phases ranges from 1 to 20 wt% of the total geothermal fluid content; the average composition is 93.8 vol% CO_2, 2.6 vol% H_2S, 1.8 vol% H_2, 1.1 vol% CH_4, and 0.65 vol% N_2.

About 20% of the waste liquid is injected. Injection experiments have been performed at the periphery of the field and in the producing regions. In one instance, channeling of cold water quenched a producing well. This was attributed to flow of cooler water along a major fault into the producing region. One set of injection tests was undertaken in 1973 in the Viterbro region, injecting 62°C water at rates of 3.5 to 35 l/s. Gravity feed was used for the injection into an 1100-m deep well that passed through a very permeable carbonate formation (first encountered at ~700 m). This test was continued for 9 days. No seismic effects were noted at five microseismic monitoring stations. Extensive injection modeling analysis is in progress for the Larderello site.

8.6 NEW ZEALAND

8.6.1 Wairakei[b]

Wairakei has been in production since 1960 and is an example of a field operated without injection. Loss of production, subsidence, and surface contamination have occurred. Some characteristics of the geothermal fluid at this liquid-dominated reservoir are given in Table 8.8. The wells at Wairakei are flashed to produce at two and three pressure levels; a considerable reduction in field pressure has occurred during the lifetime of the project. A high pressure loss approaching 50% has occurred. To maintain production in the face of declining output from high-pressure turbines, additional intermediate- and low-pressure capacity was installed. Figure 8.3 relates the decline of high-pressure capacity at Wairakei and the largely successful maintenance of field

(a) See DiPippo (1980); Kestin (1980); Schroeder et al. (1982).
(b) See DiPippo (1980); Horne and Grant (1982); Stacy and Thain (1984).

TABLE 8.8. Characteristics of Wairakei Geothermal Fluid

Gas	High Pressure, ppm	Intermediate Pressure, ppm	Species	Hot Liquid Composition, ppm
CO_2	4857	3467	Cl	2318
H_2S	132	70	SiO_2	300
N_2	7	17	$H_2B_2O_4$(a)	116
CH_4	3	5	HCO_3	39
H_2	1	1	SO_4	34
			F	10
			pH condensate	8.6

(a) Metaboric acid.

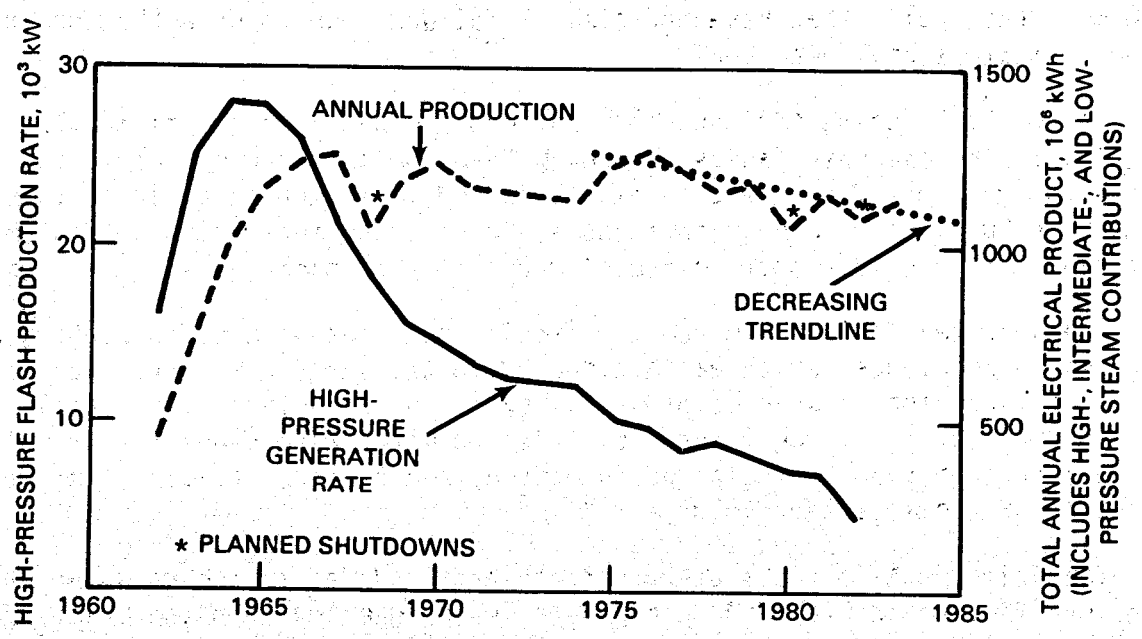

FIGURE 8.3. Maintenance of Field Production Despite Lower Pressures; No Injection; Wairakei (adapted from Stacy and Thain 1984).

output through bringing lower pressure (less-efficient) units on-line. In 1975, the total installed power capacity of Wairakei was 192.6 MWe. This reservoir has passed its peak of production; it is hoped that production will stabilize at between 125 and 140 MWe for an indefinite period.

At least partial injection of spent fluid is under consideration to prolong output. The field pressure recovered somewhat during a 3-1/2 month field shutdown in 1968; maximum subsidence rates of up to 1 ft/yr (a total of 23 ft to date) have been measured. The first injection tests at Wairakei were performed in 1982. Some unintentional injection has been taking place for some time in this field. In 1969, a production well ceased after a downflow from its shallow feeder zone at 360 m to a deeper zone at 600 m. Another well also ceased production in 1976 and a downflow of 160°C water was also shown at this well. This well was worked over in 1980, and the upper feed zone was successfully sealed off. After 4 years of accepting 300 t/h of 160°C water, this well again produced at its earlier temperature. Another well had a downflow of 175°C water from 300 to 600 m, although this well has continued to produce steam from ~300 m. Other wells that have had similar failures due to breakthrough into lower formations have been sealed.

Tracer tests using ^{131}I and ^{82}Br have shown that injected fluid flow is clearly within reservoir faults, although the flow is often by very circuitous routes through this fracture complex. Injected fluid movements in Wairakei are as much as 20 times greater than those at Broadlands, indicating a greater potential for reservoir short-circuiting during the injection.

The Wairakei field exhibited a rapid pressure response to injection compared with Broadlands, which was attributed to the large NCG content at Broadlands and hence the greater compressibility of the Broadlands geothermal fluid. As with Broadlands, strong returns of injected water were generally in wells that were deeper than the point of injection, suggesting a tendency for downward migration of the injected fluid.

Initial injection tests at both Broadlands and Wairakei have shown that water supersaturated with SiO_2 can generally be injected into the fractured reservoir without difficulty. Injectivity has tended to increase with injection due to thermal contraction of fissures or to pressurization and inflation of the formation.

8.6.2 Broadlands[a]

Two-phase conditions exist at the Broadlands site down to ~660 ft due to NCG pressure. Some of the characteristics of the geothermal fluid at this site are presented in Table 8.9.

Injection has been a prominent technical subject at Broadlands because this field is bisected by the Waikato River and any subsidence would probably cause flooding or a course change for this river. Injection testing has taken place at the following wells at Broadlands: Br7, 13, 23, 28, 30, 33, and 34. In all cases except Br34, injectivity increased with time, probably due to thermal contraction of fissured rock. In the case of well Br34, the injectivity declined due to SiO_2 deposition. This well was a shallow, cold well that brought SiO_2 into a precipitation regime. The other wells injected into a hot formation, which precluded SiO_2 precipitation. In wells Br7 and 28, static formation pressure fell with injection, probably as a result of injection of cooler water into the two-phase reservoir.

Tracer studies with ^{131}I showed that injected fluid migrates over long distances due to the fractured nature of the reservoir. Migration velocities of up to 0.5 m/h were indicated. Tracer studies also indicated a slightly downward flow of the injected fluid. Only a small percentage of the tracer fluid was recovered in all tests; therefore, the path of the injected fluid is not well understood. No thermal effects have been observed at neighboring wells despite

TABLE 8.9. Characteristics of Broadlands Geothermal Fluid

Gas	NCG Concentration
CO_2	1.2 to 10.8 wt% of steam
H_2S	0.022 to 0.077 wt% of steam
NH_3	22.8 to 49.0 ppm

Species	Contaminant Content of Liquid Separated from Wellbore at Atmospheric Pressure, ppm
Cl	1488
Na	997
SiO_2	771
HCO_3	175
K	175
B	43.7
As	3.3

(a) See DiPippo (1980); Horne and Grant (1982); Horne (1982a).

evidence that up to 12% of the injected fluid does break through into neighboring production well zones. Reservoir enthalpy is reduced in the vicinity of the injection well as was expected (e.g., ~100 to 200 kJ/kg decrease out of ~1300 kJ/kg).

The question as to where to inject has not been resolved for this site to date. Injection has been done both in and outside the field.

8.7 PHILIPPINES

8.7.1 Mak-Ban[a]

This liquid-dominated reservoir at Los Baños on the island of Luzon had an installed power capacity of 220 MWe by 1980 with an additional 100 MWe planned by 1984. Mak-Ban is the largest geothermal power complex in the world to inject all of its waste water. Most of the 14 wells are on the periphery of the production field. Published results for the Mak-Ban injection experience have been very sparse. Although the spent water has been injected without any noticeable negative effects, the chemistry of the fluids is unavailable.

8.7.2 Tongonan[a]

The liquid-dominated Tongonan field is located in the Bao River valley on the island of Leyte. The first deep well was completed in 1977 to a depth of 1942 m. Subsequently, ~45 wells have been drilled, and a 112-MWe power station was scheduled for service in 1982. Most wells are substantial producers (~72 t/h of separated steam). Before flashing, the geothermal fluid contains about 12,000 ppm TDS. Injection testing has been carried out since February 1978.

Using tracer water (^{131}I), underground liquid movements have been determined to be at rates as large as those of Kakkonda and Hatchobaru in Japan. Therefore, the potential for thermal breakthrough appears high in the Tongonan field. Injectivity does not seem to be a problem as the injection is done at separator pressure (deposition occurs at lower pressures). Increasing the injection flow rate appears to be beneficial in reducing SiO_2 deposition; a similar experience was noted at Broadlands in New Zealand. Injection of waste fluid at Tongonan appears to be a viable alternative for disposal based on the experience to date. The injection rate is expected to be ~1150 t/h of 160°C water.

(a) See Horne (1982).

8.8 SUMMARY OF INJECTION EXPERIENCE

8.8.1 Brine Treatment Approaches

Loss of injection capability due to SiO_2 deposition has been successfully avoided in New Zealand, Japan, El Salvador, and the Philippines in those cases where the injection is under separator pressure and the temperature of the injected fluid is above ~150°C. Lowering the temperature to less than ~100°C has resulted in injection losses at several sites. Injecting at high rates into a hot formation seems beneficial. Injection into a fractured reservoir is also mechanically (chemically) less troublesome, although the predictability of brine flow is poor. In the United States, the successful brine treatments have resulted from one of three approaches: hot injection above the SiO_2 saturation temperature; injection into a fractured location; or processing the brine to remove scaling conditions and particulates. The binary cycle plants inject above the SiO_2 saturation temperature, which will vary with the resource but might be ~150°F. The Raft River plant used a fractured reservoir for injection. The Union Oil Salton Sea plant processes the brine, starting at the steam production step, prior to disposal injection.

8.8.2 Reservoir Implications

At some sites, injection ability has increased with injection, either as a result of opening fractures by thermal contraction or by pressure inflation of the fractures. Injection of cooler water into two-phase reservoirs has, in some instances, reduced the reservoir pressure. This latter effect should be avoided in the design of a injection scheme if the economics can tolerate hot injection.

Tracer studies have shown that underground fluid movement can be substantially altered by injection of spent brines. Nonproducing fields tend to have slower rates of injection returns. If this indication is further substantiated, predicting thermal breakthrough from preproduction tests could prove to be quite difficult. Chemical and short-lived radioactive tracers have all been successfully used in fractured geothermal reservoirs. The very rapid return rates exhibited by fractured formations to date has allowed this success with chemical--fluorescein dye, halide ion (KI, KBr)--and short-lived radioactive tracers. Maximum tracer return velocities observed in various geothermal fields are cited in Table 8.10. As expected, there appears to be a correlation between tracer return rates and the possibility for thermal breakthrough under injection/producing conditions (i.e., fast return rates correlate with high breakthrough potential).

Injected water tends to follow faults, but the flow route can be very circuitous. There is a tendency for injected fluid to move in a downward direction, although this tendency can be overcome by vigorous production close to a injection well.

TABLE 8.10. Maximum Tracer Return Velocities in Non-U.S. Geothermal Fields[a]

Field	Velocity, m/h
Hatchobaru (Japan)	78.0
Tongonan (Philippines)	57.0
Wairakei (New Zealand)	22.0
Ahuachapan (El Salvador)	8.0
Onuma (Japan)	4.0
Broadlands (New Zealand)	1.2
Otake (Japan)	0.3

(a) Horne (1982b).

The total amount of tracer recovery is an important indicator of the possibilities of injection affecting the enthalpy of the production fluid. A close correlation has been observed in Japan between large tracer returns and subsequent degradation in well performance attributable to injection.

Frequently, using tracer tests, it has been determined that 10% to 30% of the injected water is produced again within a month or so; the remaining 70% to 90% disappears.

The environmental advantages of injection of waste geothermal fluid are well recognized. The technical and economic advantages of injection for geothermal power production are not clear-cut, particularly if 1) the reservoir is fractured, 2) environmental risks are low, or 3) near-term economic return is a dominant concern. From the results of the injection experience to date, it appears obvious that the advantages and disadvantages of injection are quite site specific. It is clear that the fluid must be physically and thermodynamically compatible with the receiving formation or it must be made compatible through a brine treatment technique.

9.0 REFERENCES

Abrams, A. 1977. "Mud to Minimize Rock Impairment Due to Particle Invasion." J. Petrol. Tech. May 1977, pp. 586-592.

Addoms, J. F., B. Breindel, and C. M. Gracey. 1978. "Wellsite Verification Testing of an Advanced Geothermal Primary Heat Exchanger (APEX)." Geothermal Resources Council Transactions 2:1-4.

Adduci, A. J. 1980. "High Salinity Geothermal Energy Conversion Based Upon the Operating Experience at the San Diego Gas & Electric/DOE Geothermal Loop Experimental Facility Located at the Niland Reservoir, Imperial Valley, California." In Proceedings of Second DOE-ENL Workshop for Cooperative Research in Geothermal Energy, October 20-22, 1980, Berkeley, California.

Alexander, G. B., et al. 1954. "The Solubility of Amorphous Silica in Water." J. Phys. Chem. 58:453-55.

Allen, C. A., T. W. Lawford, and D. H. Van Haaften. 1978. "Liquid-Fluidized-Bed Heat Exchangers for a 50-MW Plant." Geothermal Resources Council Transactions 2:5-8.

American Public Health Institute. 1981. Standard Methods for Water and Waste Water Analysis. 15 ed. American Public Health Institute, American Water Works Association, Water Pollution Control Federation, Washington, D.C.

Anastas, G. 1980. "Successful Fluid Management of the Salton Sea Reservoir." In Proceedings of Second DOE-ENL Workshop for Cooperative Research in Geothermal Energy, October 20-22, 1980, Berkeley, California.

Anderson, R. E. 1981. "Ion Exchange Softening of High-Solids Waters." Water for Subsurface Injection. ASTM STP 735, pp. 128-142.

Anfruns, J. P., and J. A. Kitchner. 1976. "The Absolute Rate of Capture of Single Particles by Single Bubbles." In Flotation - A. M. Gaudin, Memorial Volume, M. C. Fuerstenau ed., New York.

Annand, R. R., H. M. Hilliard, and W. S. Tait. 1977. "Factors in the Corrosivity of Seawater Used for Secondary Petroleum Recovery." In Oil Field Subsurface Injection of Water. ASTM STP 641, pp. 41-53.

Austin, A. L., et al. April 1977. "The LLL Geothermal Energy Program Status Report January 1976-January 1977." UCRL-50046-76.

Awerbuck, L., and A. N. Rogers. 1981. "Geothermal Scale Control by Crystallization." In Proceedings of the Fifth Annual Geothermal Conference and Workshop, July 23-25, 1981, San Diego, California, published by Attos Corp., Santa Cruz, California.

Awerbuck, L., V. C. Van der Mast, and A. N. Rogers. 1982. "Geothermal Scale Control by Crystallization." In Proceedings of the Sixth Annual Geothermal Conference and Workshop, June 28-July 1, 1982, Snowbird, Utah, published by Attos Corp., Santa Cruz, California.

Axtmann, R. C. December 22, 1980. Patent No. 4,378,295.

Ball, J. W., E. A. Jenne, and D. K. Nordstrom. 1979. "WATEQ2 - A Computerized Chemical Model for Trace and Major Element Speciation and Mineral Equilibria of Natural Waters." In Chemical Modeling in Aqueous Systems, Speciation, Sorption, Solubility, and Kinetics, E. A. Jenne, ed., Am. Chem. Soc., ACS Symp. Series 9, Washington, D.C.

Barkman, J. H., and D. H. Davidson. 1972. "Measuring Water Quality and Predicting Well Impairment." Trans. AIME (originally SEP 3543).

Barna, B. A., and J. T. Patton. 1972. "Permeability Damage from Drilling Fluid Additives." Paper SEP 3830, presented at the SEP-AIME Rocky Mountain Regional Meeting, April 10-12, 1972, Denver, Colorado.

Barnes, H. L., and J. D. Rimstidt. 1976. "Chemistry of Silica Scale Formation." In Proceedings of the Second Workshop on Materials Problems Associated with the Development of Geothermal Energy Systems, May 16-18, 1975, El Centro, California. USBM Grant No. PO 152088, Davis, California, Geothermal Resources Council.

Baumann, H. 1955. "Beitr. Silikose-Forsch." 37, p. 47.

Brown, K. L., and G. D. McDowell. 1982. "The Effect of Aeration on Silica Scaling." In Proceedings of Pacific Geothermal Conference 1982, Part 1, University of Auckland, New Zealand, pp. 127-130.

Brownell, L. E., et al. 1947. "Flow of Fluids Through Porous Media." Chem. Engr. Prog.

Buisson, D. H., H. P. Rothbaum, and W. T. Shannon. 1979. "Removal of Arsenic from Geothermal Discharge Waters After Absorption on Iron Flow and Subsequent Recovery of the Floc Using Dissolved Air Flotation." Geothermics 8:97-110.

Cassell, E. A., K. M. Kaufman, and E. Matijevic'. 1975. "The Effects of Bubble Size on Microflotation." Water Research 9:1017-1024.

Chasteen, A. J. 1975. "Geothermal Steam Condensate Reinjection." In Proceedings of Second U.N. Symposium on the Development and Use of Geothermal Resources, pp. 1335-1336.

Chemical Engineeering. "Brine Treatment Process Spurs Geothermal Progress." Chem. Eng., March 7, 1983, pp. 55, 56.

Chemical Rubber Publishing Co. 1962. Handbook of Chemistry and Physics. 44th ed., Cleveland, Ohio.

Chen, C. A., and W. L. Marshal. 1982. "Amorphous Silica Solubilities - IV. Behavior in Pure Water and Aqueous Sodium Chloride, Sodium Sulfate, Magnesium Chloride and Magnesium Sulfate Solutions up to 350°C." Geochimica et Cosmochimica Acta 46:279-287.

Churchill, R. J., and K. J. Tacchi. 1978. "A Critical Analysis of Flotation Performance," American Institute of Chemical Engineers, Symposium Series, 74(178):290-299.

Cleasby, J. L. 1972. "Fitration." In Physiochemical Processes for Water Quality Control. Wiley Interscience, New York, pp. 139-198.

Conley, W. R. 1961. "Experience with Anthracite Sand Filters." J. Am. Water Works Assn., p. 1473.

Corsi, R. 1984. "Brine Utilization Task, ENEL-DOE Agreement." Letter dated "17 Gen. 1984" to A. J. Adduci, DOE, 1333 Broadway, Oakland, California.

Cosner, S. R., and J. A. Apps. 1978. Compilation of Data on Fluids from Geothermal Resources in the United States. LBL-5936, Lawrence Berkeley Laboratory, Berkeley, California.

Cramer, S. D. 1974. "The Solubility of Oxygen in Geothermal Brines." In Corrosion Problems in Energy Conversion and Generation, C. S. Tedmon, ed., Electrochemical Society, Princeton, New Jersey.

Crane, C. H., and D. C. Kenkeremath. 1981. "Review and Evaluation of Literature on Testing of Chemical Additives for Scale Control in Geothermal Fluids." DOE/ID/12183-TL.

Cuellar, G. 1975. "Comportamiento de. la Silice en Aquas Geotermicas de Desecho." In Proceedings of Second U.N. Symposium on the Development and Use of Geothermal Resources, Lawrence Berkeley Laboratory, San Francisco, California.

Culp, R. L., G. M. Wesner, and G. L. Culp. 1978. Handbook of Advanced Waste Water Treatment. 2nd ed. Van Nostrand Reinhold Company, New York.

Dahlstrom, D. A., R. W. Moore, and R. C. Emmett. 1982. "Clarifying Geothermal Fluids." Chem. Eng. Prog. October, pp. 50-55.

Davidson, D. H. 1979. "Invasion and Impairment of Formations by Particulates." SPE 8210.

Defferding, L. J. 1980. State-of-the-Art of Liquid Waste Disposal for Geothermal Energy Systems: 1979. DOE/EV-0083, U.S. Department of Energy, Office of Environmental Compliance and Review, Washington, D.C.

DiPippo, R. 1980. Geothermal Energy as a Source of Electricity. DOE/RA/28320-1, U.S. Department of Energy, Division of Geothermal Energy, Washington, D.C.

DiPippo, R. 1984. "Worldwide Geothermal Power Development." Geothermal Resources Council Bulletin 13(1):4-16.

Donaldson, E. C., et al. 1977. "Particle Transport in Sandstones." SPE 6905, October.

Douglas, J. G., et al. 1972. Geothermal Water and Gas Collection Methods for Sampling and Analysis. BNWL-2094, Pacific Northwest Laboratory, Richland, Washington.

Earlougher, R. C. 1977. "Advances in Well Test Analysis." Society of Petroleum Engineers, Monograph Vol. 5, p. 264.

Eickmeier, J. R., and H. J. Ramey. 1970. "Wellbore Temperatures and Heat Losses During Production or Injection Operations." Paper 7016, Petroleum Society, CIM.

Einarsson, S. S., A. Vides, and G. Cuellar. 1975. "Disposal of Geothermal Waste Water by Injection." In Proceedings of Second U.N. Symposium on the Development and Use of Geothermal Resources. Lawrence Berkeley Laboratory, San Francisco, California.

Ellis, A. J. 1959a. "The Solubility of Calcite in Carbon Dioxide Solutions." Am. J. Sci. 257:354-365.

Ellis, A. J. 1959b. "The System Na_2CO_3-$NaHCO_3$-CO_2-H_2O at Temperatures up to 200°C." Am. J. Sci. 257:287-296.

Ellis, A. J. 1963. "Solubility of Calcite in Sodium Chloride Solution at High Temperature." Am. J. Sci. 261:259-267.

Ellis, A. J., and R. M. Golding. 1963. "The Solubility of Carbon Dioxide above 100°C in Water and Sodium Chloride Solutions." Am. J. Sci. 261:47-60.

Ellis, P. F., et al. 1983. Corrosion Reference for Geothermal Downhole Materials Selection. DOE/SF/11503-1.

Ellis, P. F., and M. F. Conover. 1981. Materials Selection Guidelines for Geothermal Energy Utilization Systems. DOE/RA/27026-1.

Environmental Protection Agency. 1980. Summary Report - Control and Treatment Technology for the Metal Finishing Industry - Sulfide Precipitation. EPA Technology Transfer, EPA 625/8-30-003.

Featherstone, J. L., and D. R. Powell. April 1981. "Stabilization of Highly Saline Gethermal Brines." J. Petrol. Tech., pp. 727-733.

Felmy, A. R., D. Girvin, and E. A. Jenne. 1983. MINTEQ: A Computer Program for Calculating Aqueous Geochemical Equilibria. U.S. Environmental Protection Agency, Washington, D.C.

Gaudin, A. M. 1932. Flotation. McGraw Hill, New York.

Gerlaugh, H. E., et al. 1979. Cogeneration Technology Alternatives Study (CTAS) General Electric Company Final Report. N80-24797, Vol. 1, National Technical Information Service.

Glenn, E. E., and M. L. Slusser. 1957. "Factors Affecting Well Productivity - II. Drilling Fluid Particle Invasion Into Porous Media." Trans. AIME 210:132-139.

Goyal, K. P., M. J. Lippmann, and C. F. Tsang. 1982. "Reservoir Engineering Studies of the Cerro Prieto Geothermal Field." In Annual Report 1981: Earth Sciences Division, Lawrence Berkeley Laboratory, Berkeley, California.

Gray, D. H., and R. W. Rex. 1966. "Formation Damage in Sandstone Caused by Clay Dispersion and Migration." In Proceedings of 14th Conference on Clays and Clay Minerals, Pergamon Press, London.

Grens, J. Z., and L. B. Owen. May 1977. "Field Evaluation of Scale Control Methods." Geothermal Resource Council Transactions, Vol. 1, pp. 119-121.

Gruesbeck, C., et al. 1979. "Entrainment and Deposition of Fine Particles in Porous Media." SPE 8430, September.

Gudmundsson, J. S. 1983. "Silica Deposition from Geothermal Brine at Svartsengi, Iceland." Presented at International Symposium Solving Corrosion Scaling Problems in Geothermal Systems, January 1983, San Francisco, California, National Association of Corrosion Engineers.

Harrar, J. E., et al. 1977. Determination of the Rate of Formation of Solids from Hypersaline Geothermal Brine as a Function of pH. UCID-17596, Lawrence Livermore National Laboratory, Livermore, California.

Harrar, J. E., et al. 1978. "Effects of Additives on the Formation of Solids from Hypersaline Geothermal Brine." In Transaction Geothermal Resources Council Annual Meeting, Vol. 2., pp. 259-62.

Harrar, J. E., et al. 1979a. On-Line Tests of Organic Additives for the Inhibition of the Precipitation of Silica from Hypersaline Geothermal Brine. UCID-18091.

Harrar, J. E., et al. 1979b. On-Line Tests of Organic Additives for the Inhibition of the Precipitation of Silica from Hypersaline Geothermal Brine - II. Tests of Nitrogen-Containing Compounds, Silanes, and Additional Ethoxylated Compounds. UCID-18195.

Harrar, J. E., et al. 1979c. On-Line Tests of Organic Additives for the Inhibition of the Precipitation of Silica from Hypersaline Geothermal Brine - III. Scaling Measurements and Tests of Other Methods of Brine Modification. UCID-18238.

Harrar, J. E., et al. 1979d. Preliminary Results of Tests of Proprietary Chemical Additives, Seeding, and Other Approaches for the Reduction of Scale in Hypersaline Geothermal Systems. UCID-18051.

Harrar, J. E., et al. 1979e. Studies of Brine Chemistry, Precipitation of Solids, and Scale Formation at the Salton Sea Geothermal Field. UCRL-52460, Lawrence Livermore Laboratory, Livermore, California.

Harrar, J. E., et al. February 1980. On-line Tests of Organic Additives for the Inhibition of the Precipitation of Silica from Hypersaline Geothermal Brine - IV. Final Tests of Candidate Additives. UCID-18536.

Harrar, J. E. January 1981. Final Report on Studies of Brine Chemistry and Scaling at the Salton Sea Geothermal Field, 1977-1979. UCID-18917.

Harrar, J. E., et al. 1981. Assessment of the Injectability of Brines Produced by Geopressure - Geothermal Resources of the Gulf Coast. UCRL-86547.

Harrar, J. E., et al. 1982. "Field Tests of Organic Additives for Scale Control at the Salton Sea Geothermal Field." J. Soc. Petroleum Eng. 17:26.

Harrar, J. E., et al. May 4, 1982. U.S. Patent 4,328,106. "Method for Inhibiting Silica Precipitation and Scaling in Geothermal Flow Systems."

Hedrick, R. H. 1982. "Crystallization of Silica from Geothermal Brine." Paper presented at the Southeastern Regional Meeting of the Americal Chemical Society, November 3, 1982, Burmingham, Alabama.

Helgeson, H. C. 1969. "Thermodynamics of Hydrothermal Systems at Elevated Temperatures and Pressures." Am. J. Sci. 267:729-804.

Henley, R. W. 1983. "pH and Silica Scaling Control in Geothermal Field Development." Geothermics 12(4):307-321.

Holland, H. D., and S. D. Malinin. 1979. "The Solubility and Occurrence of Non-Ore Minerals." In Geochemistry of Hydrothermal Ore Deposits, H. L. Barnes, ed. 2nd ed. John Wiley and Sons, New York.

Horne, R. N. 1982a. Effects of Water Injection into Fractured Geothermal Reservoirs: A Summary of Experience Worldwide. SGP-TR-57, Stanford Geothermal Program, Interdisciplinary Research in Engineering and Earth Sciences, Stanford University, Stanford, California.

Horne, R. N. 1982b. "Reservoir Engineering Aspects of Injection." Chinbetsu 19(3):23 (from translation furnished by author).

Horne, R. N., and M. A. Grant. 1982. "New Zealand: An Update on Injection Experience." In Proceedings of Sixth Annual Geothermal Conference and Workshop, June 28-July 1, 1982, Snowbird, Utah, published by Attos Corp., Santa Cruz, California.

Howak, T. J., and R. F. Krueger. 1951. "The Effect of Mud Particles Upon Permeabilities of Cores." In Drill and Prod. Practice. American Petroleum Insitute.

Hurtado, R. J., et al. 1981. Treatment of Cerro Prieto I Brines for Use in Reinjection; Results of Pilot Plant Tests." In Proceedings of Third Symposium on the Cerro Prieto Geothermal Field, LBL-11967, CONF-810399, Lawrence Berkeley Laboratory, pp. 513-534.

Iler, R. K. 1973. "Colloidal Silica." In Surface and Colloid Science, Vol. 6, E. Matijevic, ed. John Wiley and Sons, New York, pp. 1-100.

Iler, R. K. 1979. The Chemistry of Silica. John Wiley and Sons, New York, p. 31.

Jackson, D. H., and J. H. Hill. January 1976. Possibilities for Controlling Heavy Metal Sulfides in Scale from Geothermal Brines. UCRL-51977.

Jorda, R. M. 1978. An Analysis of Water Injection at the Niland Geothermal Test Site. SAND 78-7052, Completion Technology Company, Houston, Texas.

Jorda, R. M. 1980. Use of Data Obtained from Core Tests in the Design and Operation of Spent Brine Injection Wells in Geopressured or Geothermal Systems. SAND 80-7047, Completion Technology Company, Houston, Texas.

Kandarpa, V., et. al. 1981. "Evaluation of Geothermal Brine Treatment Facility through Particle Characterization." Geothermal Resources Council Transactions, 5:345-348.

Kandarpa, V., and O. J. Vetter. 1981. "Prediction of Salt Precipitations Due to Injecting Foreign Waters into Geothermal Reservoirs." Geothermal Resources Council Transactions 5:341-344.

Kemmer, F. N., ed. 1979. The Nalco Water Handbook. McGraw-Hill, New York, pp. 43-45.

Kennedy, J. L. 1971. "Drilling Mud Particulates Can Cause Formation Damage." Oil and Gas Journal, August 2.

Kestin, J., ed. 1980. Sourcebook on the Production of Electricity from Geothermal Energy. DOE/RA/28320-2, U.S. Department of Energy, Division of Geothermal Energy, Washington, D.C.

Kharaka, I. K., and I. Barnes. 1973. SOLMNEQ: Solution Mineral Equilibrium Computations. Geological Sur. Computer Contr. Publ., 215-899, U.S. Dept. of Interior, Washington, D.C.

Kindle, C. H. 1983. "Rankine Cycle Leak Detection via Continuous Monitoring." In Part II of Addendum to Materials Selection Guidelines for Geothermal Energy Utilization Systems, DOE/ET/27026-2.

Kindle, C. H., et al. 1984. Compendium of Selected Methods for Sampling and Analysis of Geothermal Facilities. PNL-4979, Pacific Northwest Laboratory, Richland, Washington.

Kindle, C. H. and D. W. Shannon. 1982. "Geothermal Chemistry and Corrosion: The Operating Experiences." In Proceedings of the Regional Seminar on Geothermal Energy in Eastern and Southern Africa, Nairobi, Kenya, 1982. U. N. Educational Scientific and Cultural Organization (UNESCO) and U.S.A.I.D.

Kindle, C. H., and E. M. Woodruff. 1981. Techniques for Geothermal Liquid Sampling and Analysis. PNL-3801, Pacific Northwest Laboratory, Richland, Washington.

Kitahara, S. 1960. "The Polymerization of Silicic Acid Obtained by the Hydrothermal Treatment of Quartz and the Solubility of Amorphous Silica." Rev. Phys. Chem. Japan 30:131-137.

Klassen, V. I., and V. A. Mokrausov. 1963. An Introduction to the Theory of Flotation. Buttersworth, London.

Knutson, C. F., and C. R. Boardman. 1978. An Assessment of Subsurface Salt Water Disposal Experience on the Texas and Louisiana Gulf Coast for Application to Disposal of Salt Water from Geopressurized Geothermal Wells, Topical Report. NVO-1531-2, C. K. GeoEnergy Corporation.

Kochelek, J. T., and D. F. Zienty. 1981. "Use of Organic Floculants in Spent Brine Clarification." In Geothermal Energy: The International Success Story, Transactions, Vol. 5, Geothermal Resources Council, Davis, California.

Kreissl, J. E. 1973. "Granular Media Filtration of Waste Water: An Assessment." Paper presented at Seminar on Filtration of Water and Waste Water, Ann Arbor, Michigan.

Krueger, R. F., and L. C. Vogel. 1954. "Damage to Sandstone Cores by Particles from Drilling Fluids." Drill and Prod. Practices, American Petroleum Institute.

Kunze, J. F. 1978. Geothermal R&D Project Report for Period April 1, 1977 to September 30, 1977. TREE-1256, Idaho National Engineering Laboratory, Idaho Falls, Idaho.

Kuwada, J. T. U.S. Patent 3,782,468.

Kuwada, J. T. 1982. "Field Demonstration of the EFP System for Carbonate Scale Control." Geothermal Resources Council Bulletin, September-October 1982, pp. 3-9.

Lindemuth, T. E., et al. June 1977. "Experience in Scale Control with East Mesa Geothermal Brine." Presented at the International Symposium on Oil Field and Geothermal Chemistry, La Jolla, California.

Lippman, M. J., C. F. Tsang, and P. A. Witherspoon. 1977. Analysis of the Response of Geothermal Reservoirs Under Injection and Production Procedures. LBL-7028, Lawrence Berkeley Laboratory, Berkeley, California.

Luthyl, R. G., R. E. Selleck, and T. R. Galloway. 1978. "Removal of Emulsified Oil with Organic Coagulents and Dissolved Air Flotation." Water Pollution Control Federation, February 1978, pp. 331-346.

Marsh, A. R., III, G. Klein, and T. Vermuelen. October 1975. Polymerization Kinetics and Equilibria of Silicic Acid in Aqueous Systems. LBL-4415, Lawrence Berkeley Laboratory, Berkeley, California.

Marshal, W. L. 1980a. "Amorphous Silica Solubilities - I. Behavior in Aqueous Sodium Nitrate Solutions; 25-300°C, 0-6 Molal." Geochimica et Cosmochimica Acta 44:907-913.

Marshal, W. L. 1980b. "Amorphous Silica Solubilities - III. Activity Coefficient Relations and Predictions of Solubility Behavior in Salt Solutions, 0-350°C." Geochimica et Cosmochimica Acta 44:925-931.

Marshal, W. L., and C. A. Chen. 1982. "Amorphous Silica Solubilities - V. Predictions of Solubility Behavior in Aqueous Mixed Electrolyte Solutions up to 300°C." Geochimica et Cosmochimica Acta 46:289-291.

Marshal, W. L., and J. M. Warakomski. 1980. "Amorphous Silica Solubilities - II. Effect of Aqueous Salt Solutions at 25°C." Geochimica et Cosmochimica Acta 44:915-924.

Martinez, E. N., et al. 1983. "Treatment and Disposal of Geothermal Brines at Los Azufres Field in Michoacom, Mexico." In Chemical and Geochemical Aspects of Fossil Energy Extraction, pp. 245-257, Ann Arbor Science.

Matthews, C. S., and D. G. Russell. 1967. "Pressure Buildup and Flow Tests in Wells." Society of Petroleum Engineers, Monograph Vol. 1, p. 167.

McCune, C. C. January 1977. "On-Site Testing to Define Injection-Water Quality Requirements." J. Petrol. Tech.

McDuff, R. E., and F.M.M. Morel. 1973. Description and Use of the Chemical Equilibrium Program REDEQL2. EQ-73-02, California Institute of Technology, Pasadena, California.

McIndre, R. W., Jr. 1969. "Diatomaceous Earth Filtration for Water Supplies." Water and Sewage Works, p. 50.

McKee, C. R., and M. E. Hanson. 1976. Predicting Explosive-Generated Permeability Around Geothermal Wells. UCRL-77637.

Meinhold, T. F., and J. W. Walker. 1968. "Flotation Separator Ups Lithium Concentrate Recovery 11%." Chemical Processing 21(11):33, 104, 105.

Mercer, B. W., et al. 1982. Evaluation of Physical-Chemical and Biological Treatment of Shale Oil Retort Water. PNL-3449, Pacific Northwest Laboratory, Richland, Washington, pp. 55-56.

Messer, P. H., D. S. Pye, and J. P. Gallus. 1978. "Injectivity Restoration of a Hot-Brine Geothermal Injection Well." J. Petrol. Tech., p. 1225.

Metcalf and Eddy. 1979. Waste Water Engineering: Treatment Disposal and Reuse. 2nd ed., revised by G. Tchobanoglous. McGraw-Hill, New York.

Michels, D. E. 1979. "Reaction Mechanisms Associated with $CaCO_3$ Scale and Release of CO_2 at East Mesa." Geothermal Resources Council Transactions, Vol. 3.

Michels, D. E. 1981. CO_2 and Carbonate Chemistry Applied to Geothermal Engineering. LBL-11509, GREMP-15.

Mickley, M. C., and G. Coury. 1982. "Parameters of Silica Scaling in Reverse-Osmosis Systems." Water Supply Improvement Assoc. J. 9(1):11-23.

Moss, W. E., O. D. Whitescarver, and R. N. Yamasaki. 1982. "The Salton Sea 10 MWe Power Plant, Unit 1." Geothermal Resources Council Transactions, Vol. 6, pp. 373-376.

Nagahama, T. 1974. "Treatment of Effluent from the Kamioka Concentrator by Flotation Techniques, Including the Development of the Nagahm Flotation Machine." Canadian Institute of Mining and Metallurgy Bulletin, April 1974, pp. 79-89.

Nakazawa, H., I. Matsuoka, and J. Shimoiizaka. 1980. "The Removal of Arsenic in Waste Water by Precipitate Flotation. The Chemical Society of Japan, No. 11, pp. 1792-1799.

Narasimhan, T. N., et al. 1977. Recent Results from Tests on the Republic Geothermal Wells, East Mesa, California. LBL-7017, Lawrence Berkeley Laboratory, Berkeley, California.

Neasham, J. W. 1977. "The Morphology of Dispersed Clay in Sandstone Reservoirs and Its Effect on Sandstone Shaliness, Pore Space and Fluid Flow Properties." SPE 6858.

Needham, P. B., A. P. Murphy, and F. X. McCawley. 1976. "Scaling in Both High- and Low-Salinity Brines." In Proceedings of Conference on Scale Management in Geothermal Energy Development, August 2-4, 1976, San Diego, California, COO-2607-4, pp. 127-144.

Neis, U., and K. P. Kiefhaber. 1980. Differences Between Particle Flotation and Floc Flotation. In Fine Particle Processing, P. Somasundaran ed., Amer. Inst. Min. Met. and Pet. Engrs., New York, Vol. 1, pp. 755-766.

Nicholson, R. W. 1984. "Unique Aspects of Geothermal Casing Design." Geothermal Resources Council Bulletin. 13(4):18-20.

Ostroff, A. G. 1979. Introduction to Oilfield Water Technology. 2nd ed. National Association of Corrosion Engineers, Houston, Texas.

Owen, L. B. 1975. Precipitation of Amorphous Silica from High-Temperature Hypersaline Geothermal Brines. UCRL-51866, Lawrence Livermore Laboratory, Livermore, California.

Owen, L. B., et al. 1978. Predicting the Rate by Which Suspended Solids Plug Geothermal Injection Wells. UCRL-80529.

Owen, L. B., et al. 1979. An Assessment of the Injectability of Conditioned Brine Produced by Reaction Clarification. UCID-18488, Lawrence Livermore Laboratory.

Ozawa, T., and Y. Fujii. 1970. "A Phenomenon of Scaling in Production Wells and the Geothermal Power Plant in the Matsukawa Area." Geothermics, Special Issue 2, 2(2):1613-1618.

Parkhurst, D. L., C. Thorstenson, and L. N. Plummer. 1980. "PHREEQE: A Computer Program for Geochemical Calculations." U.S. Geological Survey, Water Resources Investigations, pp. 80-96.

Peters, M. S., and K. D. Timmerhaus. 1968. Plant Design and Economics for Chemical Engineers. McGraw-Hill, New York.

Phillips, S. L., A. K. Mathur, and R. E. Doebler. 1977. A Study of Brine Treatment. Lawrence Berkeley Laboratory, Research Project RP-791-1 for the Electric Power Research Institute.

Pitzer, K. S., "The Treatment of Ionic Solutions Over the Entire Miscibility Range," Ber. Bunsenges. Phys. Chem. 85(11):952-9 (1981); "Characteristics of Very Concentrated Aqueous Solutions," Phys. Chem. Earth 13-14(Chem. Geochem. Solutions High Temp. Pressures):249-72(1981); "Electrolytes. From Dilute Solutions to Fused Salts," J. Am. Chem. Soc., 162(9):2902-6(1980).

Purcell, W. R. 1949. "Capillary Pressures - Their Measurement Using Mercury and the Calculation of Permeability Therefrom." Trans. ASME.

Quong R. F., et al. 1978. "Processing of Geothermal Brine Effluents for Injection." Geothermal Resources Council Transactions, Vol. 2, pp. 551-554.

Quong, R. F., F. Schoepflin, and N. D. Stout. 1978. Conditioning of Geothermal Brine Effluents for Injection - Use of Coagulants. UCID-17716, Lawrence Livermore Laboratory, Livermore, California.

Ralston, P. H. August 1969. "Scale Control with Aminomethylenephosphonates." J. Petrol. Tech. 1029-36.

Reay, D., and G. A. Ratcliff. 1973. "Removal of Fine Particles from Water by Dispersed Air Flotation: Effects of Bubble Size and Particle Size on Collection Efficiency." Can. J. Chem. Eng. 51:178-185.

Repubic Geothermal. 1979. Geothermal Reservoir Well Stimulation Project, Reservoir Selection Task. DOE/AL/10963-72.

Republic Geothermal. 1980. Geothermal Reservoir Well Stimulation Program - First-Year Progress Report. DOE/AL/10563-T1.

Reynolds, S. L. October 1979. The Effect of Acid Addition for Scale Control on Geothermal Field and Plant Systems. Proceedings of Third Annual Geothermal Conference and Workshop, Electric Power Research Institute.

Rimstidt, J. D., and H. L. Barnes. 1980. "The Kinetics of Silica-Water Reactions." Geochim. Cosmochim. Acta 44:1683-1699.

Robertus, R. J., D. W. Shannon, and R. G. Sullivan. 1984. Report on Design, Construction and Testing of CO_2 Breakout System for Geothermal Brines." PNL-5042, Pacific Northwest Laboratory, Richland, Washington.

Rodgers Engineering. 1982. Technical Report on the Operation of the EFP Systems Demonstration Facility at Desert Peak, Nevada. LASL Contract No. 4-X11-3079V-1; available from R. J. Hanold at LASL, Los Alamos, New Mexico.

Roe, L. A. 1980. "Flotation of Liquids and Fine Particles from Liquids." In Fine Particle Processing, P. Somasundaran ed., Amer. Inst. Min. Met. and Pet. Engrs, New York, Vol. 1, pp. 871-885.

Rothbaum, H. P., et al. 1979. "Effect of Silica Polymerization and pH on Geothermal Scaling." Geothermics 8:1-20.

Rothbaum, H. P., and B. H. Anderton. 1975. "Removal of Silica and Arsenic from Geothermal Discharge Waters by Precipitation of Useful Calcium Silicates." In Proceedings of Second U. N. Symposium on the Development and Use of Geothermal Resources, May 20-29, 1975, San Francisco, California, Vol. 2, pp. 1417-1425.

Ryan, J. E. 1951. "Industrial Salts: Production at Searles Lake." Mining Eng. 3(5):447-452.

San Diego Gas and Electric. 1980. Geothermal Loop Experimental Facility - Final Report." DOE/ET/28443-T1, U.S. Department of Energy, Washington, D.C.

Schroeder, R. C., et al. 1982. "Injection Studies of Vapor-Dominated Systems." Geothermics 11(2):93.

Setchenow, M. 1892. "Action de L'Acid Carbonique sur les Solutions des Sels a Acides Forts." Ann. Chim. Phys. 6(25):226-270.

Shannon, D. W., et al. 1980. Field Evaluation of Sampling Methods for Pressurized Geothermal Liquids, Gases, and Suspended Solids. PNL-3412, Pacific Northwest Laboratory, Richland, Washington.

Shannon, D. W., R. P. Elmore, and D. D. Pierce. 1981. Monitoring the Chemistry and Materials of the Magma Binary Cycle Generating Plant. PNL-4123, Pacific Northwest Laboratory, Richland, Washington.

Shannon, D. W., R. A. Walter, and D. L. Lessor. 1976. "The Geoscale Computer Model for Geothermal Plant Scaling and Corrosion Analyses." In Conference on Scale Management in Geothermal Energy Development, COO-2607-4, EIC Corporation.

Shannon, W. T., and D. H. Buisson. 1980. "Dissolved Air Flotation in Hot Water." Water Research 14:759-765.

Shannon, W. T., W. R. Owers, and H. P. Rothbaum. 1982. "Pilot Scale Solids Liquid Separation in Hot Geothermal Discharge Waters Using Dissolved Air Flotation." Geothermics 11(1):53-58.

Spencer, S. G. 1980. An Analysis of the Response of the Raft River Monitor Wells to the 1979 Injection Tests. EGG-2057, U.S. Department of Energy, Idaho Falls Operation Office, Idaho National Engineering Laboratory, Idaho Falls, Idaho.

Sposito, G., and S. V. Mattigod. 1980. Geochem: A Computer Program for the Calculation of Chemical Equilibria in Soil Solutions and Other Natural Water Systems. University of California, Riverside, California.

Stacy, R. E., and I. A. Thain. 1984. "Twenty-Five Years of Operation at Wairakei Geothermal Power Station." Geothermal Resources Council Bulletin 13(2)7-19.

Strumm, W., and J. J. Morgan. 1981. Aquatic Chemistry. 2nd ed. John Wiley and Sons, New York.

Subcasky, W. J. 1978. "Petroleum Industry Experience in Water Injection." In Proceedings of Thermal Energy Storage in Aquifer Workshop. LBL, CONF. 78-05140.

Talmadge, W. P., and E. B. Fitch. 1955. "Determining Thickener Unit Areas." Ind. Eng. Chem. 47:(1).

Thomeer, J. H., et al. May 1977. "A Shallow Plugging - Selective Re-Entry Technique for Profile Corrections." J. Petrol. Tech.

Tsang, C. F., et al. 1981. "The Cerro Prieto Injection Tests: Studies of a Multilayer System." In Proceedings of Third Symposium on the Cerro Prieto Geothermal Field, March 24-26, 1981, Baja California, Mexico.

Vetter, O. J. August 1972. "An Evaluation of Scale Inhibitors." J. Petrol. Tech. 997-1006.

Vetter, O. J., 1978. "Injection, Injectivity and Injectability in Geothermal Operations." Transaction GRC Annual Meeting, Vol. 1, pp. 649-652

Vetter, O. J., et al. 1981. Particle Characterization for Geothermal Operations Part 2: Field Experience. Report submitted to U.S. Department of Energy, Division of Geothermal Energy, Washington, D.C.

Vetter, O. J., and D. A. Campbell. June 1979. Scale Inhibition in Geothermal Operations - Experiments with Dequest® 2060 Phosphonate in Republics East Mesa Field. LBL-9089, Lawrence Berkeley Laboratory, Berkeley, California.

Vetter, O. J., V. Kandarpa, and J. Jackson. 1981. "Suspended Solids from Removal Prior to Brine Reinjection." In Geothermal Energy: The International Success Story, Transactions, Vol. 5, Geothermal Resources Council, Davis, California.

Vetter Research. March 29, 1982. "Scale Inhibitor Evaluation for Application to Reinjection Operations." Submitted to U.S. DOE, San Francisco Office.

Vrablik, E. R. 1959. "Fundamental Principles of Dissolved-Air Flotation of Industrial Wastes." In Proceedings of the Fourteenth Industrial Waste Conference, May 5, 6, and 7, 1959, Purdue University, Lafayette, Indiana, pp. 743-779.

Wahl, E. F. 1977. Geothermal Energy Utilization. John Wiley and Sons, New York.

Wells, K. D., et al. 1981. The Cost of Meeting Geothermal Liquid Effluent Disposal Regulations. PNL-2991, Pacific Northwest Laboratory, Richland, Washington.

Weres, O., and L. Tsao. 1981. "Chemistry of Silica in Cerro Prieto Brines." Geothermiuer 10:255-276.

Weres, O., L. Tsao, and E. Iglesias. 1980. Chemistry of Silica in Cerro Prieto Brines. LBL-10166, Lawrence Berkeley Laboratory, Berkeley, California.

Weres, O., A. Yee, and L. Tsao. 1980. Kinetics of Silica Polymerization. LBL-7033, Lawrence Berkeley Laboratory, University of California, Berkeley, California.

Westall, J. C., J. L. Zachary, and F.M.M. Morel. 1976. MINEQL - A Computer Program for the Calculation of Chemical Equilibrium Composition of Aqueous Systems. Ralph M. Parsons Laboratory for Water Resources and Environ. Eng., Dept. of Civil Eng., M.I.T. Technical Note 18.

White, D. E. 1968. "Environments of Generation of Some Base-Metal Ore Deposits." Economic Geology 63:301.

Wilkins, V. H. April 5, 1977. U.S. Patent 4,016,075. "Process for Removal of Silica from Geothermal Brine."

Wolery, T. J. 1979. Calculation of Chemical Equilibrium Between Aqueous Solution and Mineral, the EQ3/6 Software Package. UCRL-52658, Lawrence Livermore Laboratory, Livermore, California.

Yanagase, T., Y. Suginohara, and K. Yanagase. 1970. "The Properties of Scales and Methods to Prevent Them." In Proceedings U.N. Sump. Devel. Util. Geother. Res. Pisa. Geothermics, Special Issue 2, 2:1619-23.

Yoshida, K., K. Tanaka, and K. Kusunoki. 1983. "Operating Experience of Double-Flash Geothermal Power Plant (Hatchobarn)." In Proceedings of the Seventh Annual Geothermal Conference and Workshop, Electric Power Research Institute.

Zilch, H. E., and P. W. Fischer. June 28, 1977. U.S. Patent 4,032,460. "Inhibition of Scale Deposition in High Temperature Wells."

APPENDIX

EXERCISE IN SUSPENDED SOLIDS DETERMINATION AND PRESERVATION

APPENDIX

EXERCISE IN SUSPENDED SOLIDS DETERMINATION AND PRESERVATION

PURPOSE: To compare methods for determining suspended particles in geothermal brines.

SUMMARY: As part of a larger effort to determine geothermal fluid sampling protocol, a one-time exploratory comparison of particulate measuring techniques was performed on a calcite scaling brine under preflash and flashing (scaling) conditions. No comparison was made on postflash, comparatively stable brine which would be the most applicable to post-treatment injection quality brine. The results of this one-time effort do not permit a distinction between the suitability of different measuring techniques except that in flashing/calcite scaling conditions a technique that is specific to particulates, such as weight gain on a filter, is superior to instrumental techniques which record bubbles as particles. The ability to preserve brine samples for later particulate analysis has not been demonstrated.

During August 1979, a field study was performed by Pacific Northwest Laboratory (PNL) at the East Mesa DOE Geothermal Component Test Facility to compare methods of suspended solid determinations in a geothermal brine. Well 6-2 was artesian-flowed through a sampling test loop. Triplicate samples were collected from two locations: Port S-3, which taps single-phase brine, and Port S-56, which is downstream of the second orifice (produces a two-phase steam/liquid flow). For each port, the suspended solid measurements were determined under identical conditions so that variations in the determined amounts reflected only the accuracy or precision of each method and not sampling or well variations. The following methods were compared: filtration of cooled and depressurized brine using single and multiple filters, filtration at in-line conditions, light-scattering method using a laser particle counter, and turbidity measurements. The details of this comparative study can be found in Shannon et al. (1980).

The results from each method of suspended solid determination are compared in Table A.1 for Ports S-3 and S-56. Using a single filter (0.45-μm pore diameter), the total suspended solids were determined to be 0.26 mg/l at Port S-3 (single-phase flow) and 0.77 mg/l at Port S-56 (two-phase flow). From these data, it appears that the quantity of suspended solids increases after the brine flashes; $CaCO_3$ scale was forming. Suspended solids were also collected in a filter chain for comparison and to determine the size distribution of these solids. More total suspended solids were measured at the two-phase regime: 1.83 mg/l (two-phase) versus 1.15 mg/l (single-phase). The fact that

TABLE A.1. Comparison of Methods for Suspended Solid Determinations for One- and Two-Phase Brine

Method	Filter Size, mm	Suspended Solids in One-Phase Brine (Port S-3)	Suspended Solids in Two-Phase Brine (Port S-56)
Filter weight gain			
Single filter	0.45	0.26 mg/l	0.77 mg/l
Filter chain	0.22	1.15 mg/l	1.83 mg/l
Laser particle counter	1.0 and up	0.77 mg/l	32.9 mg/l
Turbidity		0.23 FTU	0.57 FTU

the filter-chain technique gives a higher value of suspended solids than the single-filter method can be partially attributed to actually collecting more solids using a smaller pore size (0.22-μm) filter. Otherwise, the difference in collection capacity may mean that a filter chain is a more effective way of collecting suspended solids.

The quantity of suspended solids of varying diameter was determined using a Prototon Particle Counter® Model ILI 1000 plus the Particle Profile Attachment. Samples were collected in 8-oz clear glass bottles that were previously rinsed with filtered (0.45-μm) distilled water. The brine was cooled and depressurized through the sampling system used for the filtered samples.

Three samples of raw brine were collected at Ports S-3 and S-56 for suspended solids determination. Three additional brine samples from Port S-3 were acidified with five drops of concentrated HCl to determine if acidification preserved the samples. At Port S-3, the suspended solids totals for the three bottles were 233, 179, and 398 particles/ml. The scatter in the values indicates that three 250-ml bottles of brine do not constitute a statistically representative sample. It is interesting to note that the acidified samples were higher in total suspended solids (485, 458, and 612 particles/ml). Apparently, acidification of this particular brine does not preserve the sample for suspended solid measurements.

The concentration of solids in raw samples (Port S-3) increased during the 95 h after sampling and then decreased at 140 h. The decrease may have occurred because the solids obtained sufficient mass to settle out. Similar trends were observed at Port S-56. Suspended solids reached their maximum

®Registered trademark of Spectrex Corporation, Redwood City, California.

level at 24.0 h and then decreased. This variation in suspended solids with time proves that suspended solid measurements should be made as soon after sampling as possible.

At Port S-56, the amounts of suspended solids for the three samples did not vary as much; counts were 744, 937, and 893 particles/ml, respectively. Comparing the average for the three at Port S-56 (858) to the average for the three raw samples at Port S-3 (270), it appears that again more suspended solids are measured in the brine after flashing.

To compare the laser data with the filter data, the laser data were converted from particles/ml to mg/l. It was assumed that the particles are perfect spheres and that the density of these particles is 3 g/cm^3 (a mixture of silica and sulfides).

As can be seen in Table A.1, the total weight of suspended solids determined using the data obtained from the laser particle counter is in good agreement with the filter weight gain method for Port S-3, but it is high for Port S-56. The laser data may have been higher because 1) bubbles were still forming in the brine during counting; 2) the particle density was actually lower than the 3 g/cm^3 used for the calculations; or 3) the particle shapes were more varied from the ideal sphere volume used in the calculations. It is clear that while the laser particle counter gives useful data, more work is needed to calibrate the mass analyses.

Turbidity of the brine in formation turbidity units (FTU) was also determined simultaneously with the other sampling methods at Ports S-3 and S-56. Turbidity measurements can be performed relatively quickly and easily; since most laboratories have a spectrophotometer, the cost is minimal. At the East Mesa sampling field test, a Bausch and Lomb Minispec 20® was used for the determinations. The smallest values were obtained at Port S-3 (Table A.1).

In summary, single and multiple filter filtration, the laser particle counter, and the turbidity measurements each measured the lowest quantity of suspended solids at the single-phase sampling Port S-3 and the highest quantity at the two-phase Port S-56. Thus, each method appears to be satisfactory for monitoring relative changes in suspended solid concentration. It is much harder to say which method is the most accurate in measuring absolute quantities, but the two-phase brine appears to be harder to measure using light-scattering techniques. Several potential sampling errors were addressed with the following conclusions: acidification to preserve suspended solid samples may produce erroneous values, and the concentration of suspended solids can vary after collection and may vary with at least some preservation attempts.

®Registered trademark of Bausch and Lomb, Analytical Systems, Rochester, New York.